Filipa Isabel Peralta da Silva Pereira

Mestre em Ciências da Conservação pela Universidade Nova de Lisboa

Early metallurgical steps in the Prehistoric Portuguese Estremadura

Dissertação para obtenção do Grau de Doutor em Conservação e Restauro do Património, especialidade em Ciências da Conservação

Orientador: Rui Jorge Cordeiro Silva, Professor Auxiliar, Faculdade de Ciências e Tecnologia, Universidade Nova de Lisboa

Co-orientadores: Maria de Fátima Araújo, Investigadora Principal, C2TN, Instituto Superior Técnico, Universidade de Lisboa

António Manuel Monge Soares, Investigador Principal (Aposentado), C2TN, Instituto Superior Técnico, Universidade de Lisboa

Júri:

Presidente: Professora Doutora Maria Adelaide de Almeida Pedro de Jesus

Arguentes: Professor Doutor Luís Filipe Malheiro de Freitas Ferreira

Professor Doutor João Carlos de Freitas de Senna-Martinez

Vogais: Professor Doutor Rui Jorge Cordeiro Silva

Investigador Doutor Pedro Manuel Francisco Valério

FCt FACULDADE DE CIÊNCIAS E TECNOLOGIA UNIVERSIDADE NOVA DE LISBOA

Dezembro, 2017

Early metallurgical steps in the Prehistoric Portuguese Estremadura

Dedicated to my family

ACKNOWLEDGMENTS

"You see things; and you say, 'Why?' But I dream things that never were; and I say, 'Why not?'"

George Bernard Shaw
Irish literary Critic, Playwright and Essayist, 1925 Nobel Prize for Literature, 1856-1950

"Understanding the history of materials means understanding the history of mankind and civilisation".

Rolf E. Hummel
University of Florida
Understanding Materials Science
History – Properties – Applications
Springer 2004, ISBN: 0-387-20939-5

x

PUBLISHED WORK

The main results presented in this PhD Dissertation have been published in international journals included in the Science Citation Index (SCI) and presented at scientific meetings.

Articles published in International peer-reviewed journals:

1. Pereira, F., Silva, R.J.C., Soares, A.M.M., Araújo, M.F., Cardoso, J.L. (2017) Metallurgical production from the Chalcolithic settlement of Moita da Ladra, Portugal. *Materials and Manufacturing Processes* 32 (7-8), 781-791. doi: 10.1080/10426914.2016.1244839.

2. Pereira, F., Silva, R.J.C., Soares, A.M.M., Araújo, M.F., Oliveira, M.J., Martins, R.M.S., Schell, N. (2015) Effects of long-term aging in arsenical copper alloys. *Microscopy and Microanalysis* 21(6), 1413-1419. doi: 10.1017/S1431927615015263

3. Pereira, F., Silva, R.J.C., Soares, A.M.M., Araújo, M.F. (2013) Microscopy characterization of metallurgical production evidence from Vila Nova de São Pedro (Azambuja, Portugal). *Microscopy and Microanalysis* 19 (Suppl 4), 149-150. doi:10.1017/S1431927613001360.

4. Pereira, F., Silva, R.J.C., Soares, A.M.M., Araújo, M.F. (2013) The role of arsenic in Chalcolithic copper artefacts - insights from Vila Nova de São Pedro (Portugal). *Journal of Archaeological Science* 40(4), 2045-2056. doi:10.1016/j.jas.2012.12.015.

Articles published in peer-reviewed scientific meetings proceedings:

1. Pereira, F., Silva, R.J.C., Soares, A.M.M., Araújo, M.F. (2014) Metallurgical production evidence in Castro de Vila Nova de São Pedro (Azambuja, Portugal). In: Proceedings of the *39th International Symposium for Archaeometry*, Leuven, 96-101.

2. Pereira, F., Furtado, M.J., Silva, R.J.C., Soares, A.M.M., Araújo, M.F., Cardoso, J.L. (2013) Estudo das Evidências de Produção Metalúrgica no Outeiro Redondo (Sesimbra). In: Actas do *I Congresso de Arqueologia da Associação dos Arqueólogos Portugueses (AAP)*, Lisboa, Portugal, 463-468.

Articles published in Nacional peer-reviewed journals:

1. Pereira, F., Silva, R.J.C., Soares, A.M.M., Araújo, M.F. (2012) Estudo arqueometalúrgico de artefactos provenientes do Castro de Vila Nova de São Pedro (Azambuja, Portugal). *Estudos Arqueológicos de Oeiras*, Oeiras, 19, 163-172.

Abstracts published in peer-reviewed scientific meetings:

1. Pereira, F., Silva, R.J.C., Soares, A.M.M., Araújo, M.F. (2015) Importance of arsenic content for the perceived colour of arsenical copper artefacts. In: *Congresso Ibérico de Arqueometria* (Évora, Portugal), 96, 14 – 16 de October. Poster presentation.

2. Pereira, F., Silva, R.J.C., Soares, A.M.M., Araújo, M.F. (2015) Evidence of cubic Cu_3As as the stable arsenide at low temperatures in arsenical coppers. In: *Materiais 2015 – VII International Materials Symposium of Sociedade Portuguesa dos Materiais* (Porto, Portugal), 21-23 June, 1p. Poster presentation.

3. Pereira, F., Silva, R.J.C., Soares, A.M.M., Araújo, M.F., Cardoso, J.L. (2015) Metallurgical production evidences in the chalcolithic settlement of Moita da Ladra (Vila Franca de Xira, Portugal), In: *International Conference Archaeometallurgy in Europe IV* (Madrid, Spain), 3 - 6 June, 104-105. Poster presentation.

4. Pereira, F., Silva, R.J.C., Soares, A.M.M., Araújo, M.F. (2015) Early metallurgical steps in the Prehistoric Portuguese Estremadura, In: *V Annual Meeting i3N* (Aveiro, Portugal), 10 – 11 April. Poster presentation.

5. Pereira, F., Furtado, M.J., Silva, R.J.C., Soares, A.M.M., Araújo, M.F., Cardoso, J.L. (2013) Estudo das Evidências de Produção Metalúrgica no Outeiro Redondo (Sesimbra). I Congresso de Arqueologia da Associação dos Arqueólogos Portugueses (AAP) (Lisboa, Portugal), 21 – 24 November, Poster presentation.

6. Furtado, M.J., Pereira, F., Silva, R.J.C., Soares, A.M.M., Araújo, M.F., Cardoso, J.L. (2013) Metallurgical Production Evidences in Outeiro Redondo, Sesimbra (Portugal). In: *1st International Conference on Innovation in Art Research and Technology* (Évora, Portugal), 10-13 July, 134. Poster presentation.

Scientific meetings:

1. Furtado, M.J., Pereira, F., Silva, R.J.C., Soares, A.M.M., Araújo, M.F., Cardoso, J.L. (2013) Metallurgical Production Evidences in Outeiro Redondo, Sesimbra (Portugal), *3as Jornadas do CENIMAT, CENIMAT - i3N* (Monte de Caparica, Portugal), 28 June, Poster presentation.

2. Pereira, F., Silva, R.J.C., Soares, A.M.M., Araújo, M.F. (2012) Microscopy characterization of metallurgical production evidences from Vila Nova de São Pedro (Azambuja, Portugal). *Micros2012 (Congresso da Sociedade Portuguesa de Microscopia): Microscopy, a tool for the advancement of science*, Hospital D.Estefânia (Lisboa, Portugal) 24 - 25 September, Poster presentation.

3. Pereira, F., Silva, R.J.C., Soares, A.M.M., Araújo, M.F. (2012). *Metallurgical production evidences in Castro de Vila Nova de São Pedro (Azambuja, Portugal)*, *39th International Symposium on Archaeometry: "50 years of ISA"* (Leuven, Belgium), 28 May - 1 June, Poster presentation.

RESUMO

Na presente tese foram estudadas três colecções metalúrgicas. As colecções são datáveis do Calcolítico e provenientes de povoados da Estremadura Portuguesa, nomeadamente de Vila Nova de São Pedro (VNSP), a que pertence a maior colecção, Moita da Ladra (ML) e Outeiro Redondo (OR). O estudo destas colecções visou fornecer uma visão geral da metalurgia primitiva na região da Estremadura, bem como obter informações detalhadas sobre a metalurgia de cada sítio arqueológico. Os métodos analíticos utilizados foram a espectrometria de fluorescência de raios X dispersiva de energias (EDXRF) e a micro-EDXRF para determinar a composição elementar; a microscopia óptica e a microscopia electrónica de varrimento com microanálise de raios X, para caracterização microestrutural, e a determinação da dureza e da cor da liga.

Os principais resultados indicam que houve produção de metal em VNSP, fazendo uso de uma tecnologia de cadinho e trabalhando em condições redutoras pobres durante as operações de produção de metal, originando escórias altamente viscosas e heterogéneas e com alta retenção de glóbulos e nódulos metálicos. Por outro lado, a produção de artefactos terá ocorrido nos três povoados. Os artefactos são constituídos por cobre ou por cobre com arsénio (As ≥ 2%), estando o teor em ferro abaixo do limite de quantificação (< 0,05%), na grande maioria dos casos. A maior percentagem de artefactos de cobre arsenical da colecção da ML está possivelmente relacionada com diversificação dos depósitos de minério explorados incluindo provavelmente, além da Zona de Ossa Morena, a Faixa Piritosa Ibérica. Esta diversificação poderá dever-se ao período cronológico de ocupação mais tardio de ML, correspondente ao Campaniforme, em comparação com VNSP. No caso do OR, não se observou um maior uso de artefactos com teores de arsénio mais elevados, possivelmente devido à pequena colecção estudada. Apesar de ML e OR serem contemporâneos, a presença campaniforme parece ser mais intensa em ML do que em OR. A existência de actividades metalúrgicas em VNSP num intervalo de tempo mais longo pode também ter causado uma maior variabilidade do teor de arsénio das ligas, devido à possibilidade de ocorrência de vários ciclos de reciclagem durante esse maior intervalo de tempo. Nos três povoados, o processamento termomecânico é constituído por um ou mais ciclos de martelamento e recozimento, com uma martelagem final aplicada em menos de metade das colecções. A cor era provavelmente a principal propriedade que determinava a selecção das ligas de cobre arsenical e não as suas propriedades mecânicas.

A ocorrência do arsenieto na forma cúbica neste tipo de objectos sugere a sua precipitação por envelhecimento prolongado à temperatura ambiente, o que aponta para a necessidade de uma redefinição da fase de equilíbrio de Cu-As. Este resultado destaca a importância de compreender o impacto do envelhecimento estrutural na avaliação das propriedades originais dos artefactos arqueológicos de cobre arsenical.

PALAVRAS-CHAVE

Calcolítico; Estremadura; metalurgia primitiva; composição elementar; cobre arsenical; microestrutura

ABSTRACT

Three different metallurgical collections were studied in the present thesis. The collections originated from Chalcolithic settlements in the Portuguese Estremadura region, namely Vila Nova de São Pedro (VNSP), from where the largest group belongs, Moita da Ladra (ML) and Outeiro Redondo (OR). These studies aimed to provide a general view of the early metallurgy in the Estremadura region, as well as detailed information on the metallurgy of each archaeological site. Several analytical methodologies were involved, namely energy dispersive X-ray fluorescence spectrometry (EDXRF) and micro-EDXRF to determine elemental compositions; optical microscopy and scanning electron microscopy with X-ray microanalysis for microstructural characterization, and hardness and colour determinations of the alloy.

The main results indicate that metal was produced only in VNSP, using a crucible technology and working under poor reducing conditions during smelting operations. These conditions would result in highly viscous and heterogeneous slag and high retention of metal prills. On the other hand, artefact production was most likely accomplished in all three settlements. Artefacts were composed of copper or copper with arsenic (As ≥ 2 wt.%), being the iron content below the quantification limit (< 0.05 wt.%) in most cases. The higher percentage of arsenic content of the artefacts recorded at ML is possibly related to the diversification of exploited ore deposits, including the OMZ and the Iberian Pyrite Belt. This diversification was likely due to the shorter and later chronological occupation period (Bell Beaker Phase) of ML and OR, compared to VNSP. The increased use of copper alloys with higher arsenic contents was not observed in OR possibly due to the small artefact collection. Also, despite ML and OR being contemporaneous, the presence of the Bell Beaker period was stronger in ML than in OR. In the case of VNSP, the percentage of arsenical copper artefacts seems to be significantly inferior from ML and OR. The existence of metallurgical activities in VNSP for a longer time interval may cause higher variability in the arsenic content of the alloys as a consequence of several recycling cycles over time. The thermomechanical processing was found to be similar in all three settlements, consisting of one or more cycles of hammering and annealing, with a final forging procedure applied in less than half the artefacts in all collections. Results also suggest that colour was probably the main property determining the selection of the arsenical alloys by ancient metallurgists rather than their mechanical properties.

The occurrence of the cubic arsenide in these particular objects suggests that it was precipitated due to long-term ageing at room temperature, which points to the need of a redefinition of the Cu-As equilibrium phase constitution. These results highlight the importance of understanding the impact of structural ageing for the assessment of original properties of archaeological arsenical copper artefacts, such as hardness or colour.

KEYWORDS

INDEX OF CONTENTS

INDEX OF FIGURES

INDEX OF TABLES

SYMBOLS AND NOTATIONS

BA	Bronze Age
BCS	British Chemical Standards
BF	Bright field (in OM observations)
BSE	Backscattered Electrons (in SEM observations)
CENIMAT	Centro de Investigação de Materiais
CIELAB	or **CIE L*a*b*** colorimetric space, **L**: lightness; **a**, **b**: colour-opponent dimensions
CA	Copper Age
CRED	Cabeço Redondo
C2TN	Centro de Ciências e Tecnologias Nucleares
DCM	Departamento de Ciências dos Materiais
DCR	Departamento de Conservação e Restauro
DF	Dark field (in OM observations)
DIC	Differential Interference Contrast
EBA	Early Bronze Age
EDS	Energy-Dispersive X-Ray Spectroscopy
EDXRF	Energy Dispersive X-Ray Fluorescence
EIA	Early Iron Age
FCT	Faculdade de Ciências e Tecnologia
FE-SEM	Field Emission Scanning Electron Microscopy
h	Metric hue or hue angle
IA	Iron Age
IGESPAR	Instituto de Gestão do Património Arquitectónico e Arqueológico
I3N	Instituto de Nanoestruturas, Nanomodelação e Nanofabricação
IP	Iberia Peninsula
IST	Instituto Superior Técnico
IUPAC	International Union of Pure and Applied Chemistry
K-S test	Kolmogorov–Smirnov two-sample test
LBA	Late Bronze Age
MAC	Museu Arqueológico do Carmo
MBA	Middle Bronze Age
ML	Moita da Ladra
OM	Optical Microscopy
OMZ	Ossa Morena Zone
OR	Outeiro Redondo
POL	Cross-polarized light (in OM observations)
RH	Relative Humidity
SAM	"Studienzu den Anfängen der Mettalurgie"
SE	Secondary Electrons (in SEM-EDS observations)

SEM-EDS	Scanning Electron Microscopy – Energy-Dispersive X-Ray Spectroscopy
UL	Universidade de Lisboa
UNL	Universidade Nova de Lisboa
VHN	Vickers Hardness Number
VNSP	Vila Nova de São Pedro
XRD	X-Ray Diffraction

xxx

1. INTRODUCTION

Metallurgy can be defined as a field of material science and engineering encompassing the study of the physical and chemical behaviour of metallic elements, their intermetallic compounds, their alloys and also the technology and engineering necessary to the manufacture of metal products. Any metallurgical process begins with the extraction of metals from the ores. It can be followed by the alloying of the metal with other elements and includes all the metalworking applied until the final shape of the object.

But what were the first steps taken before metallurgy became an established field of science? The advent of extractive metallurgy, its chronology and localization, are important issues that still raise debate in prehistoric archaeology. The introduction of metallurgy had, without any doubt, significant repercussions in prehistoric societies and was also a fundamental step for the later emergence of more technologically complex societies. After the recognition of metal as a new material, it was expected an increasing development of the metallurgical abilities and complexity in the procedures taken during the manufacture of artefacts. This evolution is reflected in the Ancient World, with continuous phases being named after the main metal processed: Chalcolithic Period or Copper Age (CA), Bronze Age (BA) and Iron Age (IA). However, even if metallurgical questions are common, these phases can correspond to different chronological periods from one region to another.

Metallurgy displays unique characteristics when compared with other activities, such as lithic or ceramic production. For example, the raw materials required for metallurgy make it quite unusual compared with other traditional technologies. Except for gold or other native metals, identification of the adequate ores and all the following pyrotechnic procedures required to obtain metal must have been the result of a long and arduous learning process. From the beginning, the distinctive physical characteristics that metal exhibits such as colour, glow, plasticity and the ability to be recycled must not have been unnoticed for prehistoric communities.

The social changes and transformations that occur in Prehistory are most likely the result of utilization of new materials and innovative technologies. Therefore, it is vital to understand the emergence of metalworking to recognise some of these critical moments of change and invention.

Archaeometallurgy is a field of archaeometry dedicated to the study of production and use of metals by Man in ancient times, namely during the Prehistory. These studies contribute to understanding the evolution and importance of metallurgical activities in the social organization of pre and protohistoric communities. These objectives are achieved through the analysis of metallic artefacts and metallurgical production vestiges that include slags, crucibles, and metallic remains, among other items.

Elemental composition, microstructure and isotopic studies of archaeological metallurgical vestiges can provide valuable information about production technology of artefacts and geographic origin of the ores. However, it must be recognized that since their use and production until the moment of study, metallurgical remains have been subjected to continuous physical, chemical and biological phenomena. Therefore, information obtained from the analysis of these vestiges can be significantly

altered or partially lost by such phenomena, confounding or making impossible the correct assessment of the original composition or production technology.

The significant development in material sciences in the past decades lead to the appearance and improvement of several analytical techniques that can be applied to the study of metallic materials, providing increased information possible to obtain from archaeological vestiges.

1.1. HISTORY OF ARCHAEOMETALLURGY

Since ancient times the description of the technological production processes and uses of metallic artefacts has been a relevant field of interest for Humankind. For instance, in the encyclopaedia "Historia Naturalis", written in the first century AD, by "Gaius Plinius Secundus" (known as Pliny, the Elder), was described the use of gold and silver in coins, jewellery and several works of art. It is one of the largest single works to have survived from the Roman Empire to the modern days and proposed to cover all ancient knowledge on those metals. Nevertheless, it is only during the Renaissance that the first comprehensive texts about the production of metals appear. Georgius Agricola publishes "Bermannus" in 1530 (Halleaux and Yans, 1990) and "De Re Metallica" in 1556 (Hoover and Hoover, 1912) describing the highly developed and complex processes of mining metal ores, metal extraction and metalworking, providing valuable data about medieval metallurgical processes.

Another study, "Pirotechnia", first published in 1559 by Biringuccio, presents a detailed description of the metallurgical operations used in XVI century (Smith and Gnudi, 1990). It describes the principal ores used for gold, silver, copper, lead, tin and iron alongside with the description of the equipment and mining exploring technologies, treatment of ores and metalworking, all techniques presenting little evolution since the Roman empire.

Bishop Watson published in 1786 "Chemical Essays" with new interpretations of the "Historia Naturalis" by "Gaius Plinius Secundus" (Craddock, 1995).

On the second half of XIX century, John Percy published several studies with descriptions of the contemporary metallurgical processes and evolution of the smelting ores processing (Percy, 1861; 1864; 1870 and 1880 in Craddock, 1995).

The research about mines and prehistoric ores began only in the XX century. A reference work in this area was published in 1935 by Oliver Davis about the Roman mines in Europe (Davies, 1945 in Craddock, 1995).

Metallic artefact analysis had a significant development in XVIII century through the progress of chemical analysis. The first work in this area was done by Stanesby Alchorn in 1774 with the analysis of two BA swords from Ireland (Pownall, 1775 *in* Pollard, 2015). Other studies followed this pioneer chemistry work: gravimetric analysis of Greek and Roman copper coins (Klaproth, 1798 in Pollard, 2015), and BA artefacts from England and Ireland (Mallet, 1852 *in* Pollard, 2015). All these studies were included in a compilation of quantitative chemical analyses of archaeological copper alloy

objects, including the largest collection of 1250 analyses, presented by Baron Ernest Freiherr von Bibra in 1869 (Pollard, 2015).

The reference and addition of chemical analysis performed in metallic artefacts in an archaeological excavation report are the first significant collaboration between Archaeology and Chemistry. One of the first examples is the excavation report of "Nineveh and Babylon" in 1853, where H. Layard publishes bronze artefact analysis (Craddock, 1995).

The majority of the studies from this period mainly determine the artefact composition and technology applied in their production. Christian Thomsen first accomplished the search for a chronology of archaeological materials based on their composition, typology and excavation context in 1819 (Craddock, 1995). Thomsen chronologically divided the artefacts from the Danish national collection as belonging to the Stone Age, Bronze Age or Iron Age. In the mid-XIX century, J.E. Wocel suggested that the elemental composition of metallic artefacts could be related with their provenance and could also provide information about the period of production and function. Another author, Göbel, determined the probable Roman origin of copper artefacts from the Baltic region through comparison with other objects of known origin (Craddock, 1995). Therefore, the singular analysis of objects evolved to the establishment of sets of objects based on their elemental composition.

The development of archaeometallurgical studies provided Archaeology with new and relevant data originated from materials recovered from excavations. The innovative questions and approaches generated new insights into the archaeological record. The increased communication between different fields of knowledge has been highly productive to a better interpretation of the archaeological findings.

Alfredo Bensaúde published the first archaeometallurgical study concerning the chemical analysis of copper artefacts, demonstrating the existence of a Chalcolithic Period in Portugal contrary to the previous belief that Bronze Age followed the Stone Age for all Europe (Bensaúde, 1889).

In the XX century, the archaeometallurgical studies were significantly increased, with the development of faster analytical techniques that allow for smaller sampling quantities when compared to classical chemical methods. The growing interest in this research field contributes to the increase of archaeometallurgical studies, exploring several new analytical techniques, and leading to the development of new methodologies that aim to increase the information obtained from archaeological vestiges. The archaeometallurgical studies enable a better understanding of the technological development and the socio-economic organization of ancient communities (Montero, 1999).

Several non-destructive analytical techniques based on the emission of elements characteristic X-ray lines have been used in archaeometallurgical studies with the goal of determining the composition of archaeologic metallic materials: X-ray fluorescence, X-ray induced electron emission and thermal neutron induced analysis, particle induced X-ray emission, among others. When combining micro-analysis with some of these techniques, the elemental composition can be determined in reduced (micron-sized) areas of the artefacts (Bronk *et al.*, 2001). In the case of scanning electron microscopy,

the spot size can be smaller than 2 μm, allowing a compositional mapping and singularity determination in the studied area (Boyes, 2002).

With the advances in the analytical methodologies, archaeometallurgical studies aimed to go further the simple elemental characterization of the artefacts, correlating compositions with typologies and trying to identify the artefact provenance. Nevertheless, some previous archaeometallurgical studies, focused on the elemental characterization of artefacts and metallurgical remains, led to relevant results and important publications concerning the understanding of the early Iberian metallurgy. An important example of such studies is the analyses carried out by the project "Studienzu den Anfängen der Metallurgie" (SAM) (Junghans *et al.*, 1974, 1968, 1960) which represents the most complete set of quantitative chemical data of prehistoric copper artefacts from Europe, including artefacts from Portugal. The SAM programme quantitatively analysed more than 22,000 archaeological copper based artefacts using atomic emission spectroscopy to find similar compositional groups. Of this large dataset, 1700 analysed artefacts were recovered at the Iberian Peninsula (IP), including 88 artefacts from Vila Nova de São Pedro (VNSP) (Müller and Pernicka, 2009; Soares, 2005; Junghans *et al.*, 1974, 1968, 1960). A significant conclusion from this programme was that pure copper and arsenical copper were the dominant productions during Chalcolithic to Middle Bronze Age (MBA) in the Iberian Peninsula (Junghans *et al.*, 1968). A classification system was developed by Sangmeister to group artefacts according to their elemental composition, using a combination of three two-dimensional element diagrams (showing the contents of As-Ni, As-Bi and Sb-Ag) to define regional groups (Müller and Pernicka, 2009; Sangmeister, 1995). Based on a typological chronology Sangmeister concluded that pure copper was primarily used during the Early Chalcolithic while arsenical copper (As > 0.1 wt.%, according to this author) with low concentrations of other elements was used throughout the Chalcolithic. Arsenical copper with high concentrations of antimony, silver and nickel tended to occur in Late Chalcolithic (Müller and Pernicka, 2009; Sangmeister, 1995).

In another study, "Bronze Age Metalwork from the Iberian Peninsula", based on the metallic collection belonging to the British Museum, about 100 metallic artefacts were characterized regarding trace element patterns using atomic absorption spectrometry (Harrison and Craddock, 1981). A significant finding from this study, which also includes artefacts recovered in Portugal, was the observation of a correlation between artefact typology and arsenic content of the alloy. They observed that flat axes tend to consist of pure copper whereas Palmela points and daggers tend to show higher concentrations of arsenic (Harrison and Craddock, 1981).

In the same decade, another analytical programme called "Proyecto de Arqueometalurgia" was started in Spain. According to this programme, more than 10,000 analyses of Chalcolithic and BA copper artefacts were performed using X-ray fluorescence spectrometry in cleaned surface areas and complemented with metallographic analysis (Rovira and Gómez-Ramos, 2003; Delibes and Montero, 1999; Rovira *et al.*, 1997). This project has provided a comprehensive overview of the compositions and operational sequence involved in the production of artefacts of Chalcolithic and BA from Spanish territory. According to their findings, the arsenic content in the arsenical copper artefacts from the Chalcolithic period seems to most likely derived from the processed ores resulting in a "natural alloy" (Müller *et al.*, 2004; Rovira and Ambert, 2002b). Further studies of metallurgical remains showed that

4

a simple crucible smelting technology was primarily applied using rich oxide ores (Rovira and Ambert, 2002b).

In 2004, research projects was initiated by the German Archaeological Institute in cooperation with the Institute of Archaeometry (University of Mining and Metallurgy in Freiberg, Saxony) to chemically and mineralogically characterize the archaeometallurgical findings from Zambujal and other Chalcolithic sites of the Portuguese Estremadura, including VNSP. Several analytical techniques were used: X-ray fluorescence spectrometry and neutron activation analyses of ores, slags and copper objects, combined with lead isotope analyses and mineralogical analyses of ores, crucibles and slags (Müller and Cardoso, 2008; Müller and Soares, 2008; Müller *et al.*, 2007). This project aimed to evaluate the impact of the metallurgical activities in Chalcolithic societies. Recently, a valuable study resulting from this project added further insight to the primitive metallurgy in the Estremadura region (Gauss, 2015).

The project "Early Metallurgy in the Portuguese Territory - EarlyMetal" was initiated in 2010 by a research team comprising the Centro de Ciências e Tecnologia Nucleares (C2TN, IST–UL), Instituto de Nanoestruturas, Nanomodelação e Nanofabricação (CENIMAT/I3N, FCT-UNL), Departamento de Ciências dos Materiais (DCM, FCT-UNL) and several archaeologists. This project intended to investigate the metallurgical evolution from Chalcolithic to Late Bronze Age (LBA), including the transition to the Early Iron Age (EIA) (Orientalizing period) in the Portuguese territory. The analytical techniques used included X-ray fluorescence spectrometry in determining elemental composition, alongside with optical microscopy, scanning electron microscopy with X-ray microanalysis for microstructural characterisation and hardness and colour determination of the alloy. This project has provided a valuable characterization of metallurgical remains and artefacts recovered from archaeological sites all over the Portuguese territory with different chronologies and compositions, and consequent acquisition of relevant information on ancient metallurgy. This characterization included determination of elemental composition, determination of the involved manufacturing operations and the measurement of the artefact hardness (Valério, *et al.*, 2016a; Valério *et al.*, 2016c; Valério, 2012, Vidigal *et al.*, 2016; Figueiredo *et al.*, 2010). The present thesis was also included into this research project.

The development of lead isotope determination techniques allowed their application in provenance studies of several materials, including metals (Ciliberto and Spoto, 2000). The Pb isotope ratios ($^{208}Pb/^{204}Pb$, $^{207}Pb/^{204}Pb$ and $^{206}Pb/^{204}Pb$) depend mainly on the geologic age of the mineral deposit, and they are not changed with the metallurgical processes applied. Consequently, Pb isotope ratios are a suitable marker in provenance studies of metals.

The structural characterization of metallic materials can be obtained mainly by optical microscopy, scanning electron microscopy and X-ray radiography (Manzano and Herrero, 1998). Optical microscopy and scanning electron microscopy allow the microstructural characterization, which takes into account not only evidence left in the microstructure produced by casting, mechanical and heat treatments but also by subsequent corrosion processes (Balasbramaniam *et al.*, 2004; Sarabia-

Herrero *et al.*, 1996). X-ray radiography can reveal heterogeneities in the structure, such as internal voids and other defects.

In conclusion, the past decades of archaeological fieldwork and archaeometallurgical analysis have provided data on how the early metal production took place. With the increasing published characterizations of metal production and metalworking techniques, it is possible to compare information from different sites and to explore local or regional innovations that occurred during the spread of metallurgical technology. Furthermore, whenever possible, these changes must be placed back into their wider social context and related to contemporaneous transitions in other technological and cultural practices (Roberts *et al.*, 2009). For instance, the earliest metal objects and tools did not necessarily replace or were superior to existing tools made of flint, bone or wood. Moreover, these materials continued to be used alongside with metal for thousands of years. These observations support new theories arguing that appearance of metallurgy derived from possible socio-cultural status and aesthetics reasons rather than necessity (Smith, 1981).

1.2. ORIGINS OF METALLURGY

Despite the evidence that prehistoric man worked native metals since the Neolithic, metallurgy is considered to start only when the smelting of ores was accomplished to obtain the metal.

The use of blue and green copper ores for beads, pendants and pigments was registered in early agro-pastoral Neolithic communities (11th-9th millennia BC) in Southwest Asia, at sites such as Shanidar Cave, Zawi Chemi (North-Eastern Iraq), Hallan Çemi (Eastern Turkey) and Rosh Horesha (Israel) (Roberts *et al.*, 2009; Bar-Yosef Mayer and Porat 2008; Yener, 2000). Artefacts made of native copper have also been found in Southwest Asia long before the application of fire to naturally occurring metals (Roberts *et al.*, 2009) (Figure 1.1, a).

It is only in the subsequent millennia that the application of heat in a controlled reducing atmosphere led to the smelting of metallic ores to produce metal (Roberts *et al.*, 2009). The earlier copper artefacts known are some beads, awls and fishhooks from Çayönü Tepesi (Eastern Turkey), where metallographic analyses have shown evidence of annealing c. 8000 BC (Maddin *et al.*, 1999).

The composition of the metal obtained by the primitive processes of ore copper smelting is similar to the melted native copper, and it is often complicated to distinguish between them. Therefore it is difficult to indicate when the intentional smelting of the first copper ores started.

According to the work of Renfrew (1973), the beginning of the extractive metallurgy was attributed to the Middle East during the 6th-5th millennium BC, but it was only during the 4th millennium BC that it started to present a real importance to those ancient communities. The earlier evidence of ore smelting in the Middle East was recognized to the slags from Çatalhöyök (Turkey) 6500 BC (Hauptmann, 2007). In Europe, a more recent study documents the earliest evidence of copper smelting at Belovode (Serbia), a Vinča culture site from the end of the 6th millennium BC (Radivojević *et al.*, 2010).

Many debates have been carried out on how the spread of the metallurgical processes throughout Europe have occurred. Did copper smelting appeared simultaneously or there was a single central region of invention followed by a spread of knowledge? Evidence of copper smelting found throughout Southwest Asia, and Southeast Europe seems to support the hypothesis of a spread of the metallurgical processes invention from the central region of Anatolia (Figure 1.1, b) (Roberts et al., 2009; Thornton, 2001).
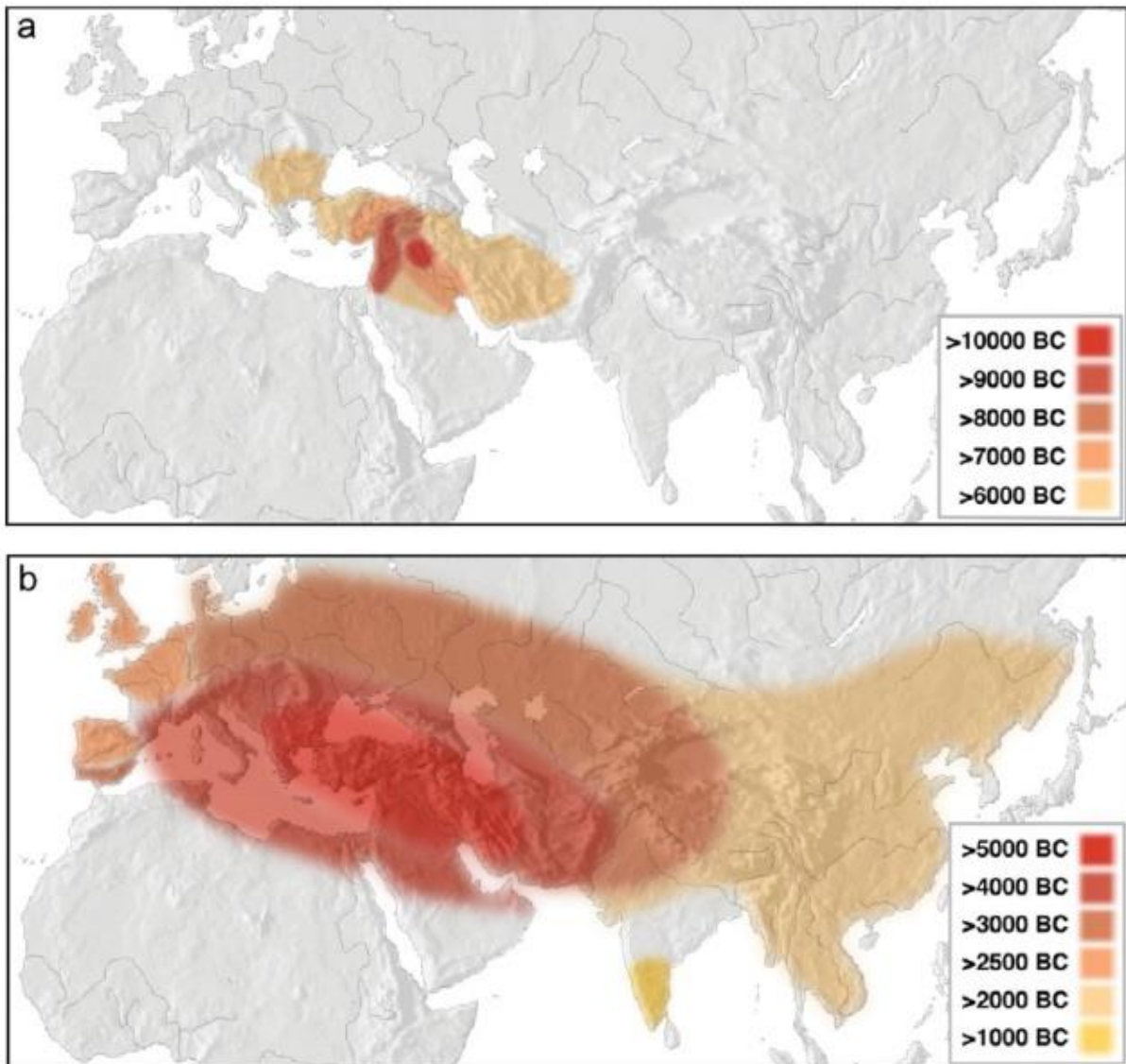
Figure 1.1. a) Exploitation of copper ores and naturally occurring copper metal; b) The spread of copper smelting technology (Figure from Roberts *et al.*, 2009).

1.3. THE CHALCOLITHIC METALLURGY

The following sections describe the most relevant characteristics of primitive metallurgical processes and metallurgical production remains like those studied in this thesis, namely crucibles, metallic nodules and slags. Also, provide some insight about arsenical copper alloys and the Chalcolithic in the IP.

1.3.1. Primitive metallurgical processes

The beginning of metallurgy is considered to have started when the prehistoric man was able to extract metal from the ore by a smelting process. Smelting is accomplished by heating the ore in a reducing atmosphere. The impurities present in the ore, alongside with the products that result from the reactions of the ore with the crucible fabric and wood or charcoal used as fuel will originate a slag. The metal should be separated from the slag during or after the ore reduction. However, the first metallurgical processes did not achieve sufficiently high temperatures and reducing atmospheres to obtain a low viscosity slag (Rovira, 2016).

The ore reduction would be made in simple shallow open forms of ceramic crucibles. The crucible would be placed directly on the ground or at the bottom of small holes, and the heating would be accomplished from the top of the crucible (Ortiz, 2003; Rovira and Ambert, 2002a).

Ancient crucibles were usually made with materials sufficiently refractory that do not break at high temperatures and are chemically inert, not reacting with metal oxides and alkalis from the fuel ash (Bayleys and Rehren, 2007). Crucibles were heated from the top, covered with wood or charcoal and presented walls several millimetres thick to withstand the high firing temperatures required during metallurgical operations and reduce heat transfer (Rovira, 2004). In that way, the underside of the crucible would remain relatively cool (Bayleys and Rehren, 2007). Extensive vitrification and alteration of the rim and inner surface of the crucible would occur while the outer surface would remain unaltered. Therefore, crucibles are reaction vessels whose contents undergo a variety of chemical and physical changes (Bayleys and Rehren, 2007). Since these ancient crucibles were possibly used for smelting the ores and melting the obtained metal, different types of residues can be found. The study of these metallurgical residues, resulting from the reaction of the ore or metal with the crucible wall and the wood or charcoal used for heating, allow identification of the type of metallurgical operation: smelting or melting.

Slags resulting from reactions between ore, the crucible fabric and wood or charcoal used as fuel are mainly composed of complex silicates. Slag analyses can always be a useful tool in reconstructing ancient metallurgical processes. An important chemical characteristic of the ancient smelting slags is the compositional heterogeneity due to the presence of all transitional stages between the thermal decompositions of the ores up to the metal phase's formation since the whole slag is not fully molten (Haupmann, 2007). The atmosphere and temperature conditions should vary with time and along the smelting volume (Rovira and Ambert, 2002b). If the atmosphere is not reducing enough, the iron

minerals present as impurities in the ore are not reduced to their metallic form and are not incorporated in the metallic copper. Consequently, the artefacts produced with copper obtained by these processes present very low iron content (< 0.05 wt.% Fe) (Craddock and Meeks, 1987).

 In several cases, it is possible to identify these early slags originated from the different operations since smelting slags tend to be richer in iron oxides and silicates than melting slags, and melting slags sometimes incorporate wood or charcoal ash (Tylecote, 1992).

In later slags, iron silicates are a common constituent. However, the poor reducing conditions and low temperatures achieved within the reaction vase during the earlier smelting operations prevent the formation of a fayalitic slag (Craddock, 1995). Fayalite (Fe_2SiO_4) is the most common mineral in later slags, and its presence or absence can give indications about the conditions of the process in question. For instance, since in fayalite the oxidation state of iron is lower (Fe^{+2}), the presence of magnetite (Fe^{+2} and Fe^{+3} oxidation states) indicate a lower reducing atmosphere in the reaction vessel (Hauptmann, 2007). However, the metallurgical processes in the origin of these fayalitic slags were introduced considerably later during the 1st millennium BC (IA) (Rovira, 2002).

The resultant high viscosity of these immature slags causes the entrapment of several metallic prills. The prehistoric man would have to crush the slag into pieces and manually collect the metallic pieces embedded in it and, afterwards, melt in another crucible (Ortiz, 2003). Although slag vestiges are a crucial indicator and evidence of early copper smelting activities, they are relatively small in size and quantity, therefore easily overlooked in the archaeological excavations. The resulting small amount of slag produced could be explained if high yield ores, namely copper oxides and carbonates were used in the smelting process.

In the Iberian Peninsula, there are vestiges of the application of this rudimentary smelting process from the Chalcolithic to the IA (Rovira, 2002). The reasons that lead to this primitive process of ore reduction in the IP are possibly related to two factors:

- This method is effective when applied to the copper oxides and carbonate ores, frequently used in this region with easily obtained high yields of copper (Figueiredo *et al.*, 2010; Rovira, 2002);
- During Chalcolithic and BA, the metallurgy in this region is mainly domestic and small scale (Rovira, 2016; Senna-Martinez and Pedro, 2000). In this context, the economic efficiency would not be significant (Ruiz-Taboada and Montero-Ruiz, 2000).

Metallic nodule is a term used in this study which comprises metallic vestiges with more rounded edges regardless of its size and origin. In this case, metallic nodule could be prills found trapped in the slag or crucible lining or a melting or casting droplet. These vestiges can be very helpful to understand the metallurgical processes that originated them. For example, the elemental composition of the metallic nodule gives an indication of the type of metal or alloy being worked by the ancient metallurgist. The microstructure present in these remains can suggest the origin of the nodule. For instance, a smelting prill, cooled inside the slag mass or attached to the slag inside the crucible would present a microstructure related to a slow cooling rate (coarse microstructure). On the other hand,

9

melting or casting droplet should exhibit a high cooling rate structure (finer dendritic structure), since it was a small portion of metal cooling in direct contact with air.

1.3.2. Arsenical copper alloys

Metallic alloys can appear in Nature. For example, gold can be found associated with silver in a natural alloy called *electrum*. Native copper is, in the majority of the cases, quite pure but can also be associated with silver or arsenic. The natural alloy of copper with arsenic can exceptionally present up to 15% of arsenic (Mohen, 1990). The prehistoric man would have recognized the advantages that these materials presented and, at some point in time, he would start to fabricate the different alloys. Would be arsenical copper alloys intentionally produced? The innovation of an alloy is that exhibits different properties when compared to the individual components. The enhanced mechanical properties, as higher hardness and different coloration of the prehistoric alloys, would be certainly the most noticed and appreciated qualities in these materials, although other advantages are also discussed in the following paragraphs.

Metallic copper is a material with relatively low hardness even after a hammering processing. However, the presence of a small quantity of arsenic introduces significant modifications in the material like increased hardness and greater workability. The hardness of an arsenical copper alloy can be significantly increased by work hardening, such as cold hammering (Figure 1.2, Left).

The arsenic addition equally increases the solidification temperature range of the cast metal, increasing its castability (with the decrease of liquidus temperature). On the other hand, the increment of hardness can make arsenical copper alloys more brittle and difficult to work although some authors state that brittleness is relatively absent until the arsenic level exceeds 10-13% (Budd and Ottaway, 1995). In the earlier studies, it was suggested that the introduction of copper alloyed with arsenic (As content ≥ 2 wt.%) was a metallurgical innovation (Craddock, 1995). In the case of copper and arsenical copper alloys, a significant increase in hardness with increasing arsenic content, especially above 2 wt.%, is observed due to solid solution hardening (Northover, 1989; Budd and Ottaway, 1995). However, as displayed in Figure 1.2, Left, the addition of arsenic to copper significantly improves the mechanical properties of the metal by work hardening up to approximately 8 wt.%, which is rarely found in ancient artefacts (Lechtman, 1996).

The high solidification range in this type of alloys, increasing the arsenic segregation effects, contributes to a heterogeneous distribution of this element in the alloy, which makes difficult to predict the material macroscopic properties only based on its average composition. The irregular distribution of arsenic can result from cored as-cast alloys, later worked producing banded structures (wrought alloys) or from inverse segregation developed during the solidification, with an arsenic enrichment at the surface of the artefact (Campbell, 2003).

Accordingly to the Cu-As phase diagram (Subramanian and Laughlin, 1988) the α-Cu phase can dissolve up to approximately 8 wt.% (7.96 wt.%) of arsenic in equilibrium conditions, before the

formation of the As-rich phase γ phase (Cu_3As) (see Figure 1.2, Right). However, due to the relatively fast cooling rates of conventional casting, this γ phase has been observed in alloys with only 2 wt.% As, suggesting the inability of ancient metallurgists in homogenising the alloy (Northover, 1989). Also, earlier studies concerning ancient arsenical coppers also indicate that the annealing was conducted at temperatures of about 300-400ºC (Northover, 1989). This range of temperatures is noticeably lower than the temperature necessary to homogenise this type of alloys (~600–700ºC) in a reasonable time. Moreover, the segregated microstructures could require an even higher temperature to be homogenized (Budd, 1991).
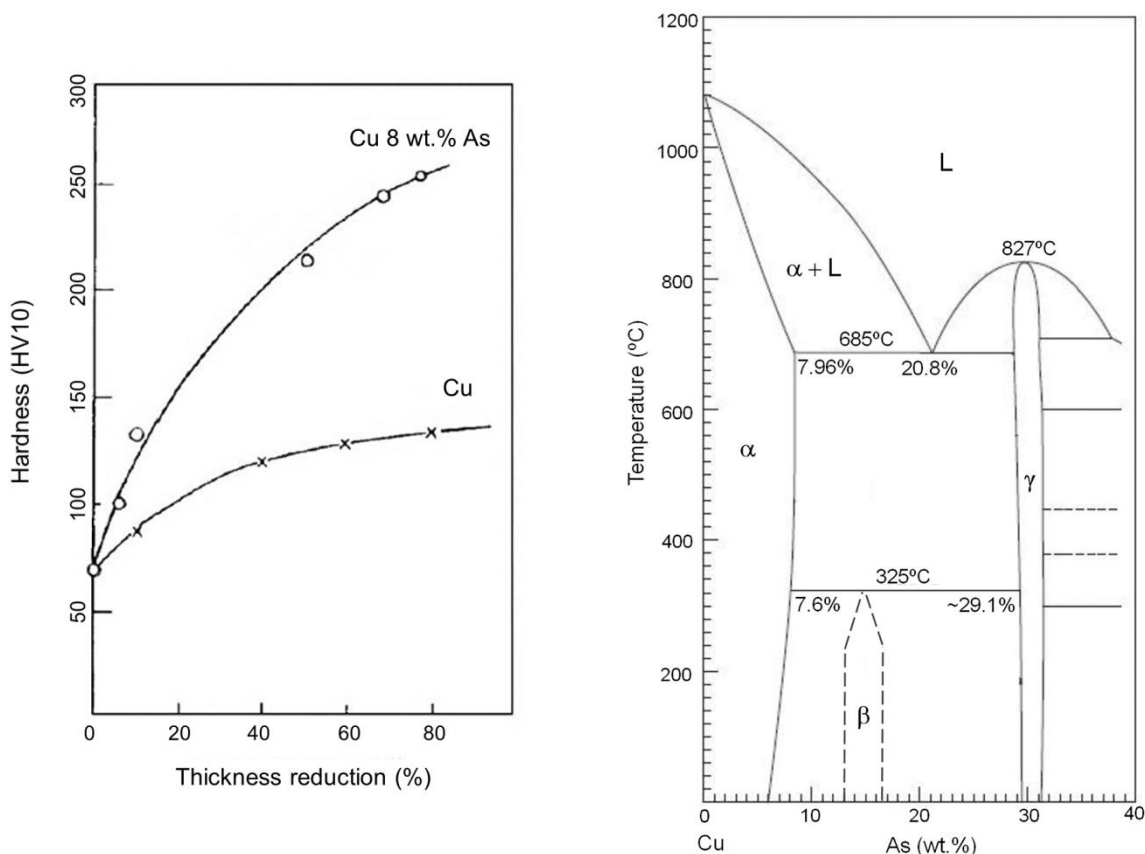
Figure 1.2. Left: Hardness increase of copper and arsenical copper alloy by cold hammering in function of thickness reduction (Adapted from Coffyn, 1985); Right: Section of Cu-As phase diagram in equilibrium conditions evidencing the formation of arsenic-rich γ phase in arsenic richer contents of the alloy (adapted from Subramanian and Laughlin, 1988).

In addition to the beneficial mechanical properties, arsenical copper alloys could have been produced for aesthetic reasons since this alloy presents a distinct colour from pure copper. Arsenic-rich prills are distinctive for their shiny silvery colour, which makes them easy to identify and select (Merkel *et al.*, 1994). A colour difference is clearly visible between prills with as little as 1 wt.% arsenic and prills without arsenic, allowing the separation of prills based on their composition. Therefore, they could have been selected and cast according to the desired colour for the artefact.

The simplest process to produce an arsenical copper alloy would be the reduction of copper ores rich in arsenic, relatively common in Portuguese territory (Ortiz, 2003). The loss of arsenic during the

smelting process of the ore, resulting from the volatility of this metal, is compensated by its high affinity to copper. Therefore, part of the arsenic is retained in the metallic copper, forming an arsenical copper alloy. Smelting experiments had demonstrated that it is possible to obtain arsenical coppers from ores with low arsenic content (Hanning *et al.*, 2010; Hauptmann, 2007).

In the case of copper oxides with arsenic, the process could be conducted through the direct reduction of the ore in reducing conditions (the generic ores formulation in the Reaction 1.1 is not stoichiometric) (Lechtman and Klein, 1999).

$$CuAsO_4 + 4CO \rightarrow (Cu,As) + 4CO_2\uparrow \qquad \text{Reaction 1.1}$$

Copper arsenate   *Cu-As alloy*
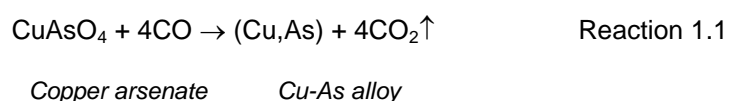
1.3.3. Chalcolithic in Iberian Peninsula

In the Iberian Peninsula (IP) the first metallurgical evidence occurs in south-east Spain territory. It is a copper slag fragment dating back to the Neolithic period (first half of the 5th millennium BC) found in the archaeological site of Cerro de Virtud (Almería, Spain) (Ruiz-Taboada and Montero-Ruiz, 1999). However, this slag fragment is isolated evidence since in this region the earliest copper artefacts and other metallurgical vestiges occur only during the 4th millennium BC, almost one millennium later (Montero-Ruiz, 1994; 2005; Roberts, 2008).

At the end of the 4th and beginning of the 3rd millennium BC, several archaeological sites with evidence of metallurgical activity, appeared in the IP. According to Renfrew and Bahn (1991), these metallurgical activities have been recognized as belonging to the beginning of copper metallurgy, suggesting that IP was an independent centre of metallurgical production.

In the Portuguese territory, the earliest sites with evidence of metallurgy correspond to most of the 3rd millennium BC, Chalcolithic, namely around 3000-2250 BC (Cardoso and Soares, 1996; Soares and Cabral, 1993). A shapeless and very pure copper artefact was recorded at Atalaia do Peixoto (Serpa, Portugal) during a surface prospection alongside with a collection of materials attributed to the Late Neolithic/Early Chalcolithic (Soares *et al.*, 1996). However, the metallographic analysis of the fragment revealed twin grains and deformation bands suggesting the understanding of a long chain production processing (hammering followed by annealing with a final hammering). This analysis indicates a more evolved metallurgy than the registered for that time, possibly Chalcolithic, but not compatible with the chronology assigned to the site (Soares *et al.*, 1996).

The Portuguese Estremadura is an important region concerning the beginning of Chalcolithic metallurgy in the IP due to the existence of impressive large settlements with evidence of metal production (Müller and Soares, 2008; Cardoso, 2000; Soares *et al.*, 1996; Soares and Cabral, 1993). In this region, several Chalcolithic settlements have been extensively excavated. It is the case of Vila Nova de São Pedro (VNSP) (Azambuja), Moita da Ladra (ML) (Vila Franca de Xira), Zambujal (Torres Vedras), Leceia (Oeiras) and Outeiro Redondo (OR) (Sesimbra) (Cardoso *et al.*, 2010/2011; Cardoso and Caninas, 2010; Soares, 2005; Kunst and Uerpmann, 2002; Cardoso, 2000; Sangmeister, 1973)

(Figure 1.3). Some of these prehistoric communities, namely VNSP, Zambujal and Leceia, at the final of the 4th millennium BC, suffered significant socio-economic transformations, other than metallurgy, that defined the transition from Neolithic to the next stage, designated Chalcolithic.

The Chalcolithic metallurgical production is characterized by a relatively reduced artefact typological diversity. The majority of artefacts typologies included relatively simple and flat forms, namely: plain axes, awls, chisels, hooks, saws, knives, daggers and arrowheads (Ferreira da Silva *et al.*, 1993).

The Iberian archaeological sites with the earlier evidence of copper metallurgy present both copper and arsenical copper artefacts, suggesting that copper does not precede arsenical copper alloys (Ruíz-Taboada and Montero-Ruíz, 1999). The first metallic artefacts were composed of copper with varying contents of arsenic, and this characteristic was present for more than a millennium (~3000–1200 BC) (Valério *et al.*, 2014; Rovira, 2002).

In the Southern Portugal, an increased number of arsenical copper artefacts occur mainly in the Late Chalcolithic and Early Bronze Age (EBA) coincident with the Bell Beaker period (Valério *et al.*, 2016; Soares *et al.*, 1994). The Bell Beaker culture emerges in this region in the transition from the 2nd to the 3rd quarter of the 3rd millennium and ends in the first quarter of the 2nd millennium BC (Valério *et al.*, 2016; Mataloto *et al.*, 2013). This culture is characterized by new forms and decoration of pottery, and by significant transformations involving not only copper metalwork with the appearance of novel artefact forms like tanged daggers and Palmela points but also with the first production of gold artefacts. Alongside with those technological innovations, new funerary rituals appear namely individual burials (Valério *et al.*, 2016c, Roberts, 2008; Cardoso *et al.*, 2003). The EBA maintains the Bell Beaker tradition, especially the predominance of copper and arsenical copper artefacts (Valério *et al.*, 2016).
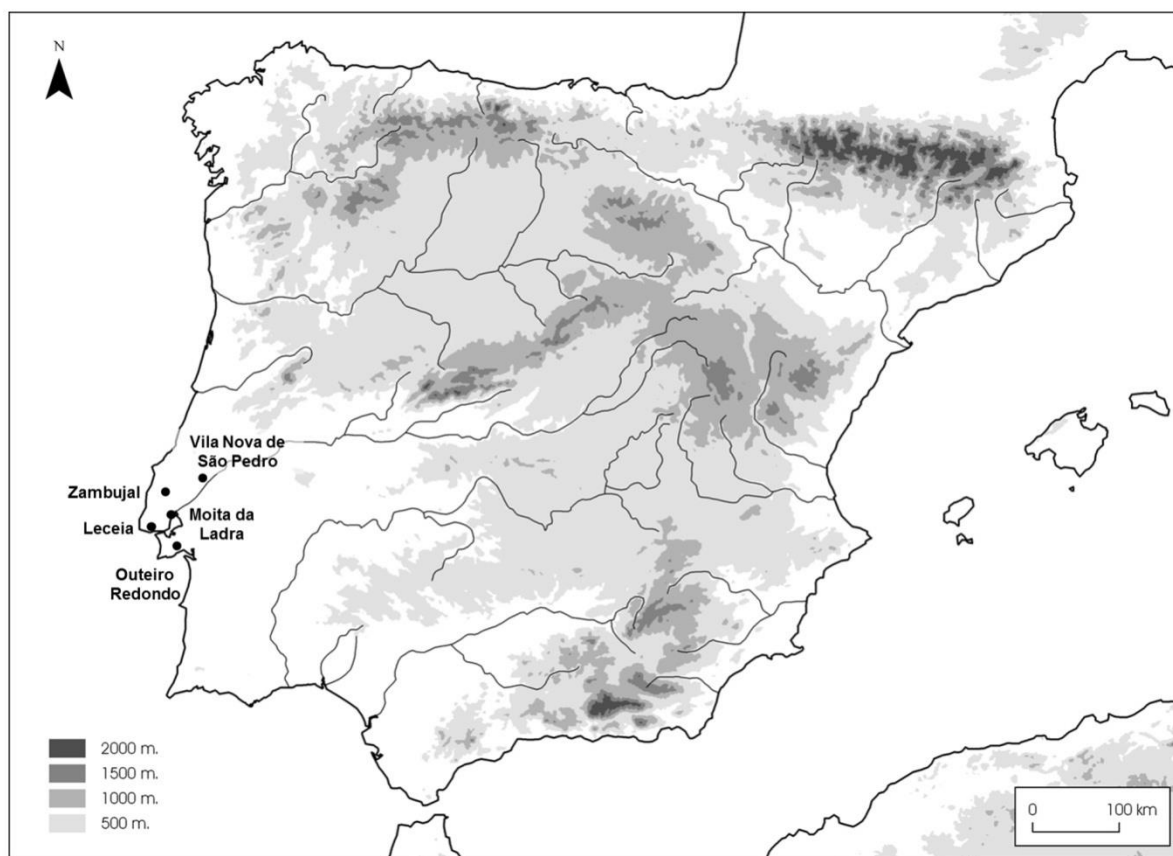
Figure 1.3. Localization of Chalcolithic settlements in Portuguese Estremadura: VNSP, ML, OR, Leceia and Zambujal.

Chalcolithic copper artefacts from VNSP analysed by the SAM project (Junghans *et al.*, 1974, 1968, 1960) exhibit a distribution of arsenic contents, resembling the "natural distribution" of minor and trace elements in minerals (Müller *et al.*, 2007). This evidence suggests that the arsenic content could not be an intentional addition, instead resulting from its natural variability in the copper ores exploited. However, as described in the subchapter 1.3.2, it is possible that ancient metallurgists recognized some properties of arsenical copper alloys such as higher hardness, better castability or different colorations. For example, Palmela points, saws, long awls and tanged daggers are the typologies with higher arsenic content at the Chalcolithic settlement of Zambujal (Müller *et al.*, 2007). In another study, a statistically significant association was found between copper alloyed with arsenic and artefacts classified as Weapons (arrowheads, daggers and knives) identified at the Chalcolithic settlement of VNSP, suggesting an intentional selection of alloys (Pereira *et al.*, 2013a). The same study also suggested that the colour of the alloy and not the hardness was most likely the criteria of choice for the alloy.

In the case of an intentional production of arsenical copper alloys, the arsenic concentration in the metallic alloy could be accomplished by selecting the ores rich in this element or selecting the resulting smelting metallic nodules based on their coloration.

The provenance of the arsenic, the technological choices involved in the production of an arsenical copper alloy and how it was recognized and finally used, intentionally or not, are all important issues to be considered and to take into account when analysing the arsenic distribution in prehistoric alloys.

The chronological period corresponding to the use of arsenical copper alloys was relatively large, and this alloy was substituted by tin alloyed with copper (bronze). There is evidence of arsenical copper alloys (As ≥ 2 wt.%) use during the 3rd and 2nd millennium BC (Chalcolithic and MBA) (Soares *et al.*, 1996). Bronze alloys were progressively introduced in the Portuguese territory during the MBA. The introduction of this new type of alloy appears to have gradually occurred from the north to the south of Portugal. The late introduction in Estremadura and southern regions could be a result of a strong regional Chalcolithic tradition (Cardoso, 2002).

In this thesis, metallurgical collections from three Chalcolithic settlements, VNSP, ML, and OR were studied. In spite of the extraordinary importance of the recovered metallurgical related materials, only a few studies have been carried out considering the copper and arsenical copper artefacts and metallurgical remains discovered at these settlements. Concerning VNSP, an earlier study was published in 1952, presenting the elemental composition of few metallic objects found at this site (Paço and Arthur, 1952). Other studies carried out by Paço were mainly concerned with descriptions of artefacts (Paço, 1955, 1964). Also, the SAM programme quantitatively analysed 88 copper-based artefacts and metallurgical remains from VNSP using atomic emission spectroscopy (Junghans *et al.*, 1974, 1968, 1960).

More recently, a study from VNSP metallurgical collection included a set of 15 copper prills and molten copper scrap (Müller and Soares, 2008) where, for the first time, lead isotope ratios were used for a provenance study in the region. Results from this study indicate that the lead isotope ratios of ore deposits from the Ossa Morena Zone (OMZ) present the best correlation to the lead isotope signatures of VNSP copper artefacts (Müller and Soares, 2008).

Another recent study from VNSP included a set of 53 copper-based artefacts, mostly in a fragmentary condition (Pereira, 2011) and was included in the present thesis.

On the other hand, ML and OR settlements have previous studies regarding the chronologies obtained through radiocarbon dating and archaeological studies concerning the description of structures and site stratigraphy (Cardoso *et al.*, 2010/2011; Cardoso and Caninas, 2010).

1.4. THESIS OBJECTIVES

The aim of this study is to understand the early metallurgical technology that took place in the Portuguese Estremadura during the Chalcolithic period. In order to clarify the first steps of the metallurgical production in this region and to bring novelty to the previous studies mentioned above, it was proposed for the metallurgical collections of VNSP, ML and OR:

- Elemental and microstructural characterization of copper-based artefacts, materials used in the metallurgical process like crucibles and other sub-products, namely slags and metallic nodules.

- Determination of alloys composition and assessment of arsenic content in copper-based artefacts to investigate possible correlation with artefact typologies, functions and correlation with thermomechanical processing applied. Such determinations allow to evaluate the intentionality in the use of arsenic and if the metallurgists acknowledge the advantages of arsenic addition in the artefact properties.

- Determination of thermo-mechanical operations involved in the production of artefacts (the so-called "châine opératoire").

- Measurement of the artefact hardness and colour to understand the metal selections of the Chalcolithic metallurgist.

- Evaluation of the metallurgical productions of VNSP, ML and OR regarding the distribution of arsenic content and fraction of arsenical copper artefacts. This assessment was extended to other collections recovered from nearby contemporary sites from Estremadura region and important settlements of other regions (Southern Portugal and Western Andalusia).

A more comprehensive understanding of these materials and prehistoric metallurgy also give valuable insights to the conservation of ancient metals.

1.5. THESIS OUTLINE

The present thesis has been organized in seven chapters. Chapter 1 presents the historical context and state of the art of the topics covered through the thesis, followed by the description of the collections analysed, study design and methodologies used in Chapter 2.

The collections were divided into production remains, that included crucibles, slags and metallic remains and copper-based artefacts. Chapters 3 to 5 describe the archaeometallurgical studies performed in the production remains, and copper-based artefacts from VNSP collection (Chapter 3), ML collection (Chapter 4) and OR collection (Chapter 5).

Chapter 6 presents an overall discussion of all the data obtained from the settlements studied.

The final Chapter 7 presents the last conclusions and future perspectives to be considered in archaeometallurgical research.

2.   MATERIALS AND METHODS

2.1. MATERIALS

The metallurgical collections from three Chalcolithic settlements, VNSP, ML, and OR, were studied (Figure 2.1). A greater focus was given to the large metallurgical collection of VNSP currently deposited in the Museu Arqueológico do Carmo (Arnaud and Fernandes, 2005). Unfortunately, it is not possible to match the recovered materials to the respective stratigraphy due to the absence of detailed field notes from the early excavations performed in VNSP. On the other hand, the collections from ML and OR have well defined archaeological contexts and more detailed archaeological excavations reports with the stratigraphy and corresponding chronology. Despite the smaller number of items in these two last collections, they are very useful for comparative analysis of the metallurgical production between settlements.

The important metallurgical collections of these three sites, including crucibles, slags, metallic nodules and artefacts, are rather valuable for understanding the early metallurgy in the Portuguese Estremadura.
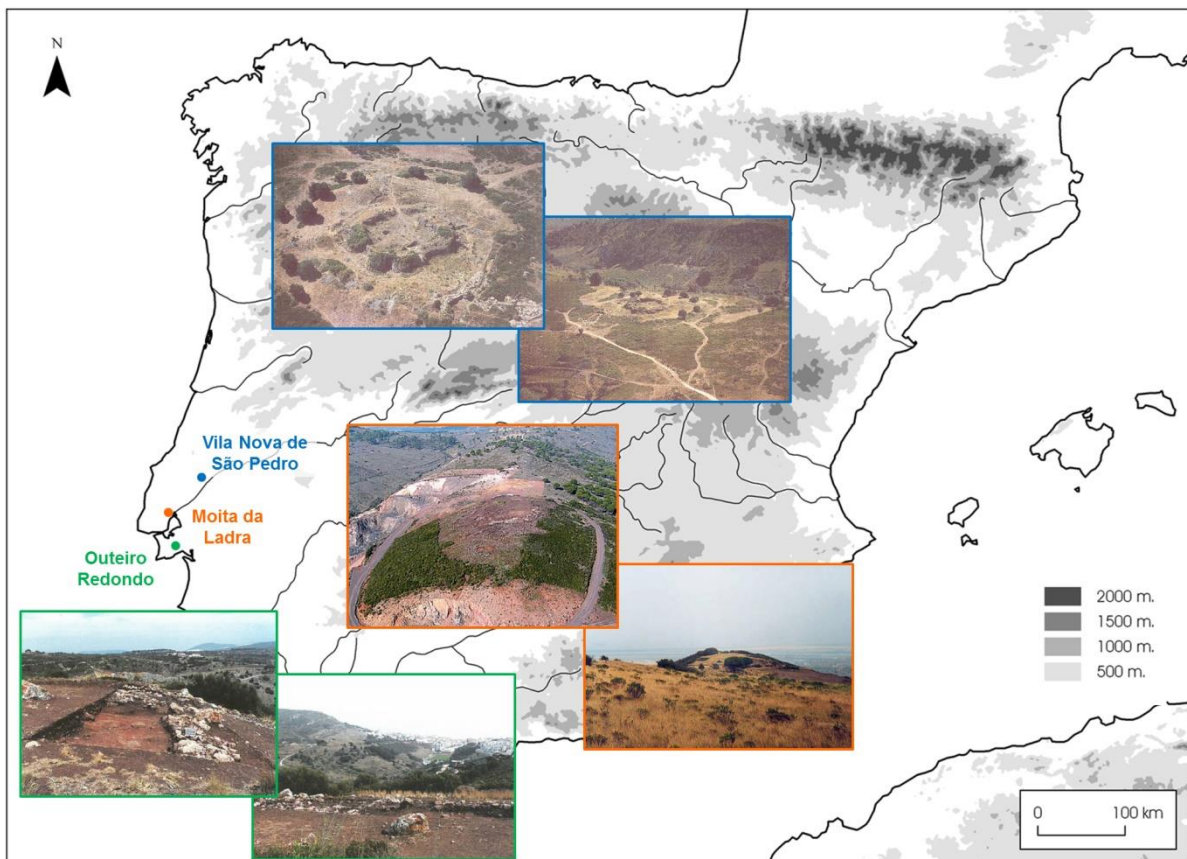
Figure 2.1. Localization of the studied Chalcolithic settlements in Portuguese Estremadura and corresponding photographies: Arnaud and Fernandes, 2005 (VNSP); Cardoso and Caninas, 2010 (ML); Cardoso *et al.*, 2010/2011 (OR).

17

The archaeometallurgical collections analysed in the present study were divided into production remains and metallic artefacts. Production remains include all materials that resulted from the metallurgical production processes namely smelting vestiges like slag fragments, all sorts of metallic nodules, like prills and droplets, and crucible fragments. No ore fragments were studied, since only small pieces of limonite with traces of malachite were found at VNSP, and these had been already analysed (Müller and Soares, 2008).

Metallic artefacts, mostly in fragmentary condition, were grouped into object categories, namely awls, wires, chisels, axes, daggers, arrowheads, fishhooks, knives, spatulas and saws. Copper ornaments are absent in these Chalcolithic contexts. The scarcity or absence of copper ornaments in Chalcolithic contexts may suggest that this material did not possess a prestige value suitable for ornaments. Ornaments in these cases were predominantly made of gold or non-metallic materials (Murillo-Barroso and Montero-Ruíz, 2012). Some of the fragments were considered to be unclassifiable due to the small size and shapeless. Other fragments show intentional sectioning (like several axe cutting edges) and might be scraps from the manufacturing process or parts of ingots, put aside for posterior re-melting or shaping into smaller objects (Müller and Soares, 2008). Parallels of this intentional sectioning process can be found in other settlements like Leceia (Cardoso and Guerra, 1997/1998).

The classes of artefacts were grouped according to their probable utility yielding the following functional categories: "Tools", "Weapons" and "Axes". Axes could be used either as tools or ingots (Soares, 2005). The group of "Tools" includes artefacts that could be used in domestic and production activities (awls, chisels, saws, spatulas, knives and fishhooks). On the other hand, the group of "Weapons" includes objects that could be used in war or for social prestige (daggers and arrowheads) (Caramé et al., 2010).

The extensive collection of 570 metallurgical remains from VNSP was narrowed down to a set of items selected for a more detailed analysis: 17 crucible fragments, 15 pieces of slag and 147 metallic nodules. The selection of the crucibles, slags and metallic nodules resulted from a preliminary visual inspection, magnet response for ferromagnetic properties (indicative of magnetite presence in slags) and from the EDXRF analyses of the complete set (compositions are presented in Appendix I). Materials with a higher iron content evaluation, darker remains (black or dark grey) than the other items, and sometimes with small green spots at the surface (suggesting the presence of copper) or with organic adherent vestiges like charcoal and apparent lower density, were also selected from the initial collection.

The metallic nodules were chosen in order to include several morphologies. Preference was given to spherical forms and visible porosities (possibly associated with smelting operations) and to droplet or splashed shapes (eventually drops resulting from melting or casting operations). By EDXRF analyses it was possible to make an estimated evaluation of the arsenic content of the selected metallic nodules, in spite of the corrosion products influence. Quantitative elemental determination by micro-EDXRF was performed on this selected set of 147 metallic nodules (results are presented in Appendix II).

The metallic nodules from ML collection followed the same procedure of the VNSP collection. In this case were only identified eight nodules of spherical form and with a porous surface. In OR collection, no nodules were present, only artefacts, fragments of artefacts and one crucible fragment.

The final selection included a total of 188 metallurgical remains and 169 artefacts from the three Chalcolithic settlements from the Portuguese Estremadura (Table 2.1).

Table 2.1. Number of production remains and artefacts studied from each settlement.

Settlement	Metallurgical remains			Artefacts	Total
	Crucible fragments	Slag fragments	Metallic nodules		
Vila Nova de São Pedro	17[a]	15[a, b]	147[a]	95 (58[c])	274
Moita da Ladra	-	-	8	62	70
Outeiro Redondo	1	-	-	12	13
Total	18	15	155	169	357

[a] Set selected from the VNSP initial collection (570 metallurgical remains) after EDXRF analysis.
[b] Set includes two slags attached to crucibles.
[c] 58 artefacts from VNSP were previously studied (Pereira *et al.*, 2013a).

The artefacts collections were grouped in object categories for each settlement (Table 2.2).

Table 2.2. Typology and number of artefacts studied from each settlement.

Settlement	VNSP	ML	OR	Total
Awls	12 (11[a])	9	1	22
Wires	3 (2[a])	-	-	3
Fishhooks	-	-	2	2
Chisels	17 (12[a])	3	-	20
Saws	4 (1[a])	1	4	9
Sickle	1	-	-	1
Spatula	1	1	1	3
Knife	1	-	-	1
Daggers	15 (8[a,])	2	-	17
Arrowheads	5	2	-	7
Palmela points	4	1	-	5
Axes	27 (19[a])	4	-	31
Socket	1[a]	-	-	1
Unclassifiables	4[a]	39	4	47
Total	95	62	12	169

[a] Artefacts from VNSP were previously studied (Pereira *et al.*, 2013a).

2.2. METHODS

The methodology used in this study comprises non-invasive and microanalytical techniques due to the archaeological and museological importance of the items of the analysed collections. Applied techniques imply a careful selection of artefacts and metallurgical production vestiges taking into account aspects such as archaeological significance, typology and conservation condition.

Energy Dispersive X-Ray Fluorescence Spectrometry (EDXRF) was used for a qualitative approach concerning the elemental composition of the metal without any previous surface preparation. However, quantitative elemental determination involves the removal of the superficial corrosion in a very small area or careful sectioning (with a minimum impact on the object) of a small sample to be mounted in an epoxy resin.

It is important to keep in mind that the archaeological copper-based artefacts and metallurgical remains present a characteristic corrosion layer that depends on the burial conditions. The corrosion products layers are enriched or depleted of some elements, due to different electrochemical potentials and corrosion products stabilities of the metal constituents (Robbiola and Portier, 2006). Also, some components of the soil where the artefact was buried can be incorporated in the corrosion products. As a result, the elemental composition of archaeological copper-based objects will usually be different if determined directly on the surface or in an area cleaned of corrosion products. Therefore, macro-EDXRF was used to identify the main metal constituents, but these results can only be considered indicative due to the significant influence of the superficial corrosion layer.

Micro-Energy Dispersive X-Ray Fluorescence Spectrometry (micro-EDXRF), Optical Microscopy (OM), Scanning Electron Microscopy with Energy Dispersive X-ray spectroscopy (SEM-EDS), micro-X-Ray Diffraction (micro-XRD), Colorimetry and Vickers micro-hardness testing analytical techniques were applied after a simple sample preparation (removal of superficial corrosion or resin mounted sample).

The advantages of sampling selected artefacts, if this operation is made carefully and well designed, far outweigh the disadvantages, allowing more possibilities of analysis and consequently more relevant information collection. The removal of samples from artefacts is performed when it does not affect its visual interpretation, usually an incomplete artefact, but with a metallic core and in a stable condition. Polished samples mounted in the resin are much easier to handle and sometimes less dangerous for the artefact when compared to dealing with a localized polished area in the artefact itself. Nevertheless, sometimes the latter is the only option available to study the composition of an object. Descriptions of sample preparation and details of instrument setup will be presented in the following sections. Also, the theory concerning each analytical technique will be briefly discussed in the following paragraphs.

Artefact collections were analysed by micro-EDXRF to determine their elemental compositions quantitatively. Next, the majority of the copper-based artefacts were characterized by OM observations allowing the identification of different phases, inclusions and the thermomechanical processes applied during the artefact production (operational sequence or "chaîne opératoire"). The

microstructural characterization was complemented by SEM-EDS analysis of the main chemical phases present in the metal or alloy, determining the distribution of chemical elements and, eventually, identifying inclusions. The actual effectiveness of thermomechanical processes in the hardness of the artefact was determined by Vickers microhardness testing, while colorimetry measurements determined the colour of the alloys.

Metallurgical remains were analysed by EDXRF to identify the elements that could suggest the type of metal or alloy or the metallurgical vestige (metallic nodule, slag) produced. Selected samples from this category were further characterized by micro-EDXRF, OM, SEM-EDS and micro-XRD to obtain more information about the type of metallurgical operations that could be associated with them: smelting or melting.

In general, the experimental methodology employed in the present study was:

- Inventory and classification of the collections;
- Primary elemental evaluation by EDXRF without any previous surface preparation;
- Determination of metal composition through micro-EDXRF in prepared areas;
- Microstructural characterization by OM in prepared areas.

Characterization by OM also helps to define how other further analysis should proceed. Thus, other methodologies were applied to selected groups to clarify the microstructural interpretation (micro-XRD and SEM-EDS) and attest different properties (hardness and colour).

A summary of the techniques used to characterize different materials and the main information obtained in each case is presented in Figure 2.2.

The number of metallurgical production remains and artefacts analysed distributed by analytical technique is shown in Table 2.3
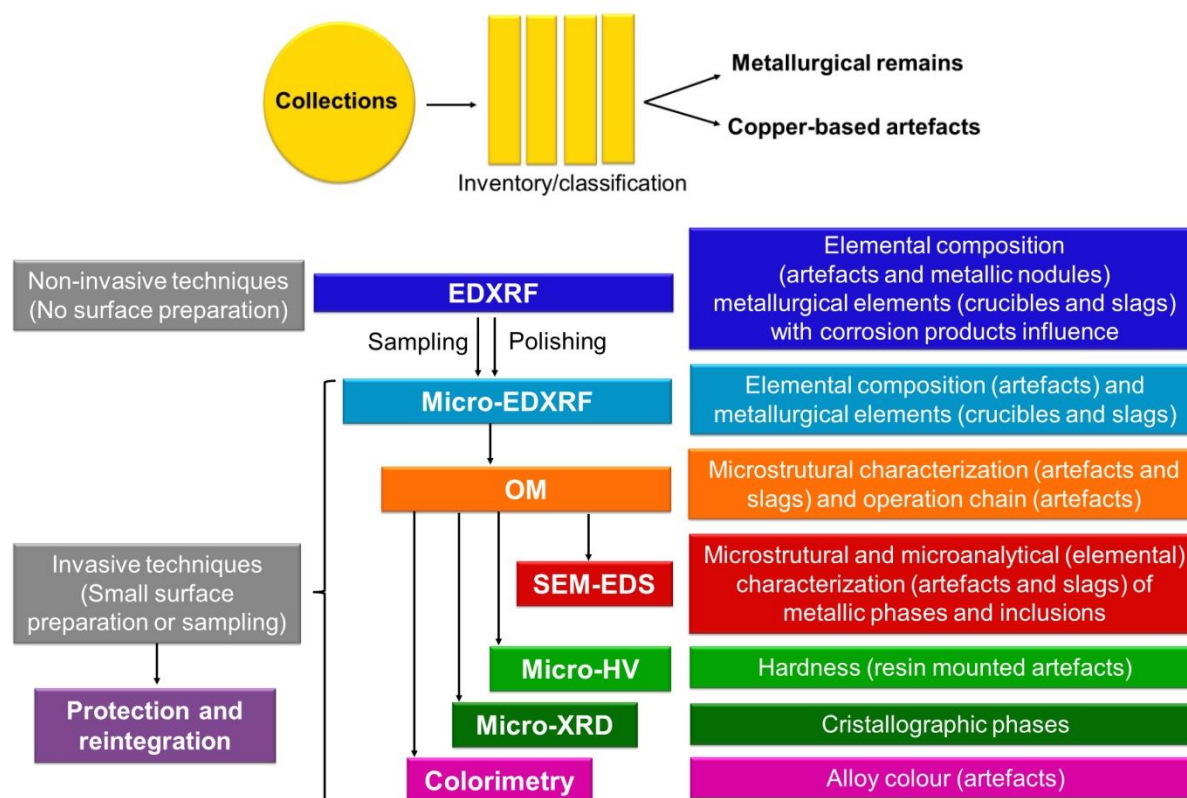
Figure 2.2. Methodology used to characterize the metallurgical remains and copper-based artefacts.

Table 2.3. Techniques used to characterize the metallurgical production remains (crucibles, slags, metallic nodules and metallic artefacts) studied and the number of items analysed in each case; A: artefact; MR: metallurgical remain.

Analytical Techniques	Items analysed	VNSP	ML	OR
EDXRF	571	570 MR	0	1 MR
Micro-EDXRF	266	147 MR + 37 A	8 MR + 62 A	12 A
OM	89	34 MR	8 MR + 34 A	1 MR + 12A
SEM-EDS	29	15 MR + 5 A	4 A	5 A
Micro-EDX	4	4 A[1]	0	0
Colorimetry measurements	25	25 A[1]	0	0
Vickers micro-hardness testing	15	0	9 A	6A

[1] Artefacts from VNSP previously analysed (Pereira *et al.*, 2013a).

Other analytical techniques were occasionally used to clarify particular questions that arise regarding the interpretation of some microstructures. These techniques were: Micro-X-Ray Diffraction and X-ray diffraction with a synchrotron radiation High Energy Materials Science beamline (HEMS) at the storage ring PETRA III.

In order to prevent any corrosion process and stabilize the cleaned areas of the artefacts resulting from the preparation for analysis, a conservation treatment was applied in these areas. This conservation treatment is described in detail after the methods description.

2.2.1. Energy Dispersive X-Ray Fluorescence Spectrometry

Energy Dispersive X-Ray Fluorescence Spectrometry (EDXRF) analyses were conducted using a spectrometer, Kevex 771, installed at Centro de Ciências e Tecnologias Nucleares (C2TN), Instituto Superior Técnico, Universidade de Lisboa (IST-UL).

In this first stage, all items were analysed with no surface preparation in two different areas whenever possible. In the case of the artefacts, it was thus possible to identify the main alloying elements. Regarding the metallurgical remains (crucibles, slags, metallic nodules) this first approach allows the identification of elements present and make a first association to the type of metallurgy they were involved.
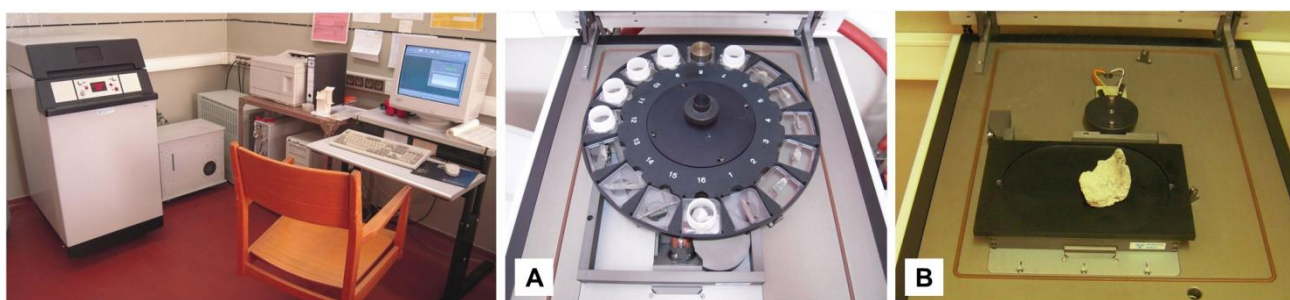
Figure 2.3. EDXRF spectrometer installed at C2TN: A: sample chamber with the automatic rotating tray for smaller artefacts; B: fixed plate that allows analyses in larger size items.

This spectrometer is equipped with a 200 W Rh X-ray tube, secondary excitation targets, radiation filters and a Si(Li) detector with a resolution of 175 eV at 5.9 keV (Mn-Kα). The characteristic X-rays emitted by chemical elements present in the excited area of the sample (circular shape with a diameter of about 2.5 cm) are measured in a liquid nitrogen cooled Si(Li) detector. The equipment has a chamber with a rotating 16-position sample tray and also a fixed plate that allows analyses in relatively large size items (artefacts with dimensions up to of 35x35x10 cm^3) (Figure 2.3. A and B). Details regarding the equipment, analytical conditions and quantifications procedures have been previously published (Kevex, 1992; Araújo *et al.*, 1993).

The quantification procedure involves fundamental parameters and experimental calibration factors (Kevex, 1992). The experimental calibration factors were calculated through the analysis of certified reference materials, whose composition should be similar to the composition of the sample to optimise the accuracy of the method.

Artefacts and production remains were analysed using two excitation conditions – Ag secondary target and Gd secondary target. The analytical conditions utilised in this study are presented in Table 2.4.

Table 2.4. Experimental conditions for EDXRF analyses of copper-based samples (artefacts and metallurgical production remains).

Excitation	Tube voltage (kV)	Current intensity (mA)	Live time (s)	Elements of interest (with respective X-ray peak)
Ag secondary target	35	0.5 (up to 3.0*)	300	Cu-K, Pb-L, As-K and Fe-K
Gd secondary target	57	1.0 (up to 3.0*)	300	Sn-K Sb-K

* In the case of crucibles, the current intensity was adjusted to obtain similar dead times.

To calculate the experimental calibration factors for the elements of interest of copper-based alloys, a certified reference material, Phosphor Bronze 551 Spectroscopic Standard from British Chemicals Standards (BCS), was analysed using the same experimental conditions. This certified reference material was used to calculate the quantification limits for the EDXRF analysis of the copper-based alloys (Table 2.5.). The quantification limit for arsenic and lead could not be accurately calculated due to spectral interferences between the As-Kα and Pb-Lα lines.

Table 2.5. Quantifications limits for EDXRF analyses of copper-based alloys (values in wt.%; calculated as 10×background$^{0.5}$/sensitivity (IUPAC, 1978) using the certified reference material Phosphor Bronze 551.

Sn	Pb	As	Fe
0.02	0.1	0.1	0.05

The obtained EDXRF results are approximate values due to the irregular, non-flat geometry and superficial enrichment in some elements caused by the corrosion products layer.

2.2.2. Surface cleaning and metallographic preparation

Samples were extracted from the artefact by conventional cutting methods, although applying a special care required for these types of archaeological materials. Due to the small size of the samples, they were mounted in an epoxy resin.

Mounted cross-sections were grinded with SiC abrasive papers (P600, P1000, P2500 and P4000 grit size) and polished with diamond paste (3 μm and 1 μm) using a rotatory polishing wheel. This equipment is installed at CENIMAT/I3N, Departamento de Ciências dos Materiais, Faculdade de Ciências e Tecnologia, Universidade Nova de Lisboa (DCM, FCT-UNL) (see Figure 2.4.A). This process intends to remove all cut marks and scratches from the cross-section allowing proper material characterization.

Preparation (without sectioning) of small observation areas directly on the artefacts (~ 3×3 mm^2) were also manually cleaned and polished with SiC abrasive papers and diamond pastes (6 μm, 3 μm and 1 μm). The cotton swabs were impregnated in diamond pastes and applied in a small rotatory tool. This

process removes the corrosion layer and allows the analysis of a clean metal surface of the artefact (see Figure 2.4.B).
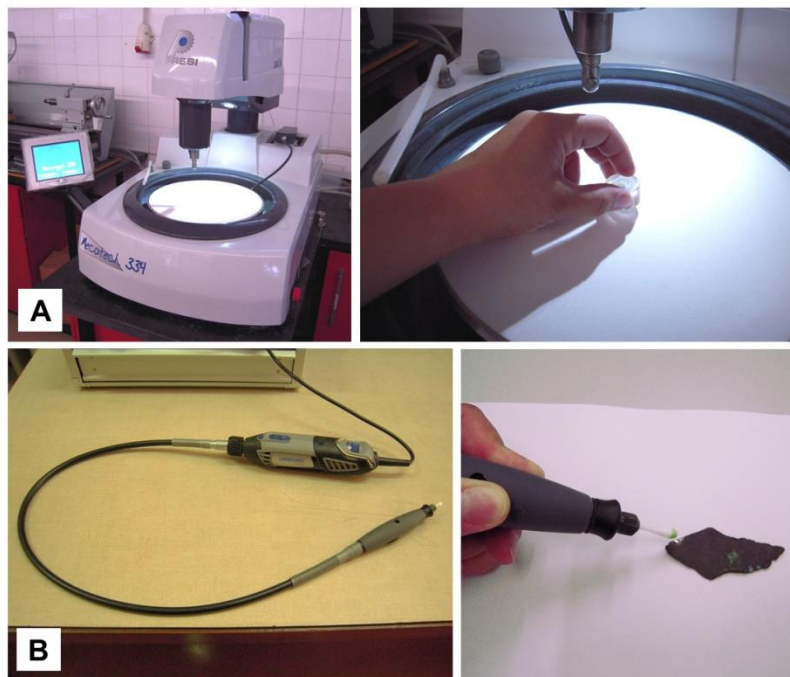
Figure 2.4. Preparation of surfaces for micro-EDXRF analysis and microstructural observation using: A: rotary polishing wheel installed at CENIMAT/I3N; B: rotary manual tool.

For metallographic observation, etching with an aqueous ferric chloride solution and a time ranging from 3 to 5 s were carried out to reveal microstructural features, like grain boundaries, coring, annealing twins or slip bands. The etching solution was prepared with 120 ml of distilled water (H_2O), 30 ml of hydrochloric acid (HCl) and 10 g of ferric chloride ($FeCl_3$) (Scott, 1991). It is very useful for all copper-based alloys such as the arsenical coppers, bronzes, brasses, etc., producing good grain contrast.

2.2.3. Micro Energy Dispersive X-Ray Fluorescence Spectrometry

Micro Energy Dispersive X-Ray Fluorescence Spectrometry (micro-EDXRF) analyses were conducted with an ArtTAX Pro spectrometer installed at Departamento de Conservação e Restauro (DCR), FCT-UNL. This spectrometer is equipped with a low power 30 W Mo X-ray tube, and an electro-thermally cooled silicon drift detector with a resolution of 160 eV (Mn-Kα). The polycapillary lenses, CCD camera and accurate positioning system (see Figure 2.5) collimate the primary X-ray beam enabling a minute spatial resolution of primary incident radiation in the sample (diameter < 100 μm) (Bronk *et al.*, 2001). Quantitative determinations were done using WinAxil software, comprising fundamental parameters and experimental calibration factors (Canberra, 2003).

Figure 2.5. Micro-EDXRF spectrometer installed at DCR and example of spot area of the artefact analysed.

The preparation of the artefacts for micro-EDXRF analysis involves the removal of the corrosion products, which was detailed in the previous subchapter of Metallographic preparation.

The analysis is performed with readings in 3 different spots on the cleaned metal surface for each artefact using a tube voltage of 40 kV and a current intensity of 0.5 mA during 300 s of live time. The X-rays of the elements of interest were: Cu-K, Sn-L, Pb-L, As-K, Fe-K, Zn-K, Ni-K and Sb-L. The experimental calibration factors were calculated through the analysis of the standard reference material Phosphor Bronze 551 from British Chemical Standards (BCS). Also, the quantifications limits for minor elements usually present in archaeological copper and copper-arsenic alloys and the accuracy of the micro-EDXRF analysis were determined by the analysis of two reference materials: Phosphor Bronze 552 (BCS) and IDLF5 ("Industries de la Fonderie") (Table 2.7). Quantification limits vary according to the atomic number, and the detected X-ray emission line, being less favourable whenever strong spectral interferences exist. A low standard deviation on the average concentrations obtained for the three different spots indicates a good representativeness of the analysed area. The accuracy of the micro-EDXRF is usually better for the major elements, mainly below 5%. The minor elements, like lead, iron, zinc and nickel, present higher relative errors. Lead emission peak overlaps with that one of arsenic and iron with the copper escape peak; zinc and nickel have a strong spectral interference with the alloy main constituent (copper).

Table 2.6. Quantification limits for micro-EDXRF analyses of copper-based alloys calculated using the standard material Phosphor Bronze 552 and IDLF5 (values in wt%; calculated as 10 × (background)$^{0.5}$/sensitivity (IUPAC, 1978)).

Cu	Sn	Pb	As	Fe	Zn	Ni	Sb
0.04	0.50	0.10	0.10	0.05	0.04	0.07	0.50

Table 2.7. Accuracy of the micro-EDXRF analyses of copper-based alloys calculated using the standard material Phosphor Bronze 552 and IDLF5 (values in wt%; average ± standard deviation of 3 independent measurements).

SS552	Cu	Sn	Pb	As	Fe	Zn	Ni
Certified	87.7	9.78	0.63	n.d.	0.10	0.35	0.56
Obtained	88.2 ± 0.4	10.0 ± 0.3	0.56 ± 0.02	n.d.	0.11 ± 0.02	0.41 ± 0.02	0.51 ± 0.02
Accuracy	0.6	2.5	11.1		10.0	17.1	8.9
IDLF5	**Cu**	**Sn**	**Pb**	**As**	**Sb**	**Zn**	**Ni**
Certified	68.5	19.9	1.42	5.755	2.23	0.94	0.67
Obtained	71.0 ± 0.05	18.9 ± 0.04	1.56 ± 0.03	5.66 ± 0.03	2.12 ± 0.03	0.81 ± 0.02	057 ± 0.02
Accuracy	3.7	5.0	9.9	1.6	4.9	13.8	14.9

2.2.4. Optical Microscopy

Metallographic observation of the cross-sections and small cleaned areas were carried out with an inverted reflected light microscope Leica DMI 5000 M installed at CENIMAT/I3N, DCM, FCT-UNL (Figure 2.6). This optical microscope is equipped with a set of objectives that allow a wide range of magnifications (5 to 100x) under bright field (BF), dark field (DF), polarized light (Pol) illumination and differential interference contrast (DIC). The DF observation reveals topographical details, such as pores, and the Pol observations allow distinguishing among non-metallic phases like copper oxides and copper sulphides. The DIC contrast was not used in the present study. After these first observations, etching of the surfaces was performed by a chemical attack with an aqueous ferric chloride solution (subsection 2.2.2) to reveal microstructural features as grain boundaries, annealing twins and slip bands among the grains.

This microscope also allows the collection of digital images at different Z-positions that can be combined into one single image with automatic compensation of different focus level. This feature is crucial in the microstructural observation of artefacts that were not sampled and the final polished surface has irregularity areas. The microscope has inverted lenses, allowing the observation of irregular shaped and large size artefacts without the need for sampling.
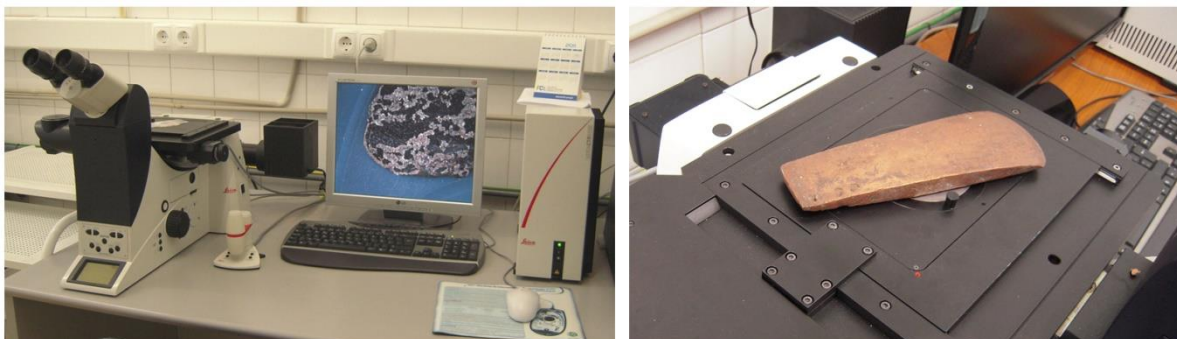
Figure 2.6. Optical microscope installed at CENIMAT/I3N, presenting an inverted design that allows the manipulation and observation of different size artefacts.

2.2.5. Scanning Electron Microscopy with X-Ray Microanalysis

Observations and microanalyses were made in a conventional scanning electron microscope (SEM) Zeiss DSM 962 equipped with secondary electrons (SE) and backscattered electrons (BSE) detectors installed at CENIMAT/I3N, DCM, FCT-UNL (Figure 2.7, A). The equipment also includes an EDS spectrometer from Oxford Instruments, model INCAx-sight, with a Si(Li) detector having a resolution of 133 eV (Mn-Kα) and an ultrathin window used for semi-quantitative elemental analysis allowing the detection of low atomic number elements, $Z > 5$. The semi-quantifications are made using the ZAF (atomic number, absorption and fluorescence) correction procedure.

Mounted samples were analysed with a gold coating or with a carbon tape bridge. Examination of non-mounted items was made with a contact of a carbon conductive bridge or copper tape bridge.

The experimental conditions of selected artefacts and production remains were 20 kV accelerating voltage, 70 μA of beam emission current and 25 mm working distance. The EDS spectra were acquired for 60 s lifetime with dead time adjusted to 30 - 40%. Co Kα radiation from pure Co sample was used for energy calibration of the detector.

Most images were collected using BSE mode due to his higher atomic number contrast, which allowed a better visual recognition of different chemical features. The EDS analysis allowed the determination of the elemental composition of these features and in some cases with the support of previous OM images.
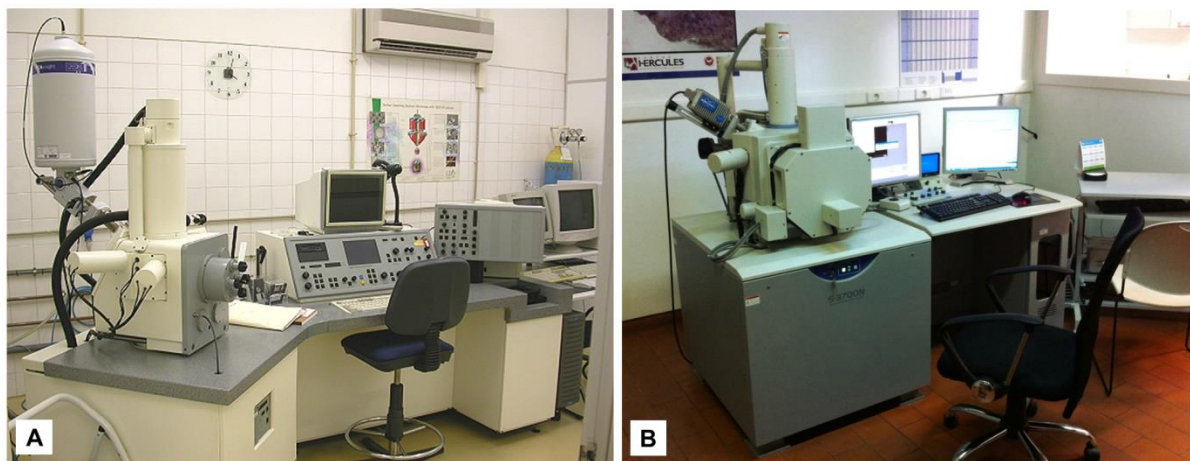
Figure 2.7. A: SEM-EDS Zeiss DSM 962 installed at CENIMAT; B: SEM-EDS HITACHI S-3700N installed at Laboratório Hércules, Universidade de Lisboa.

Microanalyses on five artefacts from VNSP were performed by a field emission scanning electron microscope (FE-SEM) HITACHI S-3700N equipped with secondary electrons (SE) and backscattered electrons (BSE) detectors installed at SEM Hercules, Universidade de Évora (UE) (Figure 2.7, B).

The equipment is operated with 20 kV accelerating voltage, 90 mA of beam emission current, 11-13 mm working distance and high vacuum. Elemental microanalysis was done in the same conditions, using a Bruker XFlash 5010 Silicon Drift Detector (SDD) with a resolution of 129 eV at Mn Kα. The

semi-quantifications were made using the ZAF (atomic number, absorption and fluorescence) corrections.

2.2.6. Micro X-Ray Diffraction

Micro X-ray diffraction (micro-XRD) analyses were performed with a Bruker AXS D8 Discover diffractometer installed at Laboratório José de Figueiredo, Direcção-Geral do Parimónio Cultural (Figure 2.8).

Figure 2.8. Micro-XRD installed at Laboratório José de Figueiredo.

The model possesses a copper anode X-ray source (Cu Kα; λ=1.5406 Å) and a Goebel mirror that converts the divergent beam emitted from the line-shaped X-ray source into a parallel beam before reaching the sample. The beam positioning is controlled by an automated laser-video alignment system that allows visualization and selection of the analysed area, using a motor that moves along the X, Y or Z axis. The diffracted beams are collected with an HI-STAR area detector and processed using a GADDS software system. The analytical conditions were: Ø=1 mm slit collimator (calculated the irradiated circular area of ~1.2 mm^2), angular variation of 12º-105º, 40 kV tube voltage, 40 mA current intensity. Acquisition time varied between 15 and 60 minutes, according to the samples. This technique was used to aid in the identification of less common crystalline metallic phases and inclusions.

Complementary experiments with a synchrotron radiation source were carried out to improve angular resolution and intensity of the diffracted X-ray beam. X-ray diffraction experiments on VNSP148D (axe cutting edge) were conducted at the High Energy Materials Science beamline (HEMS) (Schell *et al.*, 2014) at the storage ring PETRA III at DESY, Hamburg (Figure 2.9). XRD data were acquired in transmission mode (image plate MAR345) using a beam with an energy of 87 keV. The spot size was fixed to 500 µm in horizontal and 100 µm in vertical with an acquisition time of 60 s. The image plate

detector allows recording of the respective Debye-Scherrer rings. Data were processed using the FIT2D software (Hammersley *et al.*, 1996) and intensity of the diffracted beam represented as a function of the angle of diffraction (scaled to Cu Kα radiation). Identification of the crystalline phases was performed by comparing the experimental data with data sets from a Powder Diffraction File database (PDF-2) maintained by the International Center for Diffraction Data® (ICCD®).
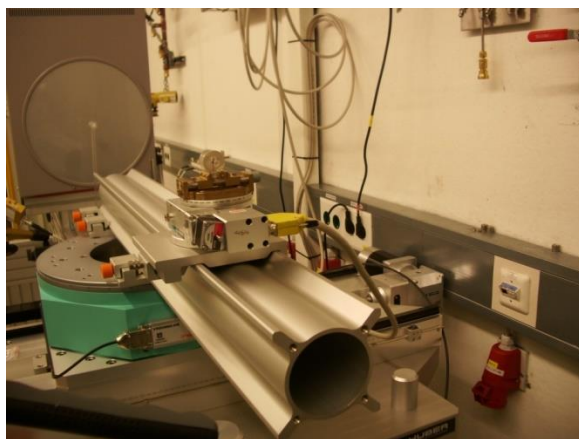
Figure 2.9. X-ray diffraction with a synchrotron radiation High Energy Materials Science beamline (HEMS) at the storage ring PETRA III.

2.2.7. Vickers Microhardness Testing

The microhardness was measured in Zwick-Roell Indetec testing equipment installed at CENIMAT/I3N, DCM, FCT-UNL (Figure 2.10, A).

The hardness of the material is defined by its plastic deformation resistance against the penetration by a harder material. A common measure is given by the Vickers Hardness number (HV), which is calculated by the load applied (P) over the surface area of the indentation (A) by a diamond pyramid indenter into the specimen (Figure 2.10, B).

$$HV = \frac{P}{A} \approx \frac{1.8544\,P}{d^2}$$

Where d is:

$$d = \frac{d_1 + d_2}{2}$$
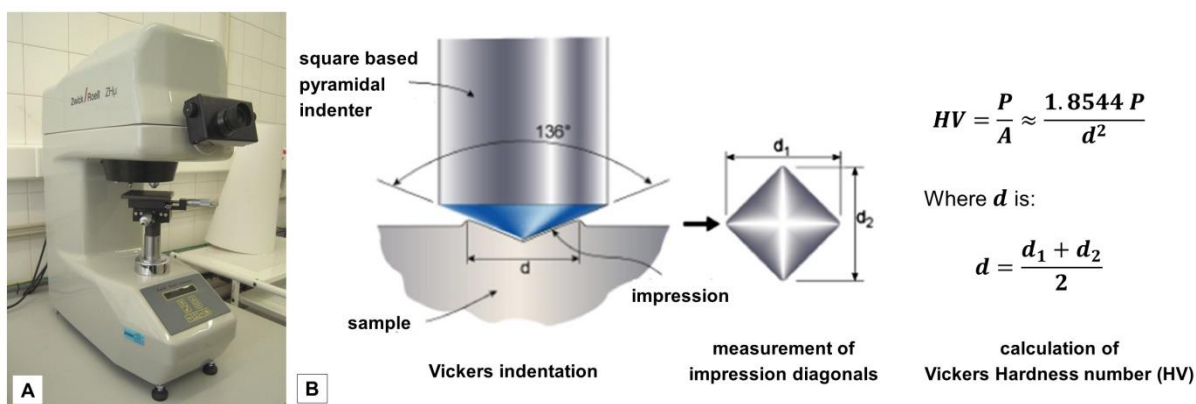
Figure 2.10. A: Microhardness testing equipment; B: Schematic of Vickers indenter and measurement of impression diagonals used in the calculation of Vickers hardness number (HV) (adapted from Maier *et al.*, 2012).

Vickers microhardness testing was made on mounted cross-sections after polishing up to 1 μm diamond paste to remove the etched layer. The Vickers microhardness was measured over the cleaned areas and avoiding the interference of coarser oxide inclusions or other less representative features. At least three indentations were made for each sample with a load of 0.2 Kgf (HV0.2) for 10 s of dwell time.

2.2.8. Colorimetry

The data were collected with a portable DataColor International spectrophotometer Microflash 200d, located at DCR, FCT-UNL, and equipped with an integrating sphere (Figure 2.11, A). The experimental conditions included diffuse illumination 8⁰ viewing (in agreement with CIE publication No15.2.Colorimetry, 1986), SCE, standard illuminant/observer CIE D65/10⁰, and a measured area of 3 mm diameter. It must be noted that the spectrophotometer area of analysis is fixed to 8 mm diameter. Since the clean metallic area of the samples was in most cases inferior, the measurement area was narrowed to 3 mm diameter with a black cardboard mask. Therefore the data obtained from these readings are only valid for comparison in this set of samples. The results are an average of five acquisitions (standard deviation always inferior to 5%) taken on the polished metallic surface of the resin mounted samples.

Colour characterization was carried out using the CIE L*a*b* (CIELAB) colorimetric space, defined by "Commission Internationale d'Eclairage" (CIE) in 1976. In CIELAB widely used colorimetric space, "L" represents lightness dimension and "a" and "b" represent the colour-opponent dimensions, on nonlinearly compressed CIE XYZ colour space coordinates (Figure 2.11, B).
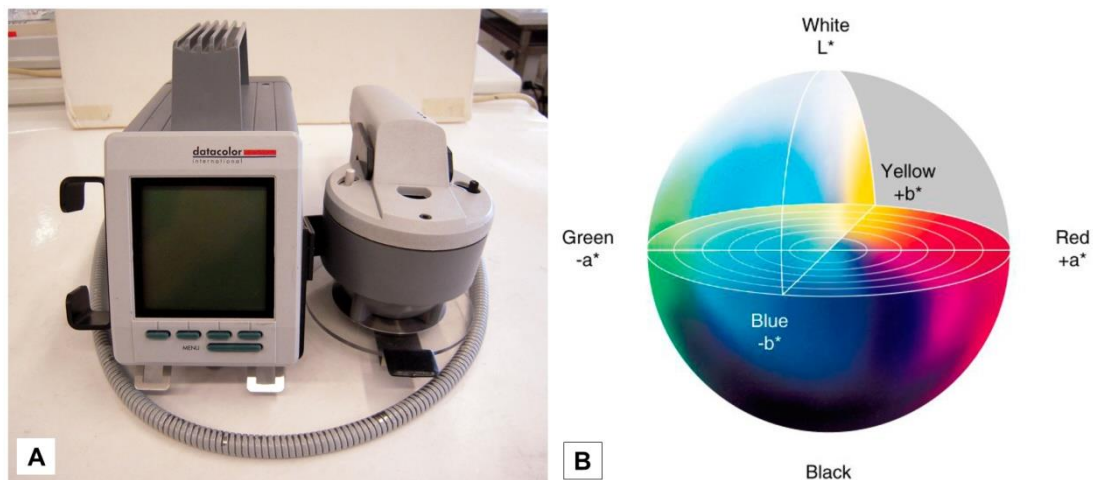
Figure 2.11. A: DataColor International spectrophotometer Microflash 200d used; B: CIE Lab colour space: *L** represents lightness: *a** > 0 represents red component, *a** <0 green component, *b** > 0 represents yellow component and *b** < 0 blue component (Adapted from Schanda, 2007).

The chromatic coordinates measured were L^*, that is always a positive value and represents lightness (0-100); a^* that stands for the red/green axes, and b^* that represents the yellow/blue hue axes. The h (metric hue or hue angle) parameter defines the colour of an object, independently of the colour saturation level and L^* (lightness) and is calculated by $h = \tan^{-1}(b^*/a^*)$ (Feller-Johnston, 2001).

2.2.9. Statistical analysis

Statistical analyses were performed using the Past software, version 2.17c, available at http://folk.uio.no/ohammer/past (Hammer, 2001).

The Kolmogorov–Smirnov two-sample test (two-sample K–S test) was used to compare distributions of arsenic found in the artefacts of the different collections to establish possible parallels and relations concerning metallurgical productions. A permutation strategy was applied to the K-S test to account for the small and unequal sample sizes of the different collections. The sample size is always an important consideration when performing statistical analysis, and accordingly, before the analysis, the Kolmogorov-Smirnov test was validated and proved robust even with unequal and small sample sizes. In the case of our study, the smaller sample size is 12 for the collection of Outeiro Redondo, with the second lowest collection having more than 30 samples.

Fisher's exact test, developed for small samples sizes, was used to evaluate the significance of the association between the presence or absence of arsenic and the artefact functional category ("Tools" and "Weapons"). The same test was also used to evaluate the significance of the association between a final forging operation applied in the artefact manufacture and arsenical copper artefacts, The null hypothesis was rejected at significance levels lower than 5% ($p < 0.05$).

Linear regressions with the determination of the 95% confidence interval for the line slope were obtained to evaluate the behaviour of the hardness measurements as a function of arsenic content in a set of artefacts. In the cases the linear model points to a positive slope, it means that the set of artefacts hardness increases with the arsenic content.

2.2.1. Conservation treatment

The artefacts and metallic nodules that have been prepared for elemental and microstructure characterization were submitted later to an intervention to avoid the occurrence of corrosion processes in the cleaned or cut area and a chromatic reintegration of the surface for aesthetic reasons. The clean metal areas exposed to oxygen are more prone to increase corrosion processes. This procedure is particularly important for objects that were buried and most likely exhibit a significant amount of chlorine. The corrosion products layers for copper-based artefacts are expected to be constituted of malachite ($Cu_2CO_3(OH)_2$), cuprite (Cu_2O) and tenorite (CuO) that are protective and stable, such as the more inner layer of cuprous chloride nantokite (CuCl) under dry conditions (Walker, 1980). However, the removal of the outer corrosion layers facilitates the contact of moisture with the internal cuprous chloride layer thus initiating the autocatalytic reaction known as "bronze

disease", which leads to the formation of paratacamite/atacamite ($4CuCl + 4H_2O + O_2 \rightarrow 2Cu_2Cl(OH)_3 + 2HCl$). The volumetric expansion of this light green corrosion product formation will destabilise and disaggregate the outer corrosion layers of the object.

The corrosion inhibitor for copper alloys used was benzotriazole (BTA) 3% (w/v) in an ethanol solution (Combarieu *et al.*, 1998; Faltermeier, 1998; Loeper-Atia and Robbiola, 1998).

The following procedures were applied to all artefacts:

- Application of a corrosion inhibitor BTA 3% (w/w in ethanol);
- Application of an acrylic resin for protection Paraloid B-72 ® 3% (w/w in ethanol);
- Chromatic reintegration of the area with a mixture of pigments in the Paraloid B-72® media solution was applied to reproduce the coloration of the surrounding corrosion layer;
- Application of a final protection with microcrystalline wax dissolved in *"white spirit"*.

A more extensive treatment was adopted to the set of 37 artefacts from VNSP. These artefacts were temporarily removed from the exhibition to be studied and, before returned to the Museu Arqueológico do Carmo (MAC), they were subjected to a stabilisation treatment. That treatment consisted in the mechanical removal of the light green instable corrosion product (paratacamite/atacamite) before the application of the corrosion inhibitor and the acrylic resin for protection in all surface of the artefacts. The following procedures remained the same.

Finally, all the artefacts were returned with an individual report indicating the location of the intervened area and the conservation treatment applied.

3. VILA NOVA DE SÃO PEDRO

3.1. INTRODUCTION

Several large settlements emerged in the Estremadura region of Portugal by the end of the 4th and the beginning of the 3rd millennium BC during the Chalcolithic period (~3000-2250 BC). The Castro of VNSP, an emblematic settlement located at Azambuja, represents one of such settlements.

Successive archaeological excavations were carried at VNSP from 1937 to 1964 by archaeologist Afonso do Paço with the support of Reverend Eugene Jalhay (Arnaud and Gonçalves, 1995, 1990; Paço and Jalhay, 1939). The structure of the settlement identified during the excavations included a more protected central fortification with several semi-circular bastions and two outer lines of defence (Müller and Soares, 2008). Alongside the practice of agriculture and grazing, some evidence of other practices such as hunting, fishing and gathering were found. Apart from the metallurgical collection (artefacts, crucibles and other remains of production), plenty of household utensils, namely pottery and loom weights, were collected in the settlement. Also an important lithic collection of arrowheads, gouges, axes, scrapers and worship idols were recovered. The majority of the artefacts found in VNSP are currently deposited in the MAC, Lisbon (Arnaud and Fernandes, 2005). Unfortunately, the field notes of the early excavations are very limited and incomplete.

Edward Sangmeister in 1955 and Hubert Savory in 1959 participated in the excavations of VNSP and, from their notes, a model for a stratigraphic sequence was developed (Müller and Soares, 2008; Savory, 1972; Paço and Sangmeister, 1956). According to these last authors, Period I of VNSP corresponds to an occupation of the settlement before the existence of protection walls and is characterized by the cylindrical vessels, "copos", with wall thicknesses about 2–3 mm and with polished fluted decorations (Müller and Soares, 2008). As stated by Savory, no evidence of archaeometallurgical remains was found in this phase of the occupation. On the other hand, in Period II, evidence for metallurgy production is abundantly present in the form of small copper tools like awls and fragments of rectangular crucibles with a low foot at each corner (Savory, 1972). Also in this period, the dominant ceramics are vessels decorated with imprinted acacia leaf and crucifera motifs. Finally, VNSP Period III corresponds to the occurrence of Bell Beaker pottery, and the metallurgy is represented by a large diversity of copper artefacts including axes, chisels and weapons (Müller and Soares, 2008). In Zambujal, a coeval settlement of VNSP, a similar occupation with four construction phases was recorded (Müller *et al.*, 2007).

A sporadic Late Bronze Age (LBA) occupation is also recognised in VNSP by the presence of some distinctive pottery and fewer tin bronze artefacts from this chronological period that were collected at a more superficial level (Arnaud and Fernandes, 2005; Soares, 2005). Unfortunately, due to incomplete field notes of the early excavations performed in VNSP and the not detailed existing documentation it is not possible to match the previous chronology to the materials excavated from VNSP.

In spite of the extraordinary importance of the recovered metallurgical related materials, only a few studies have been carried out up to the present day regarding the several hundred copper and

arsenical copper artefacts and metallurgical remains discovered at VNSP (approximately 5-6 kg). According to excavations records, a large volume of minerals was found at VNSP (Jalhay and Paço, 1945). However, as previously mentioned, in the VNSP collection deposited in the MAC, only some small pieces of limonite with traces of malachite are present. Still, they were not included in the present collection since they were previously studied (Müller and Soares, 2008). The analysis of those materials revealed they are mainly composed by iron, also containing hematite, quartz and copper carbonates. Some pieces of iron hydroxides contain traces of malachite and relics of primary chalcopyrite (Müller and Soares, 2008).

Significant amounts of technical ceramic associated with metallurgy were found during the excavations at VNSP (Soares, 2005; Paço 1955; Jalhay and Paço, 1945). The majority of crucibles are of sub-rectangular shape, flat-bottomed; some exemplars present four small feet. They also varied in wall thickness: thinner-walled crucible fragments show heavily vitrified rims and traces of copper corrosion adhering to them, which indicates that the crucibles were fired from above; thicker-walled crucibles present few signs of high-temperature exposure. There is also the possibility that these last crucibles could have been used as moulds to cast a metal ingot (Müller and Soares, 2008; Soares, 2005). Finally, there is a set of ceramic tube fragments in the VNSP collection with no apparent signs of a high-temperature alteration that could be typological compared to blowpipes found in other regions (Müller and Soares, 2008; Fasnacht 1999; Roden, 1988). Jalhay and Paço mention other fragments of blowpipes of bigger diameter and showing signs of secondary firing. Unfortunately, they could not be found in the assemblage stored at the Carmo Archaeological Museum (Jalhay and Paço 1945; Soares 2005).

An earlier study published in 1952 presented the elemental composition of a few metallic objects found at VNSP (Paço, 1955; Paço and Arthur, 1952). Other studies carried out by the first author were mainly concerned with descriptions of artefacts or the settlement (Paço, 1964; Paço and Sangmeister, 1956; Paço and Jalhay, 1939). Analyses revealed that the VNSP collection comprises artefacts made of copper as well as bronze. Due to the absence of tin in all copper droplets analysed, it was suggested that in contrast to copper, bronze was not processed at the site (Paço and Arthur, 1952; Müller and Soares, 2008). This observation was confirmed in project "Studienzu den Anfängen der Metallurgie" (SAM) that included the analyses of 88 copper-based artefacts and metallurgical remains from VNSP using atomic emission spectroscopy (Junghans *et al.*, 1974, 1968, 1960). According to the SAM analysis, 35 % of the artefacts were composed of pure copper. In the remaining set, 45% were composed of copper with arsenic (As > 0.1 wt.%) with low trace element concentrations and 20% were composed of copper with arsenic (As > 0.1 wt.%) with higher amounts of antimony (> 0.01 wt.%), silver (> 0.01 wt.%), and sometimes nickel (> 0.04 wt.%) (Müller and Soares, 2008; Sangmeister, 1995).

Sangmeister was able to demonstrate in Zambujal settlement a chronological sequence of these three types of copper. Pure copper preferentially occurred in early Chalcolithic contexts, copper with arsenic and very low trace element concentrations was used throughout the Chalcolithic period, and copper with arsenic and higher amounts of trace elements (Sb, Ag and Ni) mainly appeared in late

Chalcolithic and Bronze Age contexts (Sangmeister, 1995). However, it is not possible to compare this chronological sequence in VNSP assemblage since there is no clearly defined stratigraphy.

More recently, as mentioned in subsection 1.3.3, a study from VNSP metallurgical collection included a set of 15 copper prills and molten copper scrap (Müller and Soares, 2008) where, for the first time, lead isotope ratios were used for a provenance study in the region. Also a set of 53 copper-based artefacts from VNSP collection was studied (Pereira *et al.*, 2013b; Pereira, 2011) and the results were included in this thesis and discussed in the corresponding sections.

3.2. PRODUCTION REMAINS [1]

3.2.1. *Crucibles*

The collection of crucible fragments studied is composed of 17 fragments (Figure 3.1). In this group were included all crucible fragments with external material adherent and copper corrosion vestiges over the ceramic surface macroscopically visible (see Table 3.1). All crucible fragments have thick walls with approximately 2 cm. In this collection, VNSP276, VNSP277, VNSP279, VNSP281, VNSP282, VNSP283, VNSP286, VNSP287, VNSP288, VNSP289 and VNSP291 are rim fragments, VNSP278, VNSP280 and VNSP285 are possibly from the bottom of a crucible (flat bottom vessels). Fragment VNSP278 has a small foot suggesting a typology of crucibles with feet. In Zambujal there are some similar crucibles (Müller *et al.*, 2007). Also, the collection of VNSP in exposition in MAC has also some examples of rectangular crucibles with four feet, complete or partially reconstructed but they were not included in this set since they did not present any visible metallurgical vestige and were previously subjected to conservation procedures (Arnaud and Fernandes, 2005). The presence of feet and flat bases were most likely to confer stability. This characteristic associated with their thick clay walls suggest that these vessels most likely had been heated from above, as it was common in these ancient metallurgical operations (Barleys and Rehren, 2007; Rovira, 2004).

The remaining fragments VNSP284, VNSP290 and VNSP292 are smaller, and it was not possible to attribute them to a specific location in the crucible. In this group were included all crucible fragments with external material adherent and copper corrosion vestiges over the ceramic surface.

---

[1] Part of the content from this section was previously published (Pereira *et al.*, 2013a).
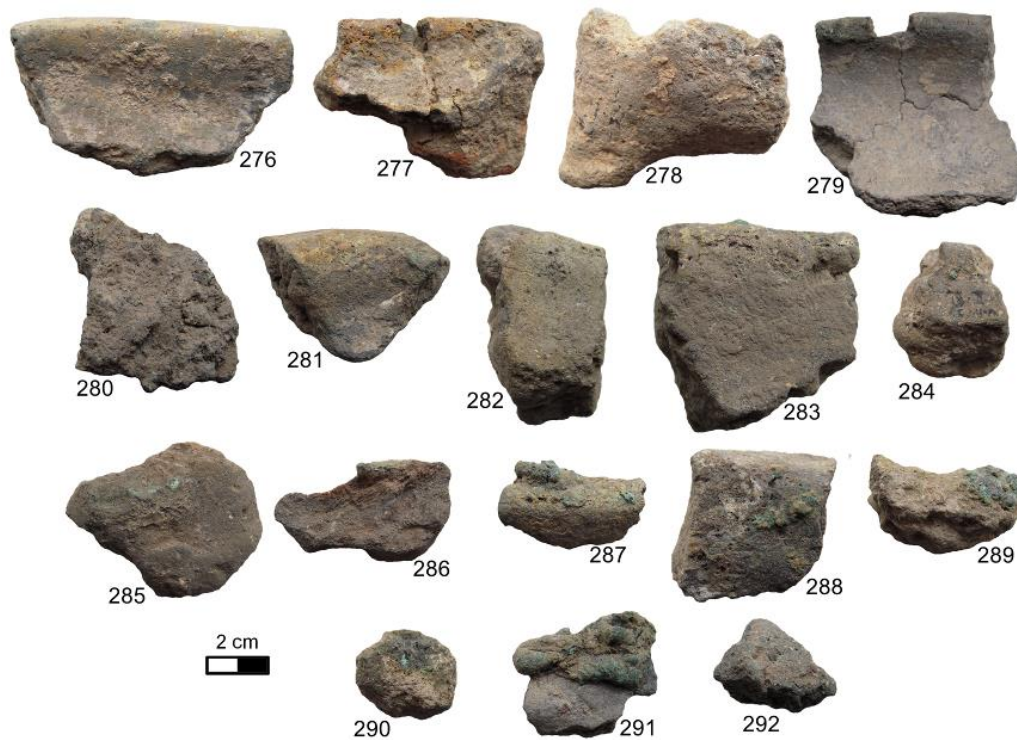
Figure 3.1. Crucible fragments from VNSP: all are presenting visible traces of copper corrosion and slag vestiges in the rim or inner wall.

The slags and clay surfaces of the crucibles were analysed by EDXRF to establish the metallic elements that enriched the areas affected by the metallurgical operation. The results from the comparison of EDXRF spectra of slags and clay surfaces of all crucibles from VNSP are summarized in Table 3.1.

An example of EDXRF spectra showing the enrichment in Cu and As elements in the inner wall surface of the crucible fragment VNSP276 or with visible slag/metallic vestige VNSP280 is presented in Figure 3.2. The enrichment in certain elements in the inner wall and rim surfaces of the crucibles is indicative of the metallurgical processes, concerning the metal or metals, performed on these ancient production remains. EDXRF results of the crucible fragments point to metallurgical activities in VNSP involving copper and copper with arsenic.

Table 3.1. Enriched elements in the surface areas of the crucibles affected by metallurgical operation: typically inner wall or rim. Macroscopically visible slag/metallic vestiges: d. – detected; n.d. – not detected.

Crucibles	Cu	As	Slag/metallic vestiges
VNSP276	+	+	d.
VNSP277	+	+	n.d.
VNSP278	+	n.d.	n.d.
VNSP279	+	++	d.
VNSP280	+	+++	d.
VNSP281	+	++	d.
VNSP282	+	+	n.d.
VNSP283	+	+	n.d.
VNSP284	+	n.d.	n.d.
VNSP285	+	n.d.	n.d.
VNSP286	+	n.d.	n.d.
VNSP287	+	n.d.	d.
VNSP288	+	+	d.
VNSP289	+	n.d.	d.
VNSP290	+	n.d.	n.d.
VNSP291	+	n.d.	d.
VNSP292	+	+	n.d.
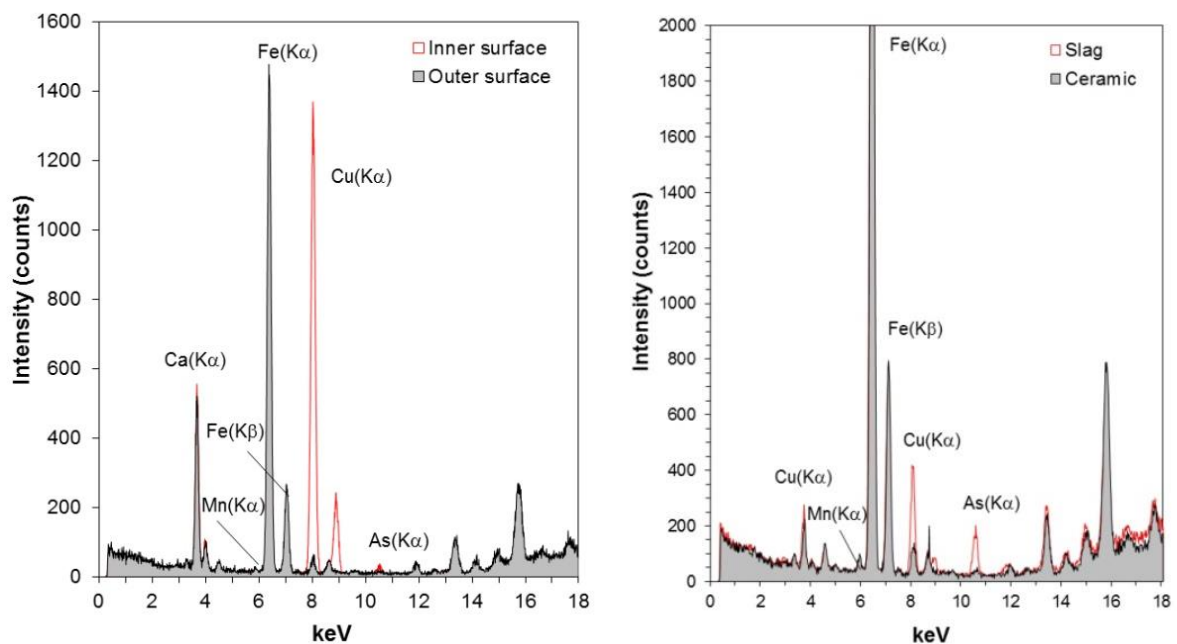
Figure 3.2. EDXRF spectrum of VNSP276 crucible inner surface (red spectrum) and VNSP280 crucible with visible slag/metallic vestige (red spectrum), both compared with the outer surface (black spectrums).

EDXRF results evidence that this set of 17 crucibles from VNSP were used in the practice of the metallurgy of copper and copper with arsenic at the settlement. A more detailed study of the adherent slags from VNSP280 and VNSP287 crucibles is included in the following section. These slags were

39

selected for their stability and size, large enough to be representative for further analysis by OM and SEM-EDS.

3.2.2. *Slags*

In this study were analysed 13 fragments of slags from VNSP (Figure 3.3) and two adherent residues from VNSP280 and VNSP287 crucibles (see Figure 3.1 and Table 3.1). The slags were manually cleaned and polished, according to the description given in subsection 2.2.2. The identification of the slags main constituents through OM and SEM-EDS characterization is presented in Table 3.2.
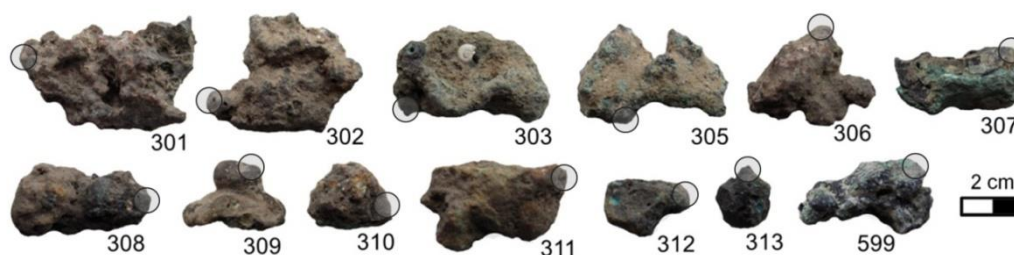
Figure 3.3. Slags fragments from VNSP collection; circles: polished areas.

Table 3.2. SEM-EDS analysis of slags from VNSP (d. – detected; n.d. – not detected); S – smelting; M – melting.

Slags	Cuprite	Tenorite	Magnetite	Delafossite	Others	Slag origin
VNSP280[a]	d.	n.d.	d.	d.	Cu-As	S
VNSP287[a]	d.	d.	n.d.	n.d.	Metallic Cu	M
VNSP301	d.	d.	d.	d.	Cu-Cl-O[b]	S
VNSP302	d.	n.d.	d.	n.d.	Metallic Cu	S
VNSP303	d.	d.	n.d.	n.d.	C+Cu+Si+Ca[c], Cu-Cl-O[b]	M
VNSP305	d.	n.d.	d.	n.d.	Metallic Cu	S
VNSP306	d.	n.d.	d.	d.	-	S
VNSP307	d.	d.	n.d.	n.d.	C+Cu+Si+Ca[d]	M
VNSP308	d.	n.d.	d.	n.d.	Metallic Cu	S
VNSP309	d.	n.d.	d.	n.d.	Metallic Cu	S
VNSP310	d.	n.d.	d.	n.d.	Metallic Cu	S
VNSP311	d.	n.d.	d.	n.d.	Metallic Cu	S
VNSP312	d.	n.d.	d.	d.	Metallic Cu	S
VNSP313	d.	n.d.	d.	d.	Cu-As	S
VNSP599	d.	n.d.	d.	n.d.	Metallic Cu	S

[a] Analysed slags attached to crucible; [b] Copper chloride; [c] Vegetal structure vestige (posterior identification indicate tree of the *genus Quercus*) [2]. [d] Organic remain: charcoal posterior dated.

---

[2] The taxonomic identification of the charcoal inclusion was made by Paula Queiroz (Terra Scenica).

SEM-EDS characterization identified in the majority of slags a vitreous and heterogeneous matrix of complex silicates (Si, Al, K, Fe and O) with spherical voids (assigned to gas pores) and several globules composed of copper oxides (cuprite and tenorite) and, sometimes, of metallic copper (prills). In all fragments of slag analysed, oxide copper globules were identified (Table 3.2). These non-metallic globules may result from re-oxidising metallic copper, indicating a limited control over the redox conditions. For instance, slag VNSP301 was identified by SEM-EDS as a high heterogeneous glassy material, alongside with magnetite, delafossite crystals and cuprite globules (Figure 3.5). Oxidized Cu-rich globules could also result from the burial of the metallurgical vestiges over archaeological times.
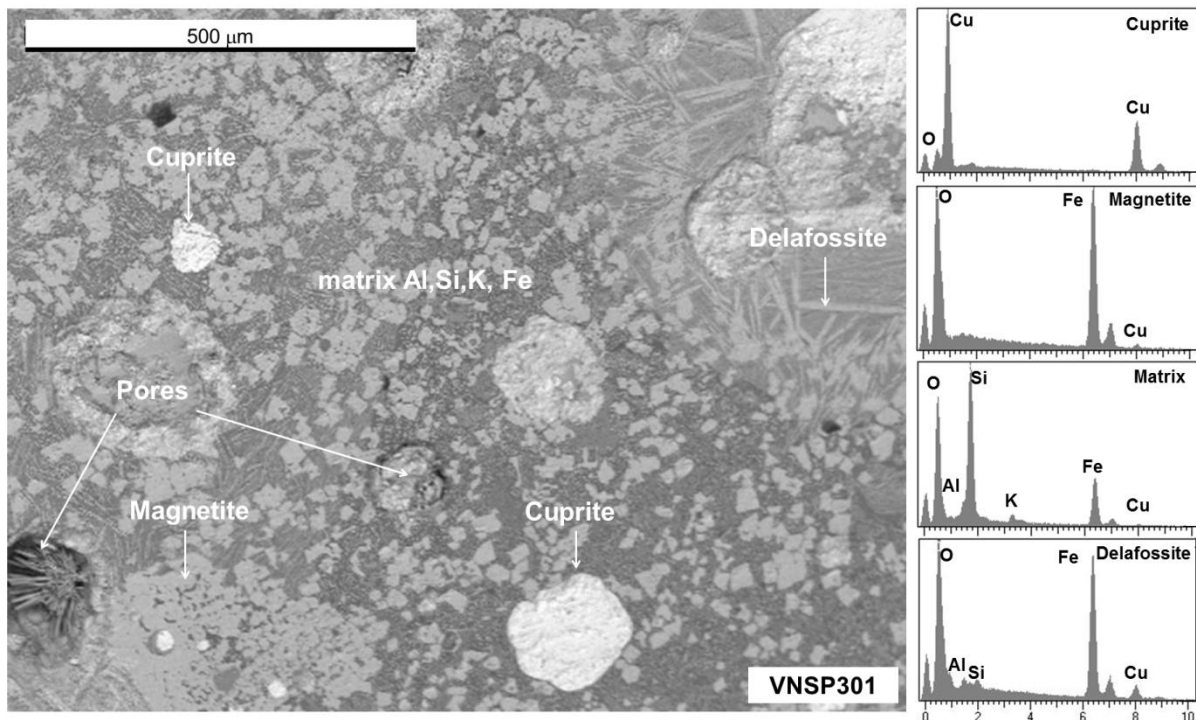
Figure 3.4. SEM-BSE image with EDS spectra of slag VNSP301 evidencing high heterogeneous matrix and identification of cuprite globules, magnetite and delafossite (phases identified by approximate stoichiometry given by EDS).

In 10 cases, small metallic copper globules were present (see Table 3.2). Copper globules with an As-rich phase (Cu_3As) were also identified in slag VNSP280 and VNSP313 (Figure 3.6).
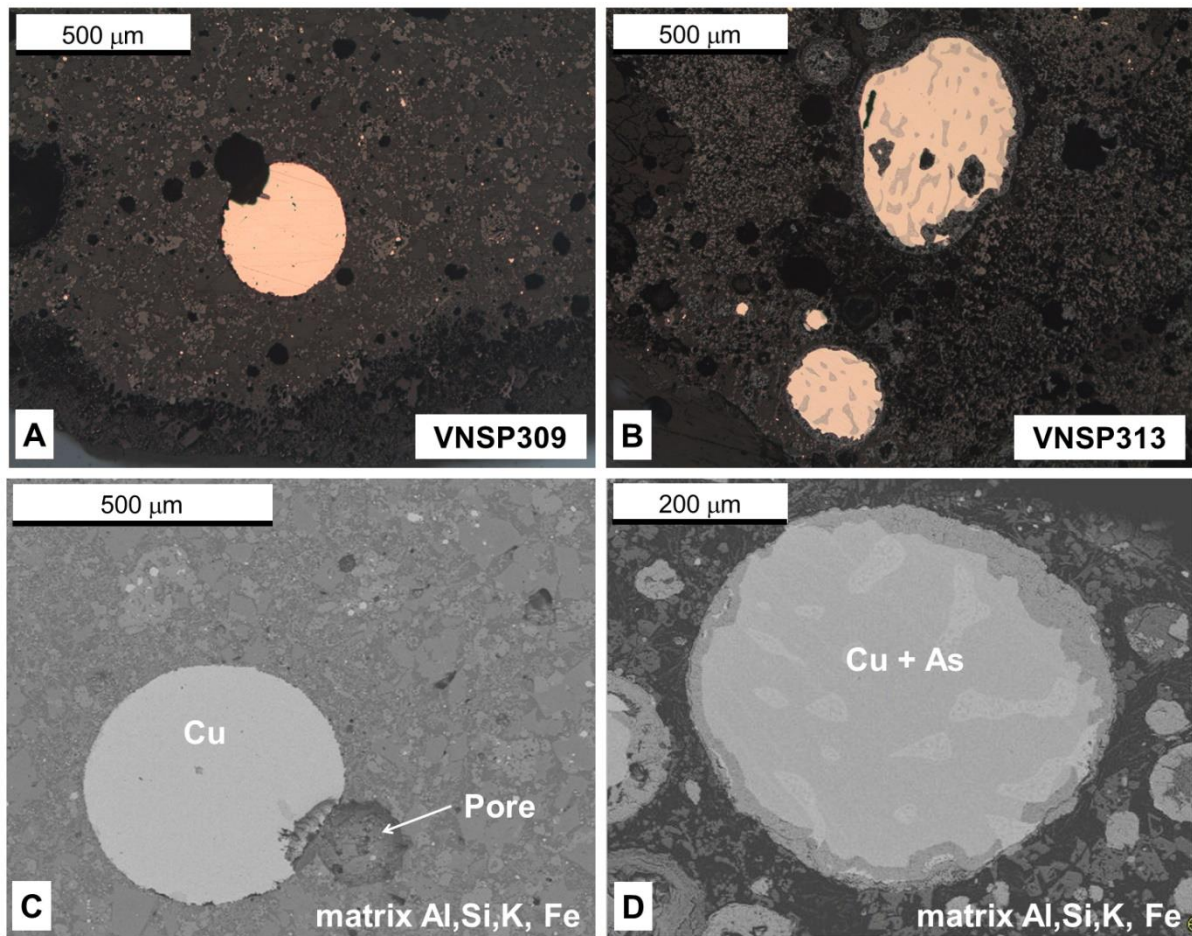
Figure 3.5. A: OM image with the corresponding SEM-BSE image (C) showing the EDS identification of the metallic globules constituents: Cu from slag VNSP309; B: OM image with the corresponding SEM-BSE image (D) showing the EDS identification of the metallic globules constituents: Cu+As from slag VNSP313. The quantification obtained for the globules with arsenic was: 2.5 wt.% As from slag VNSP280 and 27.1 wt.% As from slag VNSP313 (all OM images BF illumination; non-etched).

The prills entrapped in the slags show coarse granular microstructures that evidence the slow cooling rate of the slag inside the crucible. In slag VNSP280 (Figure 3.7) metallic prills are quite abundant and presenting variable dimensions.
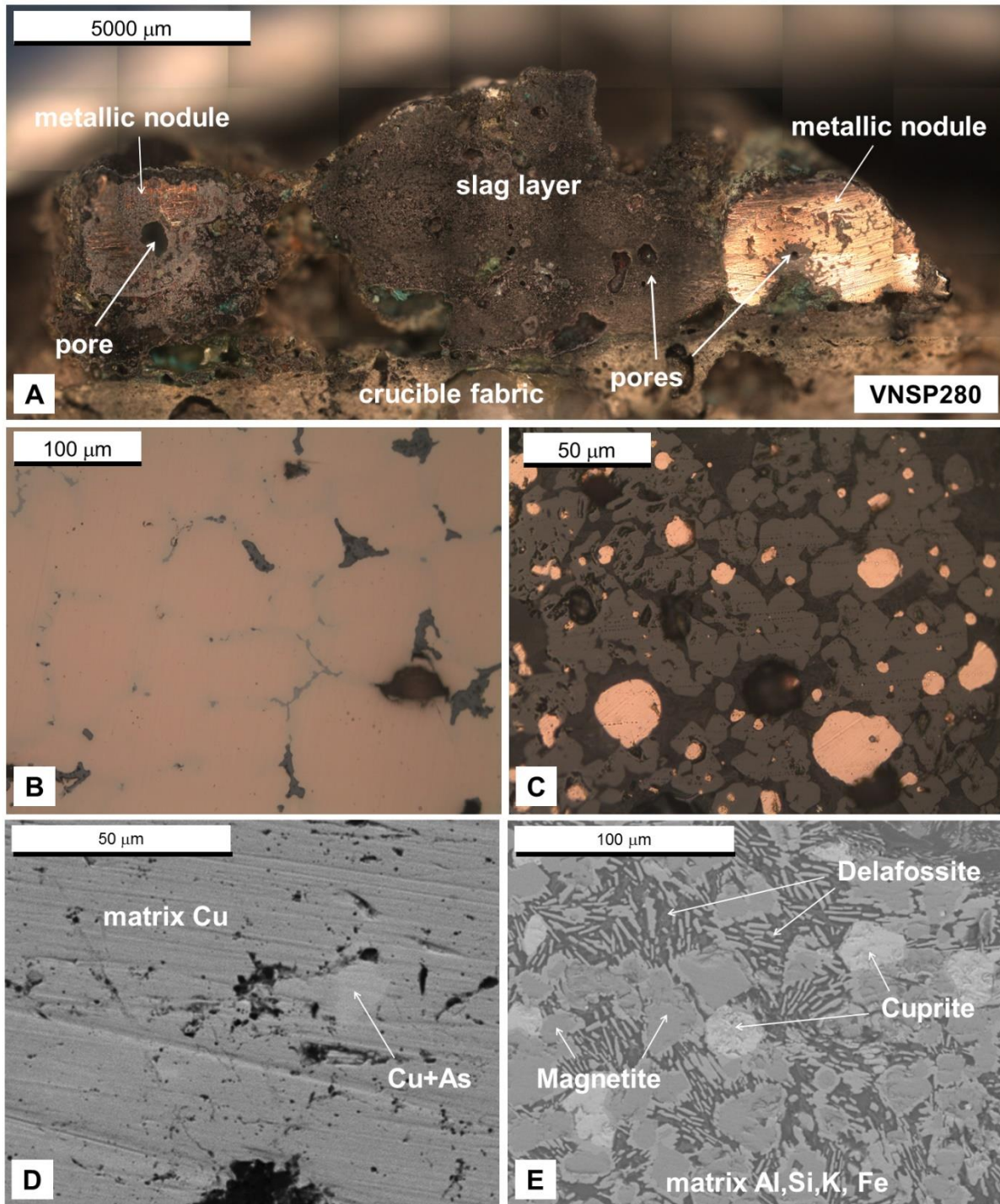
Figure 3.6. A: OM image (Pol illumination; non-etched) of the cross-section of slag VNSP280 evidencing two prills embedded in a slag adherent to the ceramic; B: OM image (BF illumination; non-etched) evidencing the coarse prill granular microstructure; C: OM image (BF illumination; non-etched) evidencing the trapped prills; D: SEM-BSE image with EDS identification of As-rich intermetallic in a Cu-rich matrix, and E: SEM-BSE image with EDS identification of cuprite globules alongside with magnetite and delafossite in a silicate glass matrix (phases identified by approximate stoichiometry given by EDS).

Almost all slags show Fe-rich products. Magnetite (Fe_3O_4 - $FeO.Fe_2O_3$) was present in all slags except VNSP287, VNSP303 and VNSP307. Delafossite ($CuFeO_2$) was identified in five cases

(VNSP280, VNSP301, VNSP306 VNSP312 and VNSP313). The abundant presence of magnetite is an indicator of poor reducing atmosphere attained in the reaction vessel during the smelting operation (Hauptmann, 2007).

The presence of some green compounds observed could be explained by the posterior formation of corrosion products during the burial of these metallurgical vestiges. Copper chlorides, identified in some slags, such as VNSP301, are possibly atacamite or paratacamite ($Cu_2Cl(OH)_3$) (Figure 3.8).

Some C-rich vestiges (assigned to vegetable remains due to its cellular structure) were observed in the slags. The result of the morphological identification of the vegetal remnant inclusion present in the VNSP303 slag indicates it provenience from a tree of the "genus Quercus". A small piece of charcoal found entrapped in the slag material VNSP307 was dated by radiocarbon (AMS). The following date was obtained: Beta 359672: 3970±30BP; 2570-2460 Cal BC (2σ).

Attributing slag fragments to melting or smelting operations is difficult. Smelting slags tend to be richer in iron compounds and silicates while the melting slags are richer in non-ferrous compounds and wood ash (Tylecote, 1992). The abundant presence of iron products like magnetite (Fe_3O_4) and delafossite ($CuFeO_2$), the entrapped globules of metallic copper (prills) or copper oxides (Cu_2O or CuO) in a heterogeneous and viscous matrix of complex silicates are characteristics of slags produced in primitive smelting operations. These matrixes of complex silicates are a result of reactions between ore/metal with the crucible ceramics and the ash resulting from the wood or charcoal used for heating during smelting or melting operations (Tylecote, 1992). It is also expected the presence of some alteration products like corrosion products in the slags.

Considering all these characteristics together, all the slags analysed in this study provide evidence of smelting operations with the exception of VNSP287, VNSP303 and VNSP307 (Table 3.2). In the case of slag VNSP303, the identification of a vegetal structure, the absence of a vitreous matrix and absence of Fe-rich oxide compounds, like magnetite and delafossite should be indicative of a melting slag (Figure 3.7). Also, in the case of VNSP287 and VNSP307, the absence of iron oxide compounds should denote melting slags (see Table 3.2 and Figure 3.8).

The heterogeneity and microstructural characteristics mentioned above for these slag fragments indicates a fairly oxidizing gas atmosphere during slag formation, but temporarily and spatially reductive enough to produce metallic copper. Silicon occurs as residual quartz, in silicates and Si-rich glasses in the matrix, while fayalite (Fe_2SiO_4), commonly present in slags formed in high reduction conditions, during the smelting process of a more advanced metallurgy, was not observed at all. The absence of the latter phase, together with the comparatively high amounts of trapped copper prills, suggests that the slags must have been very viscous. These characteristics are an indication of primitive smelting processes.
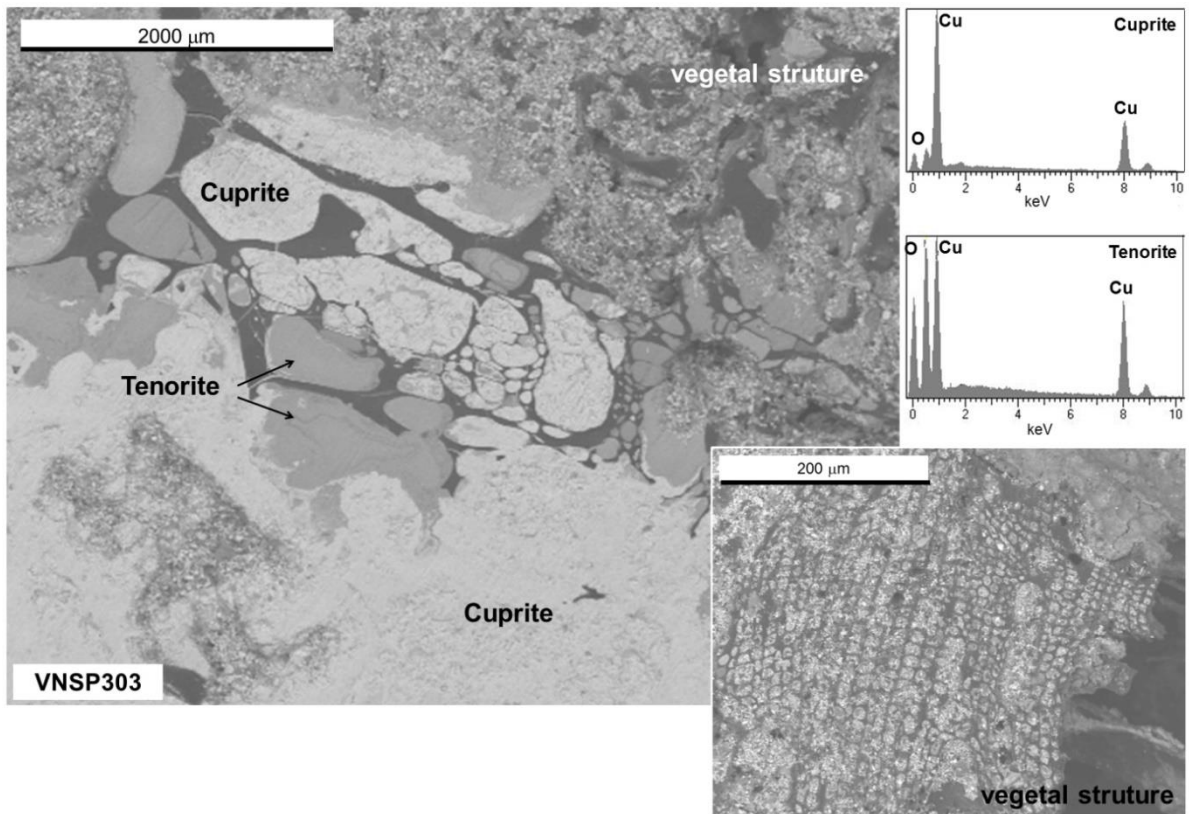
Figure 3.7. SEM-BSE image with EDS spectra of slag VNSP303 with the identification of cuprite and tenorite (phases identified by approximate stoichiometry given by EDS) alongside with a vegetal structure later identified as a tree of the *genus Quercus*.
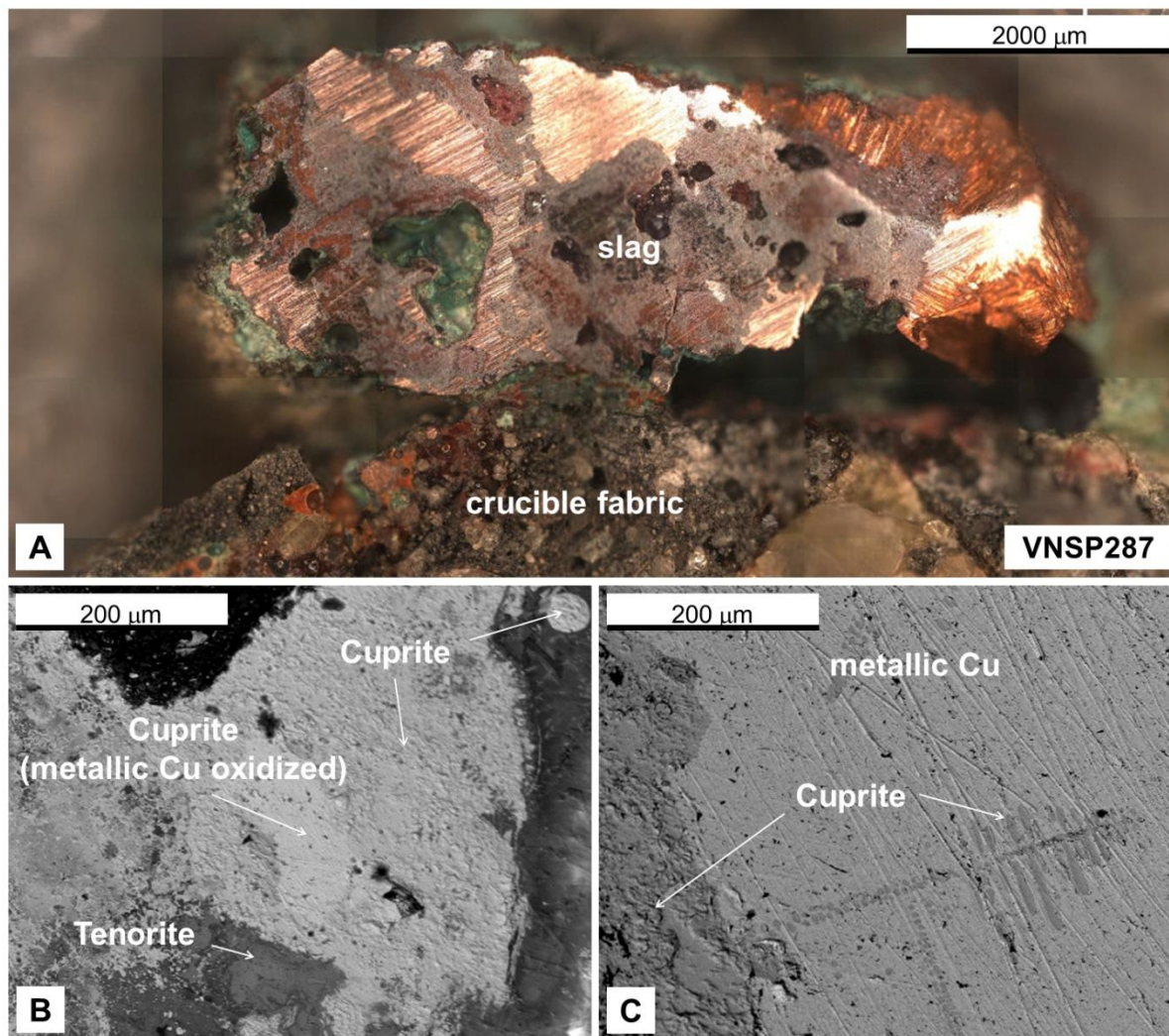
Figure 3.8. A: OM image of slag VNSP287 (Pol illumination; non-etched); B and C: SEM-BSE image with the identification of cuprite, tenorite and metallic copper (phases identified by approximate stoichiometry given by EDS).

In conclusion, evidence from the study of slags indicates crucible smelting operations for the production of copper and arsenical copper in VNSP. Items VNSP287, VNSP303 and VNSP307 are most likely melting slags since they present evidence of resulting from smelting operations (the relatively high amount of iron oxides is rather suggestive of a smelting process originated). Nevertheless, the differences between melting and smelting remains are always of difficult assessment, and more investigation in other coeval settlements is essential to combine and to attest the characteristics from each one.

The interpretation of early metallurgical vestiges is not a straightforward process since these early smelting conditions should be quite irregular. Nevertheless, the archaeometallurgical vestiges from VNSP lead to a coherent assemblage where smelting and melting operations took place.

A group of slags attributed to smelting operations were analysed by SEM-EDS to evaluate metal equivalent oxide compositions comparable to other investigations. The high heterogeneity of these

materials was taken into account in the selection of the region analysed, with the intention to be as representative as possible of the slag. Results are presented in Table 3.3.

Table 3.3. Associated oxide-types in slags from VNSP detected in SEM-EDS area analysis (wt.%). The data were normalized regarding these oxides and average composition for each distinct area. The copper and arsenic oxides detected in the samples are shown as well to give an idea of the total composition of each sample (remaining oxides forming the difference to 100% are neglected here).

Oxides / Slags	Al_2O_3	SiO_2	K_2O	CaO	FeO	CuO	MgO	P_2O_5	As_2O_3
VNSP280	1.02	8.24	n.d.	0.34	78.5	11.9	n.d.	n.d.	n.d.
VNSP301	9.70	23.7	3.77	0.97	38.6	11.3	2.78	9.18	n.d.
VNSP302	4.47	25.9	0.70	1.95	52.0	9.93	1.50	3.55	n.d.
VNSP306	2.41	23.5	0.09	n.d.	57.6	16.4	n.d.	n.d.	n.d.
VNSP309	3.65	34.9	0.52	2.07	57.6	1.26	n.d.	n.d.	n.d.
VNSP311	11.7	27.1	n.d.	n.d.	53.7	7.50	n.d.	n.d.	n.d.
VNSP313	7.02	23.7	1.13	4.34	44.8	10.3	n.d.	n.d.	8.71
VNSP599	8.09	53.9	2.39	0.32	35.3	n.d.	n.d.	n.d.	n.d.

In Chapter 6, the associated oxide-type contents presented in Table 3.3 were compared with a previous study of slags from VNSP and slags from Zambujal, another coeval Chalcolithic settlement located in Portuguese Estremadura (Gauss, 2015).

3.2.3. Metallic nodules

From the initial collection of 570 metallurgical remains, a selection of 147 metallic vestiges was analysed by micro-EDXRF (results are presented in Appendix II).

This collection is composed of copper or copper with arsenic up to 4.70 wt.%. Iron content is in the majority of the cases below the quantification limit (<0.05%), with the exception of 15 cases, although not exceeding 0.11% Fe, still a rather low amount. Other minor elements such as antimony, lead, zinc, nickel or silver were not detected or are under the quantification limit. The distribution of the arsenic content in the metallic nodules analysed evidence a distribution with a shape close to a "geometric distribution" (Figure 3.9).
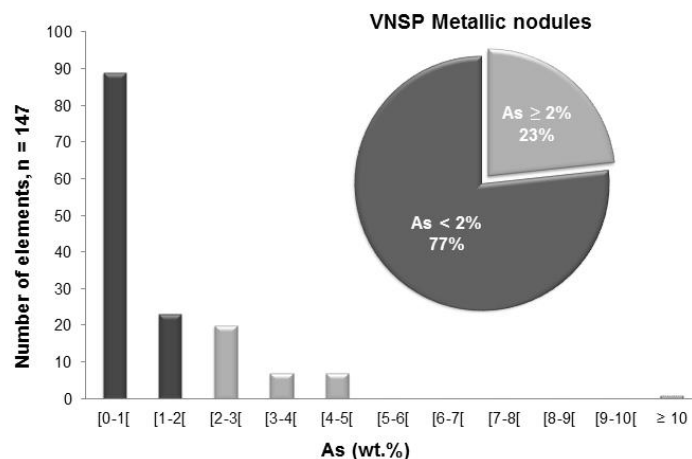
Figure 3.9. Distribution of arsenic content and percentage of metallic nodules below 2% and above 2% As in the metallurgical vestiges from VNSP.

A subset of 16 metallic nodules was selected to further analyses by OM (see Figure 3.10).
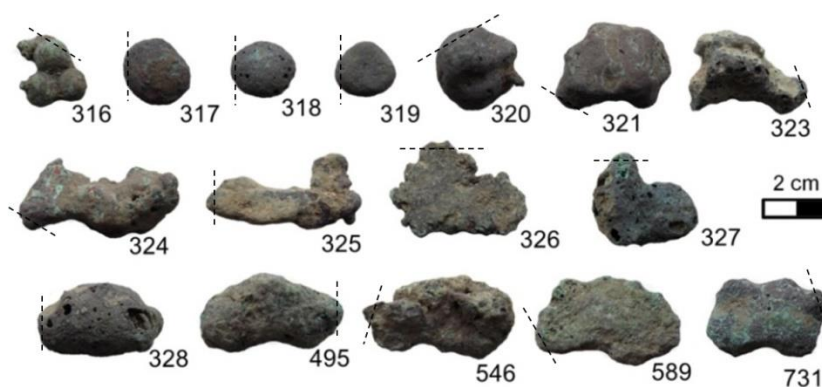
Figure 3.10. Metallic nodules from VNSP collection; dashed lines: sampled location.

The selection was made taking into consideration the less corroded metallic nodules, arsenic content and morphologies. The As-rich phase, identified later in this chapter as the Cu_3As intermetallic compound, is denoted here only by its chemical formula, notwithstanding different structural forms observed in high arsenic coppers (Pereira *et al.*, 2015). For OM observations were included metallic nodules with distinct compositions from pure copper to high arsenic content. Also, examples of two apparent types of shapes present in the collection of metallic nodules (spherical and droplet shape) were included in the final set.

The elemental composition and microstructural characterization of this set are presented in Table 3.4.

Table 3.4. Elemental composition of the metallic nodules determined by micro-EDXRF (wt%). P – prill (smelting origin); D – droplet (melting origin); P/D – inconclusive.

Metallic nodules	Elemental analysis (wt.%)			Phases	Operational sequence	Obs.
	Cu	As	Fe			
VNSP316	99.9±0.1	<0.10	<0.05	α	As-cast	P
VNSP317	97.8±0.2	2.12±0.26	0.06±0.10	α; Cu_3As	As-cast	P/D
VNSP318	98.9±0.1	1.10±0.15	<0.05	α	As-cast	P
VNSP319	99.7±0.1	0.23±0.10	<0.05	α	As-cast	P
VNSP320	98.8±0.1	1.18±0.10	<0.05	α	As-cast	P
VNSP321	98.2±0.1	1.83±0.20	<0.05	α; Cu_3As	As-cast	P
VNSP323	99.9±0.1	0.13±0.10	<0.05	α	As-cast	P/D
VNSP324	99.9±0.1	<0.10	<0.05	α	As-cast	P/D
VNSP325	99.9±0.1	<0.10	<0.05	α	As-cast	P/D
VNSP326	99.6±0.1	0.37±0.10	<0.05	α; Cu_3As	As-cast	P/D
VNSP327	99.6±0.1	0.38±0.10	<0.05	α	As-cast	P/D
VNSP328	99.9±0.1	<0.10	<0.05	α	As-cast	P
VNSP495	96.2±0.3	3.79±0.28	0.06±0.10	α; Cu_3As	As-cast	P
VNSP546	98.8±0.2	1.24±0.14	<0.05	α; Cu_3A	As-cast	P
VNSP589	99.5±0.1	0.45±0.10	<0.05	α	As-cast	P
VNSP731	95.5±0.3	4.42±0.31	<0.05	α; Cu_3As	As-cast	D

These metallic nodules with low iron contents (< 0.05 wt.% Fe) point to a poor reduction environment during the metallurgical operations involved in their production and are indicative of early smelting operations.

While the elemental composition of metallic nodules gives an indication of the type of metal being produced, the microstructure of these nodules can provide indications on the type of metallurgical operations involved in their formation.

The conditions that could suggest a prill produced by a smelting operation are: (i) higher sphericity since a round shape reflects the immiscibility between two liquid phases, slag and metal; (ii) higher amount and volume of gaseous porosities due to greater amount of evolved gas during smelting operations; (ii) coarse microstructure resulting from a slower cooling rate of the nodules inside the smelted slag; and (iv) low proportion or non-existence of Cu-Cu_2O eutectic, indicating reductive conditions. However, the characterization of these metallic nodules is not simple and may be problematic to distinguish a smelting prill from a melting droplet. For example, hammering used for the extraction of the prills from the slag could alter its shape. Also, if the prills were extracted when the slag was still hot, it would allow the introduction of oxygen into the material or differences in the arsenic content of the prills. This operation would alter the deoxidizing effect of arsenic (Hook *et al.*, 1991) and could change the proportion of the Cu-Cu_2O eutectic in the metal.

The optical microscopy observations, based on these parameters, characterize the nodules microstructure (Appendix III) of the selected group in the following categories: P – prill (smelting

origin); D – droplet (melting origin) and S/D - inconclusive (Table 3.4). Furthermore, optical microscopy observations also revealed α and α + Cu_3As phases.

Examples of metallic nodules with morphological characteristics indicative of being produced during a smelting operation are presented in Figure 3.11. These nodules exhibit higher sphericity and coarser microstructures, indicating liquid (metal and slag) immiscibility and low cooling rates. The porosities present in the microstructures also suggest the formation of the nodules from an ore reducing operation (smelting), since it is a process that evolved gas and it is subjected to higher contaminations than a melting operation. On the other hand, a metallic nodule with more irregular shape and finer dendritic structure, suggesting a faster cooling rate, is presented in Figure 3.12. These characteristics are consistent with a small piece of metallic copper that falls from the crucible during a melting or casting operation and cools extremely fast due to the rapid temperature difference and metal small volume. In these cases, the pores present are essentially attributed to solidification shrinkage.
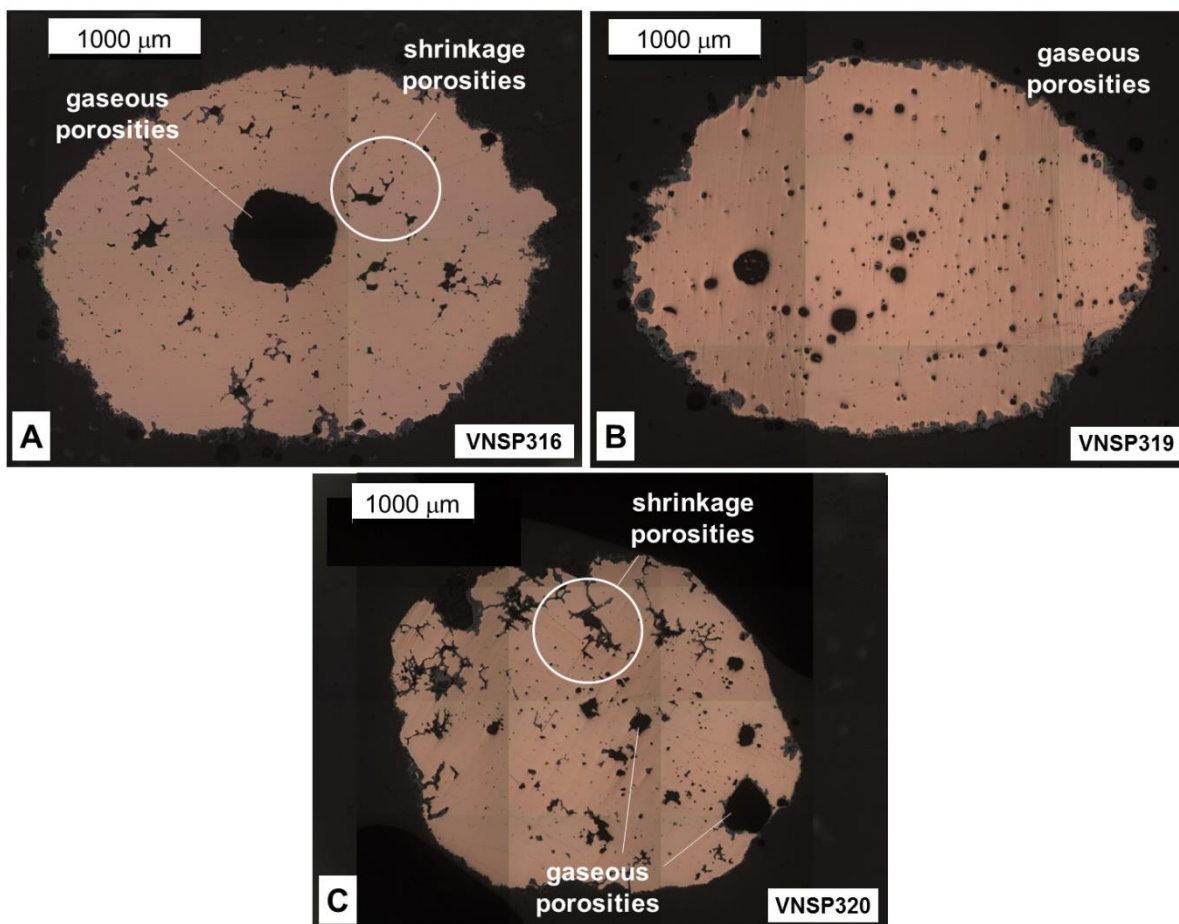
Figure 3.11. A – C: OM images (BF illumination, non-etched) evidencing structures of metallic nodules from VNSP with spherical shapes, evidencing shrinkage and relatively large gas porosities.
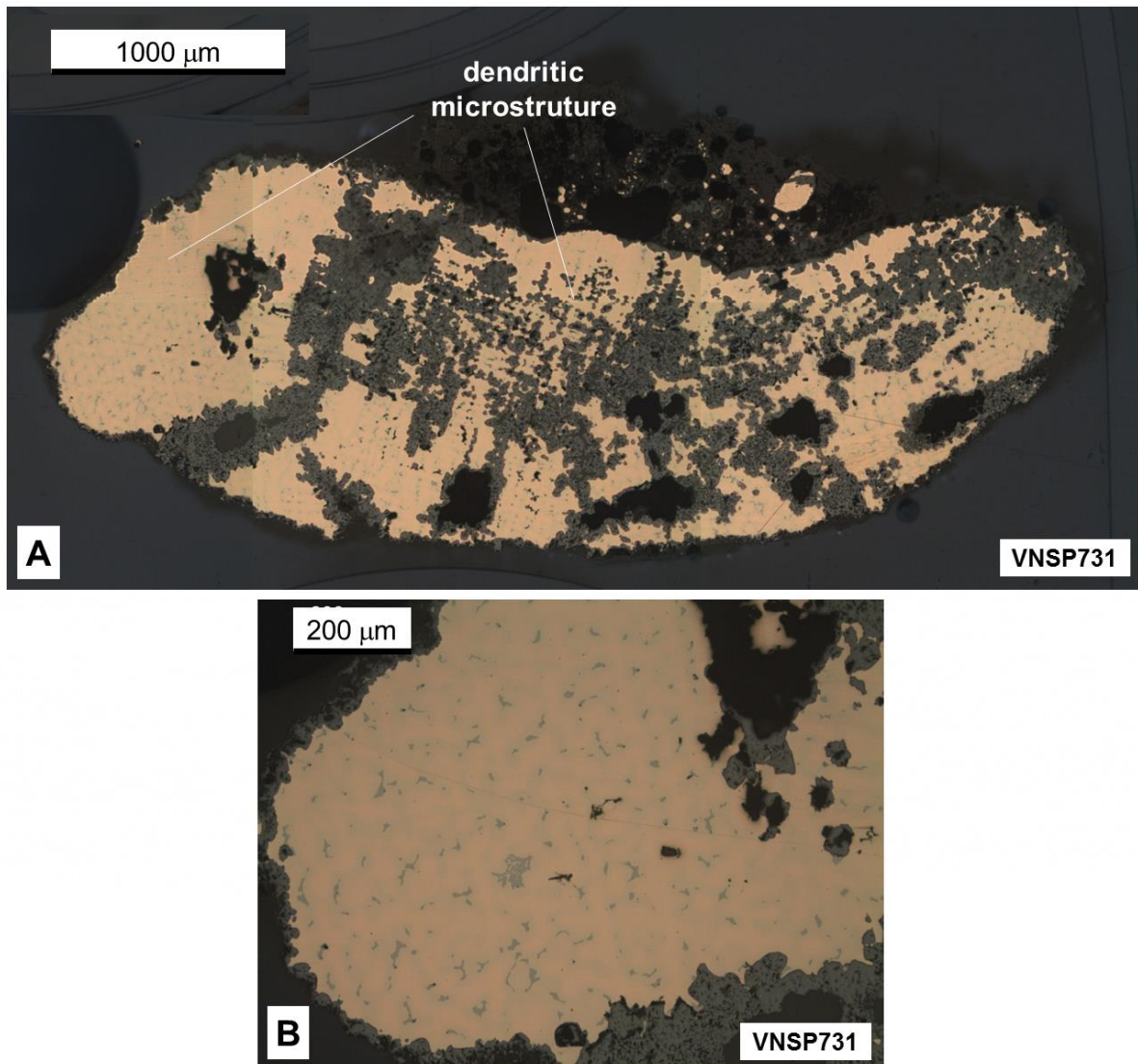
Figure 3.12. A and B: OM images (BF illumination; non-etched) of metallic nodule VNSP731 evidencing microstructure with more irregular shape and fine dendritic microstructure, which suggest a high cooling rate.

3.3. COPPER-BASED ARTEFACTS

In the present study, a significant number of copper-based artefacts with different typologies, part of the VNSP collection that remained unpublished, were analysed. This study intended to determine the involved manufacturing operations, "châine opératoire", to better understand the choices of the Chalcolithic metallurgist and also to assess the arsenic content of copper-based artefacts and to establish its correlation with artefact typologies and functions.

The copper-based collection comprises 37 artefacts with identified typologies (Figure 3.13). The artefact set includes one awl, one wire, chisels, saws, one sickle, one spatula, one knife, daggers, arrowheads (some are Palmela points) and axes. The shape of the dagger VNSP875G stands out from the remaining daggers and most common dagger models from this period. However, a similar

shape is known to be very popular in Chalcolithic Beaker period settlements from Central Europe and also found a parallel in Ciempozuelos, near Madrid in Spain (Rovira *et al.*, 2011).
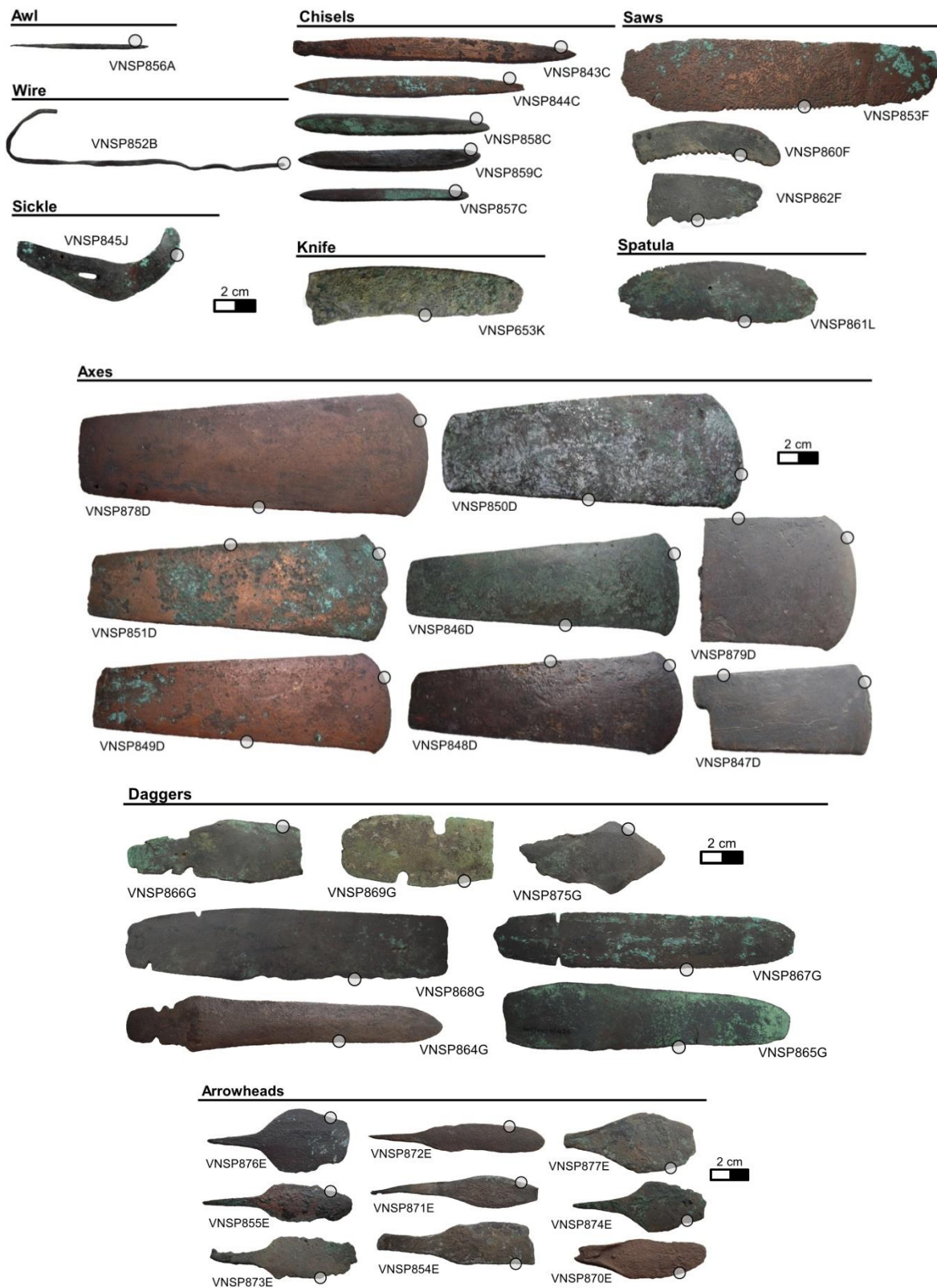
Figure 3.13. Copper-based artefacts collection from VNSP; circles: polished areas for analysis.

To a better systematization and interpretation of the results, the artefact collection was divided into three major groups, according to their probable function: "Tools" (include awl, chisels, saws, one sickle, one spatula and one knife), "Axes" and "Weapons" (include daggers and arrowheads, containing some Palmela points). Axes were grouped separately because it is assumed they could be used either as tools or ingots (Soares, 2005). The group of "Weapons" include artefacts that could be used as weapons for social prestige, although some of them, such as daggers, may have been used as tools in domestic activities (Caramé *et al.*, 2010).

It was considered necessary to analyse more than one area to ascertain about possible particularities in the manufacturing procedures of the axes. For that reason, two areas were prepared for analysis: one near the cutting edge and one in the main axis of the axe. The areas were selected accordingly with the state of conservation of each artefact and takingo into account the stability of the object. All selected areas of the artefacts were manually cleaned to remove corrosion products (see the procedure in subsection 2.2.2).

A summary of the elemental composition determined by micro-EDXRF (wt.%) as well as the results of the microstructural characterization of the metallic artefacts are presented in Table 3.5.

The microstructural observation allowed the identification of the main phases and some typical features (such as coring, annealing twins and slip bands) that allowed to establish the used processing sequence (Figure V.1 in Appendix V).

Micro-EDXRF results indicate that the selected artefacts are composed by copper or copper with arsenic (arsenic contents up to 8.66 wt.%). These results were added to the results obtained from the artefact collection previously studied (see Appendix IV) (Pereira *et al.*, 2013b). As observed in Figure 3.14, 65% of the collection exhibits an arsenic content that could be considered as an impurity (As < 2 wt.%) and the remaining 35% present an arsenic content that could be considered as an alloying element (As ≥ 2 wt.%). The arsenic content distribution is close to the shape of a "geometric distribution", with an average content of 1.86 wt.% As (Figure 3.14).

Iron content is always below the quantification limit (<0.05%) except for dagger VNSP869G that contains 0.06 wt.% Fe. Other minor elements, such as antimony, lead, zinc, nickel or silver, were not detected or are under the quantification limit and, consequently, they were not mentioned in the tables of results.

Table 3.5. Composition of copper-based artefacts from VNSP (content in wt.% average ± standard deviation; n.d.: not detected); microstructural interpretation of the artefacts processing (C: Casting; F: Forging; A: Annealing; FF: Final forging).

Typology	Artefacts	Elemental analysis (wt.%)			Phases	Operational sequence
		Cu	As	Fe		
Awl	856A	96.3±0.6	3.78±0.28	<0.05	$\alpha+Cu_3As$; coring	C+(F+A)
Wire	852B	99.8±0.1	0.20±0.02	<0.05	α	C+(F+A)
Chisels	843C	99.9±0.1	<0.10	<0.05	α	C+(F+A)
	844C	99.9±0.1	<0.10	<0.05	α	C+(F+A)
	857C	99.4±0.1	0.61±0.08	<0.05	α	C+(F+A)
	858C	98.3±0.2	1.64±0.20	<0.05	α	C+(F+A)
	859C	96.3±0.4	3.64±0.35	<0.05	α; coring	C+(F+A)+FF
Saws	853F	99.9±0.1	<0.10	<0.05	α	C+(F+A)
	860F	95.6±0.3	4.36±0.32	<0.05	α; coring	C+(F+A)+FF
	862F	94.4±0.3	5.59±0.26	<0.05	$\alpha+Cu_3As$; coring	C+(F+A)
Sickle	845J	99.9±0.1	<0.10	<0.05	α	C+(F+A)
Spatula	861F	99.9±0.1	n.d.	<0.05	α	C+(F+A)
Knife	863F	99.9±0.1	n.d.	<0.05	α	C+(F+A)
Daggers	864G	95.9±0.2	4.09±0.30	<0.05	$\alpha+Cu_3As$; coring	C+(F+A)+FF
	865G	98.4±0.2	1.56±0.18	<0.05	α; coring	C+(F+A)
	866G	96.9±0.1	2.75±0.05	<0.05	α; coring	C+(F+A)
	867G	99.9±0.1	n.d.	<0.05	α	C+(F+A)
	868G	99.6±0.1	0.32±0.04	<0.05	α	C+(F+A)
	869G	98.9±0.2	1.04±0.18	0.06±0.01	α; coring	C+(F+A)
	875E	91.4±0.4	8.66±0.36	<0.05	$\alpha+ Cu_3As$	C+(F+A)+FF
Arrowheads	854E	97.3±1.1	2.73±0.73	<0.05	$\alpha+ Cu_3As$	C+(F+A)+FF
	855E	97.7±0.6	2.34±0.96	<0.05	α; coring	C+(F+A)+FF
	870E	99.9±0.1	n.d.	<0.05	α	C+(F+A)
	871E	91.8±0.4	8.14±0.36	<0.05	$\alpha+Cu_3As$; coring	C+(F+A)+FF
	872E	98.9±0.2	1.01±0.24	<0.05	α; coring	C+(F+A)+FF
Palmela points	873E	98.7±0.2	1.27±0.2	<0.05	α	C+(F+A)+FF
	874E	97.3±0.2	2.67±0.18	<0.05	$\alpha+Cu_3As$; coring	C+(F+A)
	876E	95.7±0.3	4.2±0.28	<0.05	α; coring	C+(F+A)+FF
	877E	94.8±0.3	5.2±0.26	<0.05	$\alpha+Cu_3As$	C+(F+A)+FF
Axes	846D	99.7±0.1	0.28±0.04	<0.05	α	C+(F+A)
	847D	98.2±0.1	1.84±0.33	<0.05	α; coring	C+(F+A)
	848D	99.9±0.1	<0.10	<0.05	α	C+(F+A)
	849D	99.9±0.1	<0.10	<0.05	α	C+(F+A)
	850D	99.9±0.4	0.11±0.16	<0.05	α	C+(F+A)
	851D	99.9±0.1	<0.10	<0.05	α	C+(F+A)
	878D	99.9±0.1	n.d.	<0.05	α	C+(F+A)
	879D	99.9±0.1	n.d.	<0.05	α	C+(F+A)
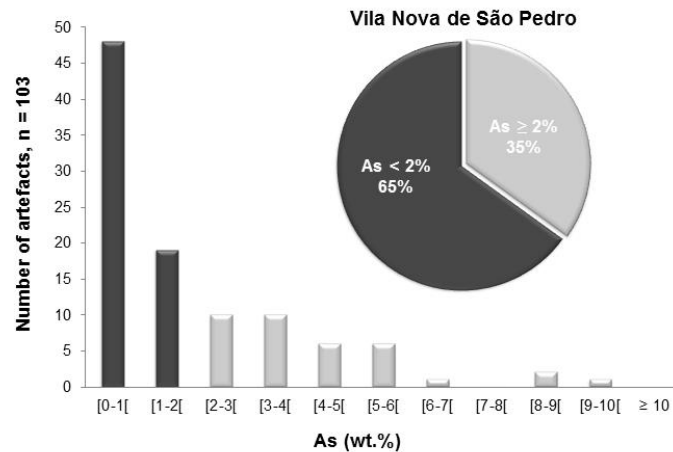
Figure 3.14. Distribution of arsenic in artefacts in VNSP collection.

Assuming a distinction in this collection between copper (< 2 wt. %As) and arsenical copper alloys, the distribution of arsenic content through the groups of typologies shows a tendency for higher levels of this element in the weapons group (Figure 3.15, Left).
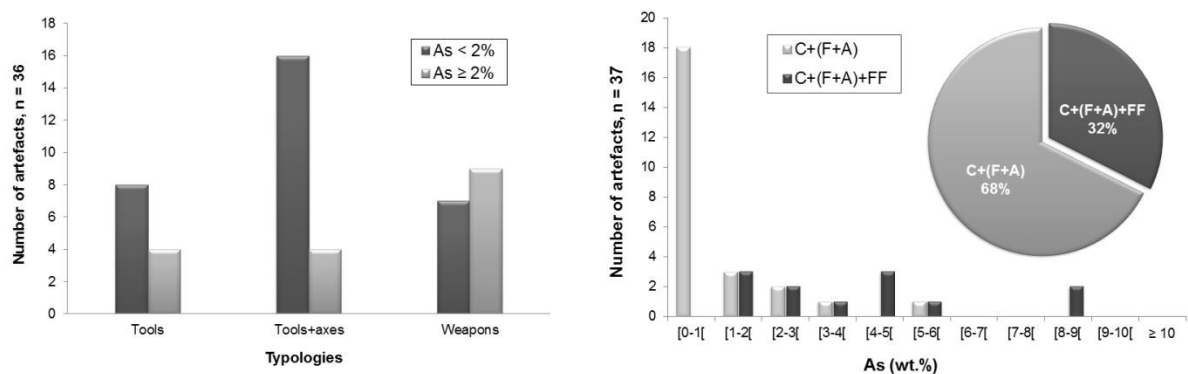
Figure 3.15. Left: distribution of arsenic in the VNSP collection (excluding one wire); Right: distribution of manufacture processes by arsenic content.

A possible association between the presence of arsenic in the alloy and the artefact typology was tested using a Fisher's exact test applied to three groups: "Tools", "Tools + Axes" and "Weapons" (the artefact typologies included in each group were previously described in subchapter 2.1). In the first group it was assumed the hypothesis that axes could be used as ingots, and therefore they were not included in the "Tools" group. An analogous study carried out using similar groups of artefacts from VNSP was added to the collection to obtain a larger sample size (Pereira *et al.*, 2013b). Therefore, to the "Tools" group was added 10 awls, 11 chisels, 3 saws, to the "Axes" group were added 12 axes and to the "Weapons" group were added 7 daggers (see Table 2.1 and Table 2.2).

Results obtained regarding the elemental composition determination by micro-EDXRF and the microstructural characterization from the previous study are presented in Appendix IV.

A statistically significant association was found between the "Weapons" and the presence of arsenic (As ≥ 2 wt.%) (p = 0.029 when comparing "Tools + Axes" and p = 0.027 when comparing "Tools",

excluding axes). A similar result was obtained with the previously studied set of artefacts from VNSP, but the addition of more elements strengthens the analysis. Consequently, it can be hypothesized that there was an intentional selection of an arsenical copper alloy (As ≥ 2%) for the manufacture of this set of weapons.

The microstructural characterization of these artefacts by OM and SEM-EDS is summarized in Table 3.6. In Appendix V is presented OM image of each artefact from the collection analysed, in BF illumination and etched.

The most common microstructural features found were near-equiaxed α-Cu grains with annealing twins (Figure 3.16, A, C and D) and, more rarely, slip bands (Figure 3.16, B). The annealing twins appear after a metal has been subjected to mechanical work and softened by heat treatment. Slip bands appear in the cold work condition without posterior heat treatment. Therefore, from the microstructural analysis, it can be inferred that the majority of the artefacts from VNSP (68%) were manufactured with forging plus annealing operations (Figure.3.15, Right, pie chart). The operational sequence of forging plus annealing, followed by final forging operation was applied to 32% of the artefacts. The results also point out to an association between the presence of final forging treatment and artefacts presenting higher arsenic content (As ≥ 2 wt.%) (Figure 3.15, Right).

Once again, the microstructural data obtained in a previous study of VNSP were added to the present observations (Pereira *et al.*, 2013b). The combined data was tested using the Fisher's exact test for association between the presence of final forging treatment and As-richer artefacts (As ≥ 2 wt.%). A statistically significant association was found in the tested group (p = 0.0003). Therefore, the application of a final forging operation on the manufacture of artefacts presenting higher arsenic contents, and therefore with a different colouration from pure copper, could be justified to obtain a harder alloy. Another hypothesis would be the application of a finishing operation with the only intention of improving the surface aspect after annealing. These results suggest that As-rich alloys would have been recognzed and selected for an application requiring a final forging treatment.

It must be taken into consideration that we are only observing a small cleaned area of the artefact; two regions in axes (see Figure 3.13), and these could not be entirely representative of the artefact microstructure. For instance, the identification of final forging treatment, which was possibly not applied to the entire artefact, could be missing.
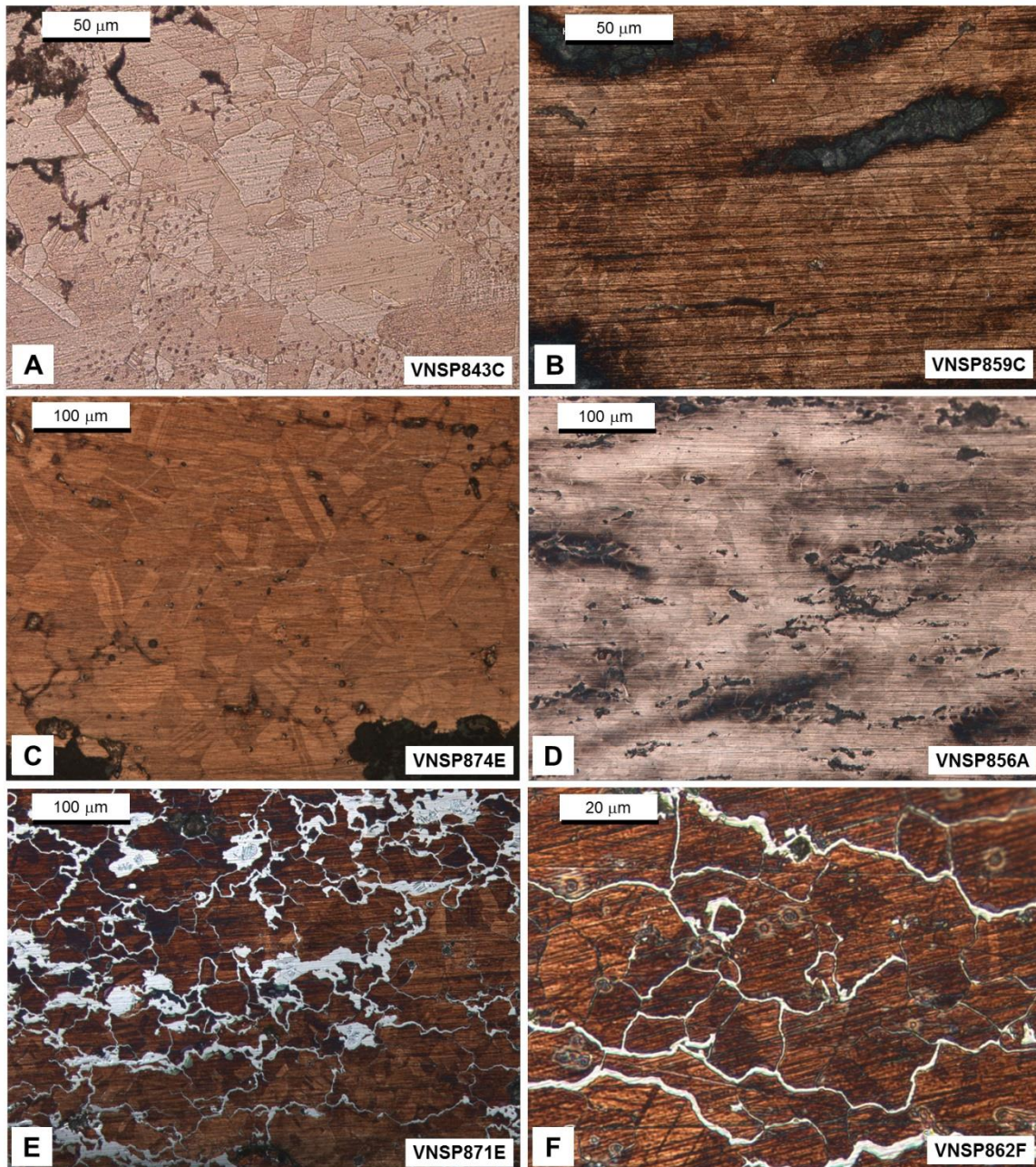
Figure 3.16. OM images of: A: chisel VNSP843C (As < 0.10 wt.% As); B: chisel VNSP859C (3.64 wt.% As); C: arrowhead VNSP874E (2.67 wt.% As); D: awl VNSP856A (3.78 wt.% As); E: arrowhead VNSP871E (8.14 wt.% As); F: saw VNSP862F (5.59 wt.% As) (all BF illumination, etched).

For copper or lower arsenic content artefacts, a commonly observed feature was the presence of inclusions, identified by SEM-EDS (Figure 3.17) as being a Cu-O compound and assigned as cuprous oxide (Cu_2O). These inclusions are formed due to a eutectic decomposition in Cu-O systems. This Cu-O eutectic appears as an interdendritic network of oxide inclusions in the α-Cu matrix, and it was observed in some microstructures (Figure 3.16, A). The finer, aligned and elongated shapes of the above mentioned oxides observed in some of the microstructures are usually a consequence of the thermomechanical treatments applied. As expected, the presence of cuprous oxide inclusions in

copper-arsenic alloys is much reduced due to the deoxidizing properties of the arsenic (Hook *et al.*, 1991) (Figure 3.16, B-D).

A common consequence of non-equilibrium solidification in copper-arsenic alloys is the coring (compositional gradient) in the primary α-phase grains. Intense mechanical work elongates these features resulting in what is normally designated as segregation bands, clearly visible after etching (Figure 3.16, B and D). In some samples, a blue-grey phase observed by OM and identified by SEM-EDS (Figure 3.17, A) as the Cu_3As intermetallic compound (Figure 3.16 E and F) was observed along the α-copper grain boundaries. These arsenide formations will be carefully analysed and interpreted in the section 3.5.
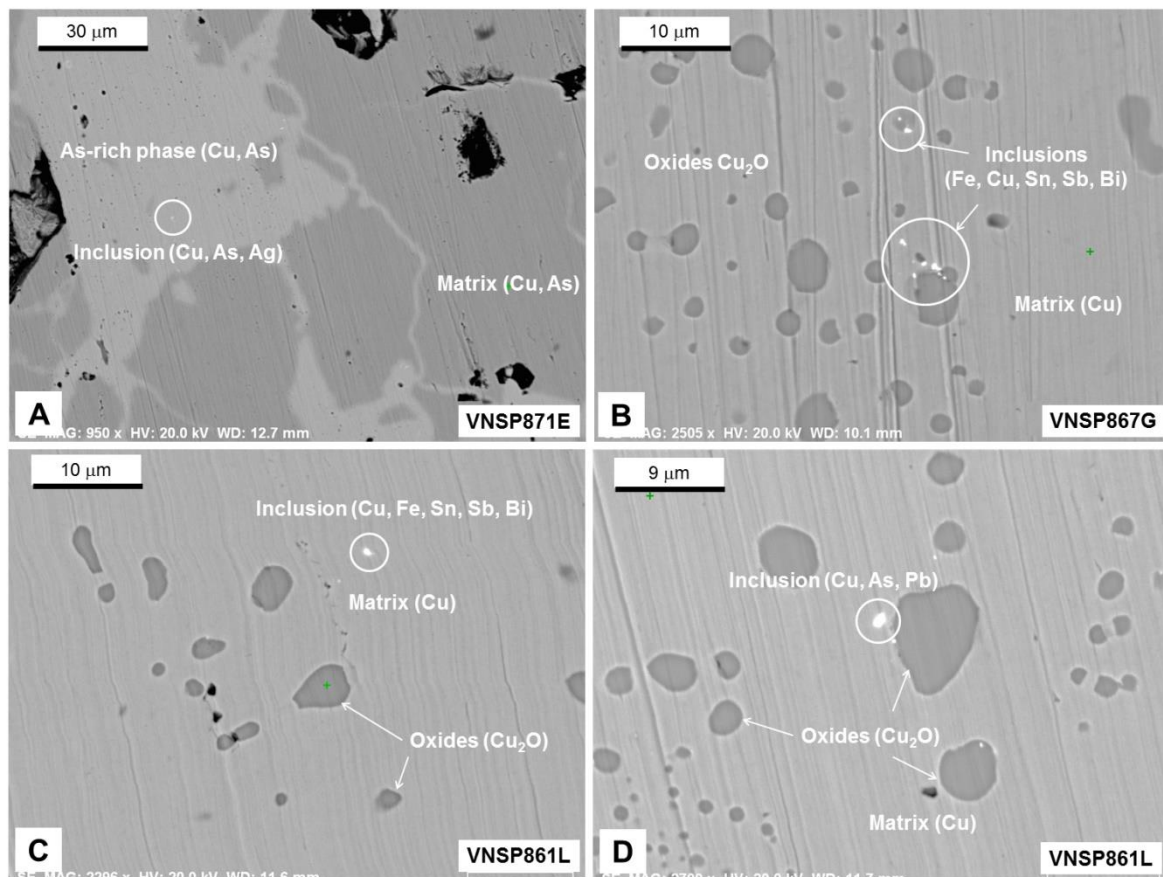
Figure 3.17. SEM-BSE image of: A: arrowhead VNSP871E (8.14 wt.% As) presenting the EDS identification of Cu_3As (As-rich phase) and a metallic inclusion composed of Cu, As and Ag; B: dagger VNSP867G (As content n.d.) presenting the EDS identification of Cu_2O oxides and metallic inclusions composed of Fe, Cu, Sn, Sb and Bi; C and D: spatula VNSP861L (As content n.d.) presenting the EDS identification of Cu_2O oxides, a metallic inclusion composed of Fe, Cu, Sn, Sb and Bi and a metallic inclusion of Cu, As and Pb.

The microstructure identified (near-equiaxed α-Cu grains with annealing twins) and hardness obtained in the cutting edges of axes (between 45 HV0.2 and 95 HV0.2) and corresponding central areas (41 HV0.2 to 64 HV0.2) from a previous study of artefacts from VNSP, seem to indicate that the increase of hardness is a consequence of more work applied to the shaping of the cutting edge than to intentionally produce a harder tip of the object (Pereira *et al.*, 2013a).

However, some marks displayed on the cutting edge of the axes analysed in the present study may indicate that the final obtained hardness, even if not intentionally obtained, was enough to its use as a tool. The thin corrosion products layer and apparently stable corrosion processes allow a more detailed observation of the surface of the blade of axe VNSP847D (1.87 wt.% As) (Figure 3.18). In this axe, there are several visible marks on the cutting edge that could be attributed to a largely used tool. However, the nature and extent of their use before deposition is widely varied and very difficult to access (Roberts and Ottaway, 2003).
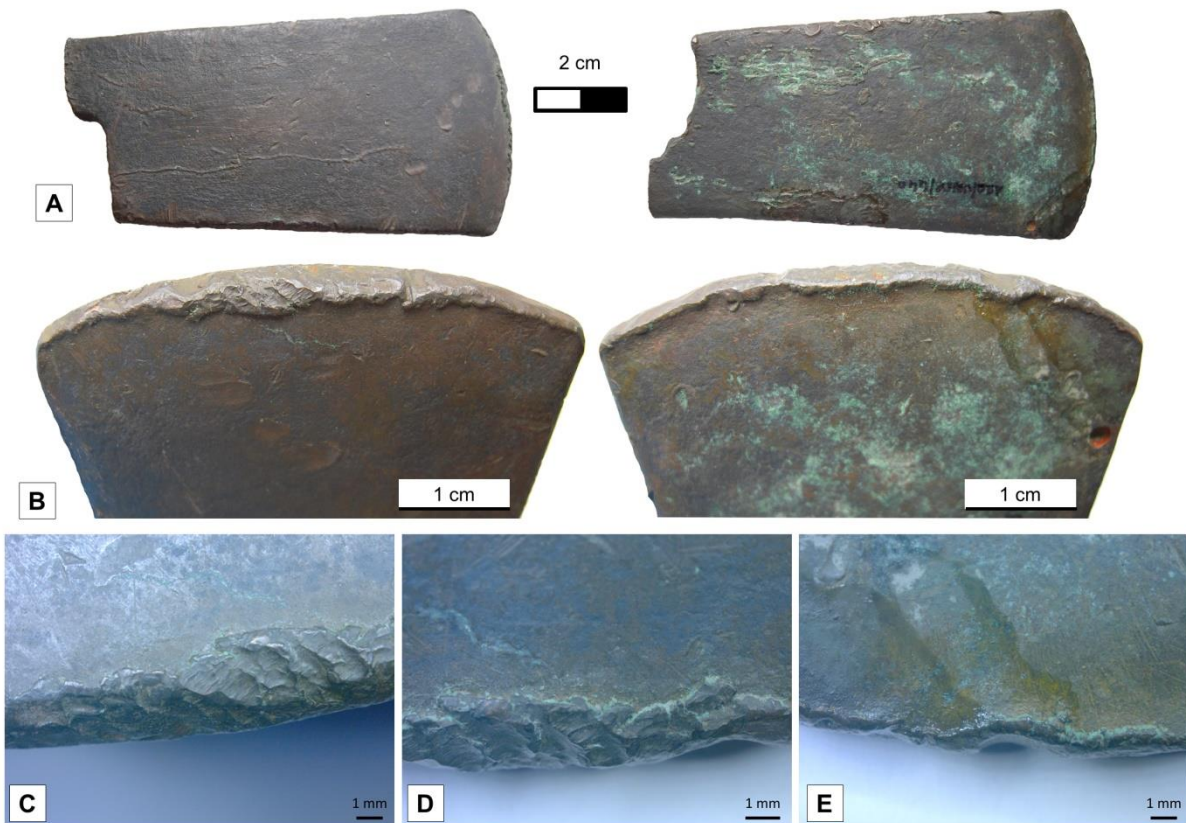
Figure 3.18. Binocular images of axe VNSP847D (1.84 wt.% As): A: view from both sides; B: detail of the cutting edge from both sides; C-E: details of the cutting edge marks.

The next section is dedicated to the use of the copper wires found in the VNSP as a probable intermediate product.

3.4. INTERMEDIATE PRODUCTS: WIRES

VNSP assemblage included three wires with no apparent function. One wire was characterized in the above subsection, and the other two wires belong to the collection from VNSP artefacts previously studied (Pereira *et al.*, 2013a). A summary of the elemental composition determined by micro-EDXRF, microstructural interpretation and Vickers microhardness testing of the metallic wires is presented in Table 3.6.

Table 3.6. Characterizations of the wires from VNSP (C: Casting; A: Annealing; F: Forging; FF: Final Forging).

Wires	Cu (wt%)	As (wt%)	Fe (wt%)	Phases	HV0.2 centre	blade	fract.	Operational Sequence
VNSP123B	99.8±0.1	0.21±0.01	<0.05	α	84	-	-	C+(F+A)
VNSP124B	99.8±0.1	0.19±0.01	<0.05	α	91	-	-	C+(F+A)
VNSP852B	99.8±0.1	0.20±0.02	<0.05	α	-[a]	-	-	C+(F+A)

[a] Vickers microhardness testing was made only in mounted cross-sections (HV0.2).

Micro-EDXRF results indicate that the wires are made of copper with low arsenic content, close to 0.20 As wt.%. Iron content is always below the quantification limit (<0.05 wt.%). Other minor elements such as antimony, lead, zinc, nickel or silver were not detected or under the quantification limit and, consequently, they are not mentioned in the table of results.

Their approximate length is between 10 cm to 20 cm and present a rectangular section (Figure 3.19). In the surface of all wires are visible incision marks, sometimes double incisions (see Figure 3.19, C).

The microstructural characterization of the wires cross-sections show near-equiaxed α-Cu grains with annealing twins indicating that forging and annealing operations were applied in their manufacture (Figure 3.19, E – I). Another feature typical of the lower arsenic content artefact was the presence of copper oxide inclusions (Cu_2O). In the three wires, these inclusions are elongated by deformation in the same direction, revealing a hammering operation intending to produce a sheet. However, an unusual characteristic observed was a change of shape of the copper grains and oxide inclusion orientations next to the smaller sides of the rectangular cross-section (Figure 3.19, G and I). This change of orientation is compatible with a break-in cut (or cutting break). Therefore it can be hypothesized that these wires could have been cut from a metal sheet and the incisions are some longitudinal notch to position the cut.

These wires would be in that case an intermediate material to further thermomechanical shaping.
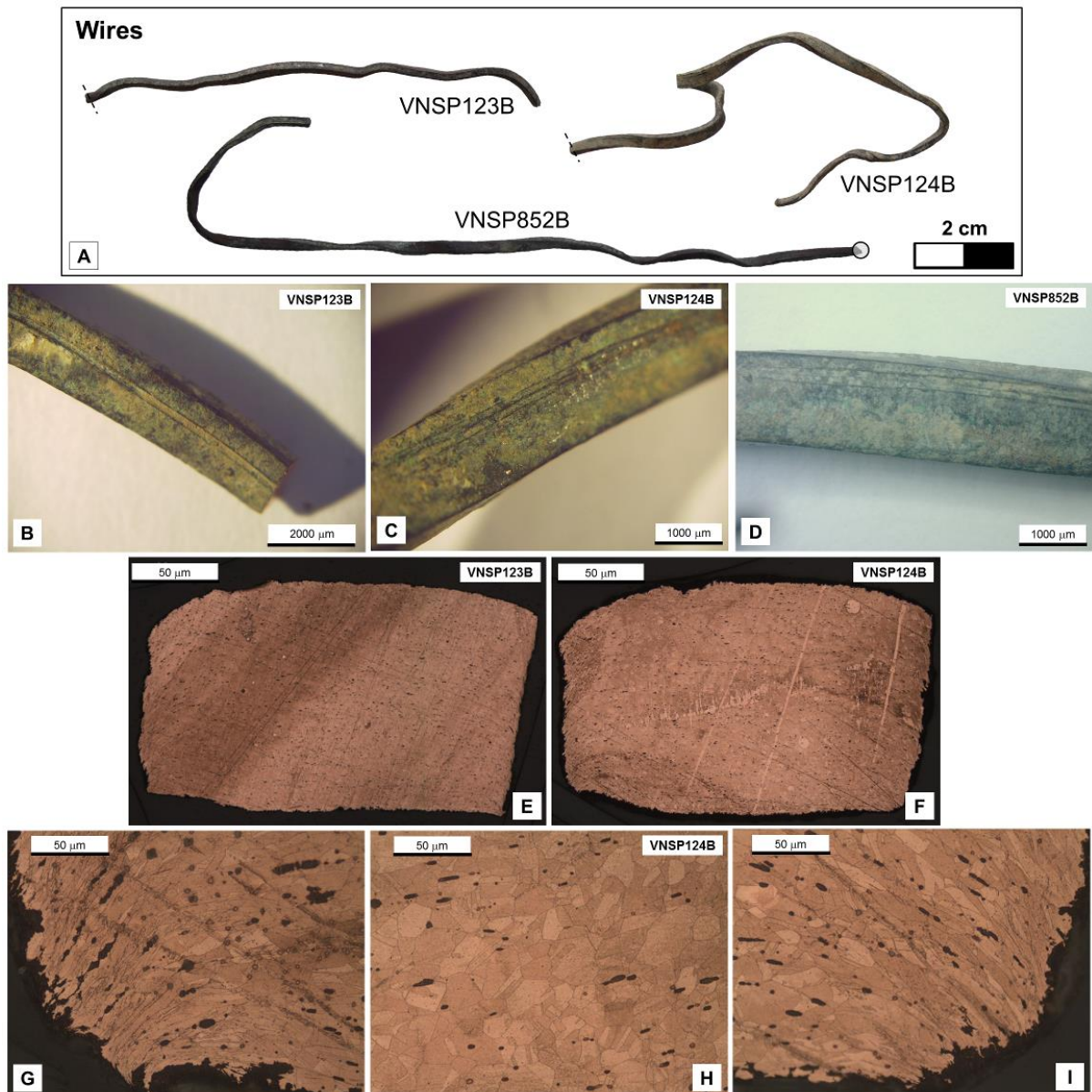
Figure 3.19. A: Wires from the VNSP collection with localization of observation (dashed lines: sampled locations; circles: polished areas); B-D: Binocular images evidencing the detail of the notches in the surface for each wire; E-I: OM images evidencing microstructure (BF illumination, etched).

A previous study describes the manufacture of wires (Asderaki and Rehren, 2008). In this case, several gilded wreaths, dated from the middle 4th up to 2nd centuries BC, were found in the cemetery of the ancient Demetrias in Volos (Greece). They were studied to understand their manufacturing techniques as well as the composition of the metals used and gilding techniques. The wires were made from pure copper which was easy to hammer into thin sheet metal and then cut into strips using chisels. Similar to the VNSP wires, OM observations of the wires showed the copper oxides inclusions elongated and parallel to the long edge of the rectangular section, reflecting the mechanical deformation of the metal. The etched sample shows an annealed, recrystallized texture of copper grains with no preferential orientation in the centre. At the edges, the deformation pattern indicates the flow of the metal made by the chisel (Asderaki and Rehren, 2008).

As previously mentioned, the microstructure analysis provides some insight into the manufacturing processes of the objects. Few studies approach this subject, but it seems possible that in the Chalcolithic period in the Estremadura region, some copper sheets were manufactured and cut into rectangular or square cross-section wires (intermediate product) and therefore shaped into objects with a similar cross-section. The tools necessary for this operation are not fully understood, but it would be possible to cut a pure copper sheet into strips of metal with a flint chisel.

The microstructural characterization from previously studied examples seems to indicate thermomechanical operations to shape a rectangular cross-section into a rounder section used in several typologies. Possible uses for this intermediate material would be awls and fishhooks since the composition and dimensions are compatible (examples in Figures 3.20).
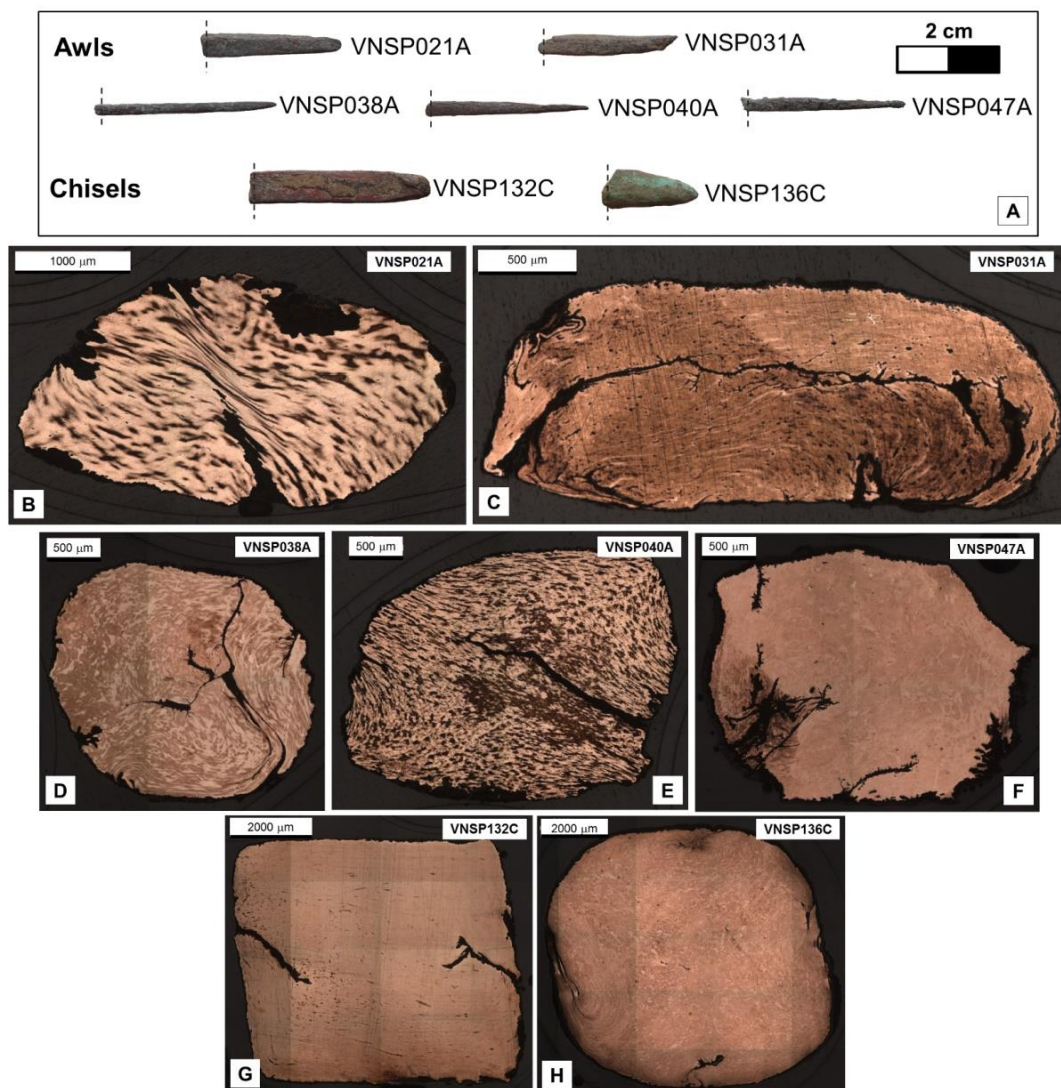
Figure 3.20. A: Examples of artefacts from VNSP copper-based artefact collection (dashed lines: sampling locations), presenting microstructure orientation of grains evidencing a manufacturing intermediate from square or rectangular section into oval or circular sections (B – H: OM images BF illumination; etched).

Although chisels usually present a cross-section too large to be produced from an intermediate material, such as the wires above presented, they were most likely manufactured from a square or rectangular metallic bar (Figure 3.20, G and H).

Fishhooks present in the OR artefact collection possibly also use wires as an intermediate material. A detailed discussion is presented in Chapter 5.

To better understand arsenical copper alloys, two additional sub-sections were performed in this thesis. One study aimed to characterize the arsenic-rich phase present in the microstructure of copper-based artefacts with higher arsenic content. The second study intent to characterize the resultant colour of alloys with increasing arsenic content by spectral colorimetry. Since these studies required resin mounted samples, they were performed in a collection of artefacts from VNSP previously presented (Pereira *et al.*, 2013a).

3.5. AS-RICH PHASE IDENTIFICATION [3]

The presence of arsenic could cause the microstructure of as-cast archaeological arsenical copper artefacts to exhibit two main types of features: coring of primary α-Cu phase grains and, in arsenic richer alloys (arsenic content above 1 - 2 wt.%), the occurrence of a second phase consisting of silvery arsenides (Budd, 1991; Northover, 1989; Ravič and Ryndina, 1984). Post-casting processing, such as thermomechanical treatments, could further alter the quantity and distribution of both these features. Concerning the arsenide formations observed in arsenical copper alloys, it is well recognized that they have a chemical formula close to Cu_3As and these often appear as a continuous network in the microstructure.

There are two explanations for these formations in Cu-As alloys with arsenic contents lower than 7.96 wt.% As (see Cu-As equilibrium phase diagram in Figure 1.2, Right). One explanation states that these arsenide formations should result from non-equilibrium solidification. In some cases, due to an intense inverse segregation phenomenon, this non-equilibrium response can produce silvery surfaces in the cast objects (Giumlia-Mair, 2008; Scott, 1991; McKerell and Tylecote, 1972). Other interpretation is that an important portion of the observed arsenides is formed as a consequence of a long-term precipitation during archaeological times from an As-supersaturated α-Cu phase matrix (Budd and Ottaway, 1995; Budd, 1991).

However, these interpretations for the arsenical copper microstructures are not fully met by the known equilibrium phase diagrams (Okamoto, 1991; Subramanian and Laughlin, 1988; Hawkins *et al.*, 1973; Smithells, 1962). For instance, the solidification of hypoeutectic Cu-As alloys should lead to the formation of the α-Cu+Cu_3As eutectic, but instead, it is often observed pure arsenide formations (Cu_3As) (Budd, 1991). Also, the solubility of arsenic in α-Cu phase presented by those diagrams does not significantly change with temperature. This makes the proportion of Cu_3As observed in some

---

[3] This section was previously published (Pereira *et al.*, 2015).

thermomechanically processed low arsenic-bearing alloys (Valério *et al.*, 2016b; Valério *et al.*, 2014; Pereira *et al.*, 2013a;) difficult to explain, since, for these contents, annealing should dissolve any excess of copper arsenides (formed in non-equilibrium conditions) into the α-Cu phase.

To understand the arsenide formations in arsenical copper alloys, it is important to overview the available information concerning the phase diagrams for the Cu-As system.

Some phase diagrams published for the Cu-As system (Pei *et al.*, 1994; Teppo and Taskinen, 1991) were built up based on thermodynamic models. Inferred phase diagrams can be very unrealistic if the thermodynamic model or data used are inappropriate (Okamoto, 1991). Therefore they will not be considered in the present study. In a review of the Cu-As system, Subramanian and Laughlin (1998) proposed an equilibrium phase diagram based directly on the known experimental data. According to their phase diagram (Figure 1.2, Right); two intermetallic arsenides are likely to occur at low temperatures. These phases are assigned as β and γ in this phase diagram.

According to these authors, the β phase should have a stoichiometry between Cu_6As and Cu_9As and is formed by a peritectoid reaction around 325 ºC. The inclusion of the β phase in the binary diagram was done with some caution concerning its temperature range stability since it is difficult to synthesize and even harder to stabilize at room temperature. X-ray diffraction measurements assigned the chemical formula of this arsenide to Cu_6As, with Pearson symbol hP2 and space group P63/mmc (Naud and Priest, 1972).

The γ phase, with chemical formula close to Cu_3As, crystallizes in a hexagonal structure, with Pearson symbol hP24 and space group $P\bar{3}c1$ (Bengough and Hill, 1910). It is the intermetallic arsenide obtained by casting processes of Cu-As alloys (Skinner and Luce, 1971). It was also reported a high-temperature form for Cu_3As, also with a hexagonal structure (Pearson symbol hP8 and space group $P6_{3/mmc}$) (Bengough and Hill, 1910). According to Subramanian´s and Laughlin´s review (1998), this was the only report of the existence of a high-temperature form for Cu_3As. Furthermore, this high-temperature phase was not confirmed in subsequent investigations of the Cu-As system.

Disregarding the controversial existence of β phase at room temperature, the α-Cu phase can dissolve up to approximately 6 wt.% As at room temperature without precipitation of the γ arsenide (see Figure Figure 1.2, Right).

In the present study, we intended to understand the formation process of the arsenide phases observed in prehistorical arsenical copper artefacts. With that purpose, artefacts with relatively high arsenic contents (As > 5 wt.%) and in which significant arsenide segregations are to be expected, were characterized. Therefore, the metallic set selected for this study was composed of four artefacts in fragmentary condition (see Figure 3.21) from VNSP (Pereira *et al.*, 2013a).
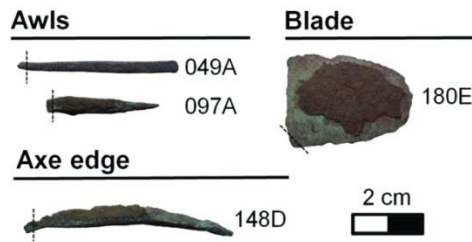
Figure 3.21. Analysed artefacts from VNSP; dashed lines: sampling locations.

Since the artefacts were in a fragmentary state, it was possible to apply a small sampling with a minimum impact on their shape (sampling locations indicated by dashed lines in Figure 3.21) and fixed them in an epoxy resin before metallographic preparation (a detailed procedure is presented in subsection 2.2.2).

These artefacts were characterized by micro-energy dispersive X-ray fluorescence spectrometry, optical microscopy, scanning electron microscopy with X-ray microanalysis, micro-X-ray diffraction and synchrotron radiation micro- X-ray diffraction.

A summary of the elemental composition determined by micro-EDXRF (wt.%) and also the results of the microstructural characterization of the metallic artefacts are presented in Table 3.7.

Table 3.7. Elemental composition and microstructural characterization (C: Casting; A: Annealing; F: Forging; FF: Final Forging; ↓: Low amount).

Typology	Artefact	Cu (wt.%)	As (wt.%)	Fe (wt.%)	Phases	Operational Sequence
Awl	VNSP049A	94.2±0.1	5.59±0.08	<0.05	α-Cu, Cu_3As	C+(F+A)
Awl	VNSP097A	93.7±0.1	6.04±0.11	<0.05	α-Cu, Cu_3As	C+(F+A)+FF↓
Axe	VNSP148D	90.6±0.2	9.13±0.23	0.07±0.01	α-Cu, Cu_3As	C+(F+A)
Blade	VNSP180E	94.2±0.4	5.57±0.38	<0.05	α-Cu, Cu_3As	C+(F+A)+FF↓

Micro-EDXRF results indicate that the selected artefacts were made of copper with arsenic (5.57 < As wt.% < 9.13). Iron content was always below the quantification limit (< 0.05 wt.%) except one artefact presenting 0.07 wt.% Fe (axe VNSP148D). Other minor elements such as antimony, lead, zinc, nickel or silver were not detected or were under the quantification limit and, consequently, are not mentioned in the table of results (Table 3.7).

Near-equiaxed α-Cu grains with annealing twins and, more rarely, slip bands were the common microstructural features found (Figure 3.22). The annealing twins reveal that the alloy has been mechanically worked and softened by post-heat treatments. On the other hand, slip bands appear in the cold work condition without posterior heating. No significant coring effects were observed in the samples, revealing that annealing temperatures should be higher than 600-700ºC to remove these cast-in features (Northover, 1989). A coloured grey constituent was also observed (Figure 3.22). According to microscopy observations, these grey formations present two different morphologies:

thicker formations (drawing roughly parallel formations with irregular thickness, sometimes forming a banded structure visible under etching conditions with different shades of grey) and thinner formations (appearing more homogeneous and regular). These grey constituents were later analysed by SEM-EDS and proved to be the copper arsenide with chemical formula close to the Cu_3As in both morphologies (see Figure 3.23).

As mentioned above, there are two basic morphological types of arsenides, depending on their thickness. These types of formations are hardly associated with the eutectic transformation since they do not show a biphasic structure. However, thicker arsenide formations should be related to non-equilibrium casting features, like strong coring and segregation that further annealing heat treatments were unable to eliminate completely. The thinner arsenide formations can be observed around grain boundaries of recrystallized grains. Recrystallization annealing only occurs after thermomechanical processing. Therefore, when these post-casting arsenide formations occur, they can only be explained by solid-state transformations. Consequently, these types of arsenide formations reinforce the idea that long-term ageing over archaeological time should precipitate the copper arsenide in the α-Cu phase grain boundaries due to arsenic segregation from a supersaturated solid solution at low temperatures.
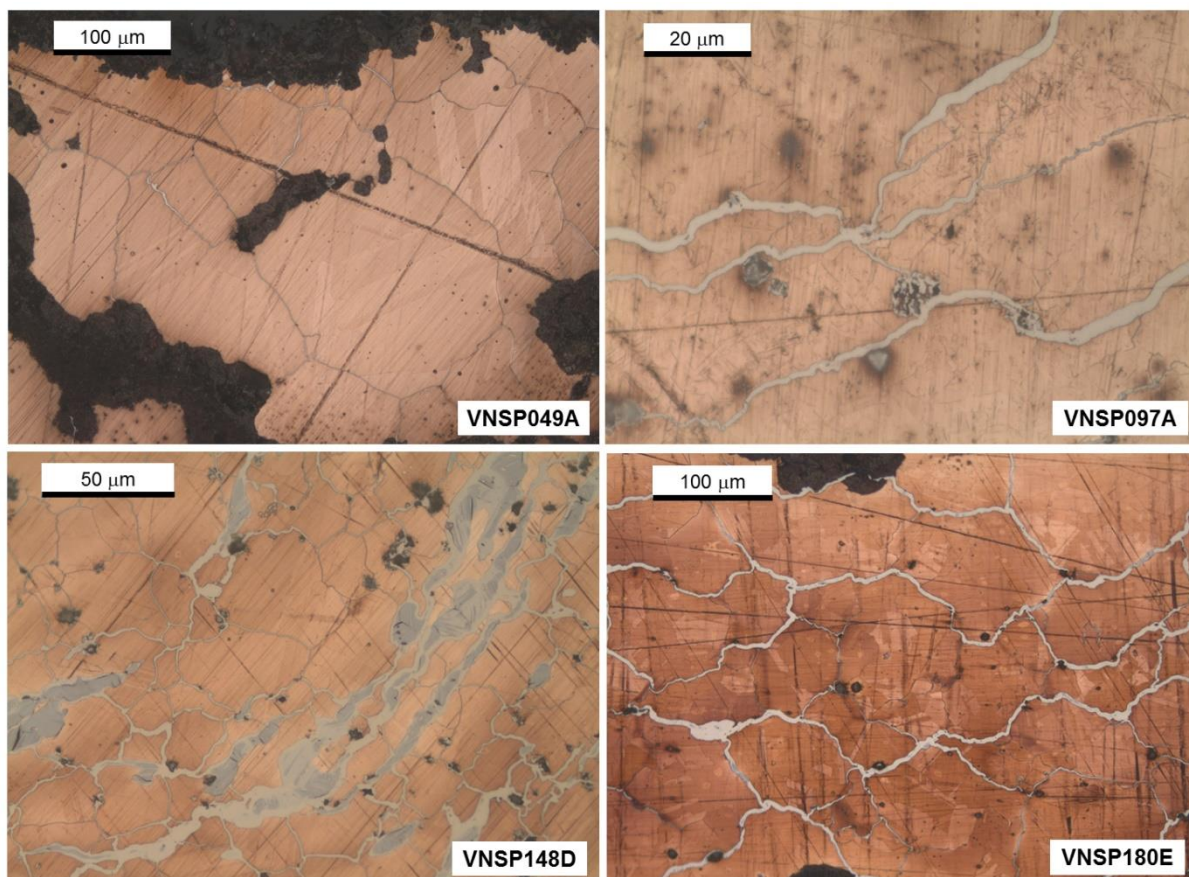
Figure 3.22. OM images of the artefacts revealing the main microstructural features (all BF illumination and etched); VNSP097A, VNSP148D and VNSP180E images show thicker arsenide formations; VNSP148D image also evidences the thicker arsenide formations two blue-grey tones; VNSP049A, VNSP148D and VNSP180E show thinner arsenide formations around annealed grains.
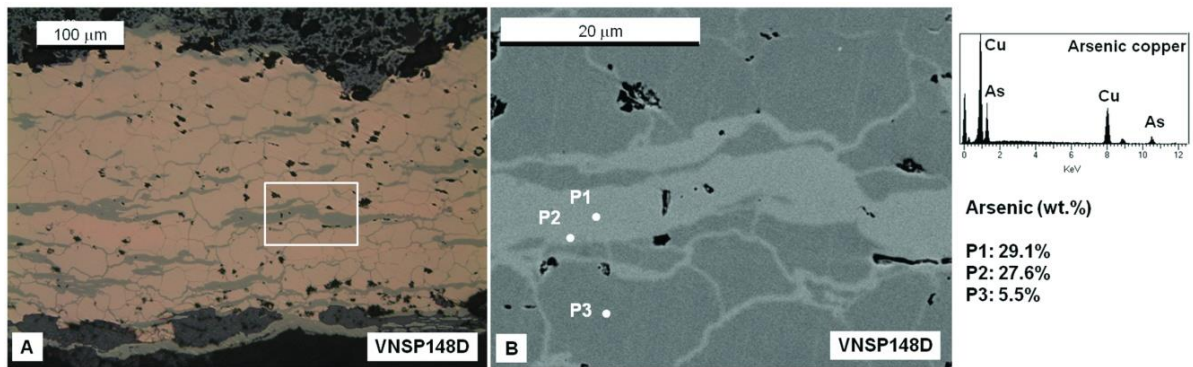
Figure 3.23 A: OM image of axe VNSP148D revealing a thicker arsenide formation following the grain boundaries (BF illumination; non-etched); B: SEM-BSE image of a detail of area signalized in A; P1, P2 (intermetallic/matrix), and P3 (α-Cu matrix) mark the EDS analysis spots.

In the case of VNSP148D, examined by OM, it was observed in the thicker arsenide formations two blue-grey tones (darker grey in central regions) (Figure 3.22). Unlike OM, backscattering SEM observations (BSE) does not reveal any contrast between the two regions (Figure 3.23, A). Since BSE images are associated with a high atomic number contrast, these observations indicate that they should have a similar composition.

SEM-EDS semi-quantitative spot analyses were also performed in this sample to allow a better elemental characterization of those microstructural features. The arsenide presented a composition of 29.1 wt.% As (25.8 at.% As) in a central (spot P1) and 27.6 wt.% As (24.4 at.% As) near the arsenide/matrix interface (spot P2). The As content of spot P2 should be underestimated by the α-Cu phase vicinity. For the α-Cu matrix (spot P3) the arsenic content obtained is 5.5 wt.% (4.7 at.% As) (Figure 3.23). The spot analyses confirm a copper arsenide with chemical formula close to that of Cu_3As. The α-Cu matrix analysis shows an arsenic content slightly lower than predicted by current Cu-As phase diagrams (Predel, 2006; Subramanian and Laughlin, 1998; Teppo and Taskinen, 1991).

A summary of the phases identified by micro-XRD results is presented in Table 3.8.

Table 3.8. Micro-XRD results (P: Present).

Typology	Artefact	Matrix α-Cu	Cuprite Cu_2O	cubic Cu_3As	hexagonal Cu_3As
Awl	VNSP049A	P	P	P	-
Awl	VNSP097A	P	P	P	-
Axe	VNSP148D	P	P	P	P
Blade	VNSP180E	P	P	P	-

Surprisingly, micro-XRD analyses identified the arsenide as cubic Cu_3As, alongside with α-Cu phase, cuprite (Cu_2O) and minor corrosion products in all samples. Only axe VNSP148D shows the expected hexagonal Cu_3As besides the cubic Cu_3As.

The arsenide structures were also analysed by X-ray diffraction experiments on VNSP148D, carried out at HEMS beamline at PETRA III (Figure 3.24). The XRD results confirm the presence of both intermetallic types of Cu_3As (cubic and hexagonal phases) in this artefact.
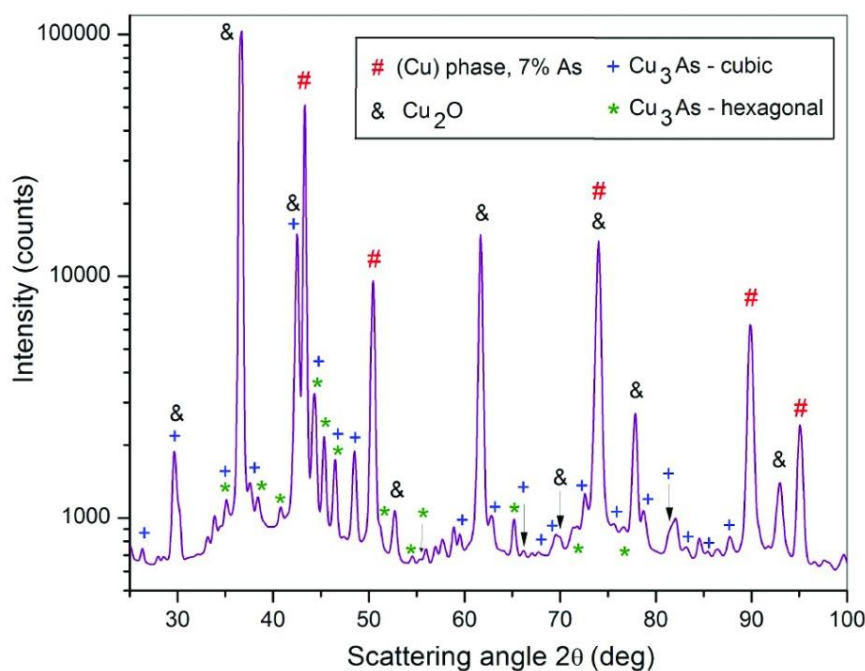
Figure 3.24. Synchrotron radiation-based XRD data obtained for VNSP148D.

Therefore, since the hexagonal Cu_3As is only clearly observed in the arsenic richer artefact, this arsenide form should be part of as-cast formations, not re-dissolved in the α-Cu matrix at the time of its production, and prevailing at lower temperatures in a metastable condition until today. On the other hand, the cubic Cu_3As, since it is observed in all artefacts, should be related to the arsenide fraction precipitated by natural ageing (slow evolution to a more stable condition) during thousands of years in a burial context.

The present identification of a cubic Cu_3As in these archaeological samples help to clarify some differences between metallurgical and mineral interpretations of the Cu-As system. Mineralogical information about copper arsenide deposits is important since this data could be useful to understand the implications of the slow atomic diffusion and sluggish phase transformations in this system at low temperatures. Regarding mineralogical data, the most common natural occurrence form of Cu_3As is designed as α-domeykite or "mineral domeykite" (Heyding and Despault, 1960). The α-domeykite exhibits a cubic structure, and it was assigned to space group $I\bar{4}3d$ (Iglesias and Nowacki, 1977). It has been stated that this mineral decomposes on heating at 225 ºC into β-domeykite and algodonite (Heyding and Despault, 1960). From a crystallographic point of view, the mineral β-domeykite, also called "artificial domeykite", corresponds to the intermetallic γ phase represented in Subramanian and Laughlin phase diagram (Padera, 1952). The mineral algodonite matches to the intermetallic β phase structure (Heyding and Despault, 1960). A Cu-As mineral phase diagram, proposed by Skinner and Luce (1971), includes both α-domeykite and β-domeykite arsenides as low-temperature mineral

phases, assuming Cu_3As and $Cu_{2.7}As$ for the α-domeykite and β-domeykite chemical formulas, respectively. According to this mineralogical diagram, the upper stability of pure α-domeykite mineral at 1 atm should lie close to 90ºC (a lower temperature than the previously 225ºC).

Although the cubic Cu_3As (α-domeykite) structure was never identified in arsenical copper alloys prepared by casting (melting processes), this mineral information suggests that the cubic structure could be the stable Cu_3As form in the Cu-As system at room temperature. Nevertheless, we should keep in mind that in geological materials the probable presence of other minor elements should affect its thermodynamic behaviour considerably. It may also be important to note that synthesis of cubic Cu_3As has also been performed. A mixture of this compound with some hexagonal Cu_3As was achieved at 154 ºC by reaction of copper with arsenic in the presence of glycerine at atmospheric pressure (Heyding and Despault, 1960). On the other hand, pure cubic Cu_3As was synthesized by electrochemically induced co-deposition of copper and arsenic from H_2SO_4-$CuSO_4$-As_2O_3 solutions at room temperature and under atmospheric pressure (Dewalens *et al.*, 1951).

The overall results (microstructural observations and XRD identifications) suggest that the lighter grey formations, surrounded by the α-Cu phase grains, should correspond to the arsenide precipitation at low temperatures. Therefore, these formations are assigned to the lower temperature arsenide form, the cubic Cu_3As (corresponding to the mineral α-domeykite). On the other hand, the darker grey arsenides, clearly observable in the arsenic richer sample (VNSP148D), should result from higher temperature transformations, and, consequently, these formations are assigned to the hexagonal Cu_3As structure (mineral β-domeykite).

This identification of cubic Cu_3As in artificial materials prepared by thermal synthesis (melting) was only possible to observe in ancient alloys, proving that this precipitation, involving slow diffusion of As towards α-Cu grain boundaries, occurs gradually during long periods of time. These results, describing the cubic Cu_3As as the stable arsenide at room temperature and the hexagonal Cu_3As as a metastable arsenide, have strong implications for the archaeometallurgical studies in the characterization of these alloys. They also reveal that properties like hardness and colour measured in archaeological arsenical copper alloys are most likely altered from the initial conditions. These results highlight the importance of understanding the impact of structural ageing for the assessment of original properties of archaeological arsenical copper artefacts, such as hardness or colour.

3.6. COLOUR STUDY

The prehistoric man earliest interest in copper minerals was most likely based on their distinctive colour properties. As mentioned in section 1.2, the use of blue and green copper ores for beads, pendants and pigments goes back to the early agro-pastoral Neolithic communities (11th-9th millennia BC) in Southwest Asia (Roberts *et al.*, 2009; Bar-Yosef Mayer and Porat 2008; Yener, 2000). Therefore, it is expected that visual properties were immensely appreciated in other materials.

During the Chalcolithic period, copper would be a relatively scarce and valuable material. Among several physical properties that provide unique characteristics to this material, visual properties would have had a significant role. The colour and luminosity of metallic surfaces are unique. Some discussion has been previously made in the present thesis regarding the deliberate selection of arsenical copper alloys to produce more prestigious objects like daggers, in contrast to the purer copper alloys selected for tools. Functional considerations and enhanced properties may influence the selection of copper with more arsenic content, for instance, the need for tools to withstand percussive impact and cutting edges to retain their sharpness. Nevertheless, the colour of the produced alloy may also be a decisive factor.

A previous study mentioned that pure copper has a reddish appearance while the addition of arsenic in copper produces whitening (Budd and Ottaway, 1991). Another author, Pearce (1998) suggests that different arsenic content in the alloys may reflect a distinction between cult and utilitarian artefacts. The conjugation of copper with arsenic produces an alloy colour that ranges from red to white (silver) (Keates, 2002). The luminous property of the metal is enhanced by producing flat-surface objects which are polished to create a reflective surface, creating an aesthetically pleasing and dazzling effect, an effect which would certainly be apparent on axes and daggers. Also, the tonalities possible to obtain in copper objects can be associated with solar symbolism (Brunod, 1998) with the whiter alloys (arsenical copper) suggesting the fully ascendant sun or the more red/pink copper to the colour of sunrise or sunset (Keates, 2002).

The VNSP assemblage presents artefacts with varying arsenic contents. The colour measurements made in this collection intended to characterize the colour of the alloys with different arsenic contents in original, ancient samples, and compare with data from previous studies.

Colour measurements were made using a Datacolor International Spectrophotometer, Microflash 200d, with an integrating sphere in the mounted and polished 27 cross-sections of the artefact collection from VNSP previously published (Pereira *et al.*, 2013b). The measurement was made in areas without intergranular corrosion to minimize the error and to obtain the colour parameters more close to the alloy as possible. Measurements were also performed in three pure metals: 100% Cu; 100% Ag and 100% Au. The analysed area of the spectrophotometer is fixed to 8 mm diameter. Since the clean area of the samples was in most cases smaller, the metallic exposed area to the measurement was narrowed to 3 mm diameter with a black cardboard mask. Therefore, the data obtained from these readings are only valid for comparison inside this set of samples.

A summary of CIE *L*a*b** chromatic coordinates and calculated *h* hue angle of the analysed VNSP artefact collection is presented in Appendix VI. Results were projected in a representation of CIE *a** and *b** (see Figure 3.25) and *h* hue angle versus As content (see Figure 3.26). The axis *a** and *b** were selected to include the results showing a chromophore content in the red and yellow and green domains and its intermediary hues.

Results indicate that the colour of the alloy is influenced by the arsenic content in the alloy. When the arsenic content is low (< 0.1 wt.% As), samples present a more positive *a** value (around 3.50 *a**) resulting in a more red colouration. The addition of arsenic in the alloy significantly reduces the *a**

value linearly (lower *a** value: 0.29, with 9.1 wt.% As). Moreover, the increasing of arsenic content not only reduces the red *a** but also slowly reduces the yellow *b** of the alloy, driving the alloy colour towards a more silvery shade. Between the two extremities, copper alloys with increasing arsenic content present a more yellow coloration due to the reduction of redness before turning into more silvery tonality. In conclusion, the addition of arsenic to copper has a visible and quantifiable effect on the colour properties in an alloy with colour ranging from a red hue to a silver coloration, including a golden hue in the middle colour range (Figure 3.25).
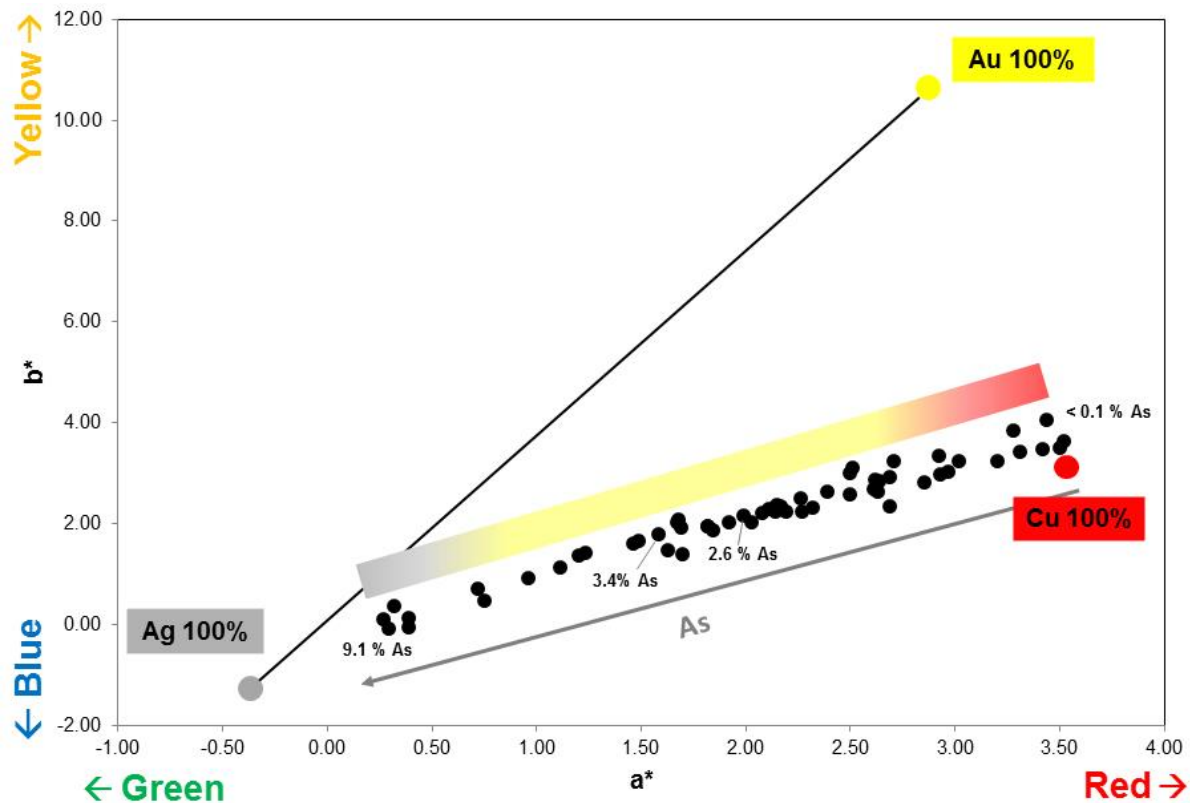
Figure 3.25. Representation of CIE *a** and *b** colour space under restrictive conditions (use of a black mask), from selected artefacts from VNSP collection, and pure Au, Ag and Cu specimens.

Another approach to evaluating the colour change with the increase of arsenic content in the alloy is the determination of the *h* hue angle. As observed in Figure 3.26, *h* shows a drop in values close to 5.5 wt.% As and matches five artefacts: VNSP049A: 5.59 wt.% As; VNSP180E: 5.57 wt.% As; VNSP191I: 5.49 wt.% As; VNSP148D: 9.13 wt.% As (see Appendix VI).

The arsenic content of VNSP049SA, VNSP180E and VNSP191I is similar to the composition in the α-copper phase of the arsenic richer artefact (VNSP148D), obtained by SEM-EDS (see Figure 3.23 in section 3.5). Therefore, 5.5 wt.% As should be a good approach to the solubility limit of As in α-copper phase at room temperature (dashed line in Figure 3.26). This arsenic content is slightly inferior to the 6.1 wt.% As value given by Cu-As phase diagram (after Subramanian and Laughlin, 1988) at room temperature.

The VNSP001A sample presents a deviation that could be due to the small dimension of the sample, and the colorimetry measurements could be affected by a surrounding epoxy resin.
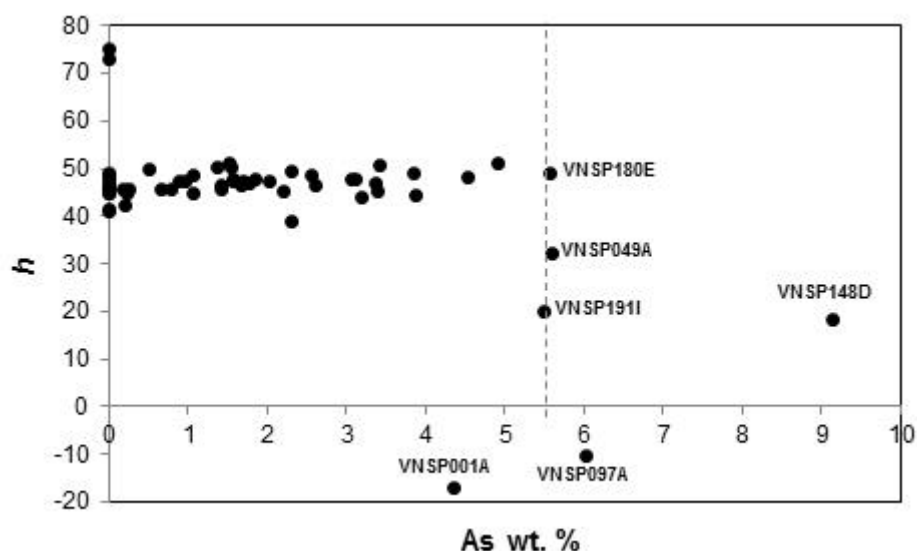
Figure 3.26. Representation of *h* hue angle space versus As wt.% content from selected artefacts from VNSP collection, and pure Au, Ag and Cu specimens.

A previous study, using measurements of the UV-visible spectrum of manufactured copper samples with varying arsenic content, obtained similar results (Berger, 2012). It was also observed the decrease of red colouration and an increase of yellow/silver colouration with the increase of arsenic content.

The collected colour data from this set of artefacts with varying amounts of arsenic supports the idea that possibly the initial use of arsenical copper alloys was with the intention of imitating the colour of gold or silver with associated higher prestige. The silver colour measured could be a consequence of the Cu_3As precipitation during burial. If that was the case, in the past, the golden alloy colour selection by aesthetic reasons may have equal or greater importance than the physical and mechanical properties of the object.

Future work could include the measurement of the UV-visible spectrum to a better comparison of the colour of the sample and compare with archaeological specimens. The objective will be to evaluate if the precipitation of the γ phase (Cu_3As, As-rich phase) (see section 3.3) provides an incorrect or less adequate perception of the aspect of the artefact at the time of manufacture since we only access the metallic collection after ageing through archaeological times.

4. MOITA DA LADRA [4]

4.1. INTRODUCTION

The walled Chalcolithic site of ML is located downstream on the right bank of the Tagus River, being mainly occupied during the second half of the 3rd millennium BC. This occupation is characterized by the presence of Bell Beaker ceramics associated with local decorated ware (acacia-leaf and crucifera patterns). According to the archaeological excavation record, copper metallurgy was a common activity at the site alongside with weaving, dairy products production and stone polishing (Cardoso and Caninas, 2010). The chronology, determined by radiocarbon dating carried out on materials from several archaeological contexts, points to a time interval of c. 2560-1820 cal BC (2 σ) (Cardoso *et al.*, 2013) (Figure 4.1). The metallurgical collection recovered from the excavations in this settlement was analysed.
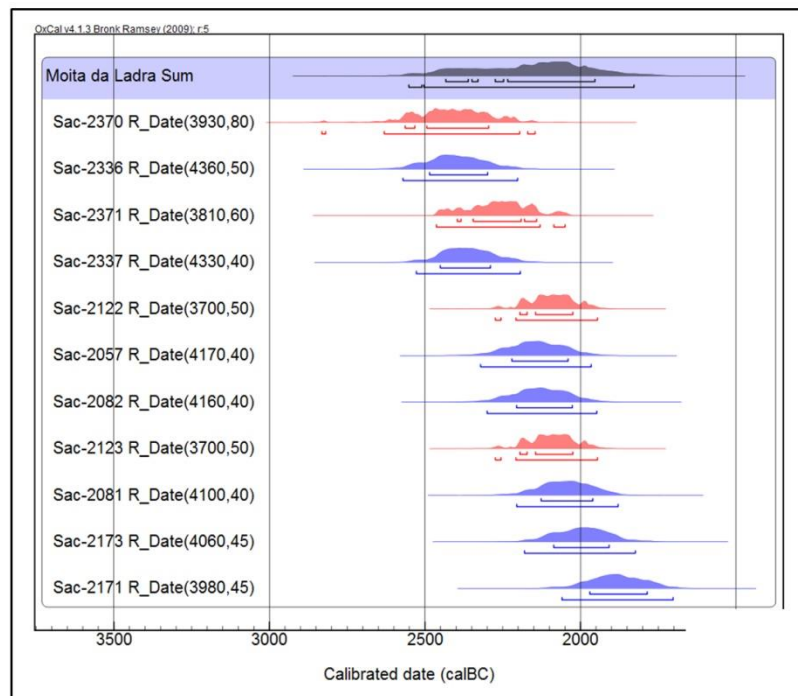
Figure 4.1. Calibrated radiocarbon dates for ML settlement using the IntCal13 calibration curve (Reimer *et al.*, 2013) and the OxCal program (V4.2.3) (Ramsey, 2014) following Cardoso *et al.*, 2013.

---

[4] Part of the content from this section was previously published (Pereira *et al.*, 2017).

4.2. PRODUCTION REMAINS

4.2.1. Metallic nodules

The metallurgical remains collection of ML consists of eight metallic nodules (Figure 4.2) with different dimensions and irregular shapes. Small open pores are observed at the surface on most nodules, possibly due to high degasification processes during its formation.

Figure 4.2. Metallic nodules from ML collection; dashed lines: sampling locations.

Small samples were taken from the metallic nodules with a minor effect on the original shape of the object (see Figure 4.2 for the location of the sampling sections) and mounted in an epoxy resin, and the exposed cross-section surfaces were subjected to a metallographic preparation (a detailed procedure in subsection 2.2.2).

The elemental composition and microstructural characterization of this set are presented in Table 4.1. The microstructural observations allowed the identification of main phases, shrinkage and gas pores, besides other typical characteristics related to as-cast features, such as coring effects. The As-rich phase, identified as the Cu_3As intermetallic compound, is denoted here only by its chemical formula, notwithstanding other possible crystalline forms observed in high arsenic coppers (see section 3.3).

Table 4.1. Elemental composition of metallic nodules from ML (content in wt.% average ± standard deviation; n.d.: not detected); microstructural characteristics (↓: Low amount); S – smelting origin.

Metallic nodules	Elemental analysis (wt.%)			Phases	Microstruture	Obs.
	Cu	As	Fe			
ML07	97.2±0.3	2.78±0.28	<0.05	α; Cu_3As	As-cast	S
ML13	98.6±0.3	1.38±0.28	<0.05	α	As-cast	S
ML20	98.0±0.3	1.79±0.23	<0.05	α	As-cast	S
ML21	97.4±0.4	2.54±0.32	<0.05	α; Cu_3As↓	As-cast	S
ML22	98.1±0.3	1.88±0.27	<0.05	α	As-cast	S
ML48	99.0±0.2	0.73±0.21	<0.05	α	As-cast	S
ML49	98.3±0.3	1.66±0.38	0.07±0.01	α	As-cast	S
ML51	99.7±0.2	0.37±0.16	<0.05	α	As-cast	S

Micro-EDXRF analyses indicate that the collection of metallic nodules from ML is composed of copper and copper with arsenic (0.37 wt.% < As < 2.78 wt.%) (Figure 4.3). Iron content is in the majority of the cases below the quantification limit (<0.05%) except ML49 with 0.07 wt.% Fe, still a rather low

content. Other minor elements such as antimony, lead, zinc, nickel or silver were not detected or were under the quantification limit. The average content of arsenic is 1.6 wt.%. The low number of items in this set hinders a more precise observation and evaluation of the shape of the arsenic distribution.
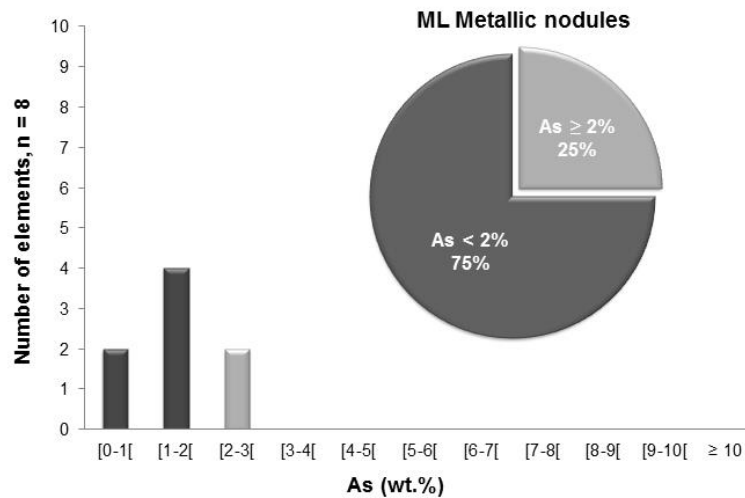
Figure 4.3. Distribution of arsenic content and percentage of metallic nodules below 2% and above 2% As in the metallurgical vestiges from ML.

The coring observed by optical microscopy observations reveals that all the nodules present a coarse dendritic structure of α phase, indicating a relatively slow cooling rate (Figure VII.1 in Appendix VII). No fine dendritic structures were observed in this set of nodules. These observations suggest that they were formed by a smelting operation and left inside the slag mass during cooling down (Figure 4.4).
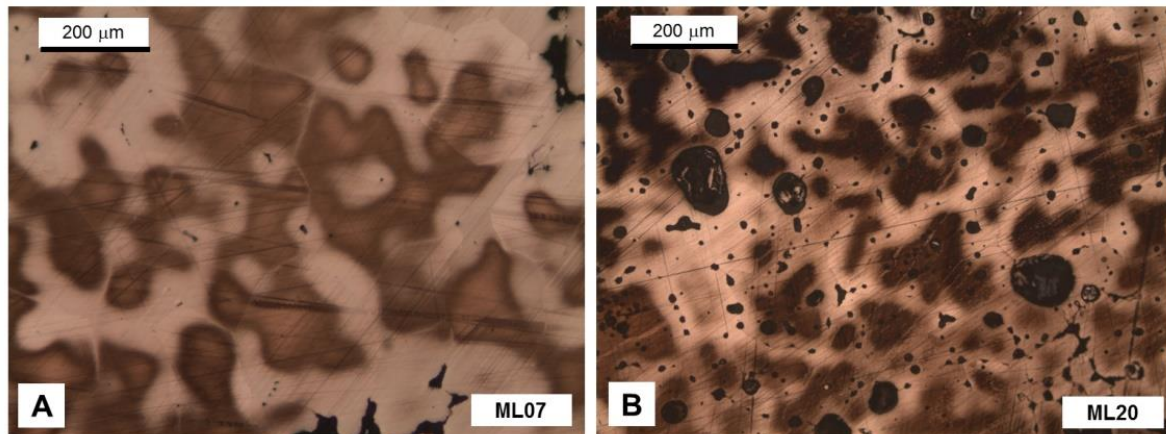
Figure 4.4. OM images of: A: prill ML07 (2.78 wt.% As) and B: prill ML20 (1.79 wt.% As) (all BF illumination, etched). Coring effects, revealing a coarse as-cast structure, gas and shrinkage pores are clearly observed.

SEM-EDS analysis identified inclusions of copper and arsenic oxides in the case of nodule ML20 (Figure 4.5). A lower oxide density is observed in the microstructure of ML07 as compared to ML20, possibly since arsenic act as a deoxidizing element (Figure 4.4) (Hook *et al.*, 1991). In conclusion, the

metallic nodules composition is copper or copper with arsenic and presents a microstructure that suggests a smelting origin. Therefore these nodules could be identified as metallic prills.
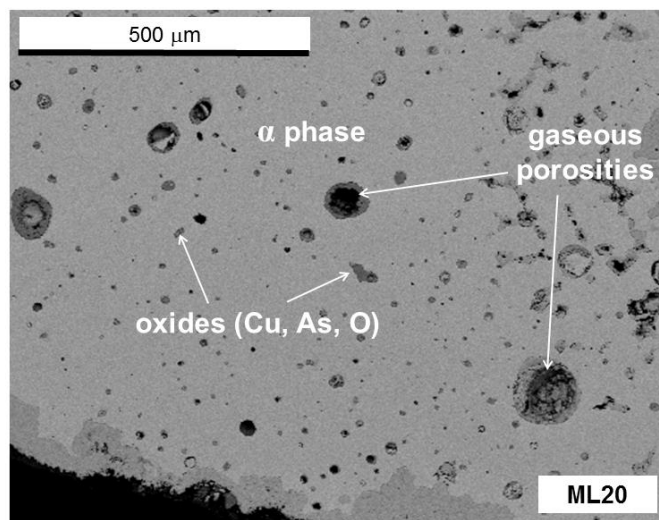
Figure 4.5. SEM-BSE image of: A: prill ML20 (1.79 wt.% As) presenting the EDS identification of oxide elements, Cu and As. Gas pores (rounded voids) are also visible.

4.3. COPPER-BASED ARTEFACTS

The copper-based metal finds selected for this study consist of 23 artefacts with identified typologies, plus 39 fragments of artefacts of unknown typologies. Only artefacts with identified typologies were represented in Figure 4.6. The artefact collection includes awls, chisels, axes, daggers, arrowheads (including one Palmela point), one spatula and one saw. The remaining artefacts are in a very fragmentary state suggesting the practice of recycling operations at the settlement.

Similar to the classification made for VNSP, the selected artefacts were grouped into the following functional categories: "Tools" (including awls, chisels, the spatula and the saw), "Axes" and "Weapons" (including daggers and arrowheads).

Figure 4.6. Copper-based artefact collection from Moita da Ladra (reproduced from Pereira *et. al.*, 2016); dashed lines: sampled locations; circles: polished areas.

Complete artefacts were manually cleaned on a small area (approximately 4 mm^2). On the other hand, nine small samples were taken from fragmented artefacts with a minor effect on the original shape of the object (see Figure 4.6 for the location of the sampling areas). Samples were mounted in resin, and the corresponding cross-sections were prepared for analysis (detailed procedure in subsection 2.2.2).

Table 4.2 presents a summary of the elemental composition, phase constitution and Vickers microhardness of the artefacts, according to the mentioned typologies. The inferred operational sequence is also present.

Table 4.2. Elemental composition of copper-based artefacts from ML (content in wt.% average ± standard deviation; n.d.: not detected); microstructural characteristics of artefacts (C: Casting; F: Forging; A: Annealing; FF: Final forging; ↓: Low amount; cor.: coring; microhardness Vickers: HV0.2 (mounted samples only).

Typology	Artefacts	Elemental analysis (wt.%)			Phases	HV0.2		Operational sequence
		Cu	As	Fe		Centre	Blade	
	ML04	98.3±0.8	1.71±0.80	<0.05	α; cor.	-	-	C+(F+A)
Awls	ML11	96.6±1.0	3.41±1.01	<0.05	α; Cu₃As; cor.	-	-	C+(F+A)+FF
	ML19	99.0±0.1	0.93±0.07	<0.05	α; cor	-	-	C+(F+A)+FF
	ML25	99.3±0.2	0.72±0.15	<0.05	α; cor.	-	-	C+(F+A)
	ML35	97.4±0.9	2.53±0.89	<0.05	α; cor.	-	-	C+(F+A)
	ML38	96.7±0.8	3.25±0.85	<0.05	α; cor.	-	-	C+(F+A)
	ML59	98.9±0.4	1.08±0.30	<0.05	α; cor.	-	-	C+(F+A)
	ML78	99.2±0.1	0.75±0.04	<0.05	α	-	-	C+(F+A)
	ML84	94.7±0.9	5.20±0.92	<0.05	α; Cu₃As; cor.	-	-	C+(F+A)
Chisels	ML09	94.5±0.5	5.47±0.53	<0,05	α; Cu₃As; cor.	110±1	-	C+(F+A)+FF
	ML64	99.1±0.2	0.83±0.13	<0.05	α	70±4	-	C+(F+A)
	ML69	97.8±0.2	2.14±0.21	<0.05	α; cor.	58±2	-	C+(F+A)
Saw	ML82	98.6±0.5	1.40±0.42	<0.05	α; cor.	56±2	-	C+(F+A)+FF↓
Palmela point	ML26	99.3±0.2	0.68±0.16	<0.05	α; cor.	-	-	C+(F+A)
Espatula	ML66	97.7±0.6	2.22±0.55	<0.05	α; cor.	-	-	C+(F+A)
Daggers	ML15	97.0±0.7	3.02±0.69	<0.05	α; Cu₃As; cor.	-	-	C+(F+A)+FF
	ML79	97.2±0.8	2.77±0.87	<0.05	α; cor.	-	-	C+(F+A)+FF
Daggers/ arrowheads	ML12	97.7±0.5	2.24±0.48	<0.05	α; cor.	62±2	70±2	C+(F+A)
	ML27	95.9±0.6	4.07±0.61	<0.05	α; cor.	78±2	86±2	C+(F+A)
Axes	ML06	96.9±0.4	3.04±0.35	<0.05	α; cor.	101±2	-	C+(F+A)+FF
	ML16	98.6±0.1	1.38±0.12	<0.05	α; cor.	55±2	58±1	C+(F+A)
	ML70	97.1±0.8	2.77±0.67	<0.05	α; cor.	70±2	73±2	C+(F+A)
	ML72	99.1±0.4	0.90±0.42	<0.05	α; cor.	-	-	C+(F+A)+FF↓
Unclassifiables	ML01	96.0±1.3	3.93±1.30	<0.05	-	-	-	-
	ML02	96.1±1.0	3.92±0.98	<0.05	-	-	-	-
	ML03	97.8±0.8	2.16±0.79	<0.05	-	-	-	-
	ML05	98.3±0.8	1.65±0.79	0.07±0.01	-	-	-	-
	ML14	98.5±0.6	1.44±0.56	<0.05	-	-	-	-
	ML17	98.4±1.7	1.64±1.76	<0.05	-	-	-	-
	ML18	97.3±0.8	2.23±0.30	<0.05	-	-	-	-
	ML23	99.5±0.5	0.46±0.44	<0.05	-	-	-	-
	ML28	98.2±0.6	1.76±0.58	0.06±0.01	-	-	-	-
	ML29	96.4±2.0	3.57±2.02	<0.05	-	-	-	-
	ML30	98.2±1.2	1.85±1.21	<0.05	-	-	-	-
	ML31	97.4±0.5	2.59±0.51	<0.05	-	-	-	-
	ML32	97.8±0.5	2.16±0.46	<0.05	-	-	-	-
	ML33	98.2±0.1	1.77±0.15	0.05±0.01	-	-	-	-
	ML34	98.1±1.0	1.93±0.94	<0.05	-	-	-	-
	ML36	97.7±0.7	2.30±0.64	<0.05	-	-	-	-
	ML39	97.3±0.3	2.65±0.31	<0.05	-	-	-	-
	ML40	99.3±0.2	0.62±0.15	0.07±0.01	-	-	-	-
	ML44	95.9±1.2	4.04±1.23	<0.05	-	-	-	-
	ML45	97.7±0.2	2.28±0.17	0.07±0.01	-	-	-	-
	ML46	98.4±0.6	1.58±0.58	<0.05	-	-	-	-

Typology	Artefacts	Elemental analysis (wt.%)			Phases	HV0.2		Operational sequence
		Cu	As	Fe		Centre	Blade	
	ML47	95.2±0.5	4.80±0.54	<0.05	-	-	-	-
	ML52	98.4±0.2	1.58±0.16	<0.05	-	-	-	-
	ML53	97.1±0.6	2.84±0.59	<0.05	-	-	-	-
	ML54	97.4±0.4	2.62±0.41	<0.05	-	-	-	-
	ML55	96.1±1.8	3.85±1.85	0.07±0.01	-	-	-	-
	ML56	98.3±0.3	1.62±0.29	<0.05	-	-	-	-
	ML57	97.1±0.5	2.87±0.52	<0.05	-	-	-	-
	ML58	97.0±0.6	3.04±0.63	<0.05	-	-	-	-
	ML65	99.3±0.4	0.72±0.37	<0.05	-	-	-	-
	ML68	98.6±0.3	1.37±0.30	<0.05	-	-	-	-
	ML71	99.1±0.4	0.93±0.37	<0.05	-	-	-	-
	ML73	97.3±0.8	2.70±0.72	<0.05	-	-	-	-
	ML74	99.2±0.2	0.82±0.15	<0.05	-	-	-	-
	ML75	99.0±0.1	0.98±0.10	<0.05	-	-	-	-
	ML76	97.2±1.1	2.78±1.07	<0.05	-	-	-	-
	ML77	99.0±0.1	0.95±0.03	0.06±0.01	-	-	-	-
	ML81	96.5±2.0	3.42±1.90	<0.05	-	-	-	-
	ML83	95.6±2.9	4.37±2.86	<0.05	-	-	-	-

Micro-EDXRF analyses indicate that the collection from ML consists of copper or copper with arsenic. The arsenic content present is up to 5.47 wt.%. In Figure 4.7, 45% of the collection (28 artefacts) shows a low arsenic content (As < 2 wt.%). In the remaining 34 artefacts, representing 55% of the analysed items, are assumed as arsenical coppers (As ≥ 2 wt.%). The iron content is below the quantification limit (<0.05 wt.%) with the following exceptions: ML28 and ML77 with 0.06 wt.% Fe, and ML05, ML40, ML45, and ML55 with 0.07 wt.% Fe. Other minor elements such as antimony, lead, zinc, nickel or silver were not detected or were under the quantification limit. The histogram shown in Figure 4.7 suggests a distribution close to the shape of a "normal distribution" positive skewed. The average arsenic content in this set was of 2.3 wt.%.
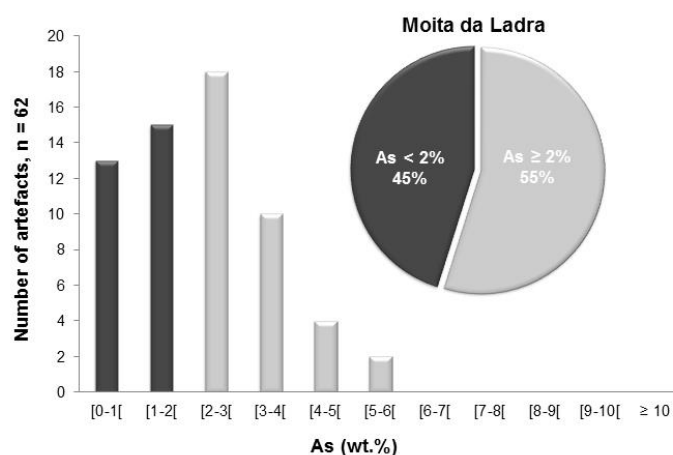
Figure 4.7. Distribution of arsenic and percentage of copper and arsenical copper artefacts in ML collection.

"Weapons" group tend to exhibit higher levels of arsenic, as it is displayed in Figure 4.8, Left. However, Fisher's exact test did not found a statistically significant association between the "Weapons" group and the presence of arsenic (As ≥ 2 wt.%) (p = 0.3378 when comparing "Weapons" with "Tools" and p = 0.3394 when comparing "Weapons" with "Tools" + axes).
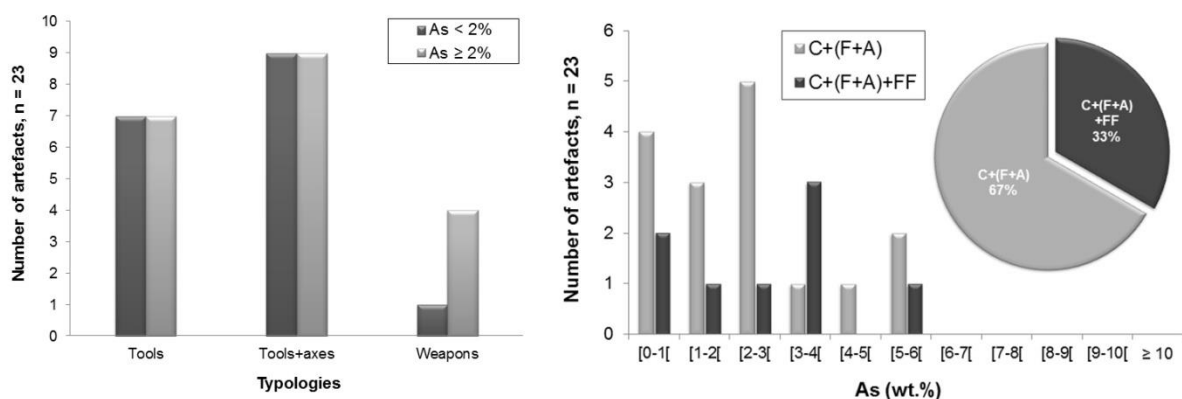
Figure 4.8. Left: distribution of arsenic in the ML objects (unclassifiable fragments and metallic nodules excluded); Right: distribution of manufacture processes by arsenic content.

Optical microscopy observations of these items revealed several features: in some cases near-equiaxial α-Cu grains with annealing twins (Figure 4.9, A), and less frequently, slip bands (Figure 4.9, B). These observations indicate that the artefacts from ML were manufactured by hammering plus annealing operations in 67% of the cases and a final forging operation was applied to only 33% of the selection (Figure 4.8, Right). Fisher's exact test was also used in this case to evaluate the significance of association between the final forging operation applied in the artefact manufacture and arsenical copper artefacts (As ≥ 2%). However, no statistically significant association was found (p = 1).

Segregation bands that resulted from subsequent mechanical work on cored structures are visible after etching in all microstructures with the exception of ML64 and ML 68, possibly due to the lower arsenic content in these alloys (Figure VIII.1 in Appendix VIII). In some samples the Cu_3As intermetallic compound was identified by SEM-EDS (Figure 4.10) alongside with the identification of oxides with Cu, As and Sb in the case of ML07. These oxide inclusions appear as blue-grey (Figure 4.9, C and D) by optical microscopy observation and are spread along the α-copper grain boundaries.

The Cu_3As intermetallic phase can be observed in the microstructure in the three morphological types: eutectic arsenide formations (biphasic structure) observed in Figure 4.9D (chisel ML09 with 5.47 wt.% As), thicker arsenide formations related to non-equilibrium casting features, and thinner arsenide formations observed around grain boundaries of recrystallized grains. The last two arsenide formations are observed in Figure 4.9C. The post-casting arsenide formations reinforce the idea of a long-term precipitation over archaeological time (see subsection 3.3).

Overall, during the artefact manufacturing, the presence of coring, eutectic arsenide and thicker arsenide formations seem to indicate an inability to achieve a chemical homogeneity by these ancient metallurgists.
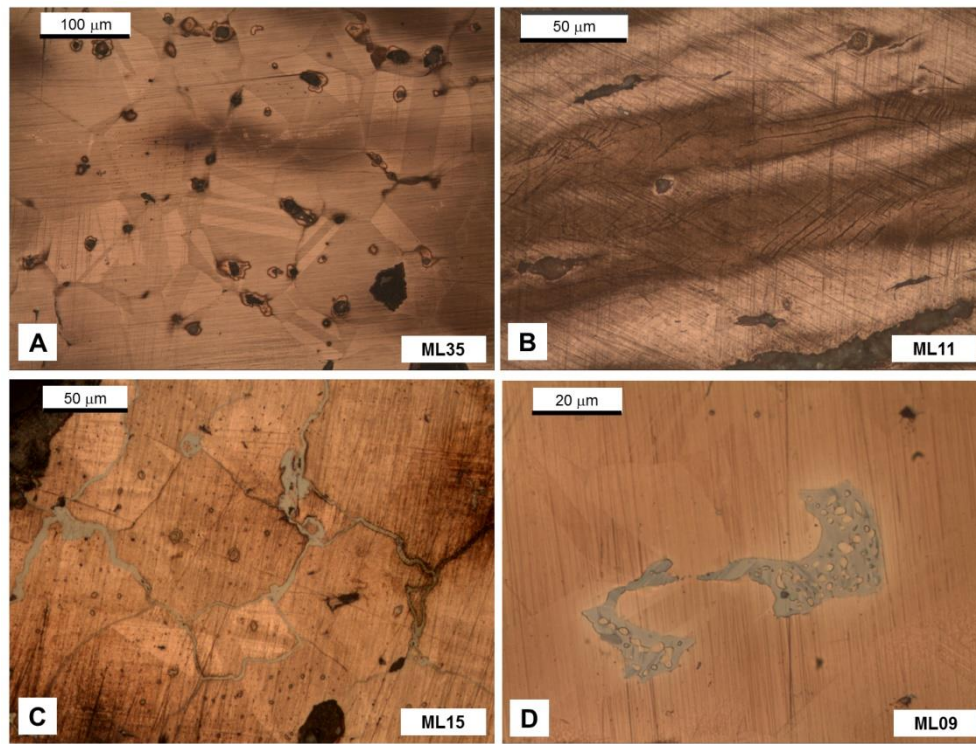
Figure 4.9. OM images of: A: awl ML35 (2.53 wt.% As); B: awl ML11 (3.41 wt.% As); C: dagger ML12 (2.24 wt.% As); D: chisel ML09 (5.47 wt.% As). Band segregations (images A and B) and different types or arsenide morphologies (images C and D) are observed (all BF illumination; etched).
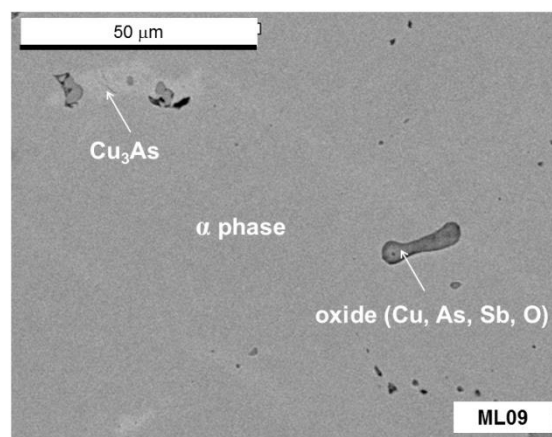
Figure 4.10. SEM-BSE image of chisel ML09 (5.47 wt.% As) presenting the EDS identification of Cu_3As, As-rich phase, and an oxide consisting of Cu, As and Sb.

Microhardness Vickers tests were performed in the centre of the nine mounted samples and, when applicable, near the cutting edge (Table 4.2). In Figure 4.11 is represented the hardness measurements as a function of arsenic content. Data are discriminated by operational sequence and typology groups. A linear regression was performed (y = 11.3x + 44.3) and the 95% confidence

interval for the line slope was also determined (slope =11.3 ± 7.52). The linear model points to a positive slope, indicating that for this set of artefacts the hardness increases with the arsenic content.

Due to the low number of artefacts in each category, when subdividing the analysis by groups of typologies and analysing them separately, they do not show any clear tendency.
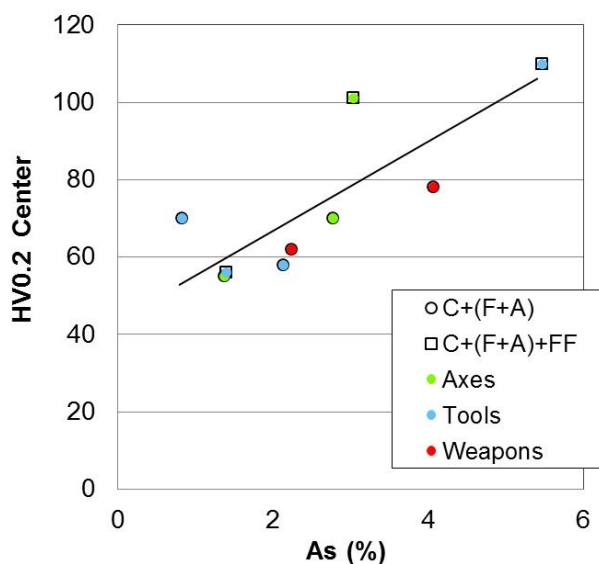
Figure 4.11. Micro-HV measurements (HV0.2) as function of the arsenic content of the artefacts (n=9). Data marker styles and colours are related to the different operational sequences, and typologies, respectively; the black line represents the linear fitting over the data points.

The two harder artefacts, chisel ML09 (5.47 wt.% As; 110 HV0.2) and axe ML06 (3.04 wt.% As; 101 HV0.2), present both higher arsenic contents and a final forging operation. Nevertheless, the sample set is too small to be certain of the intentionality of this final operation to increase the hardness. It must be noted that artefacts with this composition would obtain significant hardening (above 150 HV0.5 with only 25% of thickness reduction (Lechtmann, 1996)). These results suggest that work hardening capability of these alloys was not exploited. The hardness measured near the cutting edge and the central region was only possible to be compared in 4 cases, showing only a slight increase (not significant) in the cutting edge (Table 4.1 and Figure 4.12).
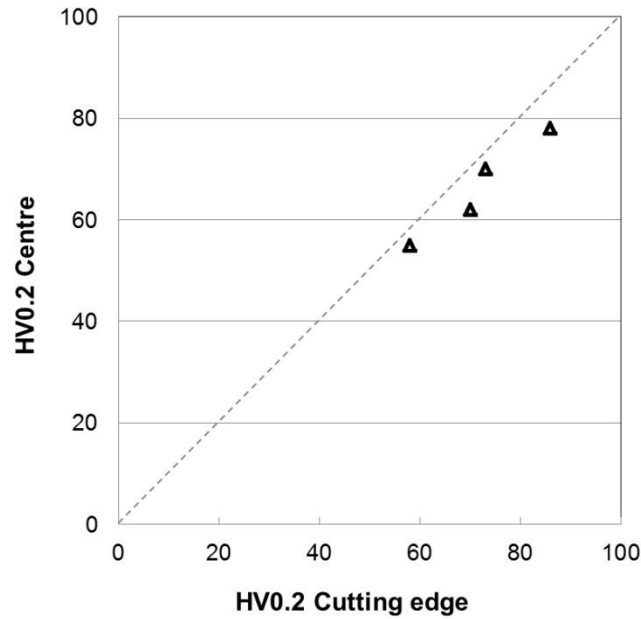
Figure 4.12. Comparison of micro-HV measurements (HV0.2, 10 s) between cutting edge and centre area (n = 4).

However, this hardness increase could be the result of the thermomechanical processing associated with the only purpose of shaping the artefacts and not to an intention to produce a harder alloy. The hammering operation reduces the distances between chemical fluctuation distances, while the heat treatment (annealing) increase the atomic diffusion rate. Both effects contribute to a more homogeneous material, reinforcing the solid solution hardening effect of arsenic in α-Cu phase.

Also, the microstructures that show post-casting arsenide formations resulting from a long-term ageing could lead to significant microstructural alterations that should be reflected in its actual hardness (see section 3.3). The Chalcolithic metallurgists may not have been aware of the hardening capacity of arsenical copper alloy but the hardness measurements made in the present may not be accurately representative of the newly finished artefact.

5. OUTEIRO REDONDO [5]

5.1. INTRODUCTION

Located near Sesimbra, OR is an important Chalcolithic settlement of the Portuguese Estremadura region (Cardoso, 2009), predominantly occupied during the second half of the 3rd millennium BC (Cardoso *et al.*, 2010/2011), similar to the period of occupation of ML. This occupation is characterized by the presence of Bell Beaker ceramics associated to regional decorated ware (acacia-leaf and crucifera patterns). According to the archaeological excavation record, copper metallurgy was a current activity in the site alongside with weaving, dairy products production and stone polishing (Cardoso, 2010; 2009). The radiocarbon dating of several archaeological contexts of the site allows ascribing a chronology of c. 2600-2100 cal BC (2 σ): (Cardoso *et al.*, 2010/2011) (Figure 5.1).

---

[5] Part of the content from this section was previously published (Pereira *et al.*, 2013c).
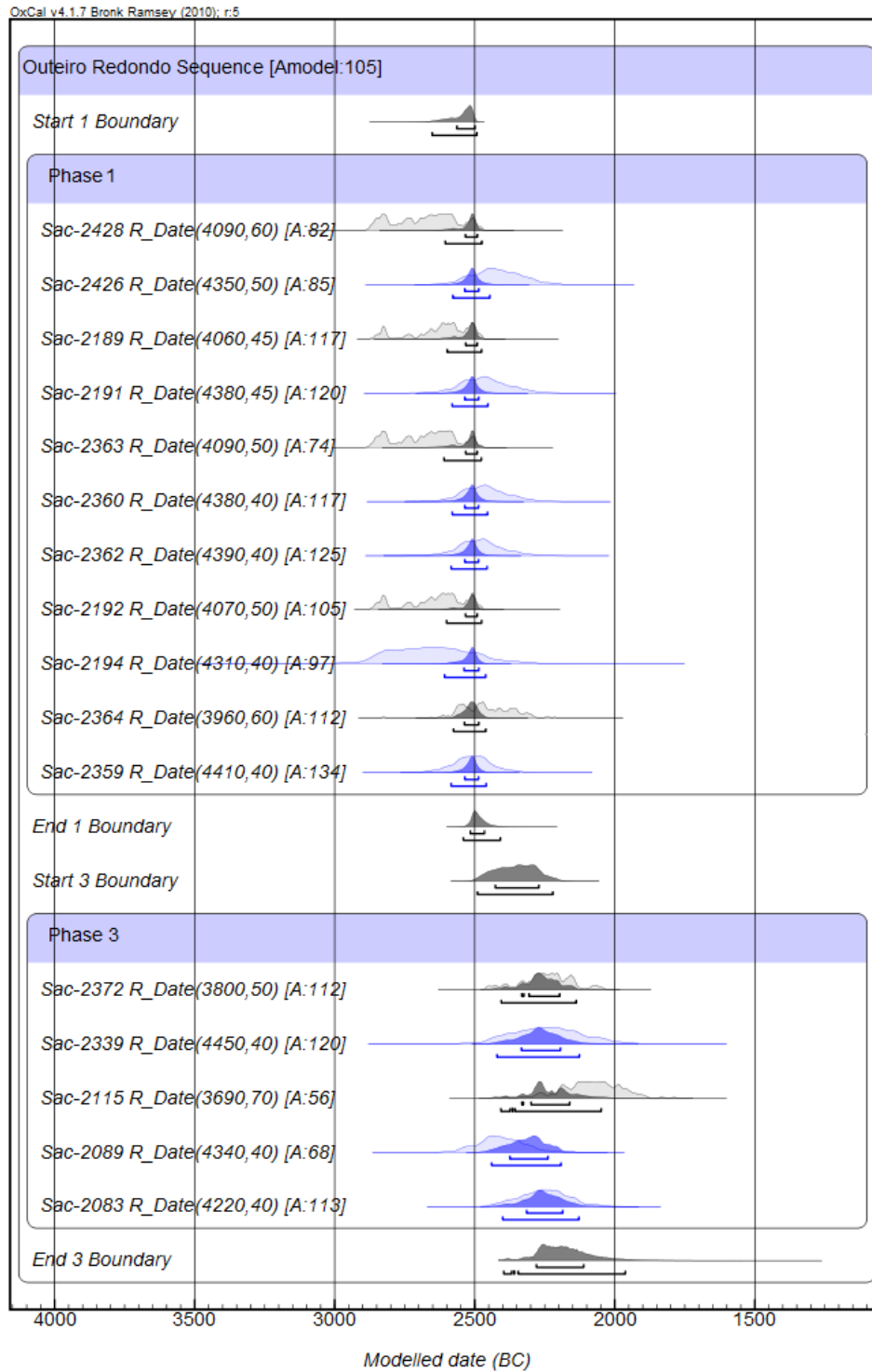
Figure 5.1. Calibrated radiocarbon dates using the IntCal13 calibration curve (Reimer *et al.*, 2013) and the OxCal program (V4.2.3) (Ramsey, 2014) following (Cardoso *et al.*, 2010/2011) for OR settlement.

5.2. PRODUCTION REMAINS

5.2.1. Crucible

The metallurgical remains of ML consist only of one crucible fragment (Figure 5.2). This fragment presents a thick wall (about 2 cm). This form is suggestive of a wall fragment with rim and bottom included and with no visible adherent material.
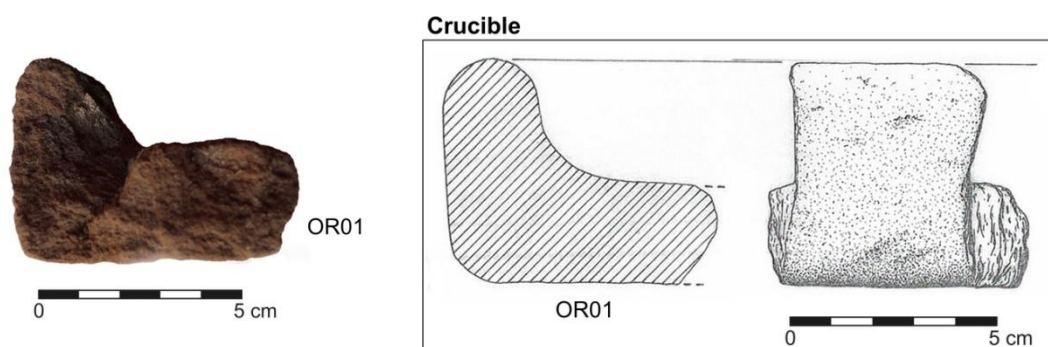
Figure 5.2. Crucible fragment from OR metallurgical collection (reproduced from Pereira *et. al.*, 2013c).

The clay surfaces of the crucible were analysed by EDXRF to establish the elements that are enriched in the areas affected by the metallurgical operation (in this case, the inner wall and rim). The results from the comparison of EDXRF spectra of clay surface from crucible fragment OR01 are presented in Figure 5.3.
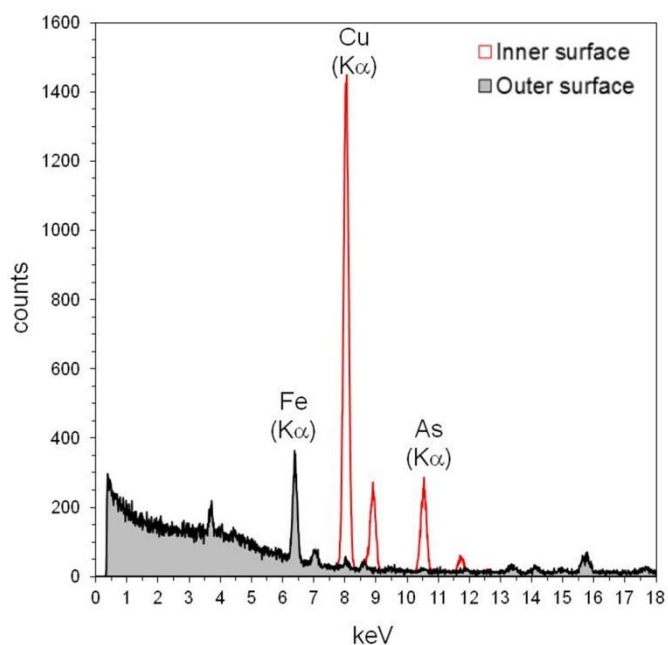
Figure 5.3. EDXRF spectrum of the inner surface (red) OR01 compared with the outer surface (black spectrum).

The enrichment in particular elements in the inner wall and rim surfaces of the crucibles is indicative of the metallurgical processes performed on this ancient remain. In this particular case, EDXRF results point to metallurgical activities in OR involving copper with arsenic.

A detailed observation of the crucible fragment by OM and SEM-EDS analysis allows the identification of small metallic nodules of Cu and As (prills) and copper oxides (cuprite) that segregated into the ceramic pores (Figure 5.4). The small sizes of these prills did not allow a valid semi-quantification.
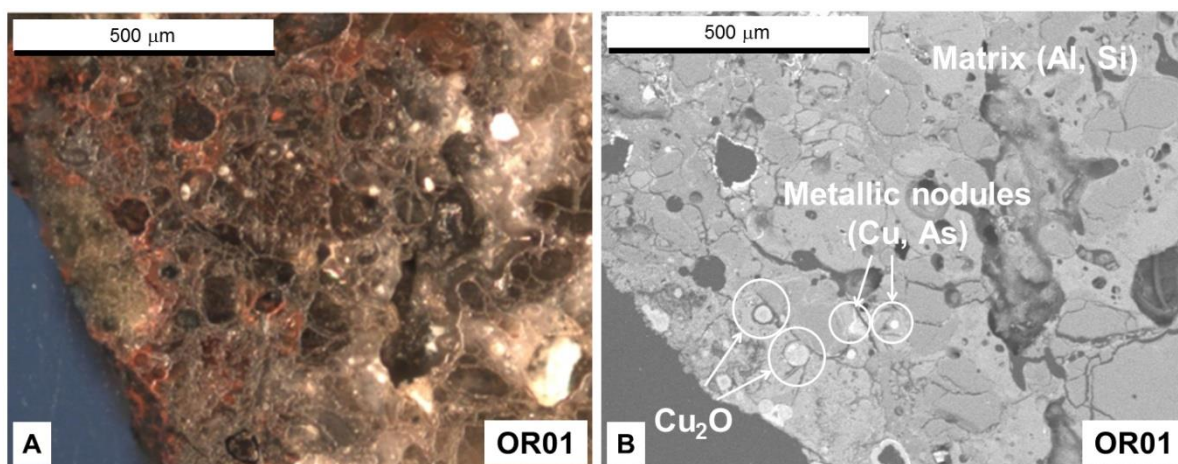
Figure 5.4. Crucible fragment from OR: A: OM image (DF illumination, non-etched) evidencing the segregation of metal to the surface of the pores in the ceramic; B: SEM-BSE image with the identification of metallic nodules of Cu and As and cuprite (oxide identified by approximate stoichiometry given by EDS).

Evidence from the study of the OR crucible fragment indicates a possible involvement of this ceramic in metallurgical operations of melting since no slag vestige is adherent to the ceramic.

5.3. COPPER-BASED ARTEFACTS

The copper-based collection of OR consists of 12 artefacts, eight with identified typologies and four fragments of unknown typologies (Figure 5.5). The artefact selection includes tools: saws, fishhooks, one awl and one spatula (Cardoso, 2010).

A summary of the elemental composition determined by micro-EDXRF, the phase constitution, the inferred operational sequence and Vickers microhardness of the metallic artefacts are presented in Table 5.1.
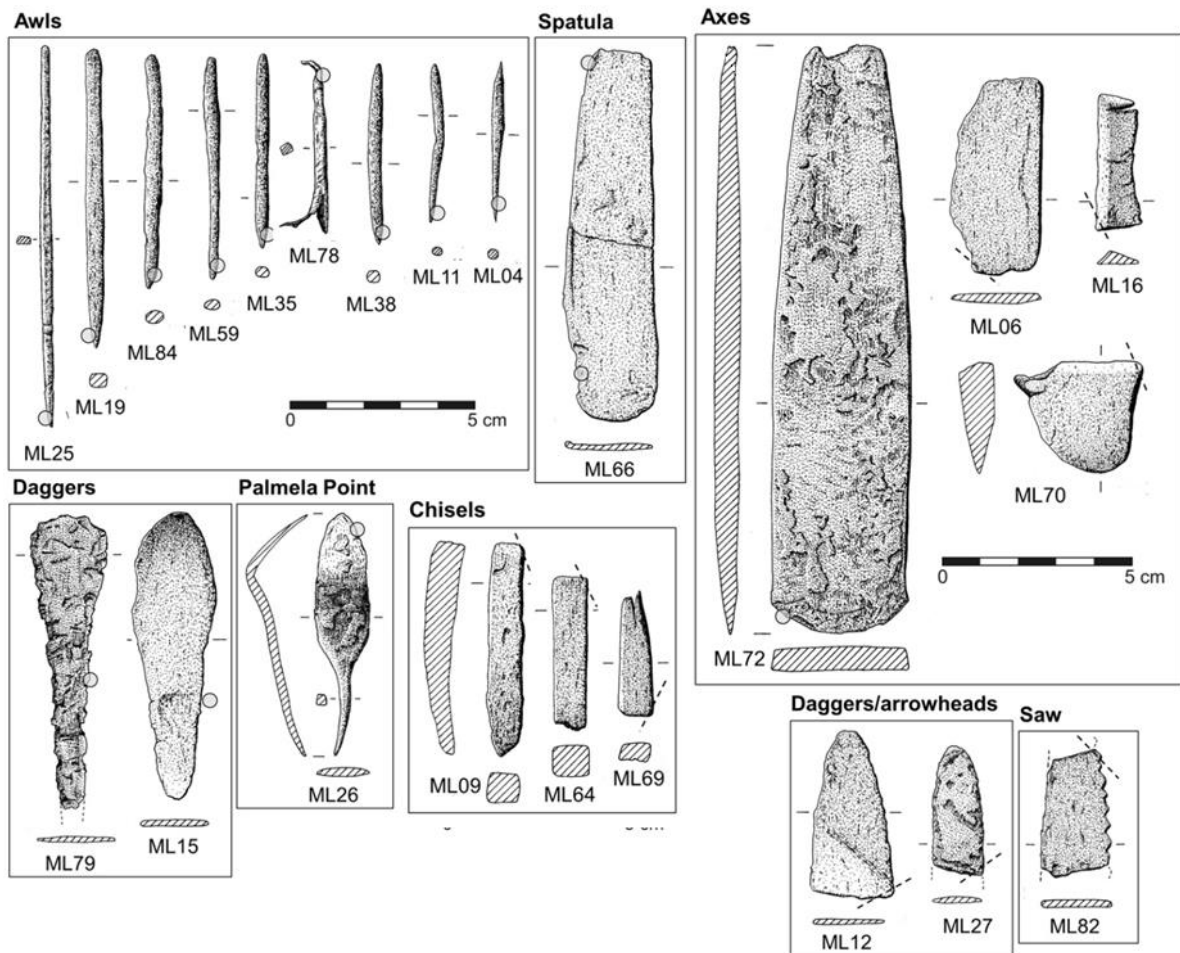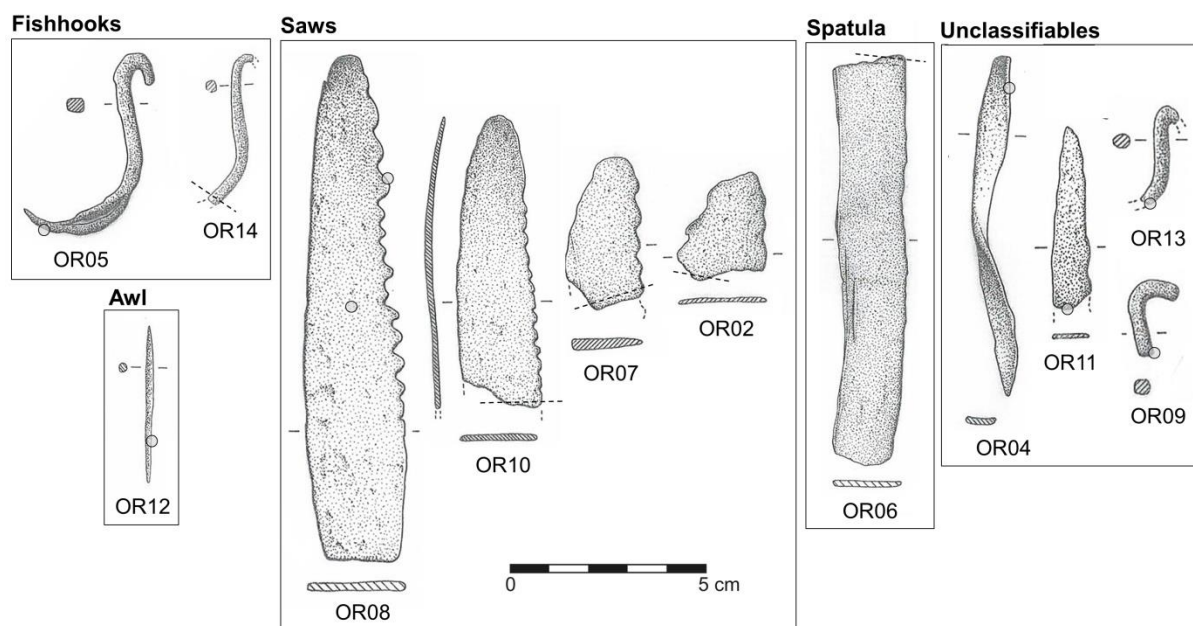
Figure 5.5. Copper-based artefact collection from OR (reproduced from Pereira *et. al.*, 2013c); dashed lines: sampled locations; circles: polished areas.

Table 5.1. Elemental composition of copper-based artefacts from OR (content in wt.% average ± standard deviation; n.d.: not detected); microstructural characteristics of artefacts (C: Casting; F: Forging; A: Annealing; FF: Final forging); cor.: coring; microhardness Vickers: HV0.2 (mounted samples only).

| Typology | Artefact | Elemental analysis (wt.%) | | | Phases | HV2.0 | | Operational sequence |
		Cu	As	Fe		Centre	Blade	
Saws	OR02	99.2±0.1	0.82±0.18	<0.05	α; cor.	45±2	67±2	C+(F+A)
	OR07	98.3±0.2	1.87±0.38	<0.05	α; cor.	99±3	111±2	C+(F+A)
	OR08	95.4±0.3	4.61±0.32	<0.05	α; Cu_3As; cor.	87±2	100±3	C+(F+A)+FF
	OR10	98.7±0.2	1.03±0.14	<0.05	α; cor.	98±2	109±2	C+(F+A)
Spatula	OR06	98.3±0.2	1.67±0.18	<0.05	α; cor.	93±1	109±2	C+(F+A)
Awl	OR12	97.8±0.3	2.14±0.20	<0.05	α; cor.	-	-	C+(F+A)+FF
Fishhooks	OR05	96.5±0.4	2.80±0.32	<0.05	α; cor.	-	-	C+(F+A)
	OR14	97.5±0.3	2.45±0.30	<0.05	α; cor.	114±2	128±2	C+(F+A)+FF
Unclassifiables	OR04	97.4±0.3	2.59±0.32	<0.05	α; cor.	-	-	C+(F+A)+FF
	OR09	99.2±0.1	0.84±0.12	<0.05	α; Cu_3As; cor.	-	-	C
	OR11	98.1±0.2	1.85±0.20	0.09±0.01	α; cor.	-	-	C+(F+A)+FF
	OR13	98.6±0.2	1.41±0.12	<0.05	α; cor.	-	-	C+(F+A)

Micro-EDXRF results indicate that the artefacts collection from OR is composed of copper and copper with arsenic (up to 4.61 wt.% As). As observed in Figure 5.6, 58% of the collection (seven artefacts) exhibit an arsenic content that could be considered as an impurity (As < 2 wt.%). The remaining five artefacts, representing 42% of the analysed collection, present an arsenic content that could be considered as an alloy element (As ≥ 2 wt.%). Iron content is below the quantification limit (< 0.05 wt.%) except for OR11 presenting 0.09 wt.% Fe. Other impurities such as antimony, lead, zinc, nickel or silver were not detected or were under the quantification limit and, consequently, they were not included in Table 5.1.

The average content of arsenic is 2.0 wt.%. The low number of items in this set does not allow a more precise observation and evaluation of the tendency of the arsenic distribution.

The saws presented variable arsenic contents (0.82 to 4.61wt.% As), while the fishhooks have a similar composition (2.80 wt.% and 2.45 wt.%). The remaining artefacts, with defined typologies, present an arsenic content near 2 wt.%.
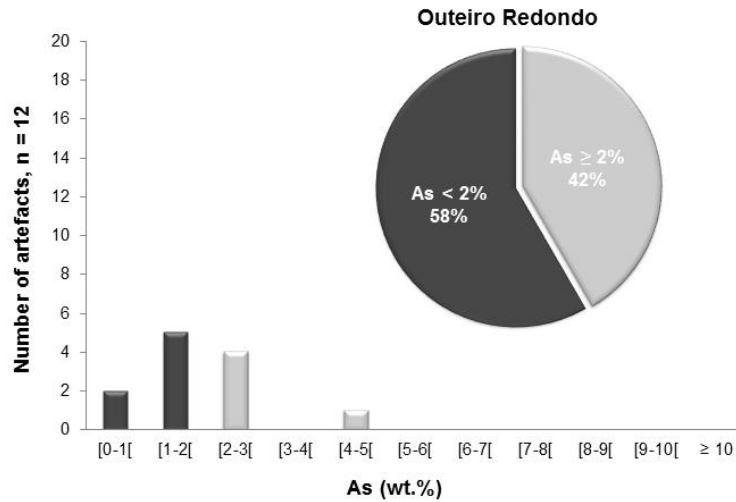
Figure 5.6. Distribution of arsenic content and percentage of copper and arsenical copper artefacts in OR collection.

Unlike the case of VNSP and ML artefacts collections, in OR collection there are only a small set of tools (eight artefacts) in the classified collection. Therefore, one cannot draw conclusions about the intentional presence or absence of arsenic and the artefact typology.

Optical microscopy observations of this collection revealed near-equiaxial α-Cu grains with annealing twins (Figure 5.7, A) and slip bands (Figure 5.7, B) as the most common microstructural features found.
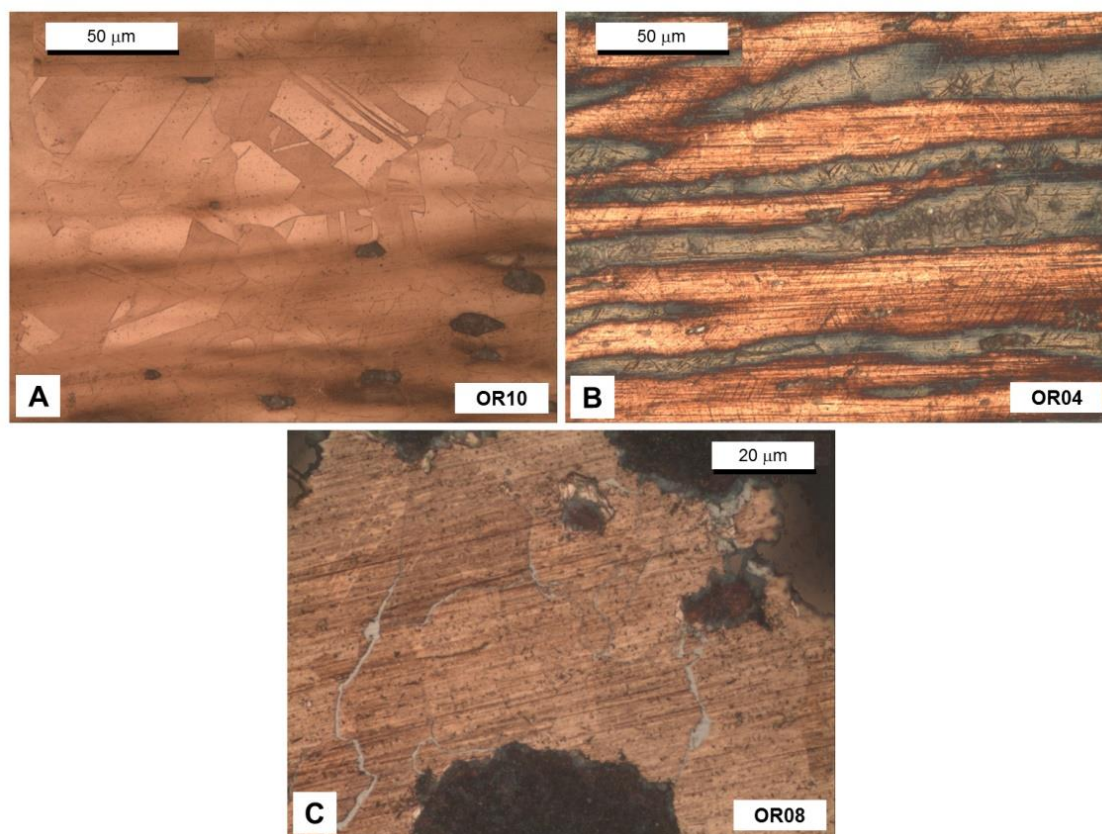
Figure 5.7. OM images of: A: saw OR10 (1.03 wt.% As) evidencing annealing twins and segregation bands; B: unclassifiable OR04 (2.59 wt.% As) evidencing annealing twins, segregation bands and slip bands; C: saw OR08 (4.61 wt.% As) showing annealing twins and Cu_3As segregations (all BF illumination, etched).

These microstructural features allow concluding that the operational sequence of forging plus annealing, followed by final forging operation, was applied to 42% of the artefacts (Figure 5.8).
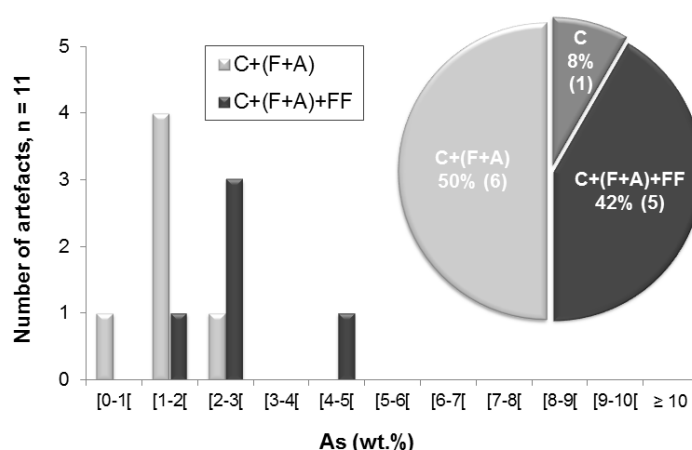
Figure 5.8. Distribution of manufacture processes by the arsenic content in OR artefacts.

In the artefact collection of OR, it is possible to find another direct example of the use of wires mentioned above in section 3.4: production of fishhooks (see Figure 5.9).
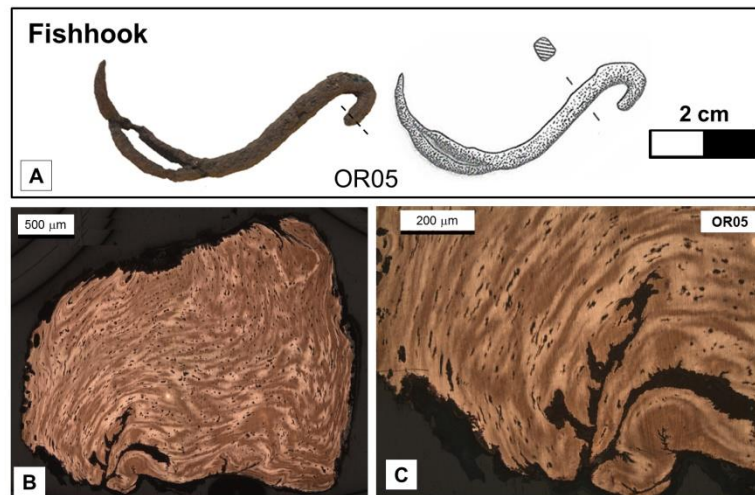
Figure 5.9. Fishhook from OR collection, microstructure evidencing the grains deformation to round up a previous rectangular section.

For copper or lower arsenic content artefacts, a commonly observed feature was the presence of red inclusions (under DF and Pol illumination in OM). These inclusions were identified by SEM-EDS (Figure 5.10, A) as being a Cu-O compound and assigned as cuprous oxide (Cu_2O). The finer and elongated shapes of the oxides mentioned above are a consequence of shaping operations.

Segregation bands were clearly visible after etching (Figure 5.7, B). In some samples, the Cu_3As intermetallic compound was identified by SEM-EDS (Figure 5.8, B) regardless of its crystalline structure. Using optical microscopy, they appear as blue-grey phase (Figure 5.7, C). As expected, the presence of cuprous oxide inclusions in copper-arsenic alloys is much reduced due to the deoxidizing properties of the arsenic.

The Cu_3As intermetallic phase can be observed in copper-arsenic alloys in three morphological types (see section 3.3). In OR artefacts, the arsenide formations that resulted from the eutectic transformation (biphasic structure) are not found. However, in saw OR08 are present the others two morphological types: thicker arsenide formations related to non-equilibrium casting features, such as strong coring that further annealing heat treatments were unable to homogenize completely, and thinner arsenide formations that can be observed around grain boundaries of recrystallized grains (Figure 5.7, C). Consequently, these post-casting formations reinforce the idea of a long-term arsenide precipitation at low temperatures during the burial of these artefacts over archaeological time. Overall, these segregation features seem to indicate an inability to achieve a homogeneous alloy.
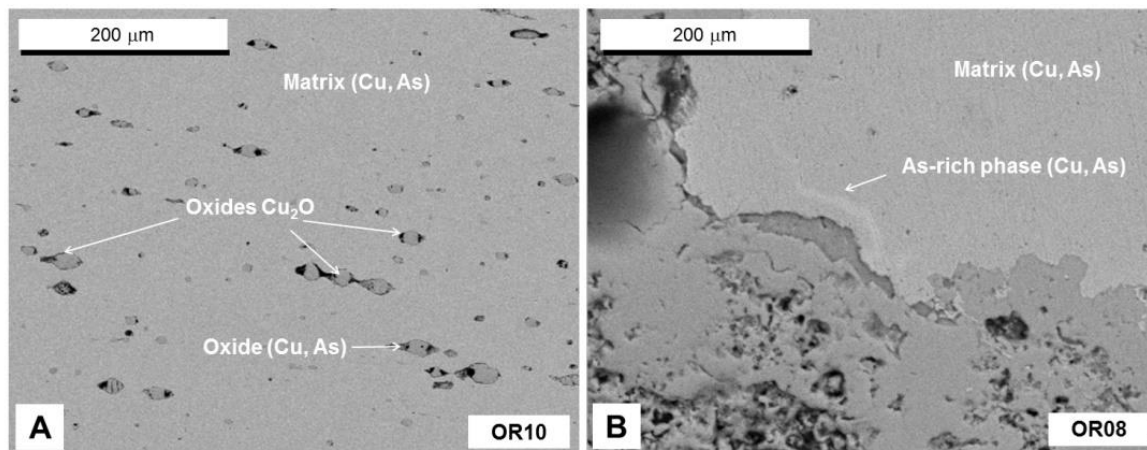
Figure 5.10. A: SEM-BSE image of saw OR10 (1.03 wt.% As) presenting the EDS identification of Cu_2O oxides and oxides consisting of Cu and As; B: SEM-BSE image of saw OR08 (4.61 wt.% As) showing the EDS identification of Cu_3As As-rich phase.

Microhardness measurements were made in the centre of the six mounted cross-sections and, when applicable, also near the borders (fracture surfaces and cutting edge). A more complete study was made in the saw OR07 since it was large enough to obtain a microhardness profile (the longitudinal cross-section profile will be presented ahead). The results for the microhardness in the centre of mounted cross-sections are presented in Figure 5.11, subdivided by attributed operational chain.

A linear regression was performed (y = 4.9x + 79.1) and the 95% confidence interval for the line slope was determined (slope = 4.9 ± 22.7). Although the measures have an apparent trend towards a positive slope (see Figure 5.11), since confidence intervals included zero, it cannot be excluded the hypothesis of no positive correlation using a linear model. It should be expected that the increase of the arsenic content would confer higher hardness to the alloy; however, no statistically significant association between the arsenic content and the measured hardness was found.

Due to the low number of artefacts, no further interpretations were made about the effect of the operational sequence and groups of typologies (all items were classified as "Tools").
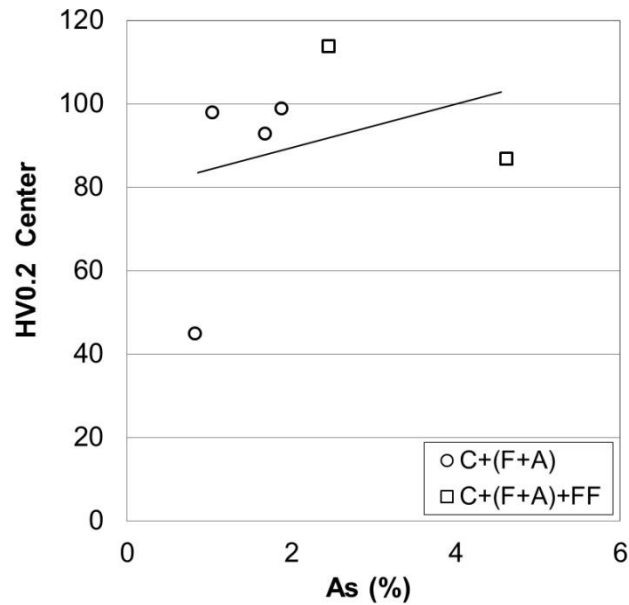
Figure 5.11. Micro-HV measurements (HV0.2, 10 s) in function of arsenic content of the artefacts (n=6) and operational sequence: C + (F + A) and C + (F + A) + FF; black line represents a linear regression over the data points.

In the "Saws" sub-group (n= 4), OR08 present higher arsenic content (4.61 wt.% As) and a final forging step in the operational sequence. However, OR08 displays a lower hardness than saw OR07 (1.87 wt.% As) and saw OR10 (1.03 wt.% As) (see Table 5.1). Saw OR08 also present lower hardness than the two artefacts from different typologies with less arsenic content: OR06 (1.67 wt.% As) and OR14 (2.45 wt.% As).

Although it was expected a significant hardening effect with a final cold hammering in arsenical coppers alloys (Rovira, 2004; Mohen, 1990; Northover, 1989), this was not the case for saw OR08. This artefact is the only presenting post-casting arsenides associated to ageing over archaeological time. So it is possible that the present hardness could be different than its original value after the object production.

Nevertheless, other variables could affect the material hardness and outweigh the influence of the arsenic content in the alloy. The different thermomechanical processing conditions applied to the artefacts (intensity and number of cycles) will result in microstructural differences among them. The great variability found in structural features, as grain size, inclusion distribution and morphologies, annealing twins and slip bands densities should contribute for the hardness dispersion observed. The different locations of sampling can also contribute to the dispersion of the hardness results.

It is expected that in some regions (tips and cutting edges) would be applied a more intense mechanical work and a harder final cold hammering than in others. Consequently, a higher increase in hardness would be obtained in the final shape. The hardness near the cutting edge and the central region for all six mounted samples were measured (Figure 5.12). In all the cases, the hardness of the cutting edge was slightly higher than in the central region but without a full exploitation of the hardening capabilities of these alloys.
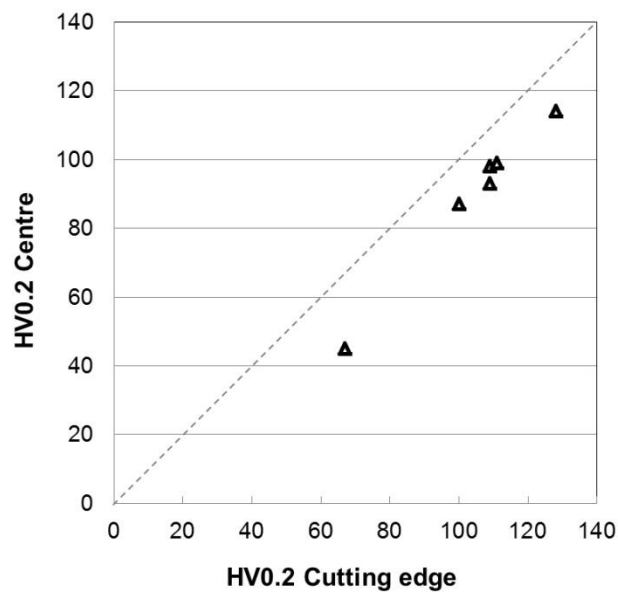
Figure 5.12. Micro-HV measurements (HV0.2, 10 s) between the cutting edge and central region (n = 6).

From this set of six artefacts, only two items present a final forging treatment. Therefore, it was not possible to have statistical evidence that the increase in hardness due to intensive mechanical work would be more significant in copper-arsenic alloys than of pure copper metal.

The artefact OR07 was sampled, and a microhardness profile was measured along the longitudinal direction (11 measurements) (Figure 5.13, A). The annealed structure shows elongated grains in all cross-section of the saw (Figure 5.13, B), indicating the application of intense thermomechanical processing in all section. The measurement data and the profile obtained are presented in Figure 5.13, C. Near the cutting edge it is observed an increase of hardness. Therefore, this profile points for an application of more intensive thermomechanical processing on the cutting edge, most likely as consequence of shaping of the blade edge and consequently increasing the hardness in this region.
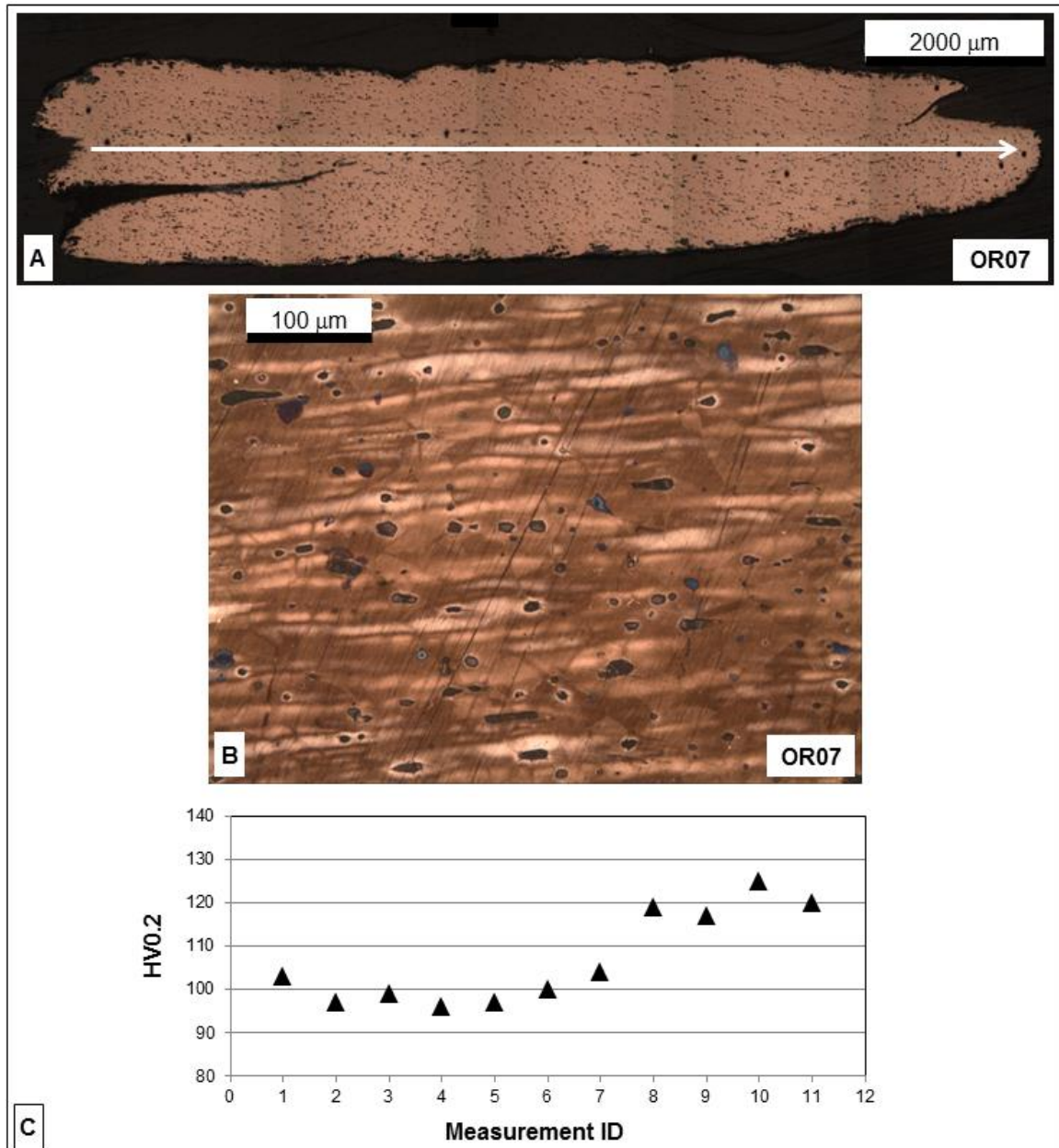
Figure 5.13. A: View of the orientation of the cut made in the saw OR07 (1.87 wt.% As) with micro-HV (HV0.2) measurements applied in longitudinal direction towards the blade (arrow); B: OM image of saw OR07 in central region evidencing segregation bands; C: Micro-HV measurements (HV0.2) in longitudinal profile of OR07.

6. DISCUSSION [6]

In this section an integrative view of the information obtained from the three Chalcolithic metallurgical collections is provided. A greater focus was given to the extensive metallurgical collection of VNPS since it represents the bulk of the data. Since VNSP has no detailed excavations reports with stratigraphy and chronology well defined, the smaller collections from the Chalcolithic sites of ML and OR should be critical for a comparative analysis of metal productions giving a broad view of the early metallurgy in Estremadura region of Portugal. It must be noted that, as referred in the Introduction, some analyses of VNSP artefacts were made before our research, in particular, within the SAM programme during which 88 copper-based artefacts and metallurgical remains were analysed using atomic emission spectroscopy. In addition to the different methodology used, this research group was interested in some particular vestigial elements to set up provenance groups that currently are not accepted and therefore those results will not be discussed in this thesis. Furthermore, another research work carried out by Müller and Soares (2008) included only a set of 15 copper prills and the so-called molten copper scrap from VNSP. Results of the elemental analysis were consistent with the already available knowledge of copper metallurgy from this settlement, but, for the first time, lead isotope ratios were used for a provenance study in the region. Thus only the results concerning the possible provenance of copper in use at VNSP will be discussed in the present work.

The scale of production can be assessed by the size of production remains and artefacts collections. It can be hypothesized that comparing the three settlements, VNSP may have been a large scale production settlement and for a longer period (~3000-2250 BC), while, apparently, ML and OR present a smaller metallurgical production and for much shorter occupation time, during the second half of the 3rd millennium BC. The apparent lower production could also be justified by the smaller settlements with less conserved vestiges recovered from the excavations.

Crucibles and slags were characterized and attributed to smelting or melting operations whenever possible. The associated oxide-type contents of the slags from VNSP were compared with a previous study of slags from VNSP and slags from Zambujal, another coeval Chalcolithic settlement located in Portuguese Estremadura. Elemental composition and microstructure observations were obtained from the selected metallic nodules.

Regarding the studied artefact collections, the elemental composition was determined in all items and manufacturing operations in identified typologies, while hardness and colour measurements were accomplished only in mounted samples, to obtain a more precise knowledge of the early metallurgical practice in this region of the Iberian Peninsula.

Results regarding the elemental composition of the artefact collections were compared between them, with nearby contemporary sites (Leceia and Zambujal) and with relevant settlements of other regions: São Pedro (Southern Portugal) and La Junta, Cabezo Juré, Valencina, Amarguillo and Necropolis Antoniana (Western Andalusia). The primary objective is to establish possible parallels and relations concerning metallurgical productions.

---

[6] Part of the content from this section was previously published (Pereira *et al.*, 2017).

6.1. EARLY METALLURGICAL EVIDENCE

All three settlements present evidence of the practice of metallurgical activities on-site. In the case of VNSP, the presence of both crucible and slag fragments alongside with metallic nodules and metallic scraps inside the settlement indicate possible smelting and casting operations in the same location. On the other hand, the only metallurgical remains of OR is a crucible fragment with evidence of being involved in melting operation. In ML collection no signs of smelting operations were present since there were not recovered any crucibles or slags. Melting operations were possibility present since a few metallic nodules were found in the settlement. There is always the possibility that these metallurgical operations occured outside the settlement limits, near the mine explored, explaining why other vestiges in the excavations were not identified. However, from the reduced information available, no evidence of these metallurgical remains was found near the mines. Therefore, metallic nodules and ingots were possibly brought from other settlements where evidence of smelting was found.

All the crucibles fragments with evidence of being involved in metallurgical activities from VNSP and OR (one item), presenting thicker walls (approximately 2 cm), point to operations involving copper and copper with arsenic.

The majority of slag fragments were constituted by iron products, magnetite (Fe_3O_4) and delafossite ($CuFeO_2$), and entrapped globules of metallic copper (prills) or copper oxides (Cu_2O or CuO) in a porous matrix of complex silicates, as well as some alteration products (corrosion products). The heterogeneity and microstructural characteristics mentioned suggest a relatively oxidizing atmosphere during slag formation, but temporarily and spatially reductive enough to produce metallic copper. Silica occurs as residual quartz, in silicates and Si-rich glasses in the matrix, while fayalite (Fe_2SiO_4), commonly present in slags formed in high reducing conditions during the smelting process of a more advanced metallurgy, was not detected at all. The absence of the latter phase together with the comparatively high amounts of trapped copper prills suggests that the slags must have been very viscous. These characteristics are an indicative of primitive smelting processes. They were most likely conducted in a ceramic crucible in an open-air fireplace loaded with crushed ore and charcoal. The redox conditions achieved in this assembly were very variable and far from the ideal.

At the end of the smelting process, the ceramic crucible was broken to recover the metallic nodules formed and trapped inside the highly viscous and heterogeneous slag. Therefore, it was expected a high retention of metal in the slags of these early smelting operations with consequent ore yield loss.

The slags analysed in this study were possibly produced from reduction of copper oxides and carbonate ores. The use of more complex copper ores like primary sulphides (chalcopyrite and bornite) (Nocete *et al.*, 2008) would possibly result in higher amounts of impurities and more complex compositions of the slag. Also, the scarcity of slags in Chalcolithic is attributed to the use of high-grade ores for smelting producing very little debris. However, it should be expected more recovered slags during archaeological excavations. It must be kept in mind that the natural corrosion and erosion processes may eliminate part of the slags. Another hypothesis is that the process of removal

of metal from the slag was made away from the smelting site or the smelting operation was accomplished outside the settlement. Nevertheless, settlements with more specialized metallurgy activity evidence present more slag findings than others with a more domestic setting (Bourgarit, 2007). In the Iberian Peninsula, there is evidence of copper smelting widely used conducted in the ceramic crucible in an open-air fireplace until pre-Roman times (Delibes de Castro *et al.*, 2001).

In the same slag, it is possible to observe prills of different sizes and coloration, from nearly pure copper to arsenical copper (Müller *et al.*, 2004). However, this was not the case in VNSP slags. In the same slag was not observed prills with significant compositional differences. This observation could be explained by the small volume of the slag material available.

In this section, the VNSP slag associated oxide-type contents are compared with a previous study of three slags from VNSP (VNSP30, VNSP31 and VNSP33) (Gaus, 2015) and a study of nine slags from Zambujal (Z9, Z43, Z62, Z87, Z98, Z151, Z192, Z194 and Z618) (Gauss, 2015). It must be taken into consideration that the differences or expected deviations could be attributed in part to the different analytical equipment used, in the different studies, or to the sampling and selection of areas analysed, which does not permit for a straightforward data interpretation and comparison with other studies.

To be able to compare slags from different studies and collections, an oxide association of the detected elements of the slags were represented in a (CuO - $SiO_2+Al_2O_3$ - $FeO+MgO+CaO$) ternary plot (compositions in wt.% - Table 6.1). The data were normalized regarding these oxide sums (remaining compounds were ignored).

Table 6.1. Normalized sum of oxides in slags from VNSP; previous studies: VNSP [a] (Gauss, 2015) and Zambujal [b] (Gauss, 2015), by SEM-EDS area analysis (wt.%).

Oxides / Slags	$Al_2O_3+SiO_2$ (wt.%)	FeO+MgO+CaO (wt.%)	CuO (wt.%)
VNSP280	9.27	79.2	11.6
VNSP301	32.0	52.7	15.3
VNSP302	32.6	57.6	9.93
VNSP306	25.9	57.6	16.4
VNSP309	39.6	59.3	1.26
VNSP311	38.8	53.7	7.50
VNSP313	36.4	53.3	10.3
VNSP599	63.5	36.6	0.00
VNSP30[a]	37.6	50.6	12.0
VNSP31[a]	62.4	22.7	14.9
VNSP33[a]	42.7	34.8	22.5
Z9[b]	9.50	39.5	50.9
Z43[b]	52.3	46.3	1.45
Z62[b]	49.9	30.5	19.6
Z87[b]	55.8	27.3	16.9
Z98[b]	30.6	34.8	34.5
Z151[b]	55.5	28.5	16.0
Z192[b]	56.6	36.4	7.01
Z194[b]	48.1	31.2	20.7
Z618[b]	52.4	40.0	8.30

In the resulting ternary plot, all the major elements are represented, thus clearly showing the high copper content in the slags from Chalcolithic settlements (expressed in CuO wt.%) (Figure 6.1).
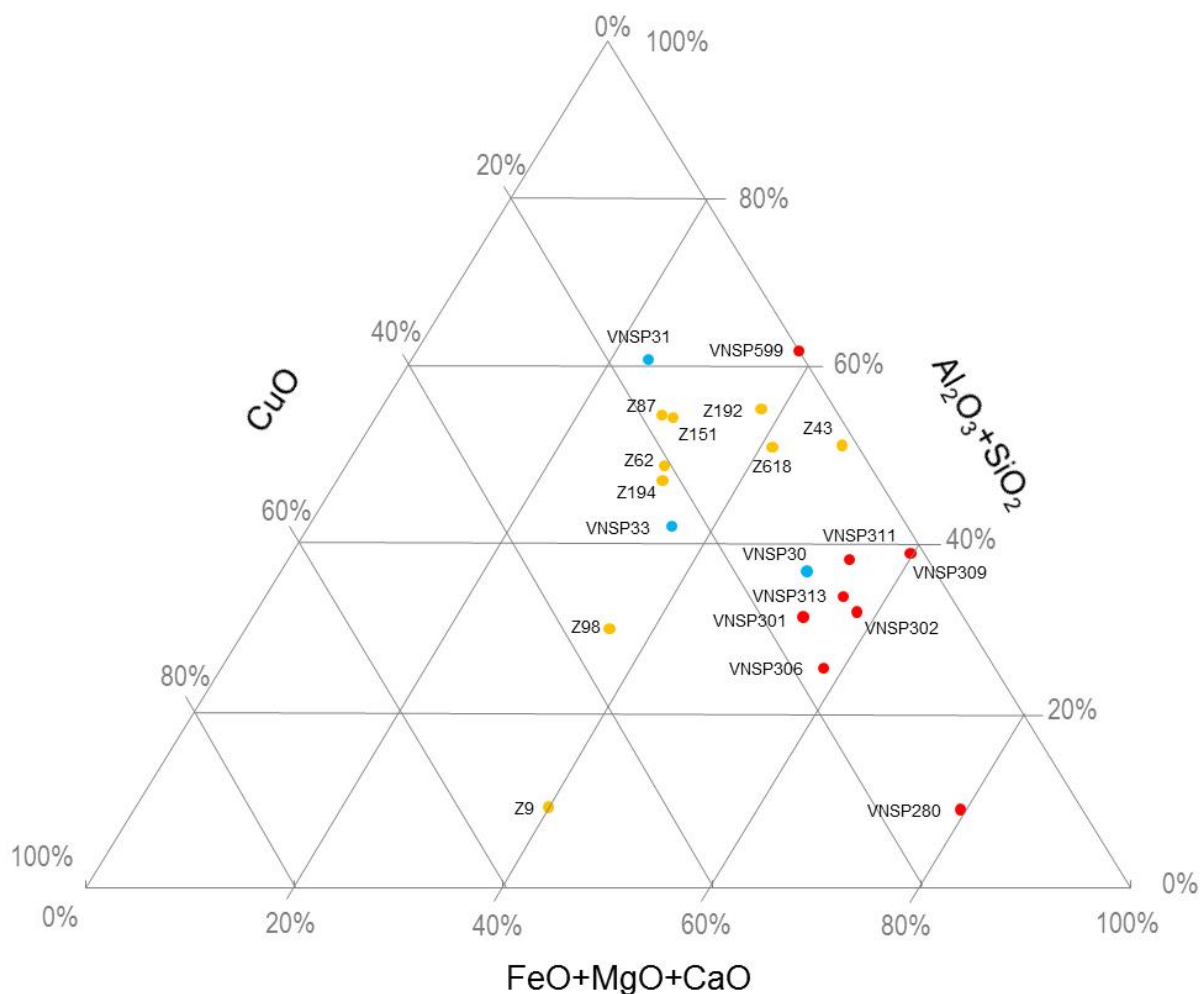
Figure 6.1. Bulk chemical compositions of the slags from the most of the Chalcolithic sites reviewed (22 analysis) plotted in a CuO - (SiO$_2$+Al$_2$O$_3$) – (FeO+MgO+CaO) diagram (compositions in wt.%). Red dots: VNSP slags; Blue dots: VNSP slags from the previous study; Orange dots: Zambujal slags (Gauss, 2015).

The data obtained from the Chalcolithic slags evidences the lack of consistency encountered at the beginning of copper extractive metallurgy. However, despite the dispersion observed, they are in accordance with the bulk chemical compositions of the slags from the most of the Chalcolithic sites (Bourgarit, 2007). Three slag samples from VNSP from the previous study (VNSP30, VNSP31 and VNSP33) are very heterogeneous, composed by magnetite, quartz inclusions, copper prills, and glass. Delafossite occasionally formed close to pores and at the edges of the slag, sometimes also interspersed among and around magnetite. The copper inclusions often show arsenic segregations with substantial variations in colour due to varying contents. Therefore, the conditions during the smelting operations were fairly oxidizing but reducing enough to form arsenical copper (Müller and Soares, 2008). The level of dispersion is similar to the VNSP slags analysed in the present study and the slags from Zambujal.

Following the smelting of the ores, all the metallic nodules would be collected and melted inside another crucible to subsequently be poured into a mould or left to cool down as an ingot. There were

no apparent differences between the ceramic or thickness of the crucible fragments from VNSP with indications of being used in smelting or melting operations.

In VNSP crucible collection, three fragments could be attributed to melting operations. In these cases, iron oxide compounds were absent, and slags were mainly composed of copper and copper oxides mixed with vegetal structures vestiges (charcoal), all characteristics consistent with a melting slag origin.

Elemental composition of the metallic nodules from VNSP (0.10 wt.% < As < 4.70 wt.%) and ML (0.37 wt.% < As < 4.78 wt.%), both collections composed of copper or copper with arsenic, is consistent with the production of the corresponding artefact collections. They also exhibit very low iron contents since the redox conditions were not sufficient to reduce the iron impurities present in the process and to be incorporated in the metal.
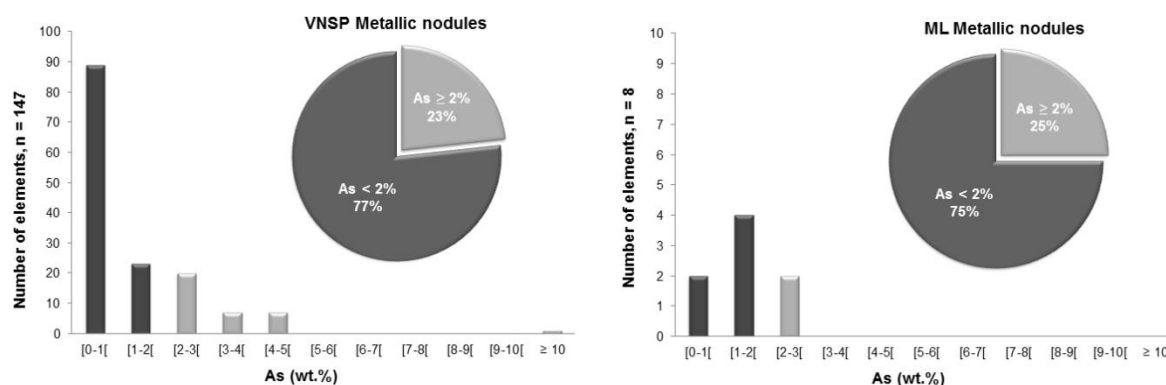
Figure 6.2. Distribution of arsenic content and percentage of metallic nodules below 2% and above 2% As in the metallurgical vestiges from VNSP and ML.

Results show that the percentage of ML nodules with As ≥ 2 wt.% (25%) is only slightly larger than the percentage of VNSP nodules (23%) (see pie charts from Figure 6.2). However, due to the small size of ML group, the difference is not statistically significant.

The distributions of arsenic found in the metallic nodules of VNSP and ML collections (see Figure 6.2) were compared using a Kolmogorov–Smirnov two-sample test (two-sample K–S test) to establish possible parallels and relations concerning metallurgical productions. The p value obtained ($p = 0.034$) rejects the null hypothesis ($p < 0.05$), confirming that the nodules do not have similar arsenic distributions.

The distribution of arsenic in the metallic nodules from VNSP is close to the shape of a "geometric distribution" (see Figure 6.2), which resembles the natural distribution of minor and trace elements in minerals (Müller *et al.*, 2007). Therefore there was no clear separation for the production of copper and arsenical copper alloys regarding the extractive processes. However, a posterior selection of the nodules based on colour could be made for the production of different artefacts or typologies.

The VNSP larger metallic nodules collection, possibly indicating a higher metallurgical production by a longer period, could also be affected by the more considerable diversity of ores compositions. On the other hand ML, with a smaller metallic nodules collection, is possibly a consequence of a lower metallurgical production during a shorter occupation period. The reasons that could lead to different arsenic contents in the artefacts produced in these settlements will be addressed in more detail in the following section.

The microstructure of the analysed metallic nodules in VNSP suggests in the majority of the cases smelting origin, more spherical forms, presenting coarse microstructure, all indicating liquid immiscibility and slow cooling rates. The porosities present in the microstructures suggest the formation of the nodules from an ore reducing operation (smelting) since it is a process that evolved gas and is subjected to more contaminations than a melting operation. On the other hand, VNSP metallic nodules found with a more irregular shape and finer dendritic structure, suggest fast cooling rate. These observations are consistent with a small piece of metallic copper that fall from the crucible during a melting or casting operation and cool down faster due to the higher temperature differences and the smaller volume. In these cases, the pores present are attributed to solidification shrinkage. In the case of ML metallic nodules collection, the characteristics exhibited are consistent with production by smelting operations.

Considering the slag compositions analysed and the low inclusion concentrations present in the metallic nodules recovered from VNSP and ML, the exploited copper ores were most likely copper oxides and copper carbonates, also presenting fewer impurities.

In conclusion, results obtained from the analysis of crucible fragments, slag and prills indicate copper and arsenical copper artefact production. The metal was obtained most likely by direct smelting of copper ores. The earlier smelting of copper ores was performed under poor reducing conditions, which naturally produce copper with very low iron contents.

The absence of ingots among the archaeological record could be explained if the smelting and casting activities were performed at the same location. If this was the case, melting with the selected prills was performed in a crucible and then poured into the final mould. There is also the possibility of not recognizing the ingots if, for instance, axes were used as ingots. The typology that required more metal to manufacture was most certainly the axes, given their volume and size. However, all the axes analysed in this thesis presented annealing operations and visible marks in the cutting edges, suggesting that were used as tools after casting into a mould. Nevertheless, in the VNSP assemblage, there is a considerable number of cutting edge fragments of axes showing intentional sectioning which objectively is unclear. They could be removed from the corresponding axe to sharpen a new edge again. In that case, the old or damaged cutting edge would be attributed to scraps from the manufacturing process or parts of ingots, put aside for posterior re-melting or shape into smaller objects (Müller and Soares, 2008). Parallels of this intentional sectioning process can be found at the settlement of Leceia (Cardoso and Guerra, 1997/1998).

It is important to explore further metallurgical vestiges to have a more consistent view of the operations used, including the determination of elemental composition and microstructural

characterization of a larger set of metallic nodules. The addition of more data will allow us to have more consistent information about the arsenic distribution in the metallurgical remains and a better comprehension of the metallurgy applied in the Estremadura region.

Evidence seems to indicate that artefacts were produced in all three settlements, using a crucible technology and working under relatively oxidizing conditions (smelting operations). Also, the large quantity of scrap material recovered in VNSP and ML suggests the existence of recycling operations.

6.2. EVALUATION OF THE METALLURGICAL PRODUCTION

Results regarding the elemental composition of the artefact collections studied in the present thesis (VNSP, ML and OR) were compared between them. They were also compared with nearby contemporary sites namely Leceia (Müller and Cardoso, 2008) and Zambujal (Gauss, 2015) and with relevant settlements of other regions: São Pedro (Southern Portugal) (Vidigal *et al.*, 2016) and La Junta, Cabezo Juré, Valencina, Amarguillo and Necropolis Antoniana (Western Andalusia) (Bayona, 2008). São Pedro (Southern Portugal) settlement presents evidence of smelting and casting operations with production of metallic artefacts, alongside with Cabezo Juré, Amarguillo and Valencina (Western Andalusia) (Vidigal *et al.*, 2016; Bayona, 2008). La Junta presents only evidence of casting operations with production of artefacts and Necropolis Antoniana only have metallic artefacts in the assemblage. These last two sites would most likely import raw copper (prills and ingots) and artefacts respectively (Bayona, 2008). The localization of these settlements is presented in Figure 6.3. The primary objective is to establish possible parallels and relations concerning metallurgical productions.

Chalcolithic data of the same type of objects from other regions close to the Portuguese Estremadura, as Central Portugal or Beiras, are scarce; therefore Southern Portugal and Western Andalusia were the only data used for this comparison. For the sake of simplicity, the Western Andalusia set comprises data from five different Chalcolithic settlements.

The distribution of arsenic content present in the artefacts collections from these sites is presented in Figure 6.4. The elemental composition of the artefact collections from VNSP, ML and OR is in accordance with the earlier evidence of copper-based metallurgical activities in the Iberian Peninsula. In this geographic region, copper and arsenical copper were the only metals used in the manufacture of artefacts, with iron contents in most cases below the quantification limits (Ruíz-Taboada and Montero-Ruíz, 1999). Also, data from VNSP previous studies are comparable with results obtained in this thesis. The results of the analysed 88 copper-based artefacts and metallurgical remains from the SAM programme indicate that artefacts are composed of copper or copper with arsenic containing very low concentrations of trace elements (Junghans *et al.*, 1960, 1968, 1974; Soares, 2005). The arsenic content ranges from 0.1 wt.% to 5 wt.% As, and only a dagger presented approximately 9 wt.% As. Also, the same analyses show that the artefacts contain a very low amount of iron, lower than 0.01% for 98% of the cases and up to 0.2% for the remaining artefacts (Soares, 2005).

Similar results were obtained from the Zambujal settlement concerning the distribution of arsenic and low levels of trace elements (Müller *et al.*, 2007). In Leceia, all the artefacts present an elemental composition similar to those from Zambujal (initial phases of occupation) and VNSP. They are all composed of copper and arsenical copper with low presence of impurities (Müller and Cardoso, 2008).
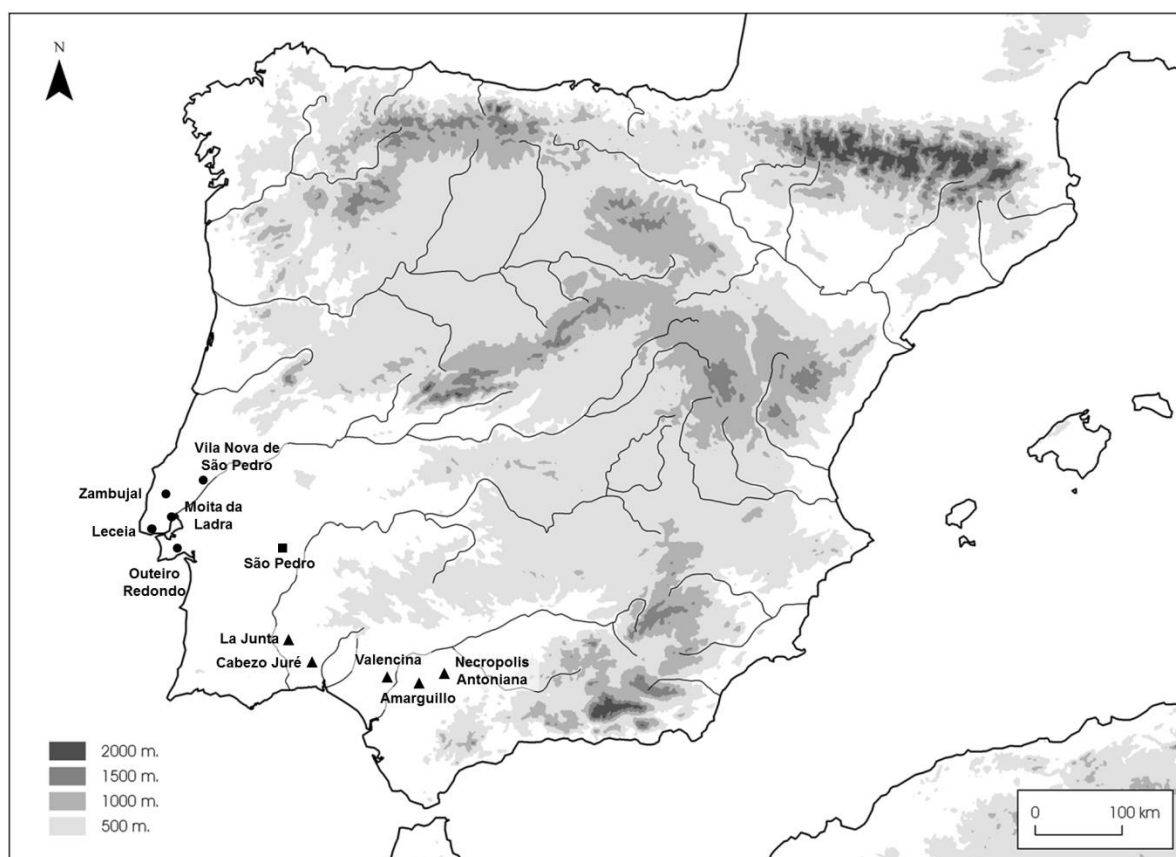
Figure 6.3. Localization of the settlements: ● Portuguese Estremadura (Moita da Ladra, Vila Nova de São Pedro, Leceia, Zambujal, Outeiro Redondo); ■ São Pedro (representing the Southern Portugal); ▲ Western Andalusia (La Junta, Cabezo Juré, Valencina, Amarguillo, Necropolis Antoniana).
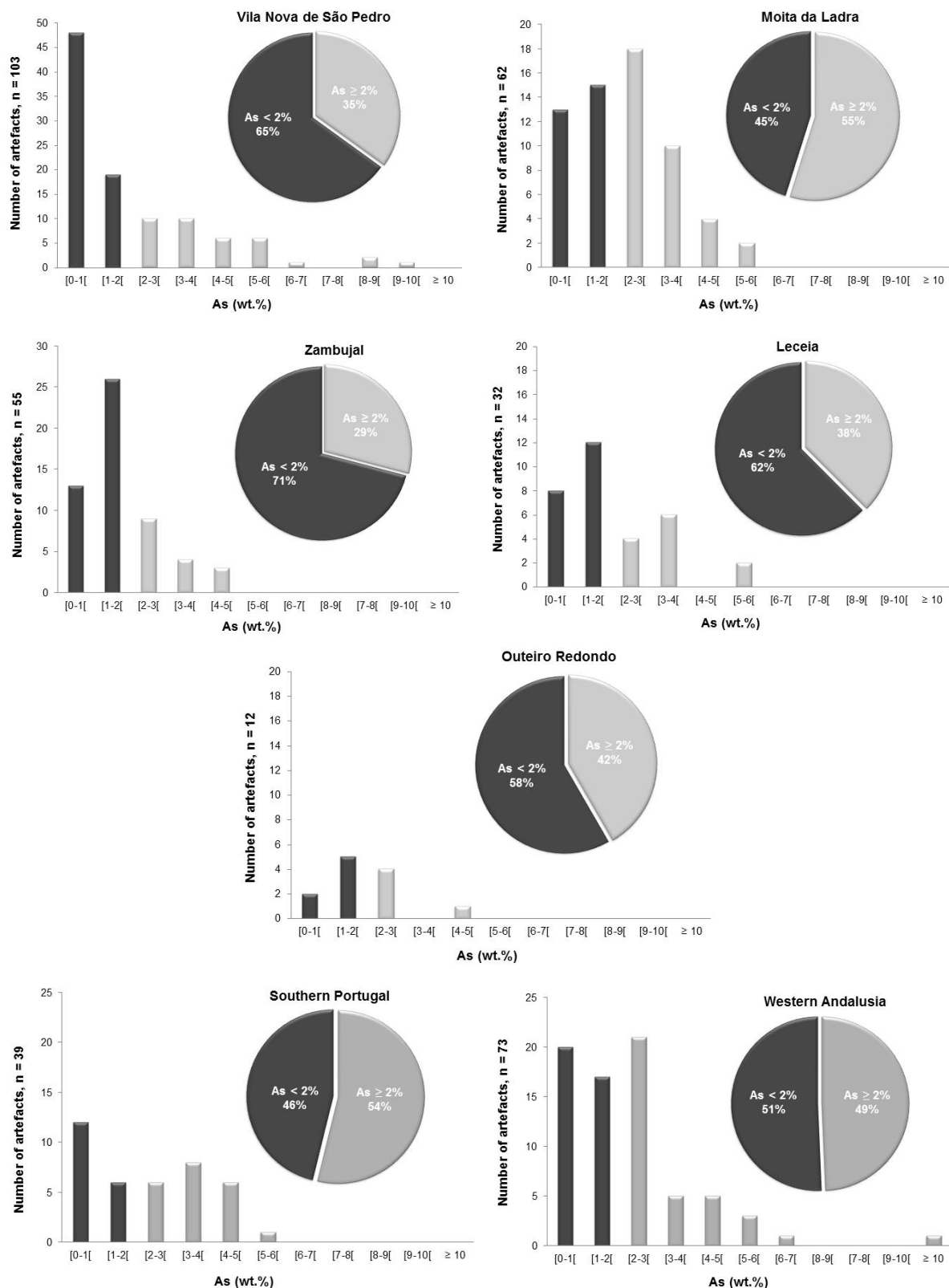
Figure 6.4. Distribution of arsenic content in finds of VNSP, ML, OR, Zambujal (Gauss, 2015) and Leceia (Müller and Cardoso, 2008) (Estremadura), Southern Portugal (Vidigal *et al.*, 2016) and Western Andalusia (Bayona, 2008).

The Kolmogorov–Smirnov two-sample test (two-sample K-S test) was used to compare distributions of arsenic found in the artefacts of the different collections to establish possible parallels and relations concerning metallurgical productions. K-S tests were applied in a pair-wise fashion to compare the distribution of arsenic found in the artefacts of different collections. Results are presented in Table 6.2. In the cases in which the K-S test rejects the null hypothesis ($p < 0.05$), the arsenic distributions are different. On the other hand, when the test does not reject the null hypothesis ($p > 0.05$), it indicates that the various sets of artefacts are not different and may have similar arsenic distributions.

Table 6.2. Results of the Kolmogorov-Smirnov test using permutation strategy: *null hypothesis was rejected at significance levels lower than 5% ($p < 0.05$).

Settlements/regions	VNSP	ML	Leceia	OR	São Pedro (Southern Portugal)	Western Andalusia	Zambujal
VNSP	-	<0.001*	<0.001*	0.027*	0.104	0.017*	0.001*
ML	<0.001*	-	0.013*	0.656	0.236	0.073	0.005*
Leceia	<0.001*	0.013*	-	0.382	0.126	0.066	0.035*
OR	0.027*	0.656	0.382	-	0.160	0.497	0.218
São Pedro (Southern Portugal)	0.104	0.236	0.126	0.160	-	0.270	0.007*
Western Andalusia	0.017*	0.073	0.066	0.497	0.270	-	0.009*
Zambujal	0.001*	0.005*	0.035*	0.218	0.007*	0.009*	-

Based on these results, the differences and probable similarities of arsenic distributions in the analysed artefacts are illustrated in Figure 6.5. The arsenic content of the São Pedro objects (Southern Portugal) could be similar to all the other settlements with the exception of Zambujal. Also, despite the proximity, ML, VNSP, Leceia and Zambujal have no similarities between their arsenic distributions. OR present possible similarities with Leceia, Zambujal, Southern Portugal and Western Andalusia.

Results indicate that in VNSP, OR, Leceia and Zambujal settlements the percentage of arsenical copper artefacts is lower than in ML, Southern Portugal and Western Andalusia (see pie charts in Figure 6.4). The settlements with longer chronologies, encompassing the entire Chalcolithic period (~3000-2250 BC) are VNSP, Leceia and Zambujal. All settlements included in this study, in the Western Andalusia, region also present chronologies encompassing the entire Chalcolithic period (Bayona, 2008).

However, the artefacts collections recovered from the settlements located in the Estremadura region (VNSP, Leceia ML and Zambujal) do not show similar arsenic distribution, despite the proximity. These sites only present possible similarities with other regions, with the exception of OR (Figure 6.5). On the other hand, the high number of Chalcolithic settlements with metallurgical activity evidence in the Portuguese Estremadura does not match the few copper ore occurrences in the region (Müller and Soares, 2008; Sousa *et al.*, 2004). Therefore, it is very likely that copper was brought from other

regions (Gauss, 2015; Müller and Cardoso, 2008) and hence a possible explanation for the potential similarities of Estremadura region production with Southern Portugal and Western Andalusia.

In the case of Leceia, raw copper (prills and ingots) would have been imported (Cardoso and Fernandes, 1995), since no evidence of smelting, but only casting remains were found at this site (Cardoso and Caninas, 2010; Müller and Cardoso, 2008). The same observations applied to ML since only prills were recovered from the settlement. In the case of OR, only a crucible fragment associated with melting operations was discovered. Prills or ingots would be likely produced from ore reduction at settlements where smelting evidence is recorded, namely at VNSP and Zambujal. In these settlements, the metallurgical finds include several crucibles and slag from smelting operations (Gauss, 2015; Pereira *et al.*, 2013a; Soares, 2005). However, the possible exportation of ores and raw copper does not explain the different percentages of arsenic between settlements in the Estremadura.
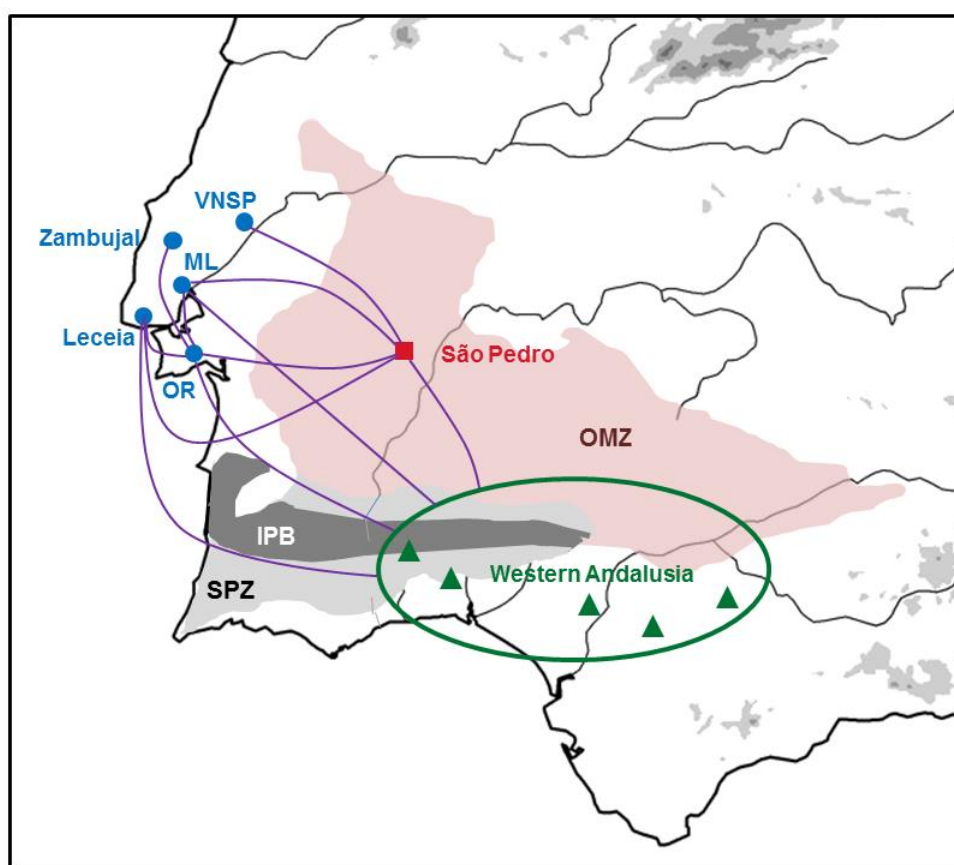
Figure 6.5. Lines between settlements indicate possible similar arsenic distributions in the artefact collection; Settlements: Estremadura region (blue), São Pedro representing Southern Portugal (red), Western Andalusia (green); Background: Ossa Morena Zone (pink area) and the South Portuguese Zone (light grey area) including the Iberian Pyrite Belt (dark grey area).

Provenance studies based on lead isotope analysis of artefacts from VNSP, Leceia, Zambujal and São Pedro (Southern Portugal) indicate that the raw materials come from ore deposits in the Ossa Morena Zone (OMZ) (pink area, Figure 6.5) (Gauss, 2015; Müller and Cardoso, 2008; Müller and

Soares, 2008; Müller *et al.*, 2007). Amarguillo (Western Andalusia) provenance studies present a compositional dispersion consistent with OMZ region (Hunt-Ortiz, 2003). On the other hand, Cabeço Juré, La Junta and Valencina used ores from Iberian Pyrite Belt (Nocete et al., 2008; Nocete et al., 2004). Copper-based artefacts belonging to La Pijotilla (Middle Guadiana basin), a coeval settlement located in the OMZ, also present identical lead isotope ratios. Furthermore, petrographic analysis has shown that polished stone artefacts of amphibolite found at Leceia and Zambujal were imported, some in unworked condition, from sources in the OMZ (Valera, 2013; Cardoso and Carvalhosa, 1995). All this suggests that, at that time, products obtained through smelting of copper ores from OMZ were part of a trade with the Estremadura region (Gauss, 2015; Müller and Cardoso, 2008). The trading of ores would possibly explain the similarities between Western Andalusia with Southern Portugal (Figure 6.5) and also the possible connections between these two regions and Estremadura. If the occurrences of ores near the Estremadura were indeed scarce, the settlements could resort to the ores deposits in OMZ.

It is important to remember that ML, OR and São Pedro (Southern Portugal) settlements were predominantly occupied during the second half of the 3rd millennium BC and the early decades of the 2nd millennium BC. In this chronological period, one important characteristic is the existence of a new cultural phase designated by Bell Beaker period characterized in more detail in section 1.3. Also, in this period, an increased use of copper alloys with higher arsenic contents and new types of metallic artefacts, namely Palmela points, appear (Soares *et al.*, 1996). These novelties might indicate that in this period different or more diversified copper ore sources were used, as shown by slightly different arsenic contents in the artefacts produced in these settlements. The increased use of copper alloys with higher arsenic contents was observed in ML and Southern Portugal but not in OR possibly due to the small artefact collection. Also, despite ML and OR being contemporaneous, the presence of the Bell Beaker period was strongly verified in ML rather than in OR.

The percentage of arsenical copper artefacts recorded in VNSP, Leceia and Zambujal seem to be significantly inferior from ML and OR contemporary settlements. However, these settlements represent chronologies encompassing the entire Chalcolithic period, contrary to ML and OR, that have shorter occupation periods between the 2nd and 3rd millennium BC, characterized as Bell Beaker period. The higher percentage of arsenical copper artefacts in ML and OR could be pointing out that, since the 2nd half of the 3rd millennium BC, there might have been different copper sources supplying the settlements of the Estremadura. Besides the hypothesis of the use of ores from OMZ, based on the lead isotope analysis of artefacts from VNSP, Leceia and Zambujal, ores might have also originated from other mining districts like the Iberian Pyrite Belt region (dark area, Figure 6.5) in the South-Portuguese Zone. The Iberian Pyrite Belt was already known to be the copper source for La Junta, Cabezo Juré and Valencina Chalcolithic settlements (Western Andalusia) (Bayona, 2008; Nocete *et al.*, 2004). This hypothesis is in agreement with the intensification and diversification of the economic activities in the south and south-east of the Iberian Peninsula that characterized the period between the 2nd half of the 3rd millennium BC.

The extended occupation chronology of VNSP and large collection of metallic artefact fragments recovered in this settlement, some with signs of sectioning, suggests the existence of a higher

number of recycling operations which could be a cause for the variable contents of this element. Frequently recycled artefacts resulting in a reduction of arsenic content since, at each melting of an arsenical copper alloy, there are losses by oxidation of the arsenic and evaporation of As_2O_3 (Mckerrell and Tylecote, 1972). The same phenomenon could also occur in the other settlements with large occupation chronologies like Leceia and Zambujal. Therefore, in such sites, the existence of metallurgical activities for longer periods of time may cause higher variability in the arsenic content of the alloys as a consequence of several cycles of recycling over time.

The distribution of arsenic content of the metallic nodules of VNSP and ML were also compared with the respective arsenic distribution of the artefacts collections (Figure 6.6).
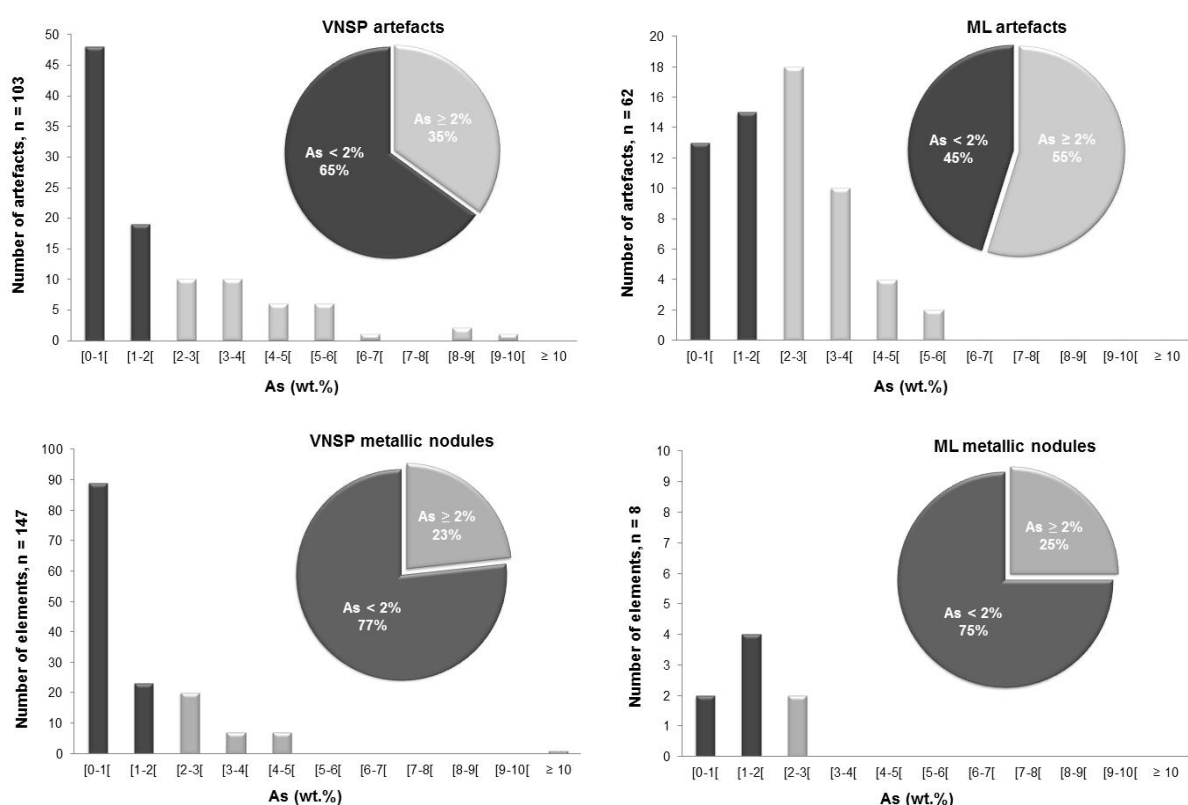
Figure 6.6. Distribution of arsenic content and percentage of artefacts and metallic nodules below 2% and above 2% As in the metallurgical vestiges from VNSP and ML.

Table 6.3. Results of the Kolmogorov-Smirnov test using permutation strategy: *null hypothesis was rejected at significance levels lower than 5% ($p < 0.05$).

Metallic nodules	vs.	Artefacts	*p* value
VNSP metallic nodules		VNSP artefacts	0.027*
ML metallic nodules		ML artefacts	0.476

From a statistical point of view, the arsenic distribution of VNSP metallic nodules has no similarities with VNSP artefacts collection. However, artefacts and metallic nodules histograms for VNSP exhibit a similar type of distribution (shape of the distribution close to a "geometric distribution"), reflecting the higher number of items with low arsenic contents (Figure 6.6). In opposition, the ML artefacts collection exhibit a shape of the distribution close to a "normal distribution". However, a higher number of arsenical copper alloys (As ≥ 2%) were found in the artefacts collection from VNSP when compared to the corresponding metallic nodules collection. If a selection based on colour was being applied to the production of artefacts richer in arsenic, the metallic nodules with more arsenic (golden) were preferentially chosen, and therefore explaining the inequalities between distributions. The majority of VNSP metallic nodules collection could be the remaining material, less used and left in the settlement.

In the case of ML, there is a possible similarity between the two distributions. The possibility of use ores richer in arsenic is in accordance with both nodules and artefacts also presenting higher arsenic contents.

It is important to be aware that the results obtained from this analysis do not have in consideration several possible confounding factors such as different stratigraphic origins or lack of stratigraphic provenance (as in the case of VNSP) or even different dimensions of the excavated settlements. Therefore, more data would be highly valuable and would strengthen the interpretation of results. However, these results already provide an extra insight based on the arsenic distribution alone.

6.3. METALLURGICAL PROCESSING

In all three collections, thermomechanical processing applied in the manufacture of the artefacts was accomplished with one or more cycles of forging and annealing operations. The final forging procedure was applied in 32% of the artefacts collection in the case of VNSP, 33% in the case of ML and 42% in the case of OR.

Regarding hardness measurements made in ML and OR collections, it was observed that the artefacts with higher arsenic content also have a higher hardness. In the case of ML, due to the low number of artefacts in each category, when subdividing the analysis by groups of typologies and analysing them separately, they do not show any apparent tendency. In OR the artefact set is composed only of "Tools"; therefore, no further observations about arsenic content were made regarding typologies and hardness. Regarding VNSP, no microhardness measurements were made in the collection presented in this thesis. In the previously studied artefact collection, although it was expected that the presence of higher levels of arsenic could confer hardness to the alloy, it was not found any statistically significant association between the arsenic content and the measured hardness (Pereira et al., 2013b).

Furthermore, in the previous analysed VNSP collection was observed an association between the presence of final forging treatment and artefacts presenting higher arsenic contents. The samples set in ML and OR are too small to be statistically certain of the intentionality of this final operation to

increase hardness. Also, artefacts submitted to a final forging step were not consistently harder with increasing arsenic contents. These observations indicate that the hardness of those arsenical copper alloys was not exploited to its full extent and therefore may not be acknowledged. The hardness increase observed in the cutting edges of some artefacts was probably a result of a more intense thermomechanical work applied with the objective of shaping the object.

In spite of the indication of some degree of control over the identification and selection of the alloys used in VNSP, it was observed that the ancient metallurgists were not completely aware of the hardening ability of alloys richer in arsenic. The thermomechanical operations applied with the intention of shaping were most likely independent of the arsenic content. Different colouration from pure copper should be considered more suitable for prestige or ceremonial artefacts. Therefore, the colour was probably the key property determining the selection of the arsenical alloys by prehistoric metallurgists rather than their mechanical properties. In those cases, the final forging operation aimed to obtain a more appellative final surface in objects with more golden or silver coloration.

With the intention of clarifying how arsenic affects the colour of copper alloys, the colour properties of an artefact collection from VNSP previously published (Pereira *et al.*, 2013a) was measured by colorimetry. Results indicate that the colour of the alloy is affected by the arsenic content in the alloy, presenting from a red to a more golden and later silver hue with the increase of arsenic. The collected colour data support the idea that the initial use of arsenical copper alloys intended to imitate the colour of gold or silver with associated higher prestige. Even if later the ancient metallurgists acknowledge the physical and mechanical advantages of the arsenical copper alloys (casting properties, increase workability and hardness), the aesthetic consideration of colour may have equal or greater importance in the past since those properties were not fully exploited.

When comparing the thermomechanical processing applied to these artefacts collections with the metallographic analysis of 64 copper objects from Zambujal (Wang and Ottaway, 2004) some differences were found. Similar to observed in VNSP, ML and OR, most of the chisels and the only saw examined were cast, cold-worked, annealed and finally cold-worked again with the exception of the awls. In Zambujal the awls were left in an annealed soft state condition in most cases. Nevertheless, very similar metallographic observations from VNSP, ML and OR were made on equivalent artefacts from Chalcolithic and Early Bronze Age Spain (Rovira and Gómez-Ramos, 2003; Hook *et al.*, 1991). It is expected in al these collections that the hardness obtained with the applied thermomechanical work would be sufficient for the use in daily activities. Small awls may have been used for leatherworking, the thin saws and knives for elaborate fine work of organic material, such as wood, bone or ivory and long awls, daggers and Palmela points as symbols of status and communication (Müller *et al.*, 2007). The massive copper axes appear heavy and less worked, especially when compared to the sophisticated amphibolite axes (cf. Lillios, 1997). The metallographic analysis of one axe from Zambujal reveals that it was left in an annealed, soft state, in agreement with results of metallographic analyses of axe cutting edges Porto Mourão (Wang and Ottaway, 2004; Soares *et al.* 1996). On the other hand, the microstructure and final hardness obtained in the cutting edges of VNSP axes (between 45 HV0.2 and 95 HV0.2) compared to the centre (41 HV0.2 to 64

HV0.2) seems to indicate an increase of hardness. This increase is most likely the consequence of more work applied to the shaping of the blade, than to intentionally produce a harder tip of the object (Pereira *et al.*, 2013a). Despite the suggestion that axes could have been more suitable for use as ingots or objects of display, rather than tools (Cardoso and Guerra 1997/98; Soares *et al.* 1996), some marks displayed in the blades of the axes analysed in the present study may indicate its use as a tool.

Generally, regarding the artefacts analysed in the present thesis, the shaping of large and more complex artefacts, like axes, daggers or arrowheads was most likely accomplished in the mould, being needed some final thermo-mechanical processing, mainly to the cutting edges. On the other hand, smaller and simpler typologies like chisels, awls and fishhooks, with a round or elliptical section, were possibly shaped from an intermediate material of rectangular section. Chisels were possibly produced by shaping pre-defined cast forms, as cast bars, through thermo-mechanical treatments and could require various cycles of plastic deformation and annealing. From the microstructural observations, it is possible to identify the recrystallized grains deformed from a previous rectangular section to a round section in some examples of these typologies. Awls and fishhooks were possibly produced from a thinner intermediate form. The wires from VNSP collection present a microstructure consistent with a sheet of cast metal that was posteriorly cut into strips of metal.

Microstructural observations in the studied artefacts collections indicate the presence of red inclusions (under DF and Pol illumination) when the alloy has lower or null arsenic content. These inclusions were recognized by SEM-EDS as being the eutectic cuprous oxide (Cu_2O). It was also observed in Cu-As alloys a reduction of this cuprous oxide formation (due to the high oxygen affinity of the arsenic). In some cases, a presence of a grey blue phase was observed. This phase was identified as the Cu_3As arsenide, an expected intermetallic compound in As-rich copper alloys. This copper arsenide was detailed studied in this thesis. Thermal synthesized Cu_3As is reported in the literature as exhibiting a hexagonal crystallographic structure. However, a cubic Cu_3As phase was identified by X-ray diffraction in all of our analysed archaeological artefacts, while the hexagonal Cu_3As phase was identified only in the artefact with higher arsenic content. The occurrence of the cubic arsenide in these particular objects suggests that it was precipitated due to long-term ageing at room temperature, which points to the need of a redefinition of the Cu-As equilibrium phase constitution by the inclusion of a low-temperature form of Cu_3As.

The artefacts with eutectic arsenide (α-Cu + Cu_3As) and thicker arsenide formations (Cu_3As) observed indicate that no chemical homogeneity was obtained in the material. In these cases, the temperatures attained during the annealing procedure probably were not sufficiently high, resulting in heterogeneous microstructures containing As-rich banding and precipitated arsenides. The arsenide segregations reduce the arsenic content of the α solid phase solution, thus decreasing the actual improvement of mechanical properties. On the other hand, thinner arsenide formations observed around grain boundaries of recrystallized grains in some examples reinforce the idea that long-term ageing over archaeological time would precipitate the copper arsenide in the α-Cu phase grain boundaries due to arsenic segregation from a supersaturated solid solution at low temperatures.

These results highlight the importance of understanding the impact of structural ageing for the assessment of original properties of archaeological arsenical copper artefacts, such as hardness or colour.

6.4. ARTEFACTS TYPOLOGIES ASSOCIATION TO DIFFERENT ARSENIC CONTENTS

The artefacts typologies identified in the three settlements are in accordance with the metallurgical production of the Chalcolithic period with a relatively reduced artefact typological diversity. The majority of artefacts typologies included relatively simple and flat forms, namely: plain axes, awls, chisels, hooks, saws, knife, daggers and arrowheads (Ferreira da Silva *et al.*, 1993). Some typologies are present in all collections, like daggers and awls. Other appear only in one collection, as the case of fishhooks in OR.

In the early metallurgy, the question of correlation between the metal composition and the artefact typology has been highly discussed by other authors. According with the SAM programme (Junghans *et al.*, 1974, 1968, 1960), the study of "Bronze Age Metalwork from the Iberian Peninsula" (Harrison and Craddock, 1981) and the "Proyecto de Arqueometalurgia" (Rovira, 2005), flat axes and awls tend to be constituted of pure copper, whereas Palmela points and daggers tend to show higher concentrations of arsenic (Müller and Soares, 2008; Müller *et al.*, 2007).

Awls and axes recovered from Zambujal excavations present low values of arsenic, with the exception of long awls that display higher amounts of arsenic (As ≥ 2 wt.%). On the other hand, sheet metal fragments, thin saws, Palmela points and tanged daggers have more frequently higher contentss of arsenic (Müller *et al.*, 2007). Similar observations were made in Leceia artefacts collection. Arsenical copper alloys seem to be reserved for long awls, sheet metal objects, Palmela points and tanged daggers (Müller and Cardoso, 2008).

Concerning the VNSP artefacts collection, previous studies based on the SAM programme argued that weapons (arrowheads and daggers) systematically contain higher amounts of arsenic than tools (chisels, awls and axes) (Soares, 2005). Therefore, it was observed a general tendency for artefacts with thinner shapes, like blades and sheet metal fragments, as well as elongated objects, like the long awls, to have higher arsenic content than other tools like axes, chisels and shorter awls. As already mentioned, axes could also be used as ingots (Soares, 2005; Soares *et al.* 1994).

In the present study, a statistically significant association was found between the presence of arsenic (As ≥ 2 wt.%) and artefacts classified as "Weapons" (arrowheads, daggers and knives) in VNSP collection. These results are in accordance with previous results from VNSP artefact collection and the metallurgical production in neighbouring sites of Zambujal and Leceia. They also strengthen the hypothesis that colour was probably the main property determining the selection of the arsenical alloys by prehistoric metallurgists rather than their mechanical properties.

Also, it must be kept in mind that the higher arsenic contents of some typologies considered of prestige objects, such as daggers and Palmela points, could be explained by those typologies being

less subject to recycling operations than everyday use objects. Therefore, less frequent re-melting of the alloy would have limited the losses of the volatile element arsenic (Rovira, 2005). On the other hand, functional artefacts would be more frequently recycled resulting in a reduction of arsenic content (Mckerrell and Tylecote, 1972). The acquire expertise of an efficient control of the reducing atmosphere during melting and annealing would prevent higher losses in the arsenic content of copper-based artefacts (Mckerrell and Tylecote, 1972).

In the case of ML, there is a tendency to the "Weapons" group to present higher levels of arsenic. However, it was not possible to obtain a statistically significant association of the use of arsenical copper alloys (As ≥ 2 wt.%) in the manufacture of artefacts classified as "Weapons". The artefacts collection of OR is constituted only by "Tools"; therefore no association was studied.

In general, the association between copper alloys with arsenic content over 2 wt.% and artefacts classified as "Weapons" point out for a deliberate selection of the alloy to the manufacture of certain typologies. One cannot rule out the hypothesis that some artefacts included in the group of "Tools" could also be considered prestigious items and that could have influenced the choice of a different colour for these artefacts. Such artefacts could have a ceremonial function explaining why some "Tools" present high arsenic content (and would be less recycled).

7. CONCLUSIONS AND FINAL REMARKS

The archaeometallurgical study presented in this thesis has proved to be very important in the definition of the copper and arsenical copper production in three Chalcolithic settlements, VNSP, ML and OR, belonging to the Estremadura region of Portugal.

The integration of data obtained from the study of the metallurgical remains from the different settlements allowed some important considerations about the Chalcolithic copper-based metallurgy of this region. This study also provided a good characterization of the alloys and the thermomechanical processes applied in artefacts manufacture.

Evidence seems to indicate that metal was produced in VNSP, using a crucible technology and working under poor reducing conditions during smelting operations. These conditions would result in highly viscous and heterogeneous slag and high retention of metal prills. The primitive smelting process was most likely conducted in a ceramic crucible in an open-air fireplace loaded with crushed ore (copper oxides and carbonates) and charcoal.

Artefact production was most likely accomplished in all settlements: VNSP, ML and OR. Furthermore, the large quantity of scrap material recovered in VNSP and ML suggests the existence of recycling operations.

The higher percentage of arsenic content determined in the artefacts recorded at ML is possibly related to the diversification of exploited ore deposits, including the OMZ and the Iberian Pyrite Belt, in the South-Portuguese Zone. This diversification was possible due to the shorter and later chronological occupation period of ML and OR, compared to VNSP, characterized as Bell Beaker period. The increased use of copper alloys with higher arsenic contents was not observed in OR possibly due to the small artefact collection. Also, despite ML and OR being contemporaneous, the presence of the Bell Beaker period was strongly verified in ML than in OR.

In the case of VNSP, the percentage of arsenical copper artefacts recorded seem to be significantly inferior from ML and OR possibly due to the existence of metallurgical activities for a longer time interval. This may cause higher variability in the arsenic content of the alloys as a consequence of several recycling cycles over time.

The thermomechanical processing was found to be similar in all three settlements, consisting of one or more cycles of hammering and annealing, with a final forging procedure applied in less than half of the artefacts in all collections.

The Chalcolithic metallurgists when working with copper alloyed with arsenic may not have been aware of the extense hardening capacity of these alloys. Nevertheless, it is possible that they were aware that visible different colours of the alloy were related to different arsenic content. On the other hand, the harder cutting edges possibly result of higher number of thermomechanical operations and some final forging applied to shape the object, and therefore achieving a better performance of the object, even if not intentionally.

Nevertheless, regarding VNSP, there is an indication of some degree of control over the identification and selection of the alloys used. The statistically significant association found in VNSP between copper alloys with arsenic content over 2% and artefacts classified as "Weapons" point out for a deliberate selection of the alloy to the manufacture of certain typologies. The distribution of arsenic content in the groups of artefacts from ML indicates that there is a tendency to the "Weapons" group to present higher levels of arsenic. However, it was not possible to obtain a statistically significant association. In case, artefacts included in the group of "Weapons" were considered prestigious items that could have influenced the choice of a different colour for these artefacts. Even if in a smaller amount, some "Tools" could have a ceremonial function or to be also considered as prestige items explaining why some exhibit high arsenic content and would be less recycled.

Therefore, results suggest that colour was probably the main property determining the selection of the arsenical alloys by ancient metallurgists rather than their mechanical properties.

The occurrence of the cubic arsenide in these particular objects suggests that it was precipitated due to long-term ageing at room temperature, which points to the need of a redefinition of the Cu-As equilibrium phase constitution. These results highlight the importance of understanding the impact of structural ageing for the assessment of original properties of archaeological arsenical copper artefacts, such as hardness or colour. Besides the better understanding and enhanced interpretation of the prehistory metallurgy, it is vital to state that greater knowledge of materials allow a better conservation approximation and preservation guidelines.

Due to the archaeological and museological importance of the analysed collections, the use of non-invasive and micro-analytical techniques proved to be adequate to the proposed objectives of studying elemental and microstructural composition, alloy hardness and colour studies, with a minimum intervention to the materials studied. Furthermore, the analytical methodology included a conservation treatment of the analysed materials, particularly for the metallic nodules and artefacts, to further minimize the impact of the performed analyses. The work presented in this thesis also demonstrated that the used experimental approach is, therefore, adequate to apply to other metallurgical collections in future studies.

The application of proven statistical analyses methodologies was also fundamental to strengthen the confidence in evaluating the hypothesis put forward in the thesis, especially when performing comparisons with small sample sizes.

In the case of VNSP artefacts collection, the current state of conservation raised some concerns since there were visible, active copper corrosion products in the surface of the objects. Therefore, to stabilize the objects, a cleaning and stabilization procedure was applied before returning the collection to the exposition vitrines of the museum. Any active corrosion processes could have led to the loss of information of the object surface.

Additional colour studies should be incorporated on ancient and experimental produced alloys to allow a better assessment of the final colour of the artefacts. The colour of the alloy observed in the present

days could be altered due to ageing processes, and also if the thermomechanical procedures applied have any influence in the final colour hue.

Besides, additional hardness studies, with ancient and experimental produced alloys, should be performed to better assess the final hardness of the artefact, taking into account the influence of the precipitation of further arsenide through archaeological times.

Archaeometallurgical studies can help archaeologists to better recognize materials, such as minerals, slags and metallurgical vestiges, that are commonly harder to identify in excavation sites, so scarce to the current record but, nevertheless, precious to help understand smelting and melting operations.

Whenever possible, archaeometallurgical studies should also be focused in artefacts from recently excavated sites with well-documented stratigraphies, to trace a local metallurgical evolution better.

Other future archaeometallurgical studies should include provenance studies based on isotope analysis to identify the sources of metal exploited during the prehistory and help clarify possible trade routes of materials and technological information. Also, experimental smelting and melting operations would allow obtaining greater sensibility of the used procedures.

In conclusion, further studies can still be made in the Portuguese territory and the data collected would raise several novel questions and identify some of the current caveats of the used methodology.

This thesis hopefully is a step forward in the comprehension of the metallurgical evolution at the Portuguese territory. Innovative analytical data and interpretations aimed to contribute to the increased knowledge about the ancient metal production, allowing the integration of the Estremadura as one of the most detailed and studied region from the Iberian Peninsula.

REFERENCES

Araújo, M.F., Alves, L.C., Cabral, J.M.P. 1993. Comparison of EDXRF and PIXE in the analysis of ancient gold coins. *Nuclear Instruments and Methods in Physics Research B* 75, 450-453.

Arnaud, J.M., Fernandes, C.V. (Eds.) 2005. *Construindo a Memória: As Colecções do Museu Arqueológico do Carmo*. Associação dos Arqueólogos Portugueses, Lisboa.

Arnaud, J.M., Gonçalves, J.L.M. 1990. A fortificação pré-histórica de Vila Nova de S. Pedro (Azambuja), Balanço de meio século de investigações – 1ª parte. *Revista de Arqueologia* 1, 25-48.

Arnaud, J.M., Gonçalves, J.L.M. 1995. A fortificação pré-histórica de Vila Nova de S. Pedro (Azambuja), Balanço de meio século de investigações – 2ª parte. *Revista de Arqueologia* 2, 11-40.

Asderaki, E., Rehren, Th. 2008. Complex Beauty: the manufacture of Hellenistic wreaths. In: Fecorellis Y., Zacharias N., Polikreti, K. (Eds.) *Proceedings of the 4th Symposium of the Hellenic Society for Archaeometry*. BAR IS 1746, Oxford.

Balasubramaniam, R., Laha, T., Srivastava, A. 2004. Long term corrosion behaviour of copper in soil: a study of archaeological analogues. *Materials and Corrosion* 55, 194-202.

Bar-Yosef Mayer, B, N. Porat. 2008. Green stone beads at the dawn of agriculture. In: *Proceedings of the National Academy of Sciences* 105(25), 8548-8551.

Bayley, J., Rehren, T. (Eds.) 2007. *Towards a functional and typological classification of crucibles.* Archetype Publications, Oxford.

Bayona, M.R. 2008. La Investigation de la Actividad Metalúrgica Durante el III Milenio A.N.E. en Suroeste de la Península Ibérica. *British Archaeological Reports International Series 1769*, 283 pp.

Bengough, G.D., Hill B.P. 1910. The Properties and Constitution of Copper-Arsenic Alloys. *Journal of the Institute of Metals* 3, 34-71.

Bensaúde, A. 1888-1892. Notice sur quelques objets préhistoriques du Portugal fabriqués en cuivre. In: *Communicações da Commissão dos Trabalhos Geologicos de Portugal* Tomo II, 119-124.

Berger, D. 2012. Bronzezeitliche Färbetechniken an Metallobjekten nördlich der Alpen – Eine archäometallurgische Studie zur prähistorischen Anwendung von Tauschierung und Patinierung anhand von Artefakten und Experimenten. *Forschungsberichte des Landesmuseums für Vorgeschichte* Halle Band 2, Landesamt für Denkmalpflege und Archäologie Sachsen-Anhalt, 331.

Bourgarit, D. 2007. Chalcolithic copper smelting, In: La Niece, S., Hook, D., Craddock, P.T. (Eds.) *Metals and Mines. Studies in Archaeometallurgy*. Archetype, London, 15.

Boyes, E.D. 2002. Analytical potential of EDS at low voltages. *Microchimica Acta* 138, 225-234.

Bronk, H., Rohrs, S., Bjeoumikhov, A., Langhoff, N., Schmalz, J., Wedell, R., Gorny, H.E., Herold, A., Waldshlager, U. 2001. ArtTAX - a new mobile spectrometer for Energy-Dispersive Micro X-Ray Fluorescence spectrometry on art and archaeological objects. *Fresenius Journal of Analytical Chemistry* 371, 307-316.

Brunod, G. 1998. Les formes solaires des stèles chalcolithique du Valcamonica. In: *Actes du deuxième Colloque International sur la statuaire mégalithique*. Archéologie en Languedoc 22, 285-97.

Budd, P. 1991. Eneolithic arsenical copper: heat treatment and the metallographic interpretation of manufacturing processes. In: Birkhäuser, B., Pernika, E., Wagner, G.A., (Eds.) *Proceedings of Archaeometry* 90, 35-44.

Budd, P., Ottaway, B.S. 1995. Eneolithic arsenical copper: chance or choice? In: Jovanovic, B. (Ed.) *International Symposium, Ancient Mining and Metallurgy in Southeast Europe*. Archaeological Institute, Belgrade, 95-102.

Budd, P., Ottaway, B.S. 1991. The properties of arsenical copper alloys: implications for the development of Eneolithic metallurgy. In: Budd, P., Pollard, A.M., Scaife, R. (Eds.) *Archaeological Sciences 1989: Proceedings of a Conference on the Application of Scientific Techniques in Archaeology*. Bradford, Oxbow Monograph 9, Oxford: Oxbow, 132-42.

Campbell, J. 2003. *Castings: Chapter 5 - Solidification structure*. Butterworth-Heinemann, Oxford, 2003, Pages 117-177.

Canberra 2003. *WinAxil Operational Guide*. Canberra Eurisys Benelux N.V., Canberra.

Caramé, C., Manuel, E., Bonilla, M.D.Z., García-Sanjuan, L., Wheatly, D.W. 2010. The Copper Age settlement of Valencina de la Concepción (Seville, Spain): Demography, metallurgy and spatial organization. *Trabajos de Prehistoria* 67 (1), 85-117.

Cardoso, J.L. 2010. O povoado calcolítico fortificado do Outeiro Redondo (Sesimbra): Resultados das escavações efectuadas em 2005. In: Gonçalves, V., Sousa, A.C. (Eds.) *Transformação e Mudança no Centro e Sul de Portugal: o quarto e o terceiro milénios a.n.e.* Cascais: Câmara Municipal de Cascais, 97-129.

Cardoso, J.L. 2009. Espólios do povoado calcolítico fortificado de Outeiro Redondo (Sesimbra): as colheitas do arq. Gustavo Marques. *Revista Portuguesa de Arqueologia* 12(1), 73-114.

Cardoso, J.L. 2002. Correspondência anotada de Abel Viana e O. da Veiga Ferreira. *Estudos Arqueológicos de Oeiras* 10, 415-608.

Cardoso, J.L. 2000. The fortified site of Leceia (Oeiras) in the context of the Chalcolithic in Portuguese Estremadura. *Oxford Journal of Archaeology* 19(1), 37-55.

Cardoso, J.L., Caninas, J.C. 2010. Moita da Ladra (Vila Franca de Xira). Resultados preliminares da escavação integral de um povoado calcolítico muralhado. Transformação e Mudança no centro e sul de Portugal: o 4.º e o 3.º milénio a.n.e. *Colóquio Internacional (Cascais, 2005)* Cascais: Câmara Municipal de Cascais, 65-95.

Cardoso, J.L., Carvalhosa, A.B. 1995. Estudos petrográficos de artefactos de pedra polida do povoado pré-histórico de Leceia (Oeiras): Análises de proveniências. *Estudos Arqueológicos de Oeiras* 5, 123-151.

Cardoso, J.L., Fernandes, J.M.B. 1995. Estudo arqueometalúrgico de um lingote de cobre de Leceia. *Estudos Arqueológicos de Oeiras* 5, 153-164.

Cardoso, J.L., Guerra, M.F. 1997/1998. Análises químicas não destrutivas do espólio metálico do povoado pré-histórico de Leceia. *Estudos Arqueológicos de Oeiras* 7, 61-87.

Cardoso, J.L., Querré, G., Salanova, L. 2003. Bell Beaker relationships along the Atlantic coast. *Trabalhos de Arqueologia* 42, 27-41.

Cardoso, J.L., Soares, A.M.M. 1996. Contribution d'une Série de Datations 14C, provenant du Site de Leceia (Oeiras, Portugal), à le Chronologie Absolue du Néolithique et du Chalcolithique de l'Estremadura Portugaise. *Actes du Colloque de Périgeux 1995. Supplément à la Revue d'Archéométrie*, 45-50.

Cardoso, J.L., Soares, A.M.M., Martins, J.M.M. 2013. O povoado campaniforme fortificado da Moita da Ladra (Vila Franca de Xira, Lisboa) e a sua cronologia absoluta. *O Arqueólogo Português* 5(3), 213-253.

Cardoso, J.L., Soares, A.M.M., Martins, J.M.M. 2010/2011. Fases de ocupação e cronologia absoluta da fortificação calcolítica do Outeiro Redondo (Sesimbra). *Estudos Arqueológicos de Oeiras*, 18, 553-578.

Ciliberto, E., Spoto, G. 2000. *Modern analytical methods in art and archaeology.* New York: John Wiley & Sons. 755 p.

Coffyn, A. 1985. *Le Bronze Final Atlantique dans la Péninsule Ibérique*. Bordeaux: Centre Pierre Paris. 441 p.

Combarieu, R., Dauchot, G., Delamare, F. 1998. Étude de l'adsorption du benzotriazole sur le fer, le cuivre et le laiton alpha par Tof-SIMS et XPS. In: Mourey, W., Robbiola, L. (Eds). *Metals 98 (Proceedings of the International Conference on Metals Conservation)*, James & James, London, 223-228.

REFERENCES

Commission Internationale de l'Eclairage. 2004. *CIE Publication* 15. Third Edition, ISBN 3-901-906-33-9. Available at: http://www.cie.co.at/publ/abst/15-2004.html

Commission Internationale de l'Eclairage. 1986. *CIE Publication* 15.2, Second Edition, ISBN 3-900-734-00-3. Available at: http://www.cie.co.at/publ/abst/15-2-86.html

Craddock, P.T. 1995. *Early metal mining and production.* The University Press, Cambridge, 363 p.

Craddock, P.T., Meeks, N.D. 1987. Iron in ancient copper. *Archaeometry.* 29, 187-204.

Davies, O. 1945. *Roman Mines in Europe*, Macmillan, London.

Delibes de Castro, G., Fernández-Manzano, J., Romero-Carnicero, F., Herrán-Martínez, J.I., Ramírez-Ramírez, M.L. 2001. Metal production at the end of the Late Bronze Age in the central Iberian Peninsula. *Journal of Iberian Archaeology* 3, 73-95.

Delibes, G., Montero, I. (Eds.) 1999. *Las primeras etapas metalúrgicas en la Peninsula Iberica II. Estudios regionales.* Instituto Ortega y Gasset, Madrid, 357 p.

Dewalens, J., Heerman, L., Simaeys, L.V. 1951. The Codeposition of Copper and Arsenic from H_2SO_4-$CuSO_4$-As_2O_3 Solutions: Electrochemical Formation of Copper Arsenides. *Journal of Electrochemistry Society* 122(4), 477-482.

Etiégni, L., Campbell, A.G. 1991. Physical characteristics of wood ash. *Bioresource Technology* 37, 173-178.

Faltermeier, R.B. 1998. A corrosion inhibitor test for copper-based artifacts. *Studies in Conservation* (43) 121-128.

Fasnacht, W. 1999. Experimentelle Rekonstruktion des Gebrauchs von frühbronzezeitlichen Blasdüsen aus der Schweiz. Kupferverhüttung und Bronzeguß. In: Hauptmann, A., Pernicka, E. Rehren, Th., Yalcin, Ü. (Eds.) *Proceedings of the International Conference: The Beginnings of Metallurgy,* Bochum 1995 (Anschnitt Beih. 9), 291-294.

Ferreira da Silva, A.C., Raposo, L., Tavares da Silva, C.T. 1993. *Pré-história de Portugal.* Universidade Aberta, Lisboa, 301 p.

Figueiredo, E., Silva, R.J.C., Senna-Martinez, J.C., Araújo, M.F., Braz Fernandes, F.M., Inês Vaz, J.L. 2010. Smelting and recycling evidences from the Late Bronze Age habitat site of Baiões (Viseu, Portugal). *Journal of Archaeological Science* 37, 1623-1634.

Figueiredo, E., Valério, P., Araújo, M.F., Silva, R.J.C., Gomes, M.V. 2010. Estudo analítico de vestígios metalúrgicos do povoado do Escoural (Évora, Portugal). In: Pérez-Macias, J.A., Romero-

Bomba, E. (Eds.) *IV Encontro de Arqueologia del Suroeste Peninsular*, Collectanea 145, Universidad de Huelva Publicaciones, Spain, (cd-rom).

Gauss, R. 2015. Zambujal und die Anfänge der Metallurgie in der Estremadura (Portugal). Technologie der Kupfergewinnung, Herkunft des Metalls und soziokulturelle Bedeutung der Innovation. *Iberia Archaeologica* 15(1), 331 p.

Giumlia-Mair, A. 2008. The metal of the moon goddess. *Surface Engineering* 24(2), 110-117.

Hammer, Ø., Harper, D.A.T., Ryan, P.D. 2001. Past: Paleontological Statistics software package for education and data analysis. *Palaeontologia Electronica* 4(1), 9. Available at: http://folk.uio.no/ohammer/past

Hammersley, A.P., Svensson, S.O., Hanfland, M., Fitch, A.N., Häusermann, D. 1996. Two-dimensional detector software: from real detector to idealised image or two-theta scan. *High Pressure Research* 14, 235-248.

Hanning, E., Gaub, R., Goldenberg, G. 2010. Metal from Zambujal: experimentally reconstructing a 5000-year-old technology. *Trabajos de Prehistoria* 67, 287-304.

Harrison, R.J., Craddock, P.T. 1981. A study of the Bronze Age metalwork from the Iberian Peninsula in the British Museum. *Ampurias* 43, 113-179.

Hauptmann, A. (Ed.) 2007. The Archaeometallurgy of Copper: Evidence from Faynan, Jordan. *Springer-Verlag*, Berlin, 388 p.

Hawkins D.T., Hultgren, R., Lyman, T. (Ed.) 1973. *Metals Handbook, Metallography, Structures and Phase Diagrams.* American Society for Metals, Materials Park, Ohio, 8th edition, 8, 259 p.

Heyding, R.D., Despault, G.J.G. 1960. The copper/arsenic system and the copper arsenide minerals. *Canadian Journal of Chemistry* 38(12), 2477-2481.

Hook, D.R., Freestone, I.C., Meeks, N.D., Craddock, P.T., Onorato, A.M. 1991. The early production of copper-alloys in south-east Spain. In: Pernicka, E., Wagner, G.A. (Eds.) *Proceedings of Archaeometry*, Birkhäuser, Base, 90, 65-76.

Hoover, H.C., Hoover, L.H. 1912. *Agricula: De re Metallica* (trans.). The Mining Magazine, London, 638 p.

Hunt-Ortiz, M.A. 2003. *Prehistoric Mining and Metallurgy in South West Iberian Peninsula.* BAR International Series 1188, Archaeopress, Oxford.

Iglesias J.E., Nowacki W. 1977. Refinement of the Crystal Struture of α Domeykite, Struture Related to the A15 type. *Zeitschrift für Kristallographie* 145, 334-345.

IUPAC 1978. Analytical Chemistry Division, Nomenclature, symbols, units and their usage in spectrochemical analysis. *Spectrochimica Acta B* 33, 242-245.

Jalhay, E., Paço, A. 1945. El Castro de Vilanova de San Pedro. *Actas y Memorias de la Sociedad Española de Antropología, Etnografía y Prehistoria* 20, 5-128.

Junghans, S., Sangmeister, E., Schröder, M. 1960. Metallanalysen kupferzeitlicher und frühbronzezeitlicher Bondenfunde aus Europa. *Studien zu den Anfängen der Metallurgie* 1. Gebrüder Mann Verlag, Berlin.

Junghans, S., Sangmeister, E., Schröder, M. 1968. Kupfer und Bronze in der frühen Metallzeit Europas. *Studien zu den Anfängen der Metallurgie* 2(1-3). Gebrüder Mann Verlag, Berlin.

Junghans, S., Sangmeister, E., Schröder, M. 1974. Kupfer und Bronze in der frühen Metallzeit Europas. *Studien zu den Anfängen der Metallurgie* 2(4). Gebrüder Mann Verlag, Berlin.

Keates, S. 2002. The Flashing Blade: Copper, Colour and Luminosity in North Italian Copper Age Society. In: Jones, A. and MacGregor, G. (Eds.) *Colouring the Past – The significance of colour in archaeological research.* Berg, Oxford, New York. 109-126.

Kevex 1992. Kevex 771-EDX spectrometer users guide. *Kevex Instruments*, Valencia, 114 p.

Klaproth, M.H., 1798. Mémoires de l'Academie Royale des Sciences et Belles-Lettres, Berlin, *Classe de Philosophie Expérimentale*, 97-113.

Kunst, M., Uerpmann, H.P. 2002. Zambujal (Torres Vedras, Lisboa): relatório das escavações de 1994 e 1995. *Revista Portuguesa de Arqueologia* 5(1), 67-120.

Lechtman, H. 1996. Arsenic bronze: Dirty copper or chosen alloy? A view from the Americas. *Journal of Field Archaeology* 23, 477-514.

Lechtmann, H., Klein, S., 1999. The production of copper-arsenic alloys (Arsenic bronze) by cosmelting: modern experiment, ancient practice. *Journal of Archaeological Science* 26, 497-526.

Lillios, K.T. 1997. Amphibolite tools of the Portuguese Copper Age (3000-2000 B.C.): a geoarchaeological approach to prehistoric economics and symbolism. *Geoarchaeology* 12(2), 137-63.

Loeper-Attia, M.A., Robbiola, L. 1998. Étude de la déchloruration de dépôts de CuCl formés sur du cuivre en absencet en presence de benzotriazole (BTA). In: Mourey, W., Robbiola, L. (Eds.) *Metals 98 (Proceedings of the International Conference on Metals Conservation).* James & James, London, 215-222.

Maddin, R., Muhly, J., Stech, T. 1999. Early Metalworking at Cayonu. In: Hauptmann, A., Pernicka, E., Rehren, T., Yalcin, Ű. (Eds.) *The Beginnings of Metallurgy.* Der Anschnitt Beiheft 9. Bochum: Deutsches Bergbau Museum, 37-44.

Maier, A., Niederbrucker, G., Stenger, S., Uhl, A. 2012. Efficient focus assessment for a computer vision-based Vickers hardness measurement system. *Journal of Electronic Imaging* 21(2), 11-14.

Mallet, J.W. 1852. *An Account of a Chemical Examination of the Celtic Antiquities in the Collection of the Royal Irish Academy.* PhD thesis, M.H. Gill, Dublin, 46 p.

Manzano, J.F. e Herrero, F.J. 1998. Arqueometalurgia del Bronce. *Introducción a la metodología de trabajo.* Universidad de Valladolid. 99-108.

Mataloto, R., Martins, J.M.M., Soares, A.M.M. 2013. Cronologia absoluta para o Bronze do Soroeste: periodização, base de dados, tratamento estatístico. *Estudos Arqueológicos de Oeiras* 20, 303-338.

McKerrell, H., Tylecote, R.F. 1972. The working of copper-arsenic alloys in the Early Bronze Age and the effect on the determination of provenance. *Proceedings of the Prehistoric Society* 38, 209-218.

Merkel, J.F., Shimada, I., Swann, C.P. and Doonan, R. 1994. Pre-Hispanic Copper Alloy Production at Batan Grande, Peru: Interpretation of the Analytical Data from Ore Samples. In: Scott, D.A., Meyers, P. (Eds.) *Archaeometry of Pre-Columbian Sites and Artifacts.* The Getty Conservation Institute, Los Angeles, 199-228.

Mohen, J.P. 1990. *Métallurgie préhistorique - introduction à la paléométallurgie.* Masson, Paris, 230 p.

Montero-Ruíz, I. 1999. Las primeras etapas metalúrgicas en la Península Ibérica. II. In: Delibes, G., Montero, I. (Coord.) *Estudios regionales.* Instituto Universitario Ortega y Gasset y Ministerio de Educación y Cultura, Madrid, 333-357.

Müller, R., Cardoso, J.L. 2008. The origin and use of copper at the Chalcolithic fortification of Leceia, Portugal. *Madrider Mitteilungen* 49, 64-93.

Müller, R., Goldenberg, G., Kunst, M., Bartelheim, M., Pernicka, E. 2007. Zambujal and the beginnings of metallurgy in Southern Portugal. In: La Niece, S., Hook, D., Craddock, P.T. (Eds.) *Metals and Mines. Studies in Archaeometallurgy* Archetype, London, 15 p.

Müller, R., Pernicka, E. 2009. Chemical analyses in archaeometallurgy: a view on the Iberian Peninsula. In: Kienlin, T.L., Roberts, B. (Eds.) *Metals and Society – Studies in Honour of Barbara S. Ottaway.* Universitätsforschungen zur prähistorischen Archäologie 169. Verlag Dr. Rudolf Habelt GMBH, Bonn, 296-306.

Müller, R., Rehren, Th., Rovira, S. 2004. Almizaraque and the early copper metallurgy of Southeast Spain. New data. *Madrider Mitteilungen* 45, 33-56.

Müller, R., Soares, A.M. 2008. Traces of early copper prodution at the Chalcolithic fortification of Vila Nova de São Pedro (Azambuja, Portugal) *Madrider Mitteilungen* 49, 94-114.

Murillo-Barroso, M., Montero-Ruiz, I. 2012. Copper ornaments in the Iberian Chalcolithic: Technology versus social demand. *Journal of Mediterranean Archaeology* 25 (1), 53-73.

Naud J., Priest P. 1972. Contributions to the Study of the Copper-Arsenic System. *Materials Research Bulletin* (in French) 7, 783-792.

Nocete, F., Queipo, G., Sáez, R., Nieto, J.M., Inácio, N., Bayona, M.R., Peramo, A., Vargas, J.M., Cruz-Auñón, R., Gil-Ibarguchi, J.I., Santos, J.F. 2008. The smelting quarter of Valencina de la Concepción (Seville, Spain): the specialised copper industry in a political centre of the Guadalquivir Valley during the Third millennium BC (2750–2500 BC). *Journal of Archaeological Science* 35, 717-732.

Nocete, F., Sáez, R., Nieto, J.M. 2004. La producción de cobre en Cabezo Juré: Estudio químico, mineralógico y contextual de escorias. In: Nocete, F. (Coord.) *Odiel: Proyecto de Investigación Arqueológica para el Análisis del Origen de la Desigualdad Social en el Suroeste de la Península Ibérica.* Junta de Andalucía, Sevilla, 273-295.

Northover, J.P. 1989. Properties and use of arsenic-copper alloys. In: Hauptmann, A., Pernicka, E., Wagner, G.A. (Eds.), *Old World Archaeometallurgy*. Der Anschnitt, Beiheft 7. Deutsches Bergbaumuseum, Bochum, 111-118.

Okamoto H. 1991. Revaluation of thermodynamic models for phase diagram. *Journal of Phase Equiibria* 12, 623-643.

Ortiz, M.A.H. 2003. Prehistoric mining and metallurgy in south west Iberian Peninsula. Oxford: *Archaeopress*, 418 p.

Paço, A. 1964. Castro de Vila Nova de S. Pedro, XVI e Metalurgia e Análises Espectrográficas. *Anais da Academia Portuguesa de História*. II Série, vol. 14, Lisboa, 159-165.

Paço, A. 1955. Castro de Vila Nova de S. Pedro, VII e Considerações sobre o problema da Metalurgia. In: *Zephyrus*. VI, Salamanca, 27-40.

Paço, A., Arthur, M.L.C., 1952. Castro de Vila Nova de S. Pedro, II - Alguns Objectos Metálicos. *Zephyrus*. III, Salamanca, 31-39.

Paço. A., Jalhay, E. 1939. A Póvoa Eneolítica de Vila Nova de S. Pedro, *Brotéria* 28/29, 687-694.

Paço, A., Sangmeister, E. 1956. Vila Nova de S. Pedro. Eine befestigte Siedlung der Kupferzeit in Portugal, *Germania* 34, 211-231.

Padera K. 1952. Revision of the Domeykite-Algodonite Group. *Acad Tcheque Sci Bull Int Classe Sci, Math, Nat, Med* 52, 53-68.

Pearce, M. 1998. Reconstructing prehistoric metallurgical knowledge: The northern Italian Copper and Bronze Ages, *European Journal of Archaeology* 1(1), 51-70.

Pei, B., Björkman, B., Jansson, B., Sundman, B. 1994. Thermodynamic assessment of the Cu-As system using an ionic two-sublattice model for the liquid phase. *Zeitschrift für Kristallographie* 85(3), 178-184.

Percy, J., 1880. *Metallurgy: Silver and Gold,* Part I, John Murray, London.

Percy, J., 1870. *The Metallurgy of Lead,* John Murray, London.

Percy, J., 1864. *Metallurgy: Iron and Steel,* John Murray, London.

Percy, J., 1861. *Metallurgy: Fuels, Fireclays, Copper, Zinc and Brass,* Part I, John Murray, London.

Pereira, F. 2011. *Archaeometallurgical Study of Artefacts from Castro de Vila Nova de São Pedro (Azambuja, Portugal)* MSc Thesis, Faculdade de Ciências e Tecnologia da Universidade Nova de Lisboa, Lisboa, 62 p.

Pereira, F., Furtado, M.J., Silva, R.J.C., Soares, A.M.M., Araújo, M.F., Cardoso, J.L. 2013c. Estudo das Evidências de Produção Metalúrgica no Outeiro Redondo (Sesimbra). *Actas do I Congresso de Arqueologia da Associação dos Arqueólogos Portugueses (AAP)* Lisboa, 463-468.

Pereira, F., Silva, R.J.C., Soares, A.M.M., Araújo, M.F. 2013b. The role of arsenic in Chalcolithic copper artefacts – insights from Vila Nova de São Pedro (Portugal). *Journal of Archaeological Science* 40(4), 2045-2056.

Pereira, F., Silva, R.J.C., Soares, A.M.M., Araújo, M.F. 2013a. Microscopy characterization of metallurgical production evidences from Vila Nova de São Pedro (Azambuja, Portugal). *SPMicros Microscopy and Microanalysis* 19 (Suppl 4), 149-150.

Pereira, F., Silva, R.J.C., Soares, A.M.M., Araújo, M.F., Cardoso, J.L. 2017. New studies in the metallic collection of the chalcolithic settlement of Moita da Ladra (Vila Franca de Xira, Portugal). *Materials and Manufacturing Processes* 32 (7-8), 781-791.

Pereira, F., Silva, R.J.C., Soares, A.M.M., Araújo, M.F., Oliveira, M.J., Martins, R.M.S., Schell, N. 2015. Effects of long term aging in arsenical copper alloys. *Microscopy and* Microanalysis 21(6), 1413-1419.

Pollard, A.M. 2015. The first hundred years of archaeometallurgy chemistry: Pownall (1775) to von Bibra (1869). *Historical Metallurgy* 49(1), 37-49.

Pownall, G., 1775. An account of some Irish antiquities. *Archaeologia* 3, 355-370.

Predel, B. 2006. As-Cu (Arsenic - Copper), Ac-Ag ... Au-Zr, 12A, Subvolume IV/5A. *Phase Equilibria, Crystallographic and Thermodynamic Data of Binary Alloys*. Madelung, Landolt-Börnstein, Berlin: Springer.

Radivojević, M., Rehren, T., Pernicka, E., Sljivar, D., Brauns, M. 2010. On the origins of extractive metallurgy: new evidence from Europe. *Journal of Archaeological Science* 37, 2775-2787.

Ramsey, C.B. 2014. *Oxcal 4.2 Manual*, Web interface build number: 86, Last Updated: 5/9/2014. Available at: https://c14.arch.ox.ac.uk/oxcalhelp/hlp_contents.html

Ravič, I.G. & Ryndina, N.V. 1984. Izučenie svojstv I mikrostrukturny splavov med'-myš'jak v svjazi s ich ispol'zovaniem v drevnosti (On the investigation of the properties and microstructure of the copper-arsenic alloys in conjunction with their use in antiquity). *Chudožestvennoe nasledie (Art Heritage)* 39(9), 114-124.

Reimer, P.J., Bard, E., Bayliss, A., Beck, J.W., Blackwell, P.G., Bronk Ramsey, C., Buck, C.E., Cheng, H., Edwards, R.L., Friedrich, M., Grootes, P.M., Guilderson, T.P., Haflidason, H., Hajdas, I., Hatté, C., Heaton, T., Hoffmann, D.L., Hogg, A., Hughen, K.A., Kaiser, K., Kromer, B., Manning, S.W., Niu, M., Reimer, R., Richards, D.A., Scott, E.M., Southon, J.R., Staff, R.A., Turney, C., van der Plicht, J. 2013. IntCal13 and Marine13 radiocarbon age calibration curves, 0-50,000 years cal BP. *Radiocarbon* 55 (4), 1869-1887.

Renfrew, C. 1973. *Before Civilization: The Radiocarbon Revolution and Prehistoric Europe.* London: Jonathan Cape, 320 p.

Renfrew, C., Bahn, P. 1991. *Archaeology: Theories, Methods and Practice.* Thames and Hudson, London, 656 p.

Robbiola, L., Portier, R. 2006. A global approach to the authentication of ancient bronzes based on the characterisation of the alloy-patina-environment system. *Journal of Cultural Heritage* 7, 1-12.

Roberts, B. 2008. Creating traditions and shaping technologies: Understanding the earliest metal objects and metal production in Western Europe. *World Archaeology* 40(3), 354-372.

Roberts, B., Ottaway, B.S. 2003. The use and significance of socketed axes during the Late Bronze Age. *European Journal of Archaeology* 6(2), 119-140.

Roberts, B.W., Thornton, C.P., Pigott, V.C. 2009. Development of Metallurgy in Eurasia. *Antiquity* 83, 112-122.

Roden, Ch. 1988. *Blasrohrdüsen. Ein archäologischer Exkurs zur Pyrotechnologie des Chalkolithikums und der Bronzezeit.* Der Anschnitt 40, 62-82.

Rovira, S. 2016. La metalurgia calcolítica en el suroeste de la Península Ibérica: una interpretación personal. *Menga. Revista de Prehistoria de Andalucía* 7, 53-67.

Rovira, S. 2005. Tecnología metalúrgica Campaniforme en la Península Ibérica. Coladas, moldeado y tratamentos post fundición. In: Rojo-Guerra, M.A., Garrido-Pena, R., García-Martínez de Lagrán, I. (Eds.) *El Campaniforme en la Península Ibérica y su Contexto Europeo*, Junta de Castilla y León, Valladolid, 495-521.

Rovira, S. 2004. Tecnología metalúrgica y cambio cultural en la Prehistoria de la Península Ibérica. *Norba, Revista de Historia* 17, 9-40.

Rovira, S. 2002. Metallurgy and society in prehistoric Spain. In: Ottaway, B., Wager, E. (Eds.) *Metals and Society - BAR International Series*, 1061. Oxford: Archaeopress, 5-20.

Rovira, S., Ambert, P. 2002a. Les céramiques à réduire le minerai de cuivre. Une téchnique métallurgique utilisée en Ibérie, son extension en France méridionale. *Bulletin de la Société Préhistorique Française* 99(1), 05-126.

Rovira, S., Ambert, P. 2002b. Vasijas cerâmicas para reducir minerales de cobre en la Península Ibérica y en la Francia meridional. *Trabajos de Prehistoria* 59(1), 1-17.

Rovira, S., Blasco, C., Ríos, P., Montero, I., Chamón, J. 2011. Yacimientos calcolíticos con campaniforme de la región de Madrid Nuevos estúdios. *VIII 1. La Arqueometalurgia, Bell Beaker International Conference. From Atlantic to Ural (15º. 2011. Poio).* Universidad Autónoma de Madrid, Madrid, 396 p.

Rovira, S., Gómez-Ramos, P., 2003. *Las primeras etapas metalúrgicas en la Península Ibérica. III Estudios metalográficos.* Instituto Universitario Ortega y Gasset, Ministerio de Cultura. Madrid.

Rovira, S., Montero-Ruiz, I., Consuerga, S. 1997. *Las primeras etapas metalúrgicas en la Península Ibérica. I Análisis de materiales.* Instituto Ortega y Gasset, Ministerio de Cultura. Madrid.

Ruíz-Taboada, A., Montero-Ruíz, I. 2000. The pattern of use of stone and copper in central Spain during the Bronze Age. *European Journal of Archaeology* 3, 350-369.

Ruíz-Taboada, A., Montero-Ruíz, I. 1999. The Oldest Metallurgy in Western Europe. *Antiquity* 73, 897-903.

Sangmeister, E. 1995. Zambujal. KupferfundeausdenGrabungen 1964 bis 1973. In: Sangmeister, E., Jiménez Gómes, M. (Eds.) *Los Amuleto de las Campaños 1964 hasta 1973*. Madrider Beiträge 5. Zabern, Mainz, 1-153.

Sarabia-Herrero, F.J., Martin-Gil, J., Martin-Gil, F.J. 1996. Metallography of ancient bronzes: study of pre-roman metal technology in the Iberian Peninsula. *Materials Characterization* 36, 335-347.

Savory, H.N. 1972. The Cultural Sequence at Vila Nova de S. Pedro. *Madrider Mitteilungen* 13, 23-37.

Schanda, J. 2007. *Colorimetry: Understanding the CIE System.* John Wiley & Sons: Vienna, Austria; Hoboken, NJ, USA, 467 p.

Schell, N., King, A., Beckmann, F., Fischer, T., Müller, M., Schreyer, A. 2014. The high energy materials science beamline (HEMS) at PETRA III. *Materials Science Forum* 772, 57-61.

Scott, David A. 1991. *Metallography and Microstructure of Ancient and Historic Metals.* Marina del Rey, CA: Getty Conservation Institute in association with Archetype Books, 185 p.

Senna-Martinez, J.C., Pedro, I. 2000. Between myth and reality: the foundry area of Senhora da Guia de Baiões and Baiões/Santa Luzia metallurgy. *Trabalhos de Arqueologia* EAM. 6, 61-77.

Skinner, B.J. & Luce, F.D. 1971. Stabilities and Compositions of α-Domeykite and Algodonite. *Economic Geology* 66, 133-139.

Smith, C.S. 1981. On art, invention, and technology. In: Smith, C.S. (Ed.) *A search for structure*, Cambridge (MA): MIT Press, 325-331.

Smith, C.S., Gnudi, M.T. (Eds.) 1942. *The Pirotechnia of Vannoccio Biringuccio*, Basic Books, Chicago, 447 p.

Smithells C.J. 1962. *Metal Reference Book* (3rd ed.) vol. 1, London, UK, 596 p.

Soares, A.M.M. 2005. A metalurgia de Vila Nova de São Pedro. Algumas reflexões. In: Arnaud, J.M., Fernandes, C.V. (Eds.) *Construindo a memória. As colecções do Museu Arqueológico do Carmo.* Associação dos Arqueólogos Portugueses, Lisboa, 179-188.

Soares, A.M.M., Araújo, M.F., Alves, L., Ferraz, M.T. 1996. Vestígios metalúrgicos em contextos Calcolíticos e da Idade do Bronze no Sul de Portugal. *Miscellanea em Homenagem ao Professor Bairrão Oleiro*. Edições Colibri, Lisboa, 553-579.

Soares, A.M.M., Araújo, M.F., Cabral, J.M.P. 1994. Vestígios da prática de metalurgia em povoados calcolíticos da bacia do Guadiana, entre o Ardila e o Chança. *Arqueologia en el entorno del Bajo Guadiana*, 165-200.

Soares, A.M.M., Cabral, J.M.P. 1993. Cronologia absoluta para o Calcolítico da Estremadura e do Sul de Portugal. *Congresso de Arqueologia Peninsular, Actas dos Trabalhos de Antropologia e Etnologia, XXXIII* (3-4), Porto, 217-235.

Solecki, R.S., Solecki, R.I., Agelarakis, A.P. (Eds.) 2004. *The Proto-Neolithic Cemetery in Shanidar Cave*. Texas A&M University Anthropology Series 7. College Station, 234 p.

Sousa, A.C., Valério, P., Araújo, M.F. 2004. Metalurgia antiga do Penedo do Lexim (Mafra): Calcolítico e Idade do Bronze. *Revista Portuguesa de Arqueologia* 7, 97-117.

Subramanian, P.R., Laughlin, D.E. 1998. The As-Cu (Arsenic-Copper) system. *Bull. Alloy Phase Diagrams* 9(5), 605-617.

Teppo, O., Taskinen, P. 1991. An Assessment of the Thermodynamic Properties of Arsenic-Copper Alloys. *Scandinavian Journal of Metallurgy* 20, 141-148.

Thornton, C. 2001. *The Domestication of Metal: A Reassessment of the Early Use of Copper Minerals and Metal in Anatolia and Southeastern Europe*. M.Phil. Thesis, University of Cambridge, 378 p.

Tylecote, R.F. 1992. *The History of Metallurgy*. The Institute of Materials, London, 205 p.

Valera, A.C. 2013. Sobreira de cima. Necrópole de Hipogeus do Neolítico (Vidigueira, Beja). *Era Monográfica*, Núcleo de Investigação Arqueológica, Lisboa,11-40.

Valério, P. 2012. *Archaeometallurgical Study of Pre and Protohistoric Production Remains and Artefacts from Southern Portugal.* PhD Thesis. Faculdade de Ciências e Tecnologia, Universidade Nova de Lisboa, 180p.

Valério, P., Soares, A.M.M., Araújo, M.F. 2016c. An overview of Chalcolithic copper metallurgy from Southern Portugal. *Menga, Revista de Prehistoria de Andalucía* 7, 31-50.

Valério, P., Soares A.M.M., Araújo, M.F., Silva, R.J.C., Baptista, L. 2016a. Middle Bronze Age arsenical copper alloys in Southern Portugal. *Archaeometry* 58(6), 1003-1023.

Valério P., Soares A.M.M., Araújo, M.F., Silva, R.J.C., Porfírio E., Serra, M. 2014. Arsenical copper and bronze in Middle Bronze Age burial sites of Southern Portugal: the first bronzes in Southwestern Iberia. *Jornal of Archaeological Science* 42, 68-80.

Valério, P., Vidigal, R.O., Araújo, M.F., Silva, R.J.C., Mataloto, R. 2017. The manufacture of copper weapons and tools from the Chalcolithic settlement of São Pedro (Portugal). *Materials and Manufacturing Processes* 32 (7-8), 775-780.

Vidigal, R.O., Valério, P., Araújo, M.F., Soares, A.M.M., Mataloto, R. 2016. Micro-EDXRF study of Chalcolithic copper-based artefacts from Southern Portugal. *X-Ray Spectrometry* 45, 63-68.

Walker, R. 1980. Corrosion and preservation of bronze artifacts. *Journal of Chemical Education 4*, 277-280.

Wang, Q. and Ottaway, B.S., 2004. *Casting Experiments and Microstructure of Archaeologically Relevant Bronzes.* BAR International Series 1331. Archaeopress, Oxford, 87 p.

Yener, K.A. 2000. *The domestication of metals.* Leiden: Brill, 252 p.

APPENDICES

APPENDIX I: SUMMARY OF SEMI-QUANTITATIVE EDXRF ANALYSIS OF METALLURGICAL VESTIGES FROM VNSP

Table I.1. Summary of semi-quantitative EDXRF analysis of metallurgical vestiges from VNSP (includes crucibles, slags and metallic nodules); * Crucible fragments.

Metallurgical vestiges	Cu	As	Fe	Metallurgical vestiges	Cu	As	Fe
VNSP276*	+	+	+	VNSP316	99.9	0.02	0.01
VNSP277*	+	+	+	VNSP317	97.8	2.12	0.06
VNSP278*	+	n.d.	+	VNSP318	98.9	1.10	0.01
VNSP279*	+	++	+	VNSP319	99.8	0.23	0.02
VNSP280*	+	+++	+	VNSP320	98.8	1.18	0.01
VNSP281*	+	++	+	VNSP321	96.4	3.36	0.24
VNSP282*	+	+	+	VNSP322	99.7	n.d.	0.22
VNSP283*	+	+	+	VNSP323	99.1	0.54	0.37
VNSP284*	+	n.d.	+	VNSP324	98.2	1.46	0.34
VNSP285*	+	n.d.	+	VNSP325	98.9	0.14	0.95
VNSP286*	+	n.d.	+	VNSP326	97.9	1.34	0.62
VNSP287*	+	n.d.	+	VNSP327	75.8	1.34	22.85
VNSP288*	+	+	+	VNSP328	99.4	0.15	0.13
VNSP289*	+	n.d.	+	VNSP329	94.0	4.41	1.57
VNSP290*	+	n.d.	+	VNSP331	96.7	0.68	2.61
VNSP291*	+	n.d.	+	VNSP332	99.4	0.15	0.50
VNSP292*	+	+	+	VNSP333	99.1	0.21	0.73
VNSP291	97.3	0.34	2.37	VNSP336	99.4	n.d.	0.57
VNSP295	99.6	0.27	0.00	VNSP337	99.2	0.60	0.18
VNSP296	99.9	n.d.	0.14	VNSP338	99.4	n.d.	0.62
VNSP297	99.4	n.d.	0.51	VNSP339	98.3	n.d.	1.62
VNSP298	97.8	n.d.	2.17	VNSP340	97.4	2.34	0.23
VNSP299	99.3	0.35	0.34	VNSP341	97.6	2.18	0.22
VNSP300	96.3	3.33	0.39	VNSP342	99.6	0.16	0.23
VNSP301	65.9	n.d.	34.10	VNSP343	99.5	n.d.	0.47
VNSP302	84.2	n.d.	15.76	VNSP344	99.5	0.19	0.28
VNSP303	99.2	n.d.	0.76	VNSP345	99.6	n.d.	0.40
VNSP304	99.1	0.11	0.78	VNSP346	99.4	n.d.	0.57
VNSP305	98.9	1.27	0.74	VNSP347	99.0	0.68	0.32
VNSP306	62.2	n.d.	37.83	VNSP348	99.3	0.13	0.56
VNSP307	99.3	n.d.	0.75	VNSP349	99.4	n.d.	0.58
VNSP308	85.5	5.75	8.78	VNSP350	99.9	n.d.	0.10
VNSP309	7.7	n.d.	92.27	VNSP351	99.0	0.13	0.86
VNSP310	88.4	0.70	10.88	VNSP352	99.4	n.d.	0.55
VNSP311	41.7	0.32	58.00	VNSP353	99.5	0.21	0.24
VNSP312	41.8	16.96	41.25	VNSP354	99.2	0.50	0.30

Metallurgical vestiges	Cu	As	Fe	Metallurgical vestiges	Cu	As	Fe
VNSP313	27.3	20.7	52.01	VNSP355	98.7	0.76	0.56
VNSP314	99.7	n.d.	0.34	VNSP356	97.7	1.77	0.54
VNSP315	98.4	1.45	0.18	VNSP357	99.1	n.d.	0.88
VNSP358	99.3	0.18	0.56	VNSP401	99.6	0.30	0.14
VNSP359	98.0	1.67	0.30	VNSP402	99.1	0.81	0.14
VNSP360	92.3	6.72	1.02	VNSP403	99.7	0.10	0.18
VNSP361	98.6	1.15	0.29	VNSP404	99.1	0.82	0.10
VNSP362	99.3	0.59	0.13	VNSP405	99.7	0.26	n.d.
VNSP363	98.8	0.42	0.76	VNSP406	94.5	0.30	5.24
VNSP364	99.9	n.d.	0.12	VNSP407	97.7	2.04	0.25
VNSP365	98.8	0.93	0.22	VNSP408	99.9	n.d.	n.d.
VNSP366	99.7	n.d.	0.20	VNSP409	99.7	n.d.	0.33
VNSP367	98.4	0.73	0.91	VNSP410	93.5	6.33	0.22
VNSP368	95.2	4.30	0.47	VNSP411	98.0	1.92	0.12
VNSP369	99.2	0.67	0.00	VNSP412	98.2	1.59	0.24
VNSP370	99.8	0.00	0.25	VNSP413	99.5	0.25	0.27
VNSP371	98.4	1.30	0.34	VNSP414	98.9	0.41	0.73
VNSP372	99.5	0.27	0.22	VNSP415	99.7	0.16	0.17
VNSP373	99.8	n.d.	0.20	VNSP416	99.8	n.d.	0.24
VNSP374	98.5	1.30	0.20	VNSP417	99.4	n.d.	0.19
VNSP375	98.1	1.42	0.44	VNSP418	98.1	1.86	n.d.
VNSP376	99.7	n.d.	0.26	VNSP419	99.6	0.37	n.d.
VNSP377	99.9	n.d.	0.12	VNSP420	98.9	1.08	n.d.
VNSP378	95.4	3.46	1.15	VNSP421	99.7	n.d.	0.28
VNSP379	96.5	3.32	0.19	VNSP422	99.6	n.d.	0.36
VNSP380	97.4	2.4	0.24	VNSP423	99.6	n.d.	0.43
VNSP381	97.5	2.31	0.16	VNSP424	99.3	0.25	0.47
VNSP382	98.8	n.d.	1.16	VNSP425	98.2	n.d.	1.81
VNSP383	99.6	0.27	0.17	VNSP426	98.7	0.98	0.28
VNSP384	99.5	0.16	0.32	VNSP427	51.1	0.66	48.2
VNSP385	99.5	n.d.	0.42	VNSP428	99.9	n.d.	n.d.
VNSP386	97.2	2.66	0.18	VNSP429	96.0	3.46	0.52
VNSP387	99.6	n.d.	0.39	VNSP430	97.6	2.35	n.d.
VNSP388	99.8	n.d.	0.25	VNSP431	99.4	0.48	0.16
VNSP389	98.2	1.66	0.12	VNSP432	98.3	1.09	0.63
VNSP390	99.8	0.11	0.15	VNSP433	97.5	1.32	1.23
VNSP391	99.6	0.22	0.20	VNSP434	99.8	n.d.	0.21
VNSP392	99.7	0.24	n.d.	VNSP435	96.0	2.70	1.30
VNSP393	99.6	n.d.	0.38	VNSP436	98.2	1.24	0.59
VNSP394	98.0	1.79	0.23	VNSP437	99.3	0.63	0.11
VNSP395	99.2	0.67	0.13	VNSP438	99.9	n.d.	0.12
VNSP396	96.7	1.41	1.94	VNSP439	98.8	1.13	n.d.
VNSP397	97.3	2.53	0.13	VNSP440	95.5	2.34	2.13
VNSP398	99.7	n.d.	0.23	VNSP441	99.8	n.d.	0.16

Metallurgical vestiges	Cu	As	Fe	Metallurgical vestiges	Cu	As	Fe
VNSP399	97.5	2.31	0.17	VNSP442	99.0	0.17	0.89
VNSP400	97.2	2.54	0.30	VNSP443	85.2	n.d.	14.83
VNSP444	97.2	2.60	0.18	VNSP487	97.9	1.98	0.12
VNSP445	99.4	n.d.	0.54	VNSP488	99.3	0.59	0.15
VNSP446	98.6	0.31	1.09	VNSP489	99.6	0.37	n.d.
VNSP447	98.0	1.74	0.22	VNSP490	99.9	n.d.	n.d.
VNSP448	99.9	n.d.	0.13	VNSP491	99.7	n.d.	0.30
VNSP449	99.0	n.d.	1.00	VNSP492	99.7	n.d.	0.31
VNSP450	99.8	n.d.	0.18	VNSP493	99.4	0.46	0.14
VNSP451	99.9	n.d.	0.10	VNSP494	99.7	n.d.	0.27
VNSP452	99.5	n.d.	0.53	VNSP495	79.5	19.61	0.85
VNSP453	98.9	0.86	0.22	VNSP496	96.7	1.23	2.09
VNSP454	99.7	0.15	0.16	VNSP497	97.6	1.21	1.24
VNSP455	99.3	0.55	0.18	VNSP498	99.1	0.60	0.14
VNSP456	99.4	0.38	0.21	VNSP499	99.9	n.d.	0.15
VNSP457	99.5	0.30	0.22	VNSP500	95.7	n.d.	4.34
VNSP458	98.7	1.21	n.d.	VNSP501	98.7	1.08	0.20
VNSP459	99.3	0.59	0.10	VNSP502	99.1	0.79	0.14
VNSP460	99.3	0.59	n.d.	VNSP503	89.5	9.69	0.83
VNSP461	99.7	0.23	0.10	VNSP504	99.1	0.75	0.16
VNSP462	97.6	n.d.	2.44	VNSP505	97.6	2.05	0.35
VNSP463	98.4	1.22	0.40	VNSP506	99.8	0.17	n.d.
VNSP464	98.8	0.22	0.95	VNSP507	99.9	n.d.	0.14
VNSP465	99.4	0.19	0.42	VNSP508	98.5	1.36	0.14
VNSP466	99.4	0.31	0.26	VNSP509	98.1	0.29	1.64
VNSP467	99.7	0.12	0.20	VNSP510	99.8	n.d.	0.20
VNSP468	98.8	0.35	0.55	VNSP511	99.4	n.d.	0.58
VNSP469	98.7	1.14	0.18	VNSP512	98.6	0.16	1.10
VNSP470	96.1	1.37	2.56	VNSP513	99.4	0.39	0.26
VNSP471	95.4	4.51	0.13	VNSP514	98.7	0.82	0.45
VNSP472	95.8	4.09	0.12	VNSP515	99.9	n.d.	0.14
VNSP473	99.3	0.23	0.46	VNSP516	99.4	n.d.	0.63
VNSP474	99.0	n.d.	0.97	VNSP517	99.9	n.d.	0.10
VNSP475	99.9	n.d.	0.12	VNSP518	97.5	1.79	0.68
VNSP476	99.6	0.34	n.d.	VNSP519	99.4	n.d.	0.57
VNSP477	99.9	n.d.	0.13	VNSP520	97.2	n.d.	2.79
VNSP478	98.9	1.02	n.d.	VNSP521	94.5	5.24	0.24
VNSP479	99.9	n.d.	0.11	VNSP522	99.3	0.49	0.19
VNSP480	98.6	1.26	0.14	VNSP523	98.6	1.31	0.10
VNSP481	99.6	n.d.	0.42	VNSP524	99.4	0.43	0.22
VNSP482	99.7	n.d.	0.33	VNSP525	94.7	5.11	0.21
VNSP483	78.5	n.d.	21.5	VNSP526	99.8	0.15	n.d.
VNSP484	99.6	n.d.	0.40	VNSP527	99.8	n.d.	0.23
VNSP485	99.7	0.16	0.19	VNSP528	99.9	n.d.	0.14

Metallurgical vestiges	Cu	As	Fe	Metallurgical vestiges	Cu	As	Fe
VNSP486	95.9	3.60	0.47	VNSP529	98.9	n.d.	1.10
VNSP530	87.7	n.d.	12.3	VNSP573	99.4	n.d.	0.58
VNSP531	99.8	n.d.	0.17	VNSP574	98.5	n.d.	1.47
VNSP532	97.0	n.d.	3.02	VNSP575	99.4	0.52	0.00
VNSP533	99.8	n.d.	0.19	VNSP576	99.7	0.16	0.00
VNSP534	99.5	0.37	0.15	VNSP577	99.8	n.d.	0.24
VNSP535	97.3	2.47	0.20	VNSP578	99.5	0.32	0.15
VNSP536	99.9	n.d.	0.15	VNSP579	99.7	0.18	0.17
VNSP537	98.7	0.55	0.75	VNSP580	99.5	0.37	0.18
VNSP538	99.8	n.d.	0.25	VNSP581	99.8	n.d.	0.21
VNSP539	98.1	0.39	0.47	VNSP582	99.8	n.d.	0.16
VNSP540	70.0	n.d.	30.0	VNSP583	99.7	0.17	0.12
VNSP541	88.8	n.d.	11.2	VNSP584	99.8	n.d.	0.22
VNSP542	97.0	1.12	1.17	VNSP585	99.8	n.d.	0.17
VNSP543	98.7	n.d.	1.31	VNSP586	99.9	n.d.	0.10
VNSP544	99.3	0.54	0.16	VNSP587	99.9	n.d.	0.12
VNSP545	93.4	5.90	0.72	VNSP588	99.5	0.42	0.12
VNSP546	83.6	15.43	0.90	VNSP589	78.4	20.7	0.99
VNSP547	84.6	n.d.	15.4	VNSP590	97.4	0.11	2.51
VNSP548	98.5	n.d.	1.51	VNSP591	99.8	n.d.	0.22
VNSP549	99.4	0.55	n.d.	VNSP592	97.3	2.51	0.20
VNSP550	99.1	0.72	0.18	VNSP593	99.5	0.34	0.21
VNSP551	99.9	n.d.	n.d.	VNSP594	99.8	n.d.	0.22
VNSP552	96.4	2.80	0.82	VNSP595	99.2	n.d.	0.83
VNSP553	98.2	1.51	0.26	VNSP596	99.7	n.d.	0.29
VNSP554	92.4	1.28	6.36	VNSP597	99.3	0.55	0.19
VNSP555	98.9	0.17	0.94	VNSP598	99.0	0.85	0.19
VNSP556	98.1	1.51	0.38	VNSP599	8.0	n.d.	92.0
VNSP557	97.6	n.d.	2.39	VNSP600	84.1	n.d.	15.9
VNSP558	99.0	0.87	n.d.	VNSP601	98.8	0.90	0.33
VNSP559	99.9	n.d.	0.15	VNSP602	99.8	n.d.	0.18
VNSP560	99.9	n.d.	0.12	VNSP603	99.9	n.d.	0.10
VNSP561	97.4	0.28	2.29	VNSP604	99.3	n.d.	0.66
VNSP562	99.7	n.d.	0.33	VNSP605	77.0	n.d.	23.0
VNSP563	99.2	0.70	n.d.	VNSP606	98.7	0.62	0.72
VNSP564	96.6	0.62	2.82	VNSP607	99.8	n.d.	0.16
VNSP565	99.9	n.d.	0.11	VNSP608	99.8	n.d.	0.24
VNSP566	98.5	1.09	0.38	VNSP609	98.1	0.59	1.31
VNSP567	99.0	0.86	0.18	VNSP610	98.9	0.76	0.38
VNSP568	99.9	n.d.	n.d.	VNSP611	99.8	n.d.	0.23
VNSP569	98.7	1.21	n.d.	VNSP612	98.8	1.12	0.00
VNSP570	97.5	2.12	0.34	VNSP613	91.0	4.25	4.38
VNSP571	99.9	n.d.	0.11	VNSP614	98.4	0.98	0.67
VNSP572	99.1	0.78	n.d.	VNSP615	99.4	0.53	n.d.

Metallurgical vestiges	Cu	As	Fe	Metallurgical vestiges	Cu	As	Fe
VNSP616	99.8	n.d.	0.24	VNSP659	99.7	n.d.	0.27
VNSP617	97.4	2.36	0.22	VNSP660	99.1	0.74	0.17
VNSP618	96.0	3.59	0.40	VNSP661	99.6	n.d.	0.44
VNSP619	98.1	0.69	0.30	VNSP662	98.9	n.d.	1.13
VNSP620	97.8	2.14	0.11	VNSP663	98.2	1.49	0.33
VNSP621	99.8	n.d.	0.18	VNSP664	99.2	0.75	0.00
VNSP622	99.8	n.d.	0.17	VNSP665	99.8	n.d.	0.23
VNSP623	99.0	0.91	0.11	VNSP666	99.7	n.d.	0.32
VNSP624	99.2	0.52	0.32	VNSP667	93.4	1.33	5.32
VNSP625	99.8	n.d.	0.20	VNSP668	93.4	0.40	6.20
VNSP626	99.7	0.13	0.16	VNSP669	99.3	n.d.	0.69
VNSP627	96.5	1.61	1.91	VNSP670	93.1	3.60	3.32
VNSP628	97.4	2.13	0.45	VNSP671	99.9	n.d.	0.13
VNSP629	99.1	0.44	0.49	VNSP672	99.9	n.d.	0.12
VNSP630	97.0	2.26	0.78	VNSP673	97.7	n.d.	2.35
VNSP631	96.2	3.32	0.52	VNSP674	99.7	0.17	0.11
VNSP632	95.5	n.d.	4.55	VNSP675	97.9	1.81	0.26
VNSP633	99.8	n.d.	0.19	VNSP676	98.9	0.17	0.98
VNSP634	99.0	0.80	0.19	VNSP677	99.0	0.47	0.51
VNSP635	98.2	1.75	0.10	VNSP678	99.4	n.d.	0.56
VNSP636	99.9	n.d.	n.d.	VNSP679	99.8	n.d.	0.20
VNSP637	95.0	n.d.	5.05	VNSP680	99.4	n.d.	0.60
VNSP638	98.9	n.d.	1.13	VNSP681	99.0	0.75	0.30
VNSP639	99.6	n.d.	0.45	VNSP682	99.3	0.44	0.29
VNSP640	99.1	0.86	n.d.	VNSP683	99.9	n.d.	0.11
VNSP641	98.5	0.87	0.61	VNSP684	99.8	n.d.	0.18
VNSP642	99.8	n.d.	0.16	VNSP685	99.9	n.d.	n.d.
VNSP643	97.1	2.72	0.19	VNSP686	98.5	1.13	0.34
VNSP644	99.8	n.d.	0.17	VNSP687	99.9	n.d.	n.d.
VNSP645	99.9	n.d.	0.11	VNSP688	98.8	0.74	0.45
VNSP646	99.9	n.d.	0.13	VNSP689	99.7	0.20	0.15
VNSP647	83.1	0.00	16.9	VNSP690	98.7	1.13	0.20
VNSP648	98.8	0.56	0.33	VNSP691	99.6	0.20	0.23
VNSP649	99.9	n.d.	n.d.	VNSP692	98.8	0.98	0.18
VNSP650	99.5	n.d.	0.51	VNSP693	98.8	0.25	0.98
VNSP651	99.9	n.d.	0.14	VNSP694	99.6	n.d.	0.40
VNSP652	43.5	n.d.	56.5	VNSP695	22.7	n.d.	77.3
VNSP653	99.4	0.50	n.d.	VNSP696	99.9	n.d.	0.12
VNSP654	99.5	n.d.	0.54	VNSP697	96.7	2.30	0.87
VNSP655	99.9	n.d.	n.d.	VNSP698	99.7	0.16	0.17
VNSP656	99.6	0.36	n.d.	VNSP699	98.8	1.07	0.14
VNSP657	61.7	n.d.	38.3	VNSP700	99.1	n.d.	0.89
VNSP658	98.6	1.20	0.25	VNSP701	99.7	0.19	n.d.
VNSP702	84.0	n.d.	16.0	VNSP745	99.1	0.67	0.24

Metallurgical vestiges	Cu	As	Fe	Metallurgical vestiges	Cu	As	Fe
VNSP703	99.4	0.17	0.41	VNSP746	99.8	n.d.	0.20
VNSP704	93.4	n.d.	6.64	VNSP747	99.4	0.46	0.16
VNSP705	99.1	0.39	0.53	VNSP748	96.8	0.45	2.75
VNSP706	97.5	1.54	0.99	VNSP749	99.3	n.d.	0.69
VNSP707	99.3	0.42	0.29	VNSP750	99.9	n.d.	0.15
VNSP708	99.0	0.66	0.32	VNSP751	99.0	n.d.	1.03
VNSP709	88.2	10.9	0.90	VNSP752	99.9	n.d.	0.13
VNSP710	99.8	n.d.	0.22	VNSP753	99.1	0.32	0.59
VNSP711	99.9	n.d.	0.14	VNSP754	95.1	1.37	3.51
VNSP712	98.9	n.d.	0.60	VNSP755	93.1	5.85	1.01
VNSP713	99.7	n.d.	0.34	VNSP756	99.0	0.88	0.10
VNSP714	99.2	n.d.	0.80	VNSP757	97.7	0.75	1.54
VNSP715	98.1	1.84	n.d.	VNSP758	98.4	1.28	0.34
VNSP716	97.3	1.69	0.96	VNSP759	98.2	n.d.	1.78
VNSP717	87.5	11.6	0.86	VNSP760	99.9	n.d.	0.15
VNSP718	95.3	4.55	0.20	VNSP761	97.1	2.71	0.16
VNSP719	98.0	1.81	0.18	VNSP762	99.8	n.d.	0.17
VNSP720	93.4	6.34	0.27	VNSP763	98.9	n.d.	1.12
VNSP721	92.1	3.63	4.24	VNSP764	99.8	n.d.	0.23
VNSP722	99.3	0.62	0.12	VNSP765	99.0	0.29	0.68
VNSP723	98.9	0.98	0.15	VNSP766	95.7	1.90	2.40
VNSP724	99.3	0.21	0.46	VNSP767	98.6	1.33	n.d.
VNSP725	98.1	1.78	0.16	VNSP768	99.9	n.d.	n.d.
VNSP726	99.0	0.77	0.22	VNSP769	99.8	n.d.	0.20
VNSP727	99.9	n.d.	0.10	VNSP770	98.7	1.19	0.12
VNSP728	98.3	1.52	0.20	VNSP771	99.6	n.d.	0.36
VNSP729	96.9	2.89	0.18	VNSP772	99.9	n.d.	n.d.
VNSP730	99.7	n.d.	0.35	VNSP773	99.9	0.00	0.15
VNSP731	82.3	10.0	7.74	VNSP774	95.5	4.27	0.28
VNSP732	98.4	n.d.	1.65	VNSP775	98.7	1.26	0.00
VNSP733	99.9	n.d.	0.15	VNSP776	99.8	n.d.	0.19
VNSP734	65.5	n.d.	34.49	VNSP777	98.8	1.05	0.19
VNSP735	99.6	0.27	0.16	VNSP778	99.8	n.d.	0.24
VNSP736	99.9	n.d.	n.d.	VNSP779	99.9	n.d.	0.10
VNSP737	92.0	2.35	5.62	VNSP780	99.4	0.49	0.11
VNSP738	99.0	0.94	n.d.	VNSP781	99.9	n.d.	0.11
VNSP739	98.8	n.d.	1.23	VNSP782	99.6	0.18	0.25
VNSP740	43.3	n.d.	56.7	VNSP783	99.0	0.91	0.13
VNSP741	99.8	n.d.	0.22	VNSP784	84.3	n.d.	15.7
VNSP742	99.1	0.41	0.54	VNSP785	16.7	n.d.	83.3
VNSP743	99.5	0.38	0.13	VNSP786	99.4	0.54	n.d.
VNSP744	99.6	n.d.	0.37	VNSP787	98.5	0.35	1.20
VNSP788	99.9	n.d.	0.13	VNSP816	99.5	n.d.	0.46
VNSP789	99.6	0.27	0.14	VNSP817	99.1	0.73	0.15

Metallurgical vestiges	Cu	As	Fe	Metallurgical vestiges	Cu	As	Fe
VNSP790	98.2	1.45	0.34	VNSP818	99.0	0.85	0.17
VNSP791	99.8	n.d.	0.18	VNSP819	98.5	1.26	0.23
VNSP792	99.7	n.d.	0.32	VNSP820	99.9	n.d.	0.13
VNSP793	99.3	0.48	0.18	VNSP821	98.4	0.72	0.88
VNSP794	99.9	n.d.	0.15	VNSP822	99.7	0.23	0.10
VNSP795	97.0	n.d.	3.00	VNSP823	99.4	0.42	0.15
VNSP796	99.7	n.d.	0.30	VNSP824	99.7	n.d.	0.26
VNSP797	85.4	n.d.	14.6	VNSP825	41.4	0.28	58.3
VNSP798	99.9	n.d.	n.d.	VNSP826	82.6	n.d.	17.4
VNSP799	94.2	n.d.	5.79	VNSP827	98.1	1.78	0.14
VNSP800	97.3	2.53	0.16	VNSP828	98.5	0.83	0.72
VNSP801	21.7	n.d.	78.3	VNSP829	99.0	0.84	0.13
VNSP802	99.6	n.d.	0.41	VNSP830	99.3	0.62	n.d.
VNSP803	25.5	n.d.	74.5	VNSP831	99.0	0.90	0.14
VNSP804	95.6	2.89	1.48	VNSP832	99.1	n.d.	0.88
VNSP805	99.6	0.29	n.d.	VNSP833	99.4	0.50	n.d.
VNSP806	48.0	n.d.	52.0	VNSP834	99.9	n.d.	n.d.
VNSP807	99.8	n.d.	0.22	VNSP835	99.9	n.d.	0.15
VNSP808	98.3	1.64	0.11	VNSP836	98.0	1.91	0.10
VNSP809	99.9	n.d.	0.14	VNSP837	98.9	0.95	0.12
VNSP810	98.7	1.17	0.10	VNSP838	98.4	1.55	n.d.
VNSP811	100.0	n.d.	n.d.	VNSP839	99.3	0.58	0.13
VNSP812	99.9	n.d.	0.10	VNSP840	99.8	n.d.	0.20
VNSP813	99.0	0.83	0.15	VNSP841	98.9	0.94	0.15
VNSP814	99.7	n.d.	0.33	VNSP842	98.5	1.38	n.d.
VNSP815	99.8	n.d.	0.23	-	-	-	-

APPENDIX II: SUMMARY OF MICRO-EDXRF ANALYSIS OF METALLIC VESTIGES FROM VNSP

Table II.1. Summary of micro-EDXRF analysis of metallic vestiges from VNSP (wt.%).

Metallic vestiges	Cu	As	Fe	Metallic vestiges	Cu	As	Fe
VNSP280	96.5±0.1	2.46±0.18	<0.05	VNSP344	99.9±0.1	<0.10	0.07±0.10
VNSP287	99.9±0.1	<0.10	<0.05	VNSP345	99.9±0.1	<0.10	<0.05
VNSP295	99.8±0.1	0.18±0.10	<0.05	VNSP346	99.9±0.1	<0.10	<0.05
VNSP296	99.9±0.1	<0.10	<0.05	VNSP347	99.6±0.1	0.43±0.10	<0.05
VNSP297	99.9±0.1	<0.10	<0.05	VNSP348	99.9±0.1	<0.10	<0.05
VNSP298	99.9±0.1	<0.10	<0.05	VNSP349	99.9±0.1	<0.10	<0.05
VNSP299	99.9±0.1	<0.10	<0.05	VNSP350	99.9±0.1	<0.10	<0.05
VNSP300	97.1±0.2	2.82±0.10	<0.05	VNSP351	99.9±0.1	<0.10	<0.05
VNSP304	99.9±0.1	<0.10	<0.05	VNSP352	99.9±0.1	<0.10	<0.05
VNSP305	99.9±0.1	<0.10	<0.05	VNSP353	99.8±0.1	0.24±0.10	<0.05
VNSP308	95.4±0.4	4.61±0.24	<0.05	VNSP354	99.7±0.1	0.26±0.10	<0.05
VNSP309	99.9±0.1	<0.10	<0.05	VNSP355	99.9±0.1	<0.10	<0.05
VNSP313D	88.9±0.6	10.44±0.31	0.08±0.10	VNSP356	98.7±0.2	1.26±0.10	<0.05
VNSP314	99.9±0.1	<0.10	<0.05	VNSP357	99.9±0.1	<0.10	<0.05
VNSP315	97.9±0.2	2.07±0.16	<0.05	VNSP358	99.9±0.1	<0.10	<0.05
VNSP316	99.9±0.1	<0.10	<0.05	VNSP359	97.7±0.2	2.29±0.11	<0.05
VNSP317	97.8±0.2	2.12±0.26	0.06±0.10	VNSP360	96.8±0.3	3.17±0.12	<0.05
VNSP318	98.9±0.1	1.10±0.15	<0.05	VNSP361	99.3±0.1	0.60±0.10	<0.05
VNSP319	99.7±0.1	0.23±0.10	<0.05	VNSP362	98.5±0.1	1.47±0.10	<0.05
VNSP320	98.8±0.1	1.18±0.10	<0.05	VNSP363	99.9±0.1	<0.10	<0.05
VNSP321	98.2±0.1	1.83±0.20	<0.05	VNSP364	99.9±0.1	<0.10	<0.05
VNSP322	99.9±0.1	<0.10	<0.05	VNSP365	99.0±0.1	1.02±0.10	<0.05
VNSP323	99.9±0.1	0.13±0.10	<0.05	VNSP366	99.9±0.1	<0.10	<0.05
VNSP324	99.9±0.1	<0.10	<0.05	VNSP367	99.2±0.1	0.76±0.10	<0.05
VNSP325	99.9±0.1	<0.10	<0.05	VNSP368	95.7±0.9	4.26±0.26	<0.05
VNSP326	99.6±0.1	0.37±0.10	<0.05	VNSP369	98.5±0.3	1.47±0.10	<0.05
VNSP327	99.6±0.1	0.38±0.10	<0.05	VNSP370	99.9±0.1	<0.10	<0.05
VNSP328	99.9±0.1	<0.10	<0.05	VNSP371	97.6±0.2	2.37±0.10	<0.05
VNSP329	97.9±0.2	2.09±0.10	<0.05	VNSP372	99.9±0.1	<0.10	<0.05
VNSP331	99.7±0.1	0.26±0.10	<0.05	VNSP373	99.9±0.1	<0.10	<0.05
VNSP332	99.9±0.1	<0.10	<0.05	VNSP374	99.0±0.1	0.99±0.10	<0.05
VNSP333	99.9±0.1	<0.10	<0.05	VNSP375	97.8±0.3	1.53±0.10	0.70±0.10
VNSP334	99.8±0.1	0.19±0.10	<0.05	VNSP376	99.9±0.1	<0.10	<0.05
VNSP335	99.9±0.1	<0.10	<0.05	VNSP377	99.9±0.1	<0.10	<0.05
VNSP336	99.9±0.1	<0.10	<0.05	VNSP378	97.3±0.3	2.22±0.10	<0.05
VNSP337	97.4±0.3	2.46±0.11	0.11±0.10	VNSP379	97.0±0.3	3.00±0.17	<0.05
VNSP338	99.9±0.1	<0.10	<0.05	VNSP380	99.7±0.1	0.27±0.10	0.07±0.10
VNSP339	99.9±0.1	<0.10	<0.05	VNSP381	97.5±0.2	2.52±0.10	<0.05
VNSP340	96.7±0.3	3.27±0.11	0.07±0.10	VNSP382	99.9±0.1	<0.10	<0.05

Metallic vestiges	Cu	As	Fe	Metallic vestiges	Cu	As	Fe
VNSP341	97.4±0.2	2.50±0.10	0.07±0.10	VNSP383	99.9±0.1	<0.10	<0.05
VNSP342	99.9±0.1	<0.10	<0.05	VNSP384	99.8±0.1	0.19±0.10	<0.05
VNSP343	99.9±0.1	<0.10	<0.05	VNSP385	99.9±0.1	<0.10	<0.05
VNSP386	99.2±0.1	0.72±0.10	<0.05	VNSP630	97.6±0.5	2.36±0.10	<0.05
VNSP387	99.9±0.1	<0.10	<0.05	VNSP631	97.4±0.5	2.58±0.11	0.06±0.10
VNSP388	99.9±0.1	<0.10	<0.05	VNSP634	97.6±0.6	2.40±0.10	<0.05
VNSP389	97.9±0.3	2.03±0.11	<0.05	VNSP670	99.9±0.1	<0.10	<0.05
VNSP390	99.9±0.1	<0.10	<0.05	VNSP394	98.1±0.2	1.85±0.10	<0.05
VNSP391	99.9±0.1	<0.10	<0.05	VNSP395	99.2±0.1	0.74±0.10	<0.05
VNSP392	99.6±0.1	0.36±0.10	<0.05	VNSP397	98.3±0.2	1.65±0.10	<0.05
VNSP393	99.9±0.1	<0.10	<0.05	VNSP398	99.9±0.1	<0.10	<0.05
VNSP394	98.1±0.2	1.85±0.10	<0.05	VNSP399	96.6±0.8	3.39±0.21	<0.05
VNSP395	99.2±0.1	0.74±0.10	<0.05	VNSP400	98.1±0.3	1.86±0.10	<0.05
VNSP397	98.3±0.1	1.65±0.10	<0.05	VNSP401	99.7±0.1	0.24±0.10	<0.05
VNSP398	99.9±0.1	<0.10	<0.05	VNSP402	98.6±0.2	1.40±0.10	<0.05
VNSP399	96.6±0.5	3.39±0.18	<0.05	VNSP403	99.9±0.1	<0.10	<0.05
VNSP400	98.1±0.4	1.86±0.10	<0.05	VNSP404	98.4±0.1	1.50±0.10	<0.05
VNSP401	99.7±0.1	0.24±0.10	<0.05	VNSP405	99.7±0.1	0.28±0.10	<0.05
VNSP402	98.6±0.2	1.40±0.10	<0.05	VNSP407	99.9±0.1	<0.10	<0.05
VNSP403	99.9±0.1	<0.10	<0.05	VNSP410	97.5±0.4	2.48±0.10	0.05±0.10
VNSP404	98.4±0.2	1.50±0.10	<0.05	VNSP429	99.9±0.1	<0.10	<0.05
VNSP405	99.7±0.1	0.28±0.10	<0.05	VNSP430	95.7±1.1	4.28±0.33	<0.05
VNSP407	99.9±0.1	<0.10	<0.05	VNSP435	98.7±0.1	1.34±0.10	<0.05
VNSP410	97.5±0.6	2.48±0.12	0.05±0.10	VNSP440	99.9±0.1	<0.10	<0.05
VNSP429	99.9±0.1	<0.10	<0.05	VNSP444	95.7±0.8	4.26±0.11	<0.05
VNSP430	95.7±0.6	4.28±0.31	<0.05	VNSP471	99.0±0.1	1.04±0.10	<0.05
VNSP435	98.7±0.3	1.34±0.10	<0.05	VNSP472	97.0±0.2	3.02±0.15	<0.05
VNSP440	99.9±0.1	<0.10	<0.05	VNSP486	99.4±0.1	0.58±0.10	<0.05
VNSP444	95.7±0.8	4.26±0.14	<0.05	VNSP487	97.7±0.1	2.19±0.11	<0.05
VNSP471	99.0±0.1	1.04±0.10	<0.05	VNSP495	96.2±0.1	3.79±0.12	0.06±0.10
VNSP472	97.0±0.2	3.02±0.12	<0.05	VNSP503	99.3±0.1	0.68±0.10	<0.05
VNSP486	99.4±0.1	0.58±0.10	<0.05	VNSP521	98.8±0.1	1.13±0.10	<0.05
VNSP487	97.7±0.2	2.19±0.12	<0.05	VNSP525	99.6±0.1	0.37±0.10	<0.05
VNSP495	96.2±0.3	3.79±0.28	0.06±0.10	VNSP535	99.2±0.1	0.78±0.10	<0.05
VNSP503	99.3±0.1	0.68±0.10	<0.05	VNSP537	99.9±0.1	0.11±0.10	<0.05
VNSP521	98.8±0.1	1.13±0.11	<0.05	VNSP545	99.9±0.1	<0.10	<0.05
VNSP525	99.6±0.1	0.37±0.10	<0.05	VNSP546	98.8±0.2	1.24±0.14	<0.05
VNSP535	99.2±0.1	0.78±0.10	<0.05	VNSP552	99.9±0.1	<0.10	<0.05
VNSP537	99.9±0.1	0.11±0.10	<0.05	VNSP570	98.4±0.2	1.55±0.12	<0.05
VNSP545	99.9±0.1	<0.10	<0.05	VNSP589	99.5±0.1	0.45±0.10	<0.05
VNSP546	98.8±0.1	1.24±0.10	<0.05	VNSP592	98.5±0.2	1.45±0.10	<0.05
VNSP552	99.9±0.1	<0.10	<0.05	VNSP613	99.9±0.1	0.15±0.10	<0.05
VNSP570	98.4±0.1	1.55±0.11	<0.05	VNSP617	98.0±0.2	2.05±0.12	<0.05
VNSP589	99.5±0.1	0.45±0.10	<0.05	VNSP618	99.1±0.1	0.87±0.10	<0.05

Metallic vestiges	Cu	As	Fe	Metallic vestiges	Cu	As	Fe
VNSP592	98.5±0.1	1.45±0.10	<0.05	VNSP628	99.3±0.1	0.67±0.10	<0.05
VNSP613	99.9±0.1	0.15±0.10	<0.05	VNSP630	97.6±0.4	2.36±0.11	<0.05
VNSP617	98.0±0.3	2.05±0.10	<0.05	VNSP631	97.4±0.3	2.58±0.12	0.06±0.10
VNSP618	99.1±0.1	0.87±0.10	<0.05	VNSP729	98.3±0.2	1.70±0.10	<0.05
VNSP628	99.3±0.1	0.67±0.10	<0.05	VNSP731	95.5±0.3	4.42±0.31	<0.05
VNSP634	97.6±0.2	2.40±0.13	<0.05	VNSP737	95.1±0.6	4.37±0.22	<0.05
VNSP670	99.9±0.1	<0.10	<0.05	VNSP755	97.6±0.4	2.42±0.12	<0.05
VNSP697	99.5±0.1	0.37±0.10	0.08±0.10	VNSP761	97.5±0.2	2.50±0.11	<0.05
VNSP709	96.7±0.5	3.24±0.16	<0.05	VNSP774	98.1±0.1	1.86±0.10	<0.05
VNSP717	98.8±0.2	1.13±0.10	0.07±0.10	VNSP800	95.3±0.7	4.70±0.31	<0.05
VNSP718	99.8±0.1	0.18±0.10	<0.05	VNSP804	98.7±0.2	1.21±0.10	<0.05
VNSP720	99.4±0.1	0.61±0.10	<0.05	-	-	-	-

APPENDIX III: SUMMARY OF MICROSTRUCTURAL OBSERVATIONS OF METALLIC NODULES COLLECTION FROM VNSP
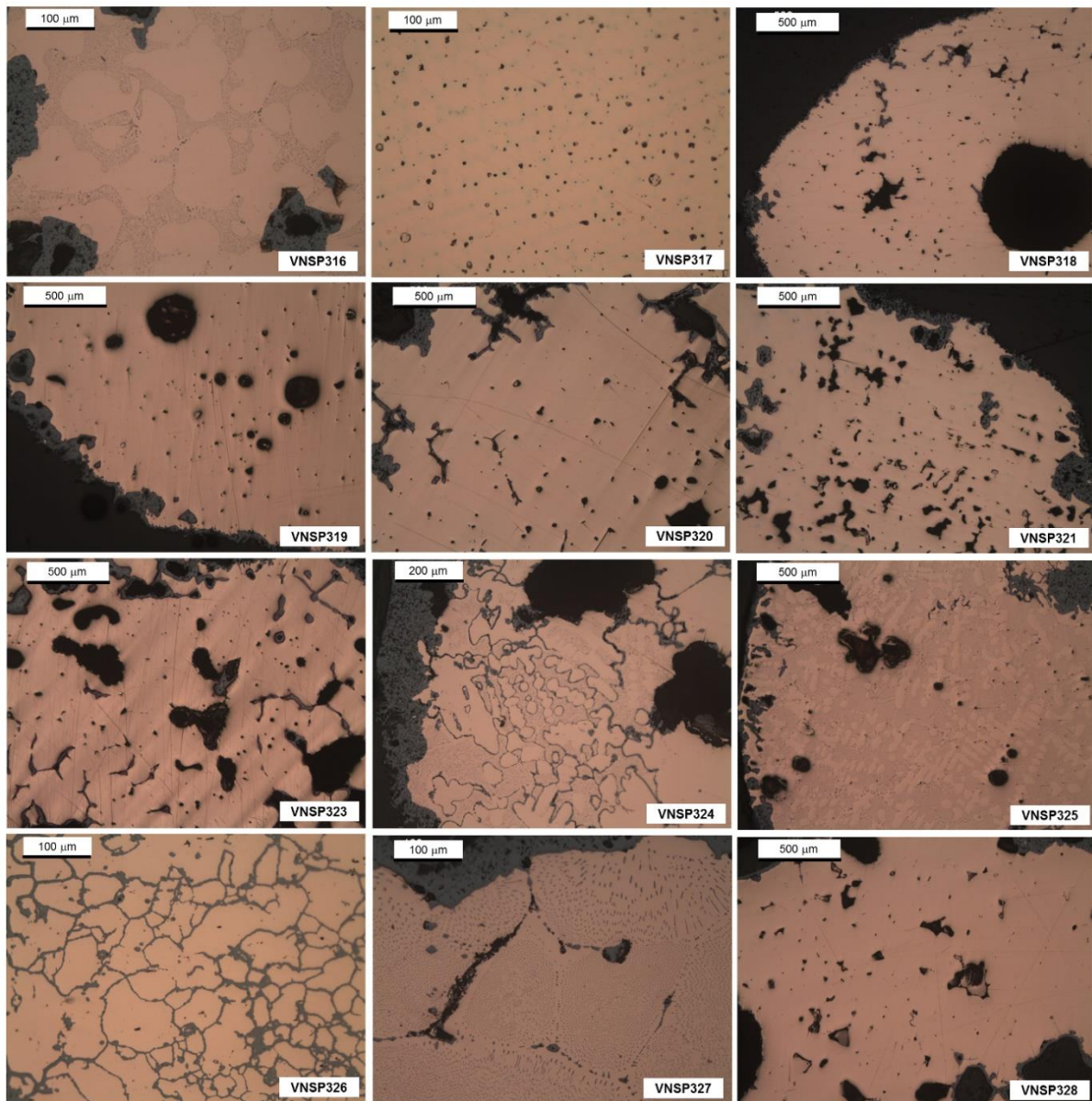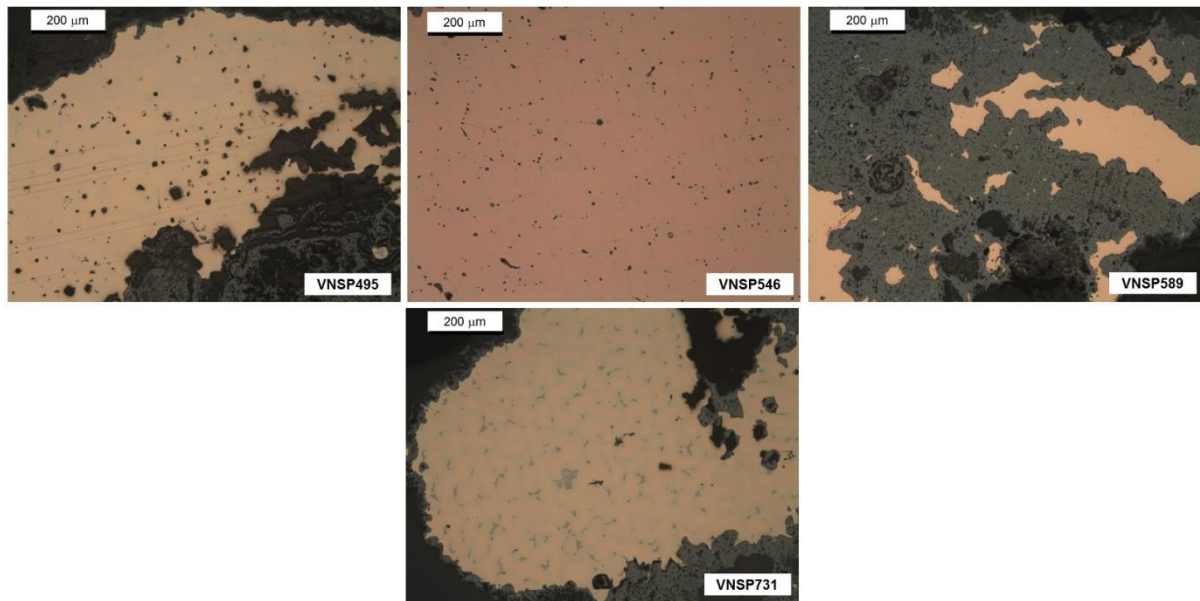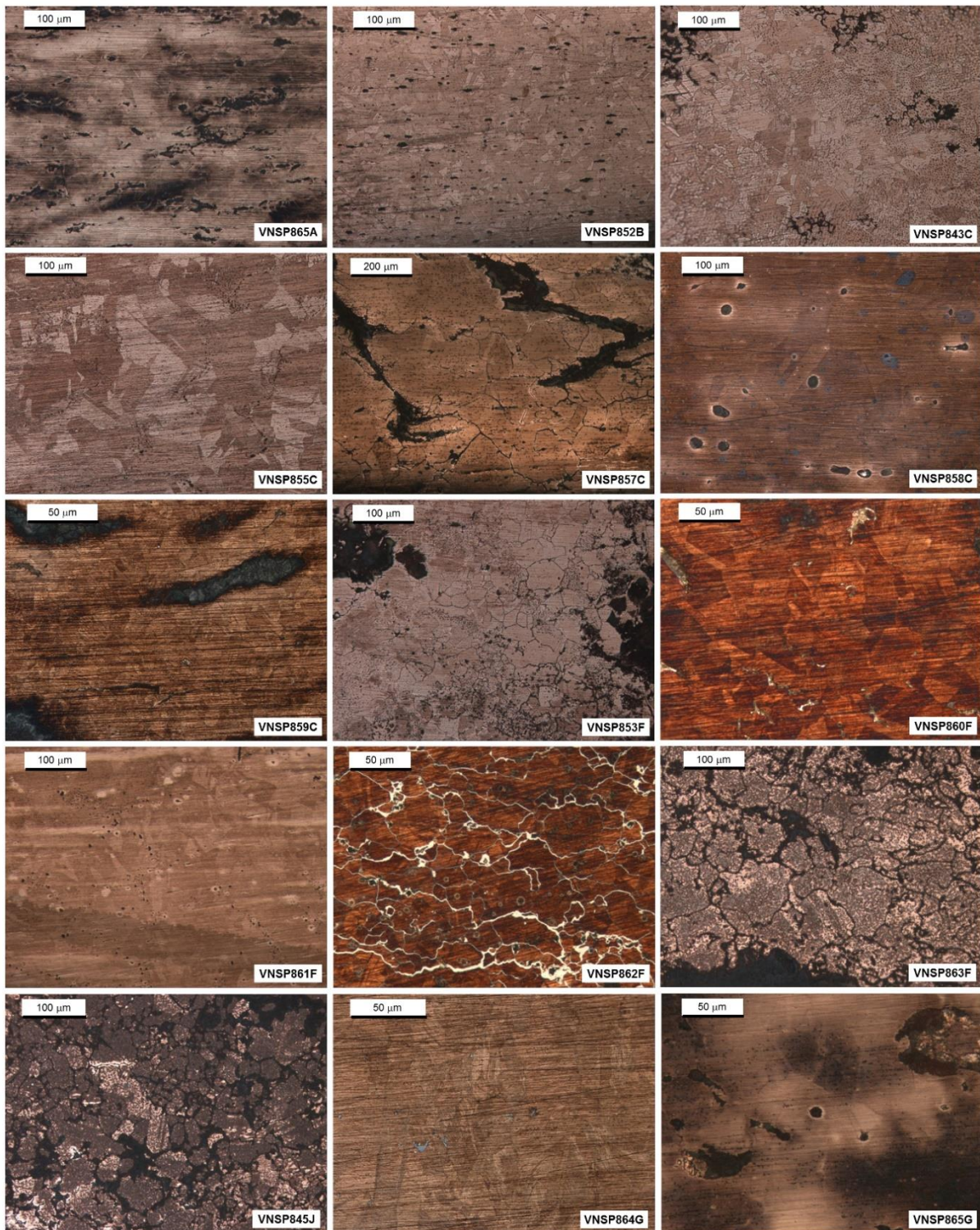
Figure III.1. OM images with the most representative microstructural observations of metallic nodules collection from VNSP (all BF, non-etched).
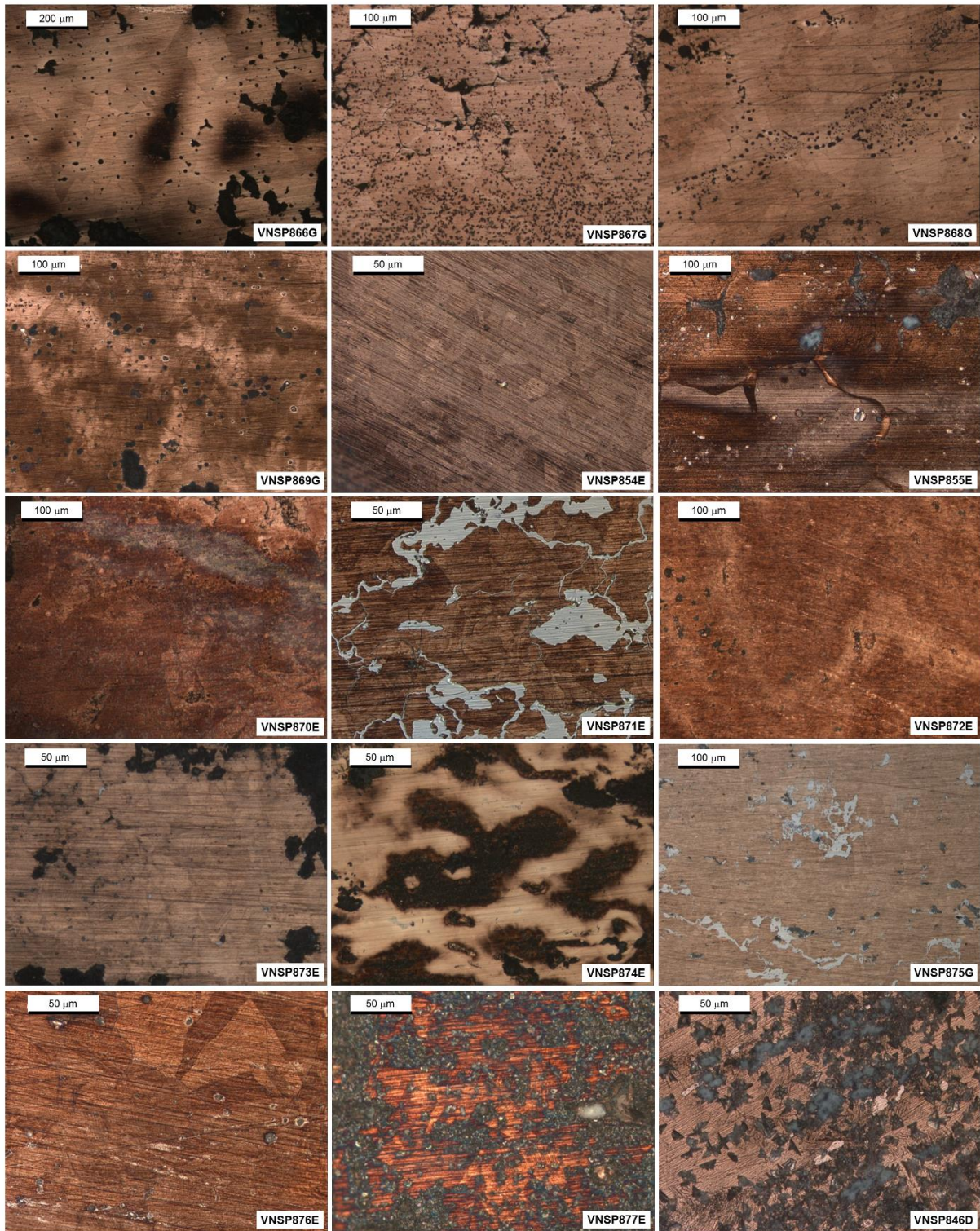
APPENDIX IV: COMPOSITION OF ARTEFACT COLLECTION FROM VNSP AND RELEVANT MICROSTRUCTURAL CHARACTERIZATION DATA FROM PREVIOUS STUDY (PEREIRA ET AL., 2013) AND MASTER´S THESIS (PEREIRA, 2011)

Table IV.1. Summary of micro-EDXRF analysis of copper-based artefacts from VNSP (content in wt.% average ± standard deviation; n.d.: not detected); microstructural characteristics (C: Casting; F: Forging; A: Annealing ; FF: Final forging; ↓: Low amount; ↑: High amount); [a]: Hardness profiles (transversal and longitudinal axis), were determined in artefact VNSP262C; [b]: Vickers microhardness testing was made only in mounted cross-sections (HV0.2).

Typology	Artefacts	Elemental analysis (wt.%)			Phases	HV0.2 [b]			Operational sequence
		Cu	As	Fe		Centre	Blade	Fract.	
A – Awls	VNSP001A	95.4±0.2	4.36±0.23	<0.05	$\alpha+Cu_3As$	80	-	-	C+(F+A)+FF
	VNSP021A	98.9±0.1	0.90±0.04	<0.05	α	40	-	-	C+(F+A)
	VNSP023A	98.7±0.1	0.96±0.08	<0.05	α	68	-	-	C+(F+A)
	VNSP029A	96.5±0.2	3.19±0.18	<0.05	$\alpha+Cu_3As$	59	-	-	C+(F+A)
	VNSP031A	98.3±0.2	1.43±0.20	<0.05	α	106	-	-	C+(F+A)
	VNSP038A	98.1±0.2	1.56±0.18	0.07±0.01	α	81	-	-	C+(F+A)
	VNSP040A	96.3±0.4	3.39±0.35	0.05±0.01	α	60	-	-	C+(F+A)+FF↓
	VNSP047A	99.7±0.1	<0.10	<0.05	α	63	-	-	C+(F+A)
	VNSP049A	94.2±0.1	5.59±0.08	<0.05	$\alpha+Cu_3As$	65	-	-	C+(F+A)
	VNSP097A	93.7±0.1	6.04±0.11	<0.05	$\alpha+Cu_3As$	86	-	-	C+(F+A)+FF↓
	VNSP123B	99.8±0.1	0.21±0.01	<0.05	α	84	-	-	C+(F+A)
	VNSP124B	99.8±0.1	0.19±0.01	<0.05	α	91	-	-	C+(F+A)
C – Chisels	VNSP132C	94.9±0.4	4.92±0.36	<0.05	$\alpha+Cu_3As$	53	-	-	C+(F+A)
	VNSP133C	99.5±0.1	0.27±0.04	<0.05	α	36	-	-	C+(F+A)
	VNSP134C	99.7±0.1	<0.10	<0.05	α	81	-	-	C+(F+A)
	VNSP135C	98.2±0.2	1.53±0.17	<0.05	α	42	-	-	C+(F+A)
	VNSP136C	99.7±0.1	<0.10	<0.05	α	94	-	-	C+(F+A)
	VNSP137C	99.8±0.1	<0.10	<0.05	α	85	-	-	C+(F+A)+FF↓
	VNSP138C	98.7±0.3	1.08±0.28	<0.05	α	44	-	-	C+(F+A)
	VNSP139C	98.1±0.1	1.71±0.15	<0.05	α	91	115	90	C+(F+A)
	VNSP140C	96.3±0.2	3.43±0.22	<0.05	α	80	105	90	C+(F+A)+FF↓
	VNSP141C	97.2±0.1	2.61±0.05	<0.05	α	97	123	98	C+(F+A)+FF↓
	VNSP261C	99.7±0.3	0.31±0.04	0.07±0.01	α	-	-	-	C+(F+A)
	VNSP262C	99.8±0.1	<0.10	<0.05	α	-[a]	-	-	C+(F+A)
	VNSP263C	99.4±0.4	0.26±0.04	<0.05	α	-	-	-	C+(F+A)
	VNSP264C	99.7±0.1	<0.10	<0.05	α	-	-	-	C+(F+A)
	VNSP265C	99.0±0.3	0.67±0.04	<0.05	α	-	-	-	C+(F+A)
	VNSP266C	99.6±0.1	<0.10	<0.05	α	-	-	-	C+(F+A)
D - Axes	VNSP144D	99.7±0.1	<0.10	0.21±0.02	α	44	66	47	C+(F+A)
	VNSP145D	99.8±0.1	<0.10	<0.05	α	48	50	49	C+(F+A)
	VNSP146D	97.7±0.1	2.04±0.10	<0.05	α	45	47	45	C+(F+A)
	VNSP147D	97.9±0.2	1.85±0.14	<0.05	α	65	57	64	C+(F+A)
	VNSP148D	90.6±0.2	9.13±0.23	0.07±0.01	$\alpha+Cu_3As$	95	95	95	C+(F+A)
	VNSP150D	99.5±0.1	0.24±0.04	<0.05	α	45	50	49	C+(F+A)
	VNSP153D	98.6±0.1	1.08±0.13	0.05±0.01	α	64	64	65	C+(F+A)

Typology	Artefacts	Elemental analysis (wt.%)			Phases	HV0.2 [b]			Operational sequence
		Cu	As	Fe		Centre	Blade	Fract.	
	VNSP154D	98.2±0.3	1.58±0.24	<0.05	α	47	46	45	C+(F+A)
	VNSP155D	98.9±0.1	0.79±0.07	<0.05	α	42	45	45	C+(F+A)
	VNSP165D	98.4±0.2	1.42±0.18	<0.05	α	42	47	46	C+(F+A)
	VNSP178D	99.8±0.1	<0.10	<0.05	α	75	-	-	C+(F+A)
	VNSP267D	99.8±0.1	<0.10	<0.05	α	-	-	-	C+(F+A)
	VNSP268D	99.8±0.1	<0.10	<0.05	α	41	50	45	C+(F+A)
	VNSP269D	97.5±0.2	2.56±0.10	<0.05	α	-	-	-	C+(F+A)
	VNSP270D	98.9±0.1	0.83±0.13	<0.05	α	-	-	-	C+(F+A)
	VNSP271D	98.6±0.2	1.37±0.18	<0.05	α	-	-	-	C+(F+A)
	VNSP272D	96.7±0.4	3.06±0.22	<0.05	α+Cu$_3$As	-	-	-	C+(F+A)
	VNSP273D	99.8±0.1	<0.10	<0.05	α	-	-	-	C+(F+A)
	VNSP274D	98.3±0.2	1.68±0.21	<0.05	α	-	-	-	C+(F+A)
	VNSP275D	97.6±0.2	2.30±0.10	<0.05	α+Cu$_3$As	-	-	-	C+(F+A)
E – Arrowheads, Daggers, Knives	VNSP177E	99.8±0.1	<0.10	<0.05	α	43	44	46	C+(F+A)
	VNSP180E	94.2±0.4	5.57±0.38	<0.05	α+Cu$_3$As	63	63	75	C+(F+A)+FF↓
	VNSP181E	97.5±0.2	2.22±0.18	<0.05	α	119	119	120	C+(F+A)+FF
	VNSP182E	94.1±0.2	5.66±0.21	<0.05	α	90	96	75	C+(F+A)
	VNSP183E	95.8±0.2	3.89±0.08	<0.05	α+Cu$_3$As	54	55	53	C+(F+A)+FF
	VNSP188E	97.9±0.4	1.79±0.39	<0.05	α+Cu$_3$As	77	80	78	C+(F+A)
	VNSP189E	95.2±0.4	4.53±0.33	<0.05	α+Cu$_3$As	155	204	119	C+(F+A)+FF
F - Saws	VNSP185F	99.7±0.1	0.10±0.01	<0.05	α	53	42	46	C+(F+A)
	VNSP186F	99.7±0.1	<0.10	<0.05	α	73	73	73	C+(F+A)
	VNSP187F	99.8±0.1	<0.10	<0.05	α	- [b]	-	-	C+(F+A)

APPENDIX V: SUMMARY OF MICROSTRUCTURAL OBSERVATIONS OF ARTEFACT COLLECTION FROM VNSP

VNSP866G · VNSP867G · VNSP868G · VNSP869G · VNSP854E · VNSP855E · VNSP870E · VNSP871E · VNSP872E · VNSP873E · VNSP874E · VNSP875G · VNSP876E · VNSP877E · VNSP846D
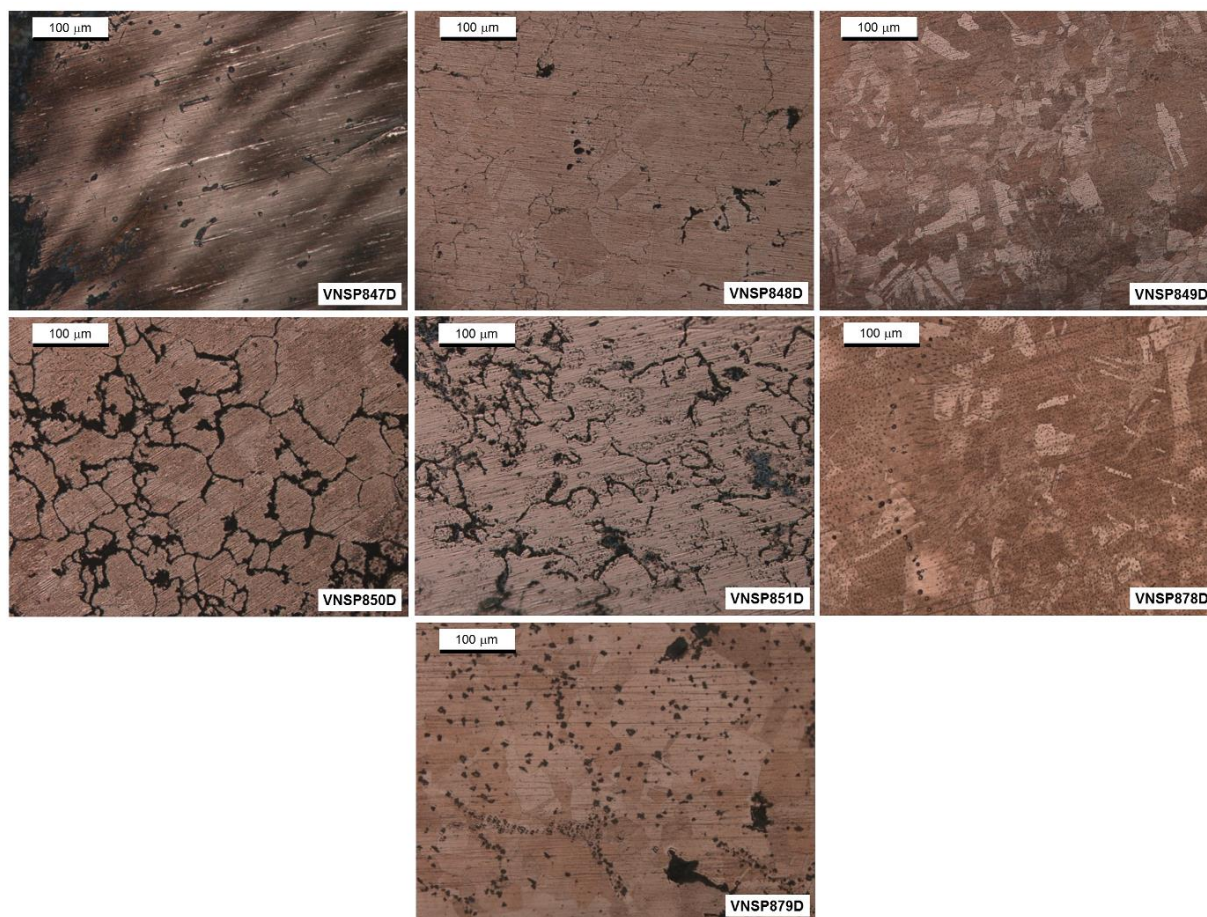
Figure V.1. OM images with the most representative microstructural observations of artefact collection from VNSP (all BF, etched).

APPENDIX VI: SUMMARY OF CIE L*A*B* CHROMATIC COORDINATES AND *H* ANGLE OF ARTEFACT COLLECTION FROM VNSP

Table VI.1. CIE *L*a*b** chromatic coordinates, *h* angle of the VNSP collection analysed and As content (wt.%).

Artefact	L*	a*	b*	h	As (wt.%)
VNSP001A	26.18	0.29	-0.09	-17.24	4.36
VNSP021A	24.99	2.17	2.34	47.16	0.90
VNSP023A	24.76	2.11	2.29	47.34	0.96
VNSP025A	23.54	1.82	1.94	46.83	3.37
VNSP029A	23.39	0.96	0.92	43.78	3.19
VNSP031A	23.19	1.84	1.87	45.46	1.43
VNSP038A	25.91	2.71	3.25	50.18	1.56
VNSP040A	22.75	2.03	2.03	45.00	3.39
VNSP047A	24.58	2.63	2.64	45.11	<0.10
VNSP049A	22.86	0.75	0.47	32.07	5.59
VNSP097A	27.00	0.39	-0.07	-10.17	6.04
VNSP123B	21.77	1.63	1.47	42.04	0.21
VNSP124B	23.22	2.93	2.98	45.48	0.19
VNSP132C	22.57	1.68	2.07	50.94	4.92
VNSP133C	25.50	2.97	3.02	45.48	0.27
VNSP134C	27.06	3.50	3.49	44.92	<0.10
VNSP135C	24.94	2.51	3.11	51.10	1.53
VNSP136C	24.97	3.20	3.24	45.35	<0.10
VNSP137C	25.31	3.31	3.42	45.94	<0.10
VNSP138C	24.72	2.85	2.83	44.80	1.08
VNSP139C	24.48	2.64	2.85	47.19	1.71
VNSP140C	24.17	1.67	2.03	50.56	3.43
VNSP141C	23.87	2.08	2.2	46.61	2.61
VNSP262C	23.18	3.42	3.48	45.50	<0.10
VNSP265C	24.79	2.61	2.68	45.76	0.67
VNSP144D	25.07	2.32	2.31	44.88	<0.10
VNSP145D	26.14	2.39	2.62	47.63	<0.10
VNSP146D	23.74	1.99	2.15	47.21	2.04
VNSP147D	23.51	2.15	2.38	47.91	1.85
VNSP148D	25.39	0.27	0.09	18.43	9.13
VNSP150D	24.33	2.27	2.25	44.75	0.24
VNSP153D	22.70	1.20	1.36	48.58	1.08
VNSP154D	23.75	2.62	2.87	47.61	1.58
VNSP155D	25.13	2.19	2.24	45.65	0.79
VNSP165D	24.09	2.14	2.25	46.43	1.42
VNSP178D	25.94	3.52	3.64	45.96	<0.10
VNSP267D	24.32	2.92	3.34	48.84	<0.10
VNSP268D	24.64	2.69	2.33	40.90	<0.10
VNSP269D	23.36	1.69	1.92	48.64	2.56
VNSP271D	24.48	2.50	3.01	50.30	1.37
VNSP272D	25.17	1.46	1.61	47.80	3.06
VNSP273D	26.18	3.02	3.23	46.92	<0.10
VNSP274D	24.45	1.92	2.03	46.59	1.68

| Artefact	L^*	a^*	b^*	h	As (wt.%)
VNSP275D	26.27	1.70	1.38	39.07	2.3
VNSP177E	25.01	2.50	2.57	45.79	<0.10
VNSP180E	22.33	0.32	0.37	49.14	5.57
VNSP181E	22.78	1.11	1.12	45.26	2.22
VNSP183E	22.15	0.72	0.7	44.19	3.89
VNSP184E	23.37	1.23	1.41	48.90	3.85
VNSP188E	23.07	1.82	1.95	46.97	1.79
VNSP189E	22.60	1.49	1.67	48.26	4.53
VNSP186F	24.07	1.58	1.79	48.56	<0.10
VNSP190H	25.39	2.69	2.91	47.25	1.57
VNSP191I	22.48	0.39	0.14	19.75	5.49
VNSP192I	22.74	2.26	2.49	47.77	3.13
VNSP193I	27.48	3.28	3.85	49.57	2.32
VNSP194I	25.36	3.44	4.06	49.72	0.51
Cu (100%)	27.25	3.52	3.11	41.46	<0.10
Au (100%)	33.35	2.88	10.62	74.83	<0.10
Ag (100%)	27.05	-0.37	-1.22	73.13	<0.10

APPENDIX VII: SUMMARY OF MICROSTRUCTURAL OBSERVATIONS OF METALLIC NODULES COLLECTION FROM ML
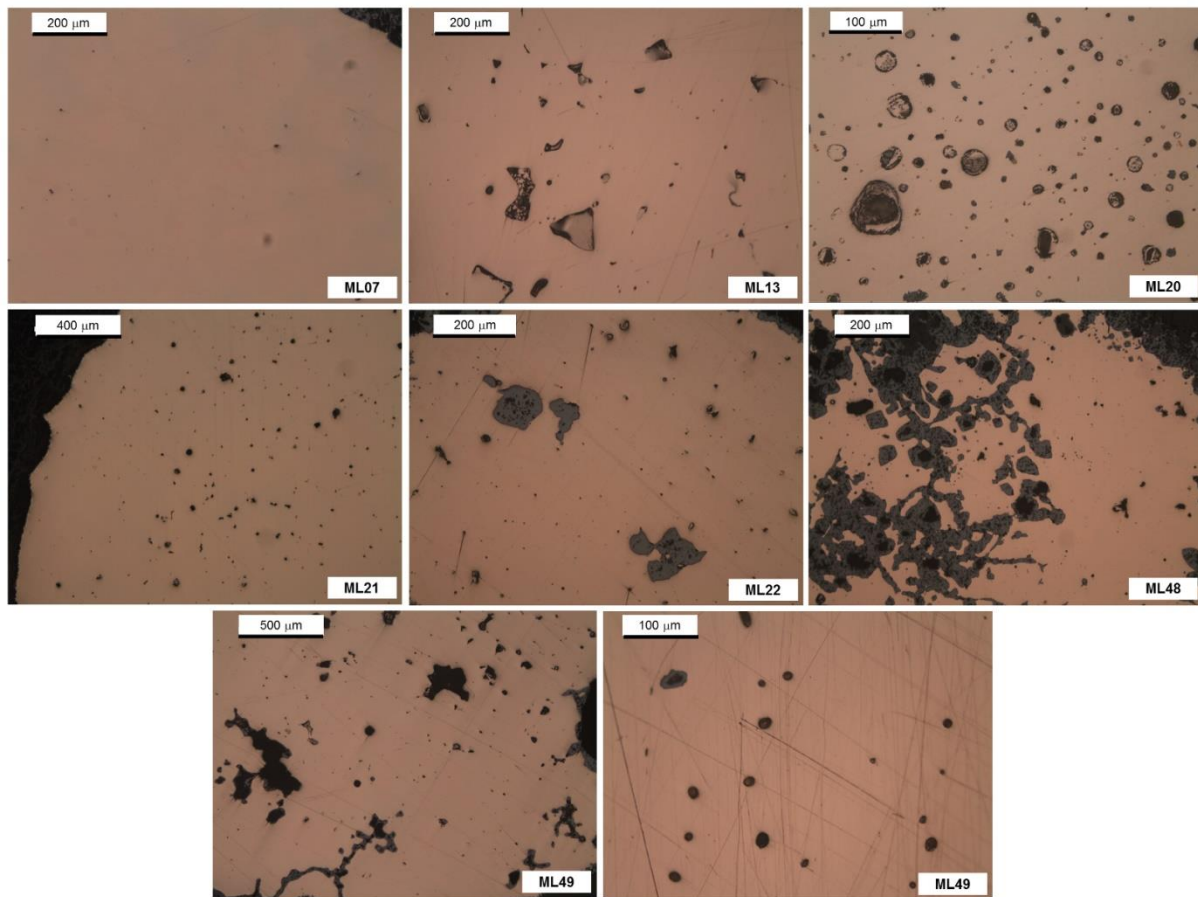
Figure VII.1. OM images with the most representative microstructural observations of metallic nodules collection from ML (all BF, non-etched).

APPENDIX VIII: SUMMARY OF MICROSTRUCTURAL OBSERVATIONS OF ARTEFACT COLLECTION FROM ML
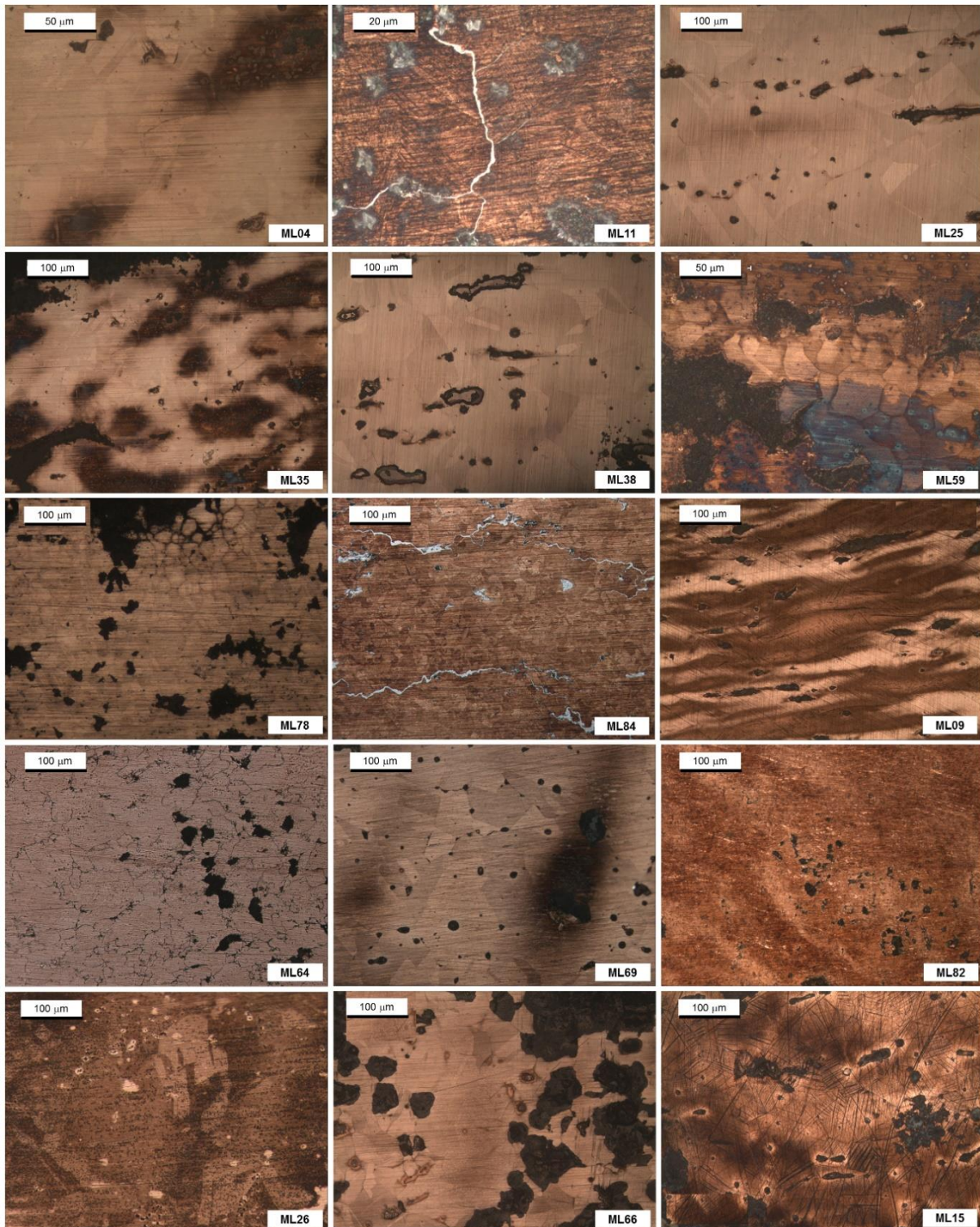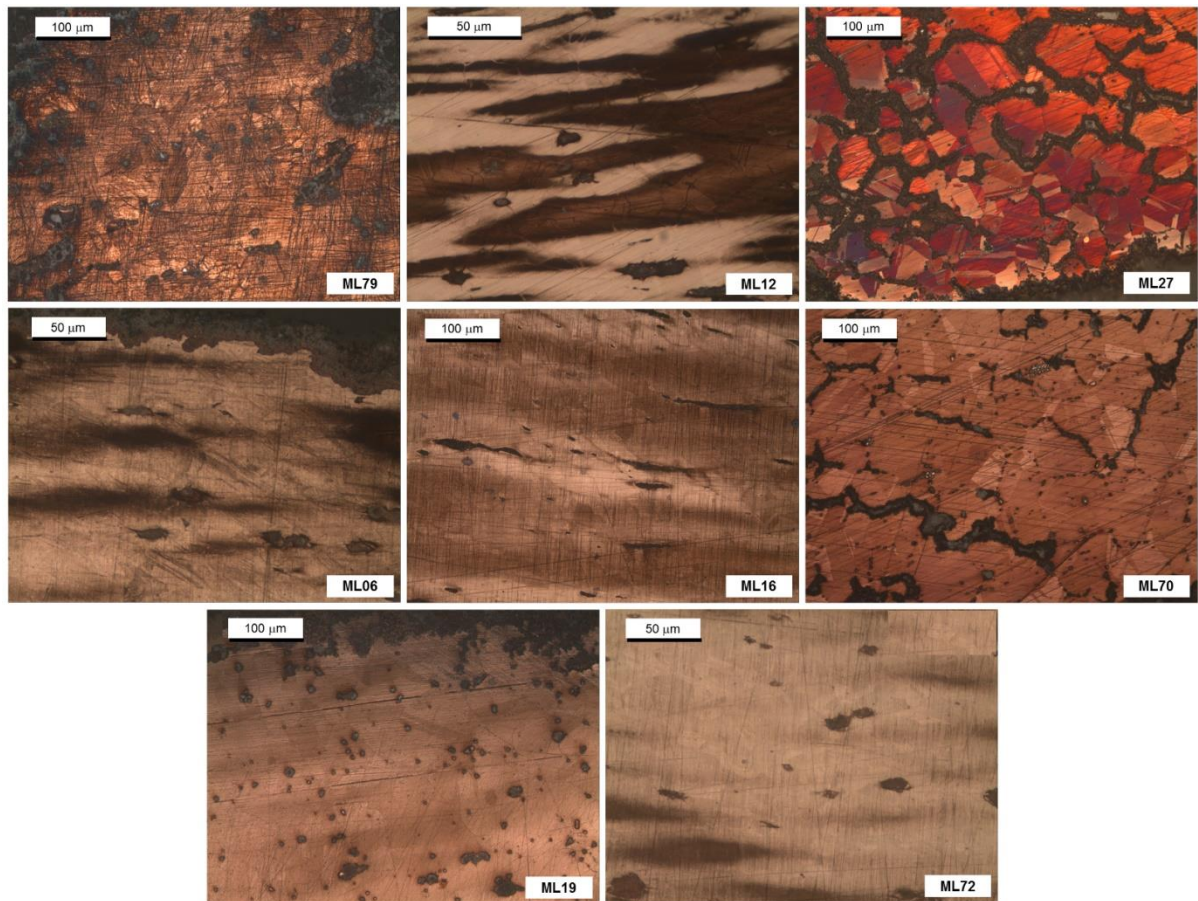
Figure VIII.1. OM images with the most representative microstructural observations of metallic nodules collection from ML (all BF, etched).
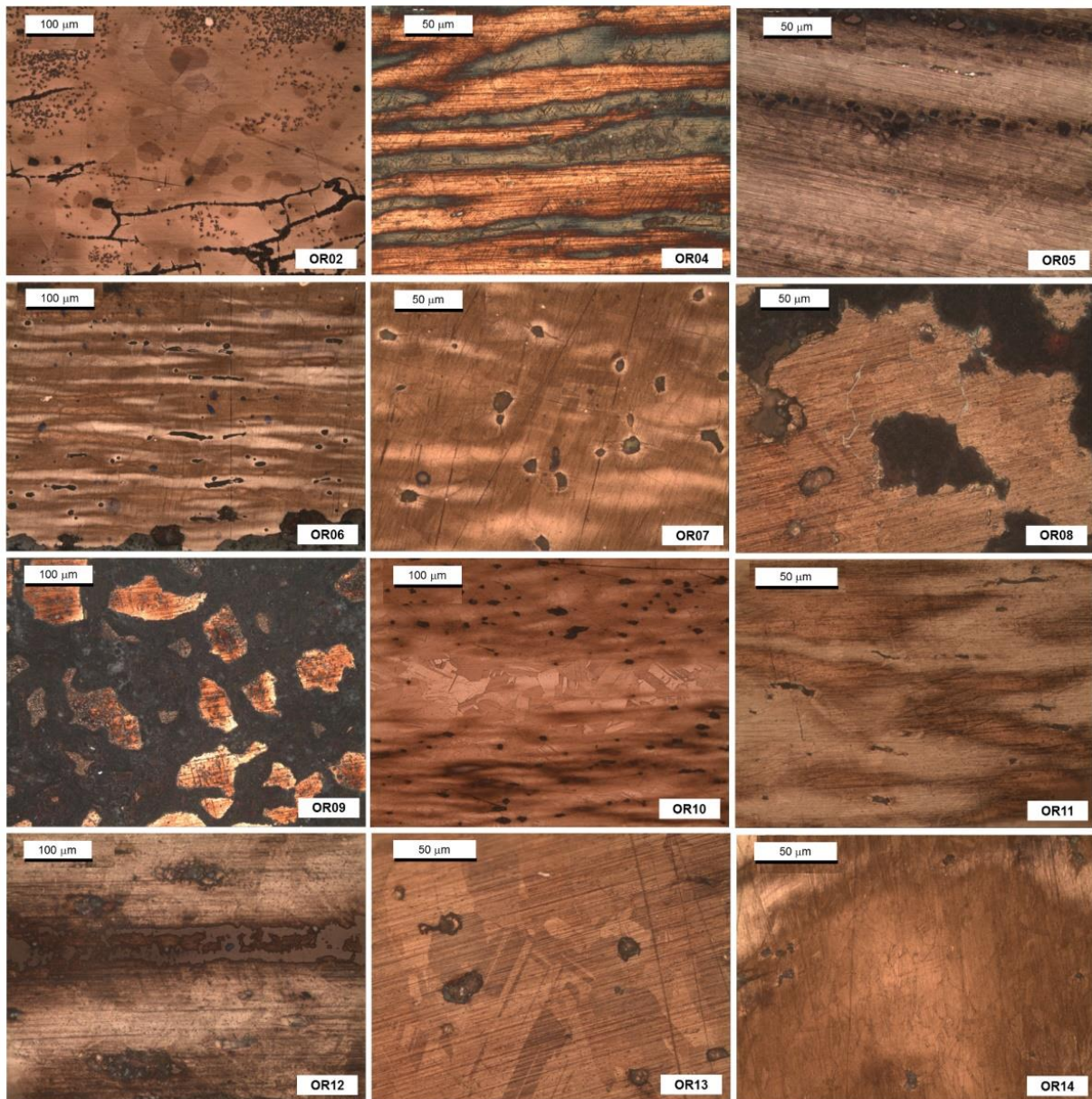
APPENDIX IX: SUMMARY OF MICROSTRUCTURAL OBSERVATIONS OF ARTEFACTS FROM OR COLLECTION

Figure IX.1. OM images with the most representative microstructural observations of artefact collection from OR (all BF, etched).